

**ASPECTS OF DEFLECTION BASIN  
PARAMETERS USED IN A MECHANISTIC  
REHABILITATION DESIGN PROCEDURE FOR  
FLEXIBLE PAVEMENTS IN SOUTH AFRICA**

**HORAK, E**

**PhD (Civil Engineering)**

**University of Pretoria**

**1987**



## CONTENTS

CONTENTS	i
SYNOPSIS	ii
SAMEVATTING	iv
ACKNOWLEDGEMENTS	vi
CHAPTER 1	LITERATURE SURVEY ON DEFLECTION BASIN MEASUREMENTS
CHAPTER 2	MEASUREMENT AND DATA PROCESSING OF DEFLECTION BASINS IN SOUTH AFRICA
CHAPTER 3	ANALYSIS OF DEFLECTION BASINS MEASURED DURING ACCELERATED TESTING
CHAPTER 4	LITERATURE SURVEY ON MATERIAL CHARACTERIZATION AND STRUCTURAL ANALYSIS USING DEFLECTION BASINS
CHAPTER 5	EFFECTIVE ELASTIC MODULI DETERMINED FROM ROAD SURFACE DEFLECTOMETER MEASUREMENTS
CHAPTER 6	RELATIONSHIPS BETWEEN DISTRESS DETERMINANTS AND DEFLECTION BASIN PARAMETERS: A LITERATURE SURVEY
CHAPTER 7	RELATIONSHIPS BETWEEN DEFLECTION BASIN PARAMETERS AND DISTRESS DETERMINANTS FOR TYPICAL SOUTH AFRICAN PAVEMENTS
CHAPTER 8	PROPOSED USE OF DEFLECTION BASIN MEASUREMENTS IN THE MECHANISTIC REHABILITATION DESIGN OF FLEXIBLE PAVEMENTS
APPENDIX A	EVALUATION OF DEFLECTION BASIN CURVE FITTING PROCEDURES
APPENDIX B	SUMMARY ON CONDITION SURVEYS
APPENDIX C	REMAINING LIFE DETERMINATION
APPENDIX D	CRITERIA FOR OVERLAY
APPENDIX E	CRACK MOVEMENT CALCULATIONS WITH DEFLECTION BASIN MEASUREMENTS ON N4/3
APPENDIX F	APPLICATION OF EQUIVALENT LAYER THICKNESS CONCEPT



## SYNOPSIS

TITLE : ASPECTS OF DEFLECTION BASIN PARAMETERS USED IN A MECHANISTIC REHABILITATION DESIGN PROCEDURE FOR FLEXIBLE PAVEMENTS IN SOUTH AFRICA.

CANDIDATE : EMILE HORAK

PROMOTOR : PROFESSOR P F SAVAGE

DEPARTMENT : CIVIL ENGINEERING

DEGREE : PHILOSOPHIAE DOCTOR ( CIVIL ENGINEERING )

The non-destructive measurement of deflection basins has come a long way from measuring only maximum deflection or radius of curvature and using empirical relationships in rehabilitation design. New equipment was developed world-wide and analysis techniques moved towards utilising the full deflection basin in fundamental analysis procedures.

This author addressed the problem of a proper description of the full deflection basin by doing a detailed literature survey on this subject. Various deflection basin parameters that describe the deflection basin are listed, as well as the various measuring apparatus related to them. The apparatus are all discussed in detail and related to the equipment available in South Africa.

The measurement of deflection basins with the road surface deflectometer (RSD) under accelerated testing with the fleet of heavy vehicle simulators (HVSs) are described in detail. An improved data manipulation procedure is proposed which simplifies the calculation of all the deflection basin parameters found in literature. Various models to fit the measured deflection basins are also investigated in an effort to describe the deflection basin in full too.

The measured deflection basin parameters of a bitumen, granular, cemented and light structured granular base pavement are discussed in detail as being tested with the fleet of HVS's. It is shown how the deflection basin parameters reflect the structural capacity of the various layers and behaviour states. A more accurate description of the behaviour states is made possible with the proposal of ranges for the various behaviour states for these deflection basins selected.

A literature study was carried out to investigate the various analysis procedures that use measured deflection basins as basic input in the characterization of materials. On the basis of this study, linear elastic programmes were used to calculate effective elastic moduli for each pavement layer, using measured deflection basins as input.

The possibility to relate typical distress determinants to measured deflection basins were investigated in the literature. Based on this, typical South African flexible pavement structures were analysed mechanistically and typical design curves were established for typical bitumen and granular base pavements. The effect of overlays were investigated too, resulting in typical overlay design curves.

In the final chapter the author endeavours to summarise the research by indicating how deflection basins can be measured and enhance the South African mechanistic rehabilitation design process. Only the latter rehabilitation design procedure is discussed with specific reference to the enhancement of the behaviour state identification, material characterization, analysis procedure and rehabilitation design with measured deflection basin parameters. The author ends off by giving an indication of the future research need in this field of deflection basins.



## SAMEVATING

TITEL : ASPEKTE VAN DEFLEKSIEKOM-PARAMETERS GEBRUIK IN 'N MEGANISTIESE REHABILITASIE-ONTWERPPROSEDURE VIR BUIGBARE PLAVEISELS IN SUID-AFRIKA.

KANDIDAAT : EMILE HORAK

PROMOTOR : PROFESSOR P F SAVAGE

DEPARTEMENT : SIVIELE INGENIEURSWESE

GRAAD : PHILOSOPHIAE DOKTOR ( SIVIELE INGENIEURSWESE )

Die nie-destruktiwe meting van defleksiekomme het 'n lang pad gevorder vanaf die meting van slegs maksimum defleksie of krommingstraal en die gebruik van empiriese verbande in rehabilitasie-ontwerp. Nuwe toerusting is wêreldwyd ontwikkel en analise tegnieke het in die rigting van die gebruik van die hele defleksiekom in meer fundamentele analiseprosedures beweeg.

Hierdie outeur spreek die probleem van die volledige beskrywing van die defleksiekom aan deur 'n diepgaande literatuurstudie oor hierdie onderwerp te doen. Verskeie defleksiekom-parameters wat die defleksiekom beskryf, word gelys, sowel as die onderskeie aparate wat daarmee verband hou. Hierdie aparate word almal in detail bespreek en in verband gebring met die toerusting wat in Suid-Afrika beskikbaar is.

Die meting van defleksiekomme met die padoppervlakte-deflektometer (POD) onder versnelde toetsing met die vloot van swaarvoertuignabootsers (SVN'e) is in detail beskryf. 'n Verbeterde datamanipulasie-prosedure is voorgestel wat die berekening van al die defleksiekom-parameters vereenvoudig soos gevind in die literatuur. Verskeie modelle wat gebruik is om die gemete defleksiekom te pas, is ondersoek in 'n poging om die defleksiekom ten volle te beskryf.

Die gemete defleksiekom-parameters van 'n bitumen, gebreekte klip, gesementeerde en ligte struktuur korrelkroonlaag-plaveisel is in detail bespreek soos getoets met die vloot SVN'e. Daar is getoon hoe die defleksiekom-parameters die strukturele kapasiteit van die onderskeie lae en gedragstoestande reflekteer. 'n Meer akkurate beskrywing van die gedragstoestande is moontlik gemaak deur die daarstelling van grense vir die verskillende gedragstate van die gesellekteerde defleksiekom-parameters.



'n Literatuurstudie is gedoen om die verskillende analise-prosedures wat van defleksiekom-parameters as basiese inset gebruik maak, in die karakterisering van materiale, te ondersoek. Op grond van hierdie studie is daar ook gepoog om gebruik te maak van linieêr elastiese programme om effektiewe elastiese moduli te bereken, vir elke plaveisellaag, vanaf gemete defleksiekomme.

Die moontlikheid om determinante vir oorspannendheid direk aan gemete defleksiekom-parameters te kan koppel, is in die literatuur nagevors. Op hierdie trant is daar toe tipiese Suid-Afrikaanse soepel plaveiselstrukture meganisties ontleed en sogenaamde ontwerpcurwes daargestel vir tipiese bitumen- en korrelkroonlaag-plaveisels. Die invloed van herdeklae is ook ondersoek en tipiese herdeklaag ontwerpcurwes is daargestel.

In die finale hoofstuk poog die skrywer om die navorsing op te som deur aan te dui hoe defleksiekomme gemeet kan word en die Suid-Afrikaanse meganistiese rehabilitasie ontwerp-prosedure kan versterk. Slegs laasgenoemde rehabilitasie ontwerp-prosedure is bespreek met spesifieke verwysing na hoe gemete defleksiekom-parameters die gedragstoestande kan identifiseer, materiale karakteriseer, die analise prosedure en rehabilitasie ontwerp kan versterk. Die outeur eindig deur aan te dui wat die navorsingsbehoefte in die toekoms is ten opsigte van defleksiekomme.

## ACKNOWLEDGEMENTS

I thank my friend and Lord Jesus Christ for setting me free to become the person He wants me to be. May this thesis also contribute to His glory!

The Chief Director of the NITRR, Mr R N Walker, is thanked for the permission to use this research work done at the Institute in this thesis.

I thank Dr Charles Freeme, former group head of the Pavement Engineering Group, for his enthusiastic support and motivation by excellent example. In the same breath I would like to thank Professor Carl Monismith from U.C. Berkeley, who initiated my interest in this field.

I thank the whole former Pavement Engineering Group for their kind co-operation and interest. Rassie Otte is singled out for his perseverance and hard work on the computer. A special word of thanks to Rolette Sutton for her meticulous editing. The typing done by the typing pool is highly appreciated.

I would like to thank my wife Mariana for her loving support, and Hèlène, Emile, Eduard and Anè for enduring the moods.

Last of all I would like to thank my parents, Markie and Bets, for their support and interest over the years. Markie, I know you would have been proud!



## **CHAPTER 1**

### **A LITERATURE SURVEY ON DEFLECTION BASIN MEASUREMENTS**



**CHAPTER 1: CONTENTS**

	PAGE
1 INTRODUCTION	1.2
2 DEFLECTION BASIN PARAMETERS	1.5
2.1 Review of parameters	1.5
2.2 Evaluation of parameters	1.7
3 DEFLECTION MEASURING	1.19
3.1 Review of devices and methods	1.19
3.2 Evaluation of devices	1.21
3.3 Correlations between devices	1.31
4 CONCLUSIONS AND RECOMMENDATIONS	1.32

## 1. INTRODUCTION

In the development of fundamental methods of pavement evaluation by means of deflection measurements it is imperative that an accurate description of the deflection basin be given. In the majority of analysis procedures only the maximum surface deflection ( $\delta_0$ ) is measured (Epps and Hicks, 1982). Owing to the empirical nature of analysis techniques in the past, a more detailed description of the deflection basin has been neglected. In Figure 1.1 it can be seen that the same maximum deflection value,  $\delta_0$ , can be measured on two pavements with totally different deflection basins and structural response characteristics. Whitcomb (1982) even concludes from various examples of this phenomenon that "...resilient moduli for layers in a pavement system cannot be back calculated using maximum surface deflection alone". In their analysis of Alaskan highways during the spring thaw period Stubstad et al. (1983) show that the same maximum deflection value could lead to wrong assumptions of thaw depth and resulting damage potential. It is only by looking at the whole deflection basin that preventative predictions of thaw depth can be made. Although South Africa does not have pavement distress due to thaw as in North America, it is significant that the whole deflection basin can be used to indicate a change of state.

Paterson et al. (1974) states that when a pavement deflects under a load, the influence of the load extends over a certain area. In one dimension and for one depth this can be regarded as a deflection profile or influence line of, say, the surface. In two dimensions the deflection at any depth is given by an influence surface. The shape of the influence surface reflects the structure of the pavement. In Figure 1.2 the typical deflection profiles for a uniform circular load and the more complex shapes of dual wheel single axle loads and how front and back axles influence each other, are shown. The depth profile of the deflection closely reflects the stiffness depth profile of the pavement in relation to the relevant stress levels.

This is best summarised by the Technical Committee Report of the XVII World Road Congress (Permanent International Association of

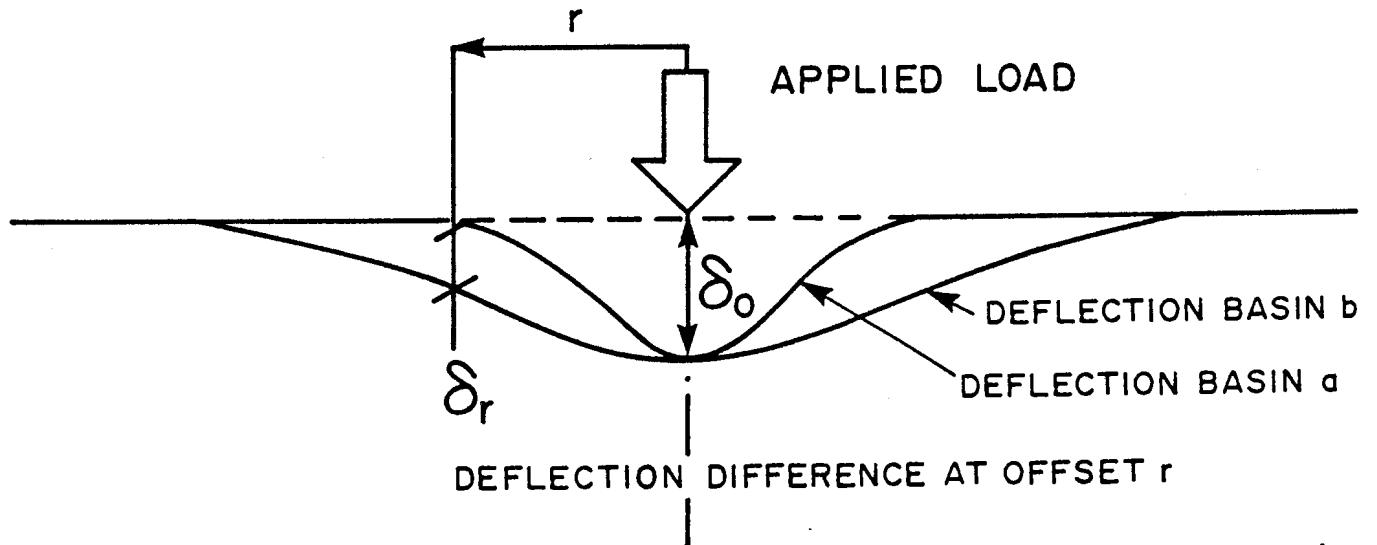


Illustration of the same maximum deflection for two different deflection basins.

FIGURE I.1  
DEFLECTION BASIN ILLUSTRATION.

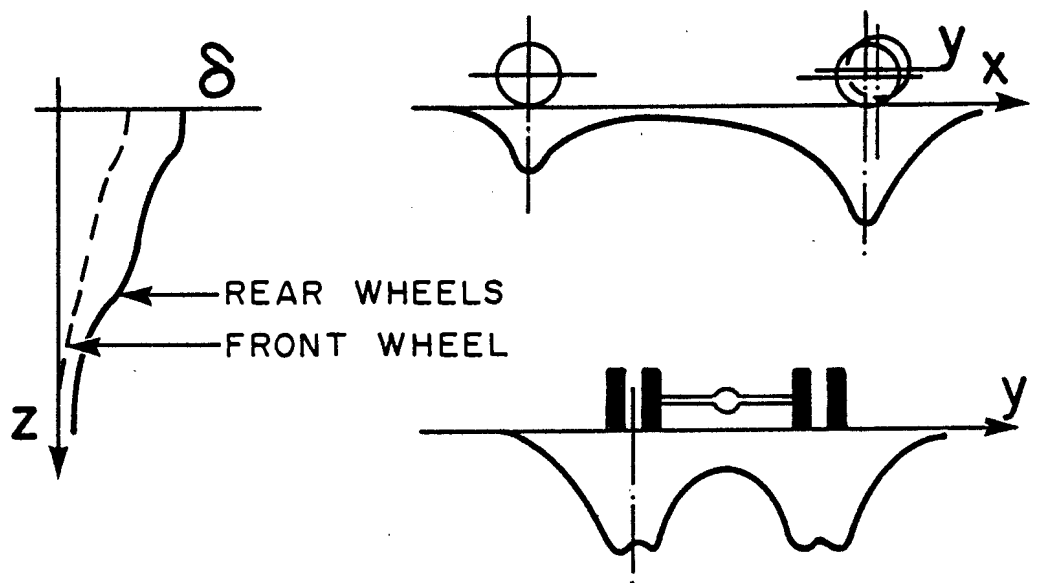
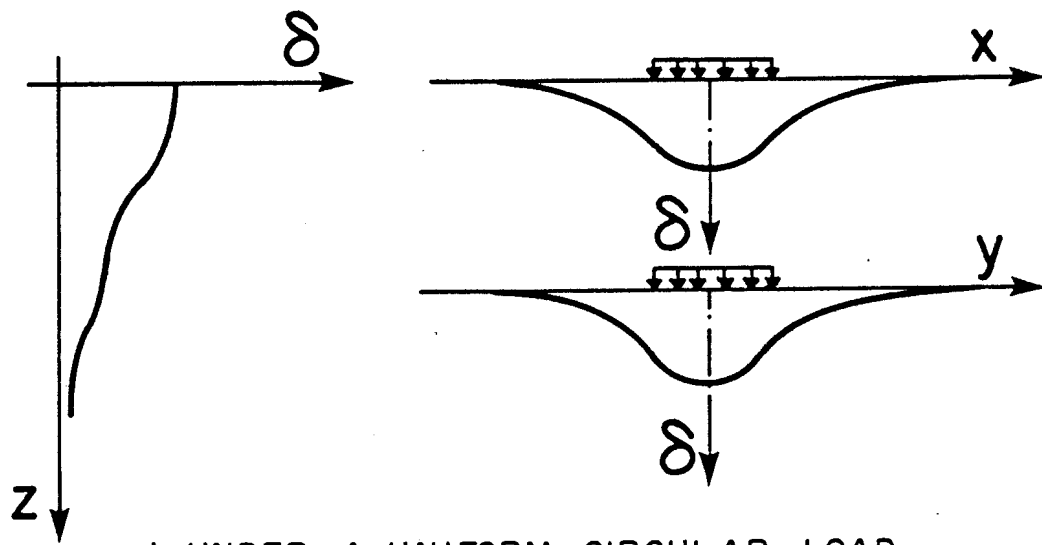


FIGURE I.2  
TYPICAL SHAPES OF DEFLECTION INFLUENCE  
LINES (Dehlen, 1962 b)

Road Congresses,1983). "There are obvious attractions in making maximum use of the information that can, in principle, be obtained by detailed evaluation of the deflected shape as it obviates or reduces the need for assumptions about, or measurement of, properties of pavement materials."

This introductory discussion clearly indicate that there is a need for the measurement and interpretation of the full deflection basin. As will be discussed in later chapters, in South Africa the full deflection basin is measured, but the analysis historically focussed on the small area surrounding maximum deflection. In order to make better use of the full deflection basin , a literature survey was conducted. This literature survey covers the work done overseas with other measuring equipment , description methods of the full deflection basin , evaluation of various deflection basin parameters and devices. In order to bring it in line with the South African scene , all these discussions are related to the practice here . Recommendations are made by this author to enhance the current practice and use of South African devices and deflection basin description.

## 2 **DEFLECTION BASIN PARAMETERS**

### 2.1 Review of Parameters

Surface deflections are generally measured by sensor(s) of various kinds located in a fixed line and normally at a fixed distance relative to the centriod of the load area. Deflection basin parameters differ in their relation to the measuring device and degree to which they describe the essential features of the deflection basin. In Table 1.1 a summary is given of the parameters, formulae, test method or device normally associated with it and at least one reference.

It is suggested that the fold-in of Table 1.1 at the back be folded out to ensure ease of reading as exhaustive reference will be made to the various deflection basin parameters in the sections to follow, as well as the chapters to follow.

TABLE I.1 SUMMARY OF DEFLECTION BASIN PARAMETERS

Parameter	Formula	Measuring device	Reference
1. Maximum deflection	$\delta_0$	Benkelman beam Lacroix deflectograph	Kennedy, et al. Asphalt Institute(1978)
2. Radius of curvature	$R = \frac{r^2}{2\delta_0(\delta_0/\delta_r - 1)}$ $r = 127 \text{ mm}$	Curvaturemeter	Dehlen (1962 a)
3. Spreadability	$S = \frac{[(\delta_0 + \delta_1 + \delta_2 + \delta_3)/5]100}{\delta_0}$ $\delta_1, \dots, \delta_3$ spaced 305 mm	Dynaflect	Vaswani (1971)
4. Area	$A = 6 [1 + 2(\delta_1/\delta_0) + 2(\delta_2/\delta_0) + \delta_3/\delta_0]$	Falling weight deflectometer(FWD)	Hoffman and Thompson (1981)
5. Shape factors	$F_1 = (\delta_0 - \delta_2)/\delta_1$ $F_2 = (\delta_1 - \delta_3)/\delta_2$	FWD	Hoffman and Thompson (1981)
6. Surface curvature index	SCI = $\delta_0 - \delta_r$ ; where $r = 305 \text{ mm}$ or $r = 500 \text{ mm}$	Benkelman beam Road rater FWD	Anderson (1977) Kilareski, et al. (1982) Molenaar (1982)
7. Base curvature index	BCI = $\delta_{610} - \delta_{915}$	Road rater	Kilareski, et al. (1982)
8. Base damage index	BDI = $\delta_{305} - \delta_{610}$	Road rater	Kilareski, et al. (1982)
9. Deflection ratio	$Q_r = \delta_r/\delta_0$ where $\delta_r \approx \delta_0/2$	FWD	Claessen and Ditmarsch (1977)
10. Bending Index	BI = $\delta/a$ where $a =$ Deflection basin	Benkelman beam	Hveem (1955)
11. Slope of deflection	SD = $\tan^{-1}(\delta_0 - \delta_r)/r$ where $r = 610 \text{ mm}$	Benkelman beam	Kung (1967)
12. Tangent slope	ST = $(\delta_0 - \delta_r)/r$ where $r$ is determined by a polynomial function	Benkelman beam FWD	University of Dundee (1980)
13. Radius of influence	RI = $R'/\delta_0$ where $R'$ is the distance from $\delta_0$ to where basin is tangent to horizon.		Ford and Bissett (1962)

The first two parameters listed in Table 1.1 are the traditional maximum deflection and radius of curvature. Their formulas show that only the small area surrounding maximum deflection (positive curvature) is utilized. The spreadability (S) and area (A) parameters obviously cover the full deflection basin. Parameters such as the shape factors (F1 and F2), surface curvature index (SCI), base damage index (BDI), base curvature index (BCI), slope of deflection (SD) and tangent slope (ST) also cover more than only part of the area of positive curvature near the load. In fact some of the aforementioned parameters try to describe either the area of positive curvature or the area of reverse curvature or the important area surrounding the point of inflection where the positive curvature changes to that of the reverse curvature. The other parameters not mentioned, do describe the deflection basin better than maximum deflection and radius of curvature, but it is not clear in which area of the deflection basin they fall with their description.

## 2.2 Evaluation of Parameters

The Technical Committee Report on flexible Roads of the XVII World Road Congress (Permanent International Association of Road Congresses, 1983) states; "The transient displacement or deflection of the road surface represents the sum of all the vertical strains in the pavement and sub-grade and remains the most widely used measurement of structural condition. Its advantages are, the relative simplicity of the measurements, the large amount of experimental data that already exists and the strong correlation found between deflection and overall performance in well defined conditions. It is however not very responsive to changes in the stiffness of upper pavement layers and is not a unique measurement of performance on all types of pavement."

A sensitivity analysis done at the University of Dundee (1980) incorporated most of the parameters listed in Table 1.1. A three-layered pavement system was analysed. All the structural parameters were varied. The sensitivity analysis was done by

converting to a standard dimensionless unit. The conclusions and summary of this study are briefly as follows:

Irrespective of the technique or measuring device, the parameters, bending index (BI) and radius of influence (RI) are difficult to determine. This is due to the fact that the length of the deflection basin is normally too long to measure accurately in situ. The value of maximum deflection ( $\delta_0$ ) was found to be unreliable when used alone owing to the difference in pavement conditions. This confirms the illustration in Figure 1.1 and conclusion by Whitcomb (1982) in Section 1.

Radius of curvature parameter (R) showed a high sensitivity to most changes in the pavement structural parameters, but was insensitive to subgrade elastic modulus. The deflection ratio (Q or Qr) and spreadability (S) showed even less sensitivity to changes in the other structural parameters. Contrary to this conclusion Koole (1979) reports that the parameter Q is a reliable parameter. The inconsistency seems to stem from the lack of adherence to Koole's (1979) precondition ( $\delta_r \approx \delta_0/2$ ) in determining Q. It seems that using a fixed value of  $\delta_r = \delta_{610}$ , as in this analysis done by the University of Dundee (1980), can result in the recorded insensitivity to changes in the pavement structural parameters. If it is taken into consideration that this parameter was developed for a specific type of pavement structure, it is to be expected that variances in structure will definitely influence its sensitivity. Rohlf et al. (1985) indicate that spreadability (S) is an indication of the ratio of the surface layer to support layer strengths.

In this sensitivity analysis by the University of Dundee (1980) the slope of deflection (SD) and tangent slope (ST) have shown a high sensitivity to changes in the pavement structural parameters. It is concluded, though, that the slope of deflection (SD) may have the same unreliability as the maximum deflection ( $\delta_0$ ) when used alone. The reason for this is that, as illustrated in Table 1.1, a fixed value of  $\delta_r = \delta_{610}$  is used. The tangent slope, on the other hand, makes use of a polynomial



function to describe the deflection basin and form the basis for the selection of  $\delta_r$  unambiguously. Dehlen (1962b) also observed that  $R$  is dependent mainly on the moduli of the upper layers of construction, and very little on those of the materials at depth. He states that; "The radius of curvature of a road surface under a given vehicle is dependent mainly on the Young's moduli of the materials in the base and subbase;... "He also observed that  $R$  is dependent to a considerable degree on tyre pressure and only to a lesser degree on the wheel load while  $\delta_0$  is dependent on wheel load and little on tyre pressure.

Hoffman and Thompson (1981) developed the area ( $A$ ) parameter from work done by Vaswani (1971). It is obviously related to the spreadability ( $S$ ) parameter and an attempt to incorporate the full deflection basin.

The surface curvature index (SCI) indicates the strength of the upper portion of a pavement according to an analysis of standard pavement structures in the State of Victoria, Australia by Anderson (1977). Generally in these pavement structures, as in the dry regions of South Africa, rather thin ( $\pm 50$  mm) asphalt surfacing layers are used. In Anderson's (1977) study, maximum deflection ( $\delta_0$ ) was used simultaneously to describe the response of the lower portion of pavements successfully.

Kilareski et al. (1982) state that the base curvature index (BCI) indicates the strength of the lower portion of the pavement system. The basis for these statements concerning SCI and BCI can be seen in Figures 1.3 and 1.4 where the related structural parameters are varied. It can be seen in Figure 1.3 that a difference in deflection at 0 and 305 mm (SCI) will reflect the change in base elastic modulus. In Figure 1.4 the difference in deflection at 610 mm and 915 mm (BCI) will reflect the change in subgrade elastic modulus.

The Technical Committee Report on flexible roads of the XVII World Road Congress (Permanent International Association of Road Congresses, 1983) concludes on the deflected shape; "The

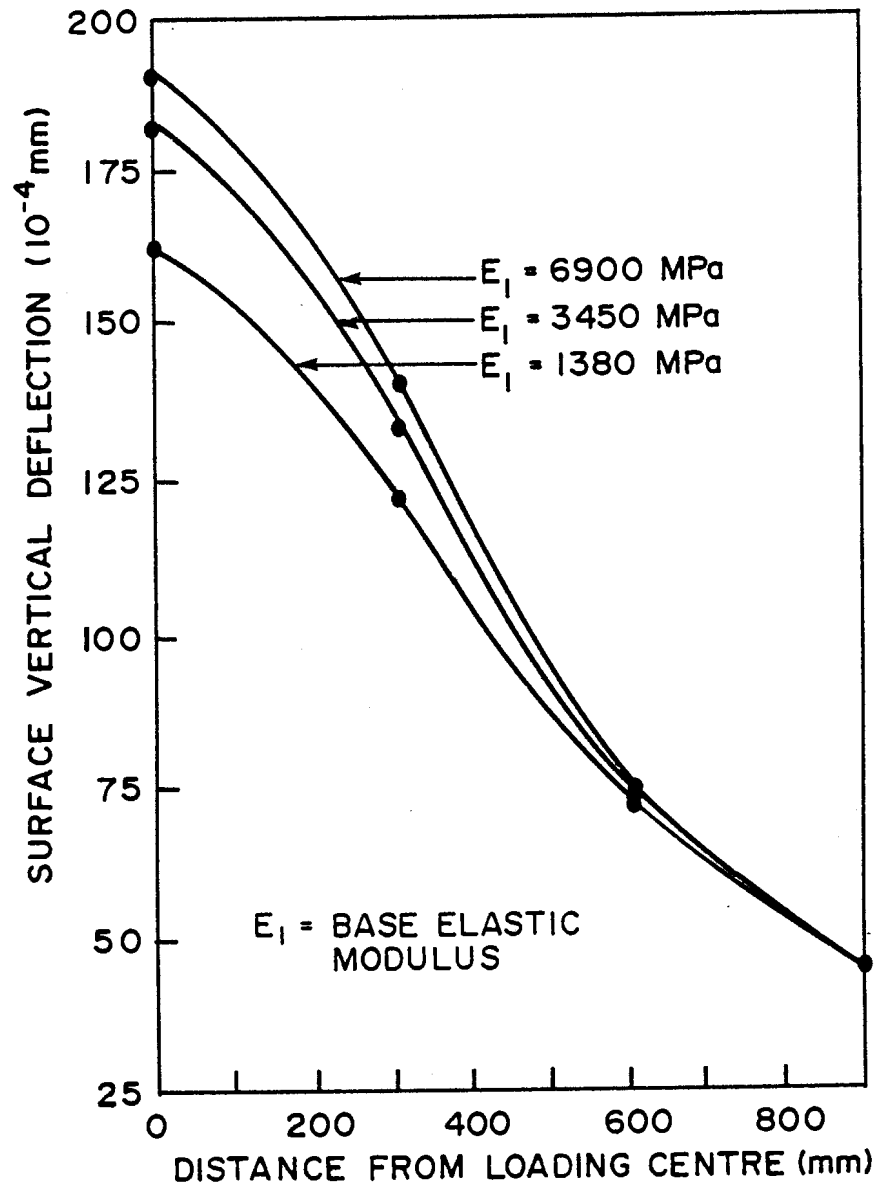


FIGURE 1.3  
 VARIATION OF SURFACE  
 DEFLECTION BASIN WITH  
 SURFACE MODULUS,  $E_1$   
 (Kilareski, et al., 1982)

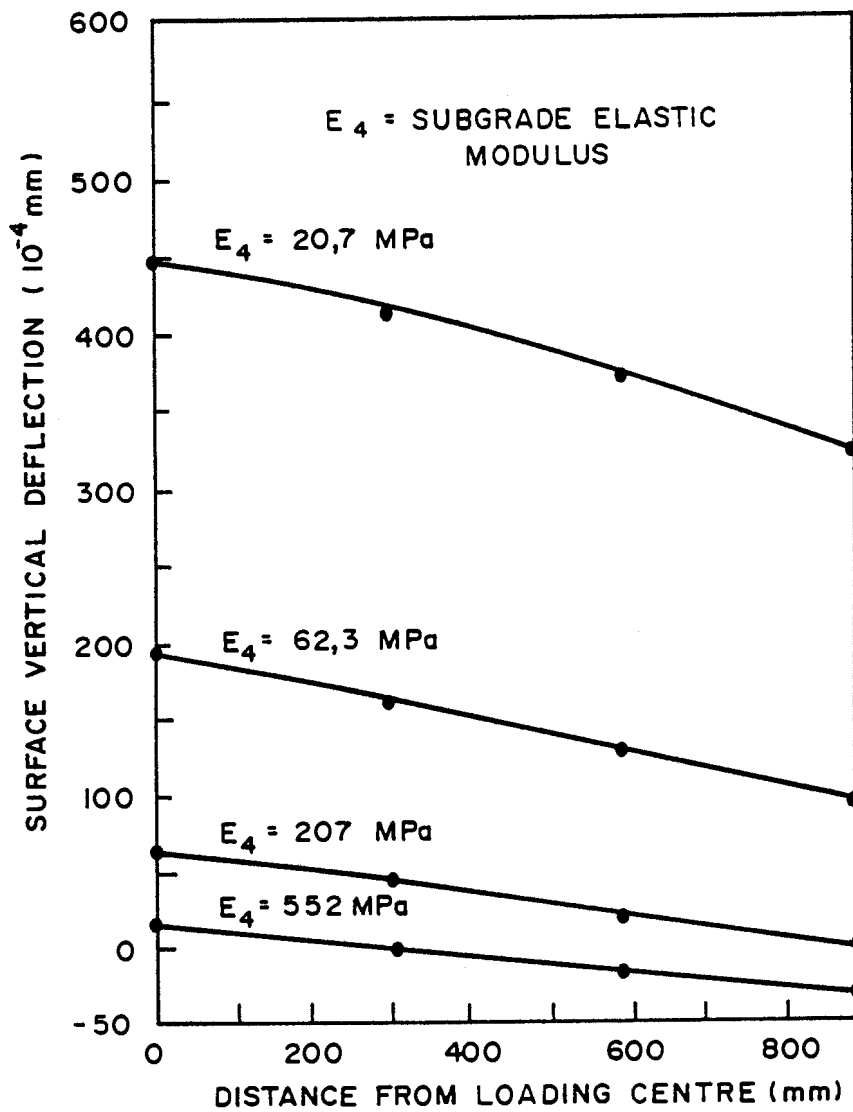


FIGURE 1.4  
 VARIATION OF SURFACE DEFLECTION  
 BASIN WITH SUBGRADE MODULUS,  $E_4$   
 (Kilareski, et al., 1982)

deflected shape near the point of maximum deflection is sensitive to changes in upper pavement layers and relatively unaffected by the subgrade. Deflection levels and their rate of change further from the maximum have been related to the stiffness of lower pavement layers and the subgrade."

Very interesting information is available on how the various deflection basin parameters relate to increase in number of standard axle repetitions. Kilaeski et al. (1982) produced the typical results of deflection versus number of equivalent axle repetitions as shown in Figure 1.5. SCI (difference between Sensors 1 and 2) and the BCI (difference between Sensors 3 and 4) are virtually constant with the increase in number of standard axle repetitions. From this follows the need for the development of the base damage index (BDI) which is the difference between Sensors 2 and 3). The values of the BDI change with the increase in repetitions of standard axles. Figure 1.6 results from work done by Molenaar (1983); in spite of the difference in measuring technique and device (see Table 1.1) it shows considerable support for this approach of relating the surface curvature index (SCI) to the repetitions of standard axles.

Rohlf et al. (1985) did a multivariate analysis of pavement Dynaflect deflection data. A relationship between Dynaflect deflections and pavement temperature, subgrade moisture, and cumulative traffic loading for a number of different pavement sections was developed. A typical Dynaflect deflection basin measurement is illustrated in Figure 1.7. The major conclusion from this study is that the base thicknesses and base layer elastic moduli had significant effects on the sensor deflections. The first sensor deflection (maximum) was directly related to the base thickness.

Tam (1985) analysed three-, four- and five-layered pavement structures and determined how the variation of structural inputs affected the deflection basin. Figure 1.8 summarizes the relative importance of the effect of varying the stiffnesses of

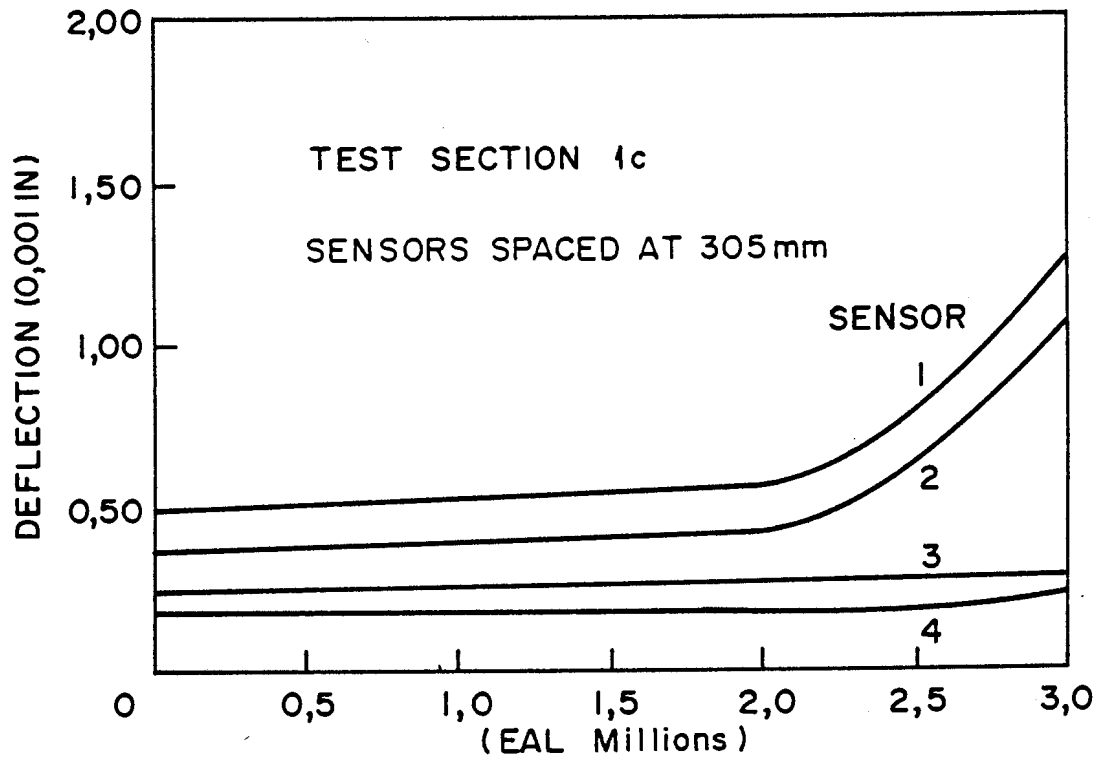


FIGURE 1.5  
CORRECTED ROAD RATER SURFACE  
DEFLECTIONS VS. 18-KIP (80 kN)  
EQUIVALENT SINGLE - AXLE LOAD  
(Kilareski, et al., 1982)

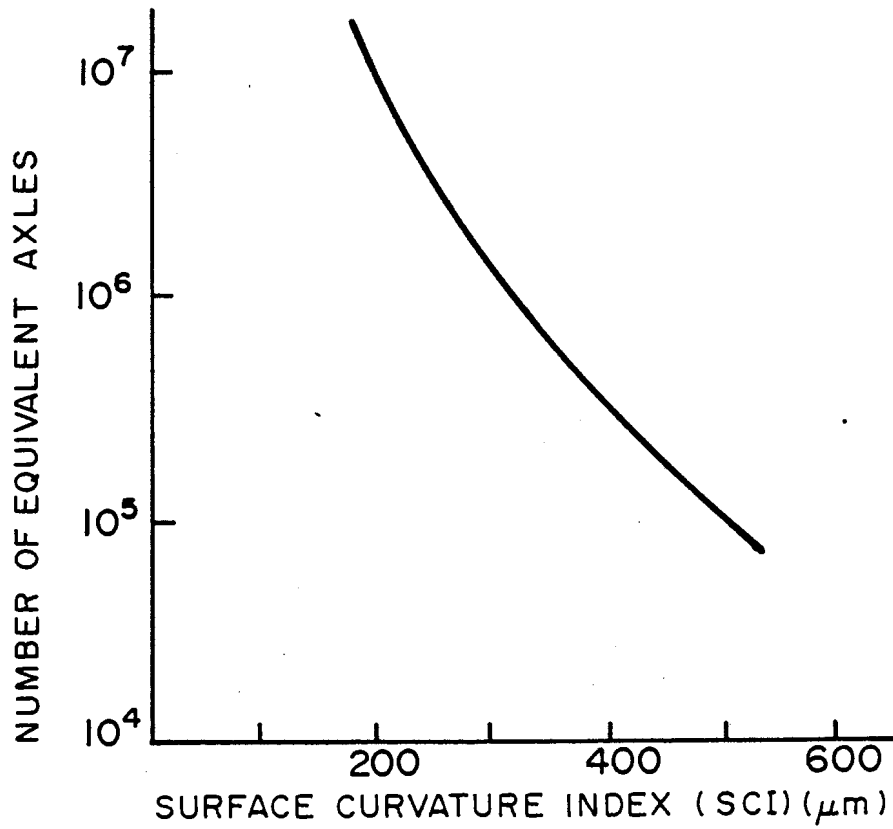
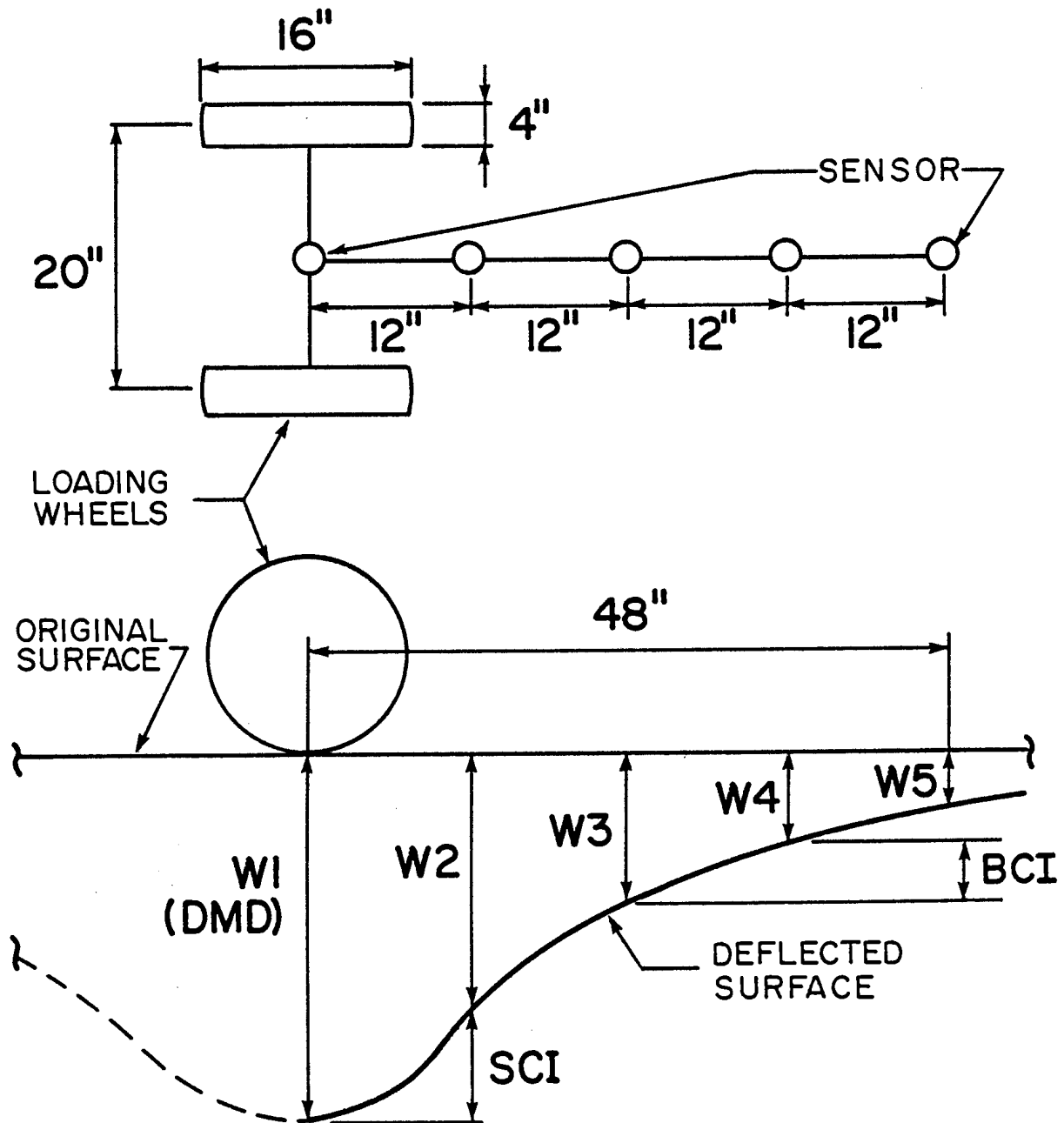


FIGURE I.6  
EXAMPLE OF A PAVEMENT DESIGN  
CURVE BASED ON THE SURFACE  
CURVATURE INDEX (SCI) (Molenaar, 1983)



NOTE : DEFLECTIONS ARE EXAGGERATED FOR CLARITY

FIGURE I.7  
 DYNAFLECT DEFLECTION BASIN (Rohlf, et al., 1985)

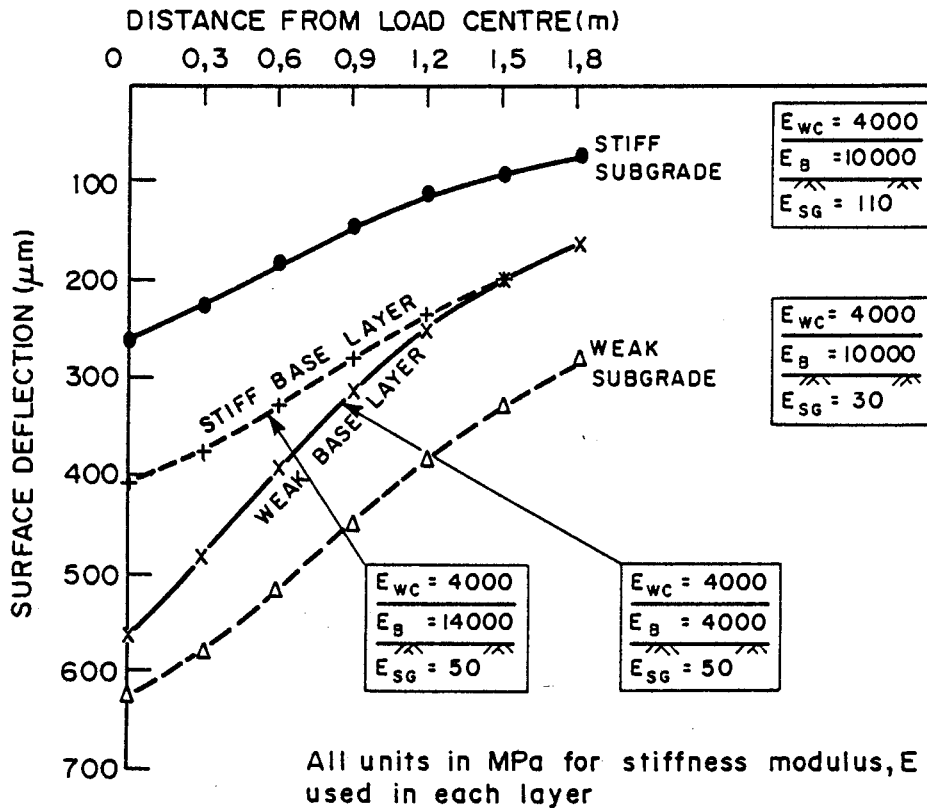


FIGURE 1.8  
RELATIONSHIP BETWEEN VARIATION OF  
STIFFNESS MODULI IN BASE LAYER AND  
SUBGRADE (Tam, 1985)



the base layer and the subgrade in a three-layered pavement structure. The main conclusions from the Tam study on three-layered pavement structures are as follows:

- (a) The variation of base layer thickness had the greatest influence on maximum deflection ( $\delta_o$ ) and spreadability (S). This was followed by the subgrade stiffness and base stiffness. Spreadability (S) had seven deflections incorporated in the calculation instead of the normal five (see Table 1.1).
- (b) As the subgrade stiffness increases (decreases), maximum deflection ( $\delta_o$ ) and spreadability (S) decrease (increase) (see Figure 1.8).
- (c) The increase (decrease) in magnitudes of pavement structural parameters reduces (increases) maximum deflection ( $\delta_o$ ), but increases (reduces) spreadability (S).

In Figure 1.9 the typical four-layered pavement system, as analysed as reference system by Tam (1985), is shown. The spreadability (S) and maximum deflection ( $\delta_o$ ) was normalized by a ratio to the value of the reference structure. The main conclusions here were the same as for the three-layered pavement system regarding the influence of the base and subgrade. It also showed that maximum deflection ( $\delta_o$ ) and spreadability (S) were hardly affected by the change of sub-base parameters at all. The implications are that the actual stiffnesses of the subbase will be difficult to determine with accuracy in evaluating existing pavement conditions and high accuracy on subbase thicknesses will not be a prerequisite for analysing such pavements. In the South African context this is a typical granular subbase pavement.

In Figure 1.10 the typical reference five-layered pavement structure is shown. In this case a cemented subbase in the pre-crack phase was analysed. The sensitivity analysis on maximum deflection ( $\delta_o$ ) and spreadability (S) are also shown.

REFERENCE STRUCTURE	
$E_{wc} = 4000 \text{ MPa}, \nu = 0,4$	$h_{wc} = 40 \text{ mm}$
$E_B = 1000 \text{ MPa}, \nu = 0,4$	$h_B = 200 \text{ mm}$
$E_{SB} = 100 \text{ MPa}, \nu = 0,3$	$h_{SB} = 200 \text{ mm}$
$E_{SG} = 50 \text{ MPa}, \nu = 0,4$	
$\delta_o = 431 \mu\text{m}, S = 0,678$	

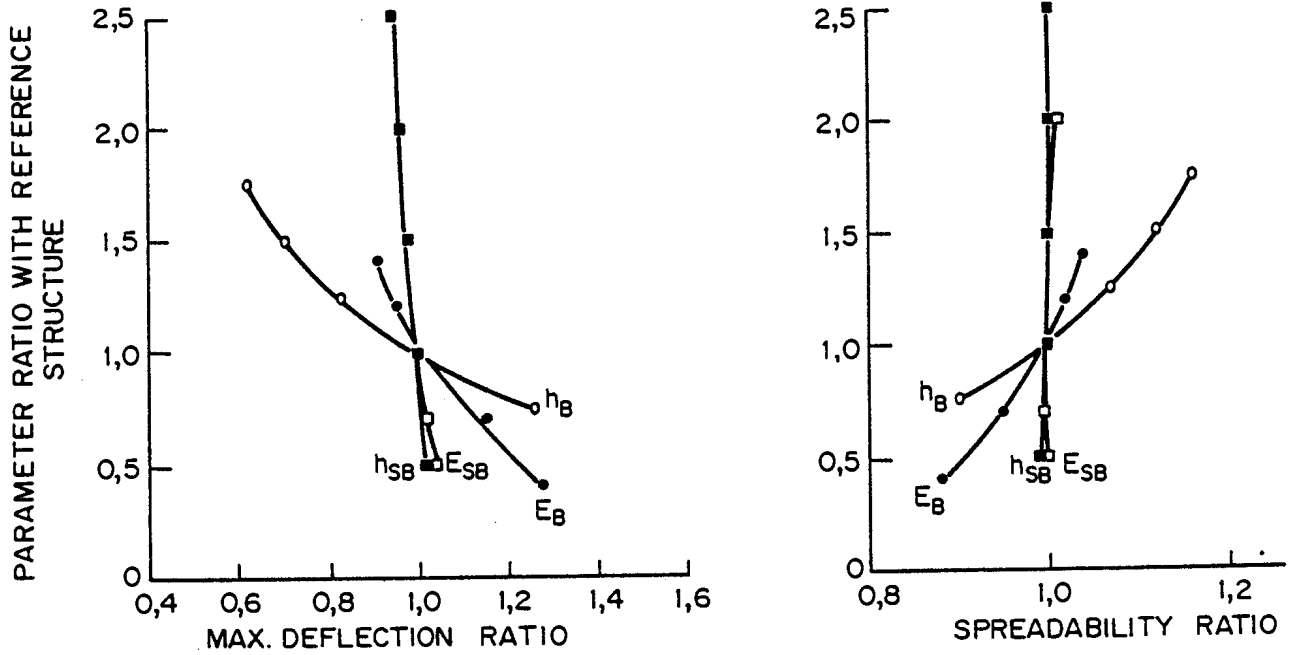


FIGURE 1.9  
RELATIVE SENSITIVITY OF PARAMETERS OF SUBBASE LAYER  
(Tam, 1985)

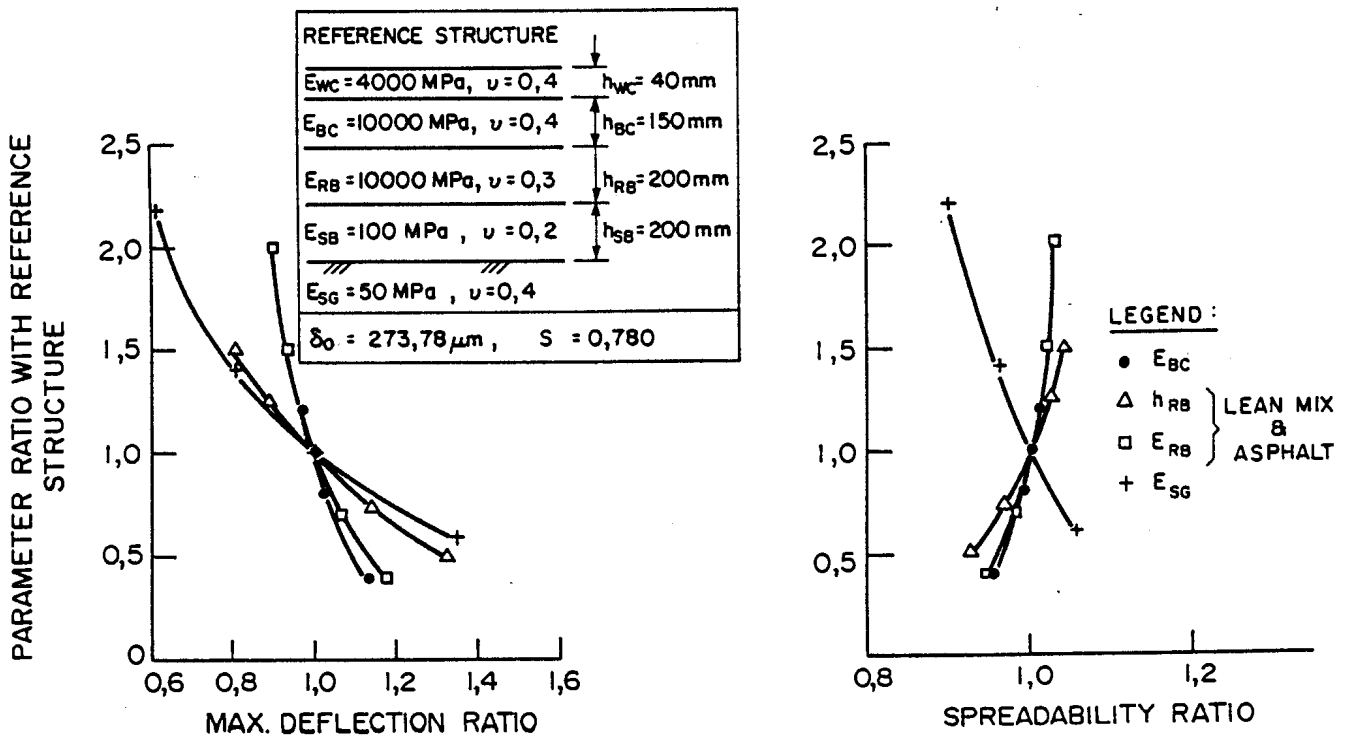


FIGURE 1.10  
RELATIVE SENSITIVITY OF PARAMETERS OF LEAN MIX AND  
ASPHALT BASE LAYER (Tam, 1985)

The main conclusion here was that deflections are sensitive to the variation of thickness of the lean concrete subbase and the asphalt base. Hence, it is important to know what their actual thicknesses are to enable one to evaluate the condition of the existing pavements with confidence.

### 3 DEFLECTION MEASURING DEVICES AND METHODS

#### 3.1 Review of devices and methods

Pavement deflection devices made their appearance in 1938 in California. The California Division of Highways installed the General Electric Travel Gauge state-wide in that year. This type of device developed evolutionarily. This process was enhanced by the use of these devices at test tracks such as those at Brighton and Stockton, and at WASHO and AASHO road tests. (Whitcomb, 1982). Since then the use of non-destructive deflection measuring devices has become standard practice world wide.

The development of new equipment has been prompted by the need to:

- a) increase the testing production rate
- b) increase the accuracy of measurements
- c) simulate moving traffic loads in terms of magnitude of load, shape and equivalent time of loading
- d) provide simplicity of operation and interpretation of results
- e) reduce the cost of testing.

Most deflection testing equipment can be classified by loading mode. Generally these devices fall into three main groups: static or slow-moving wheel devices, steadystate vibratory devices and impulse or falling weight devices. Table 1.2 lists a brief summary of the devices as classified by Monismith (1979).

Whitcomb (1982) mentions several other sophisticated devices. The moving vehicle device and accelerometers which need instrument installation in the pavement, cannot strictly be regarded as non-destructive deflection basin testing. Others mentioned are a deflection beam measuring perpendicular to a passing vehicle, laser technology and new techniques in photogrammetry. The road surface deflectometer (RSD) and multi-depth deflectometer (MDD) developed in South Africa for use with the Heavy Vehicle Simulator (HVS) described by Freeme et al. (1981) can also be seen as recent developments. Strictly speaking the MDD is a destructive deflection measuring device in terms of its installation procedure.

TABLE 1.2 - Deflection measuring devices

Method by which load is applied	Device	Organization by which used (Examples)
Slow-moving Wheel	Benkelman beam	Asphalt Institute, College Park, Maryland
	Road surface deflectometer (RSD)	NITRR, CSIR, South Africa
	Travelling deflectograph	California Department of Transportation
	Deflectograph	Transport and Road Research Laboratory, Great Britain. National Institute for Transport and Road Research, S.A. Main Roads Department, New South Wales, Australia, LCPC, France
Vibratory load	Curviameter	LCPC, France.
	Light vibrators, e.g. Road rater and Dynaflect	States: California, Kentucky, Louisiana, Utah. Federal Highway Administration
Falling weight	Heavy vibrators	U.S. Army Corps of Engineers, Waterways Experiment Station
	Falling weight deflectometer (FWD)	Shell Research, Amsterdam

### 3.2 Evaluation of devices

Whitcomb (1982) states that criteria for determining the "best" deflection testing device from a technical standpoint are difficult to describe. Various comparative studies have been made. In his comprehensive study Bush (1980) compared the operational characteristics (for example ease, speed and manpower requirements), costs (initial and operating), accuracy, reproducibility of measurements and depth of influence of several devices. The results are summarized in Table 1.3.

1438930  
1438924

Relative values of 1 to 10 were used with 1 being the most desirable and 10 the least. The results of this table clearly indicate a preference for the Dynaflect Model 2008, Road Raters and FWD.

The most comprehensive recent study comparing non-destructive testing (NDT) devices and methods for use in the overlay design of flexible pavements is that by the Federal Highway Administration (FHWA, 1984). User comments on the various devices were collected from all over the world. The following factors were considered:

- (a) time in service
- (b) crew size
- (c) professional qualifications of crew
- (d) number of test points per day
- (e) cost per test point
- (f) maintenance costs
- (g) traffic control costs
- (h) data recording methods
- (i) data storage
- (j) towing vehicle.

Typical results are summarized in Table 1.4. Most of the variation is apparently due to a difference in user rather than equipment. It does, however, give a good guide. It is obvious that the device that comes out best will depend on which factor is selected.

Another comparative study, also from the FHWA (1984) study, is shown in Table 1.5. It covers a wide range of criteria and the final result indicates that the FWD is favoured. The Road Raters and even the Dynaflect are not far behind in this rating. This emphasizes the fact that each device has its strong and weak points.

A few relevant conclusions from this study by the FHWA (1984) are as follows:

- (a) The Dynaflect, Road Raters and FWD are equipped to measure deflection basin parameters more quickly and efficiently than the static and automated beam devices;

TABLE 1.3 - Ranking of candidate devices by evaluation parameters (from Bush, 1980)

	Benkelman beam	Dynalect	FWD	Model 400 road rater	Model 510 road rater	Model 2008 road rater
Optional characteristics	6	1	5	3	4	2
Ease	6	1	5	3	4	2
Speed	6	1	5	2	2	2
Manpower	6	1	3	3	3	1
SUBTOTAL	18	3	13	8	9	5
Costs	6	1	5	2	2	4
Accuracy	3	2	1	3	3	2
Deflection	6	2	1	2	2	5
Force	1	4	3	5	5	1
SUBTOTAL	7	6	4	7	7	6
Transportability by cargo aircraft	1	2	2	3	2	2
Depth of influence	1	5	2	6	4	3
Suitability	6	3	1	5	3	1
TOTALS	23	14	16	22	18	14

TABLE I.4 : SUMMARY OF SELECTED DATA REPORTED ON VARIOUS NON-DESTRUCTIVE TESTING DEVICES

	No. of persons in crew	No. of test points per day	Man-hours per test day	Cost to analyze one day's data	Analysis cost per point	Average annual maintenance cost	Average daily traffic control costs
<u>Deflection beam</u>							
Mean	3	83	23	\$ 127	\$ 1,52	\$ 42	\$ 262
Standard deviation	0	24	1,4	\$ 106	\$ 0,99	—	\$ 12,50
<u>Dynaflect</u>							
Mean	1,8	234	14	\$ 88	\$ 0,44	\$ 2 242	\$ 408
Standard deviation	0,5	130	5	\$ 67	\$ 0,21	\$ 1 950	\$ 229
<u>Falling weight deflectometer</u>							
Mean	1,9	169	15,5	\$ 262,5	\$ 1,41	\$ 3 250	\$ 363
Standard deviation	0,2	65	0,9	\$ 237,5	\$ 1,09	\$ 1 750	\$ 274
<u>Road rater ( all models )</u>							
Mean	1,3	292	10	\$ 362	\$ 1,69	\$ 2 075	\$ 176
Standard deviation	0,4	86	2,5	\$ 178	\$ 1,17	\$ 2 104	\$ 43
<u>Travelling deflectometer /deflectograph</u>							
Mean	2	2667	18,7	\$ 278	\$ 0,10	\$ 3 312	\$ 600
Standard deviation	0	656	3,8	\$ 111	\$ 0,02	\$ 312	—



TABLE I.5: COMBINED RATINGS REPORTED IN LITERATURE (LARGER NUMBERS INDICATE BETTER RATING)

Rating Criteria	Dynalect	RR 400B	RR2000	FWD
Cost per lane mile	9.5	10.0	9.2	7.5
Operator training	10.0	10.0	10.0	10.0
Speed of operation (1)	7.5	10.0	10.0	10.0
Traffic interference (1)	7.5	10.0	10.0	10.0
Ease of data collection(2)	10.0	10.0	10.0	10.0
Ease of calibration (3)	2.0	5.0	5.0	10.0
Equipment versatility(4)	0	10.0	10.0	10.0
Actual load capability(5)	1.0	2.9	5.5	10.0
Design compatibility	<u>10.0</u>	<u>10.0</u>	<u>10.0</u>	<u>10.0</u>
Combined rating	57.5	77.9	79.7	87.5

- (1) Based on the theoretical test program.
- (2) Assumes the recommended options.
- (3) Based on the time required for calibration.
- (4) Based on ability to vary the applied load.
- (5) Based on ability to produce a 10,000 lb. dual wheel load.

- (b) The automated beam device, FWD and Road Rater model 2008 can develop loads at, or near, normal design loads;
- (c) Load as well as deflection can easily be measured. The Road Raters and FWD are equipped to measure load as well as deflection;
- (d) Devices capable of producing several load levels up to, or near, design loads can be used to determine the stress sensitivity of pavement systems, and
- (e) Steady state dynamic devices, which use a relatively heavy static pre-load, change the stress state in the pavement before the testing.

The slow-moving wheel devices like the Benkelman beam and deflectographs may be seen as representing the first generation of measuring devices; the vibratory and falling weight devices are more recent developments. Of prime concern is the fact that the slow-moving devices are normally associated with a single measuring point, whereas the later generation measuring devices are increasingly able to describe the deflection basin. This is normally achieved with the equally spaced measuring points away from the point of loading. The development of the RSD (Freeme et al. 1981) and modification of the standard Benkelman beam and Lacroix deflectograph (Anderson, 1977), which can produce a "continuous" plot of the deflection basin, overcome this disadvantage. In general it can be stated that the more accurate the measuring device can measure the deflection basin, the better it is.

The curviameter can strictly be called a fast rolling wheel technique. The Technical Committee Report on flexible roads of the XVII World Road Congress (Permanent International Association of Road Congresses, 1983) described it as follows; "The Curviameter carries a velocity-sensitive transducer on an endless moving chain that places and replaces the transducer in advance of the loaded dual wheels of a lorry moving at 20 km/h. Although the machine gives an increase in route-capacity of rolling wheel techniques the derived deflections and curvatures are of limited accuracy."

The slow-moving wheel devices generally measure deflection with a standard axle load. Depending on the measuring technique of the wheel moving to or from the measuring point, deflections can vary. Although a lot can be said for these techniques and devices simulating the actual moving wheel loads (more accurately), it must be remembered that the simulation is normally much slower than the real situation and effects like plastic deformation come into play. In this regard Whitcomb (1982) states that the input from the static and vibratory devices commonly used bears little resemblance to the input from an actual vehicle. Molenaar and Koole (1982) mention that the low force levels of the light vibrators on predicted pavement behaviour are a cause for concern. This concern is not only with respect to possible non-linear behaviour of the pavement, but also with respect to errors in measurement, particularly measurements taken at the extremes of the deflection basin where deflections measured and normal variations of instruments are of the same magnitude. The heavy vibrators described by the Federal Aviation Administration (1979) have adequate loading force, but are mainly used to evaluate airfield pavements.

The FWD meets all requirements for reliability, reproduction, accuracy, simulation of moving wheel loads and measuring the whole deflection basin and it does not alter the conditions of the pavement before loading (Whitcomb, 1982). The FWD can vary the force from 40 to 125 kN and will represent any loading

condition on a pavement or airfield realistically (Claessen and Ditmarsch, 1977 and Koole, 1979). Ullidtz (1982) concludes that the FWD simulated the influence of a heavy fast-moving wheel load on the maximum values of the deflections, stresses and strains in the pavement structure.

In the study by the University of Dundee (1980) it is shown that when equipment measuring deflection with dual wheel loads is used, (for example the Benkelman beam), the maximum deflection is not located at the centroid of the loading area. This is illustrated by the results of a typical analysis in Figure 1.11. Anderson (1977) also recognizes the importance of this phenomenon and noted that it might lead to wrong conclusions, particularly for relatively weak (thin) pavements. He suggested that field performance should be calibrated with analysed pavements before being adopted in the design phase. The former study recommended the use of a single wheel device and proved that deflections measured at the extremes of the loaded area did not significantly vary from deflections measured inside the loaded area. Dehlen (1962b) also recognized this phenomenon of  $\delta_0$  (maximum) and R minimum being situated under the loaded area. The transverse position also lead to the more severe curvature parameters measured of the deflection basin. This is illustrated in Figure 1.12. Dehlen (1962b) states; "The longitudinal elongation observed in many chicken net crack patterns is, as has been pointed out by others, another indication that the factors giving rise to cracking are most severe in the transverse direction."

The Technical Committee Report of the XVII World Road Congress (Permanent International Association of Road Congresses, 1983) states that interest in developing analytical design methods is linked more to stationary test techniques than to the rolling wheel techniques. The light vibrators are obviously ideal for standard field work as Tables 1.3, 1.4 and 1.5 indicate. In spite of the advantages of using the FWD mentioned earlier, Molenaar and Koole (1982) comment that, according to conclusions of a study group of the Dutch Study Centre for Road Construction, the

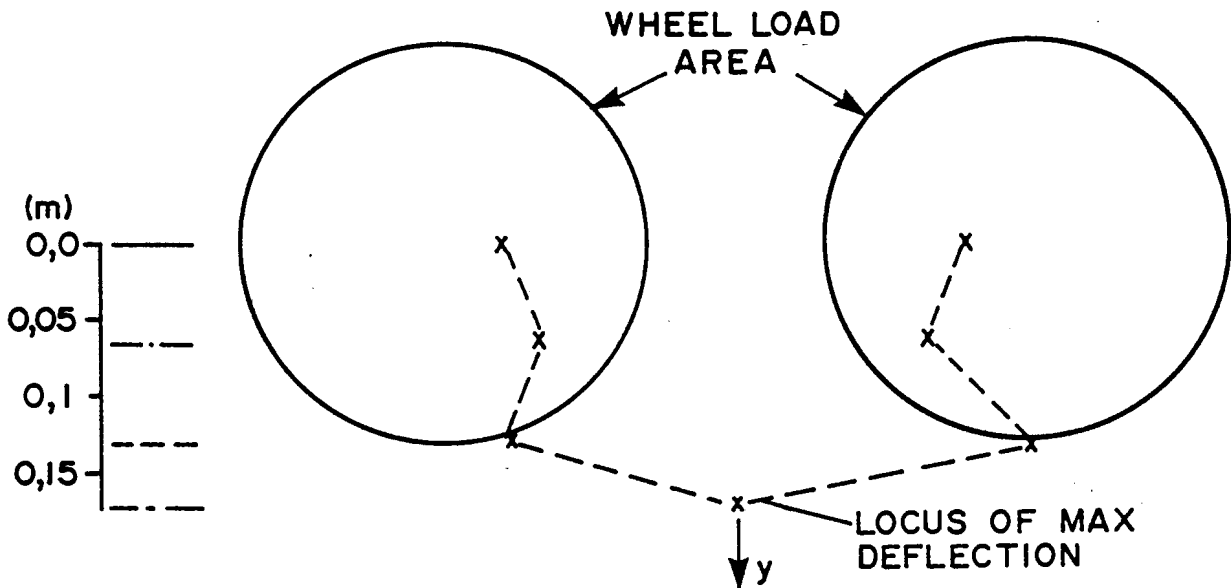
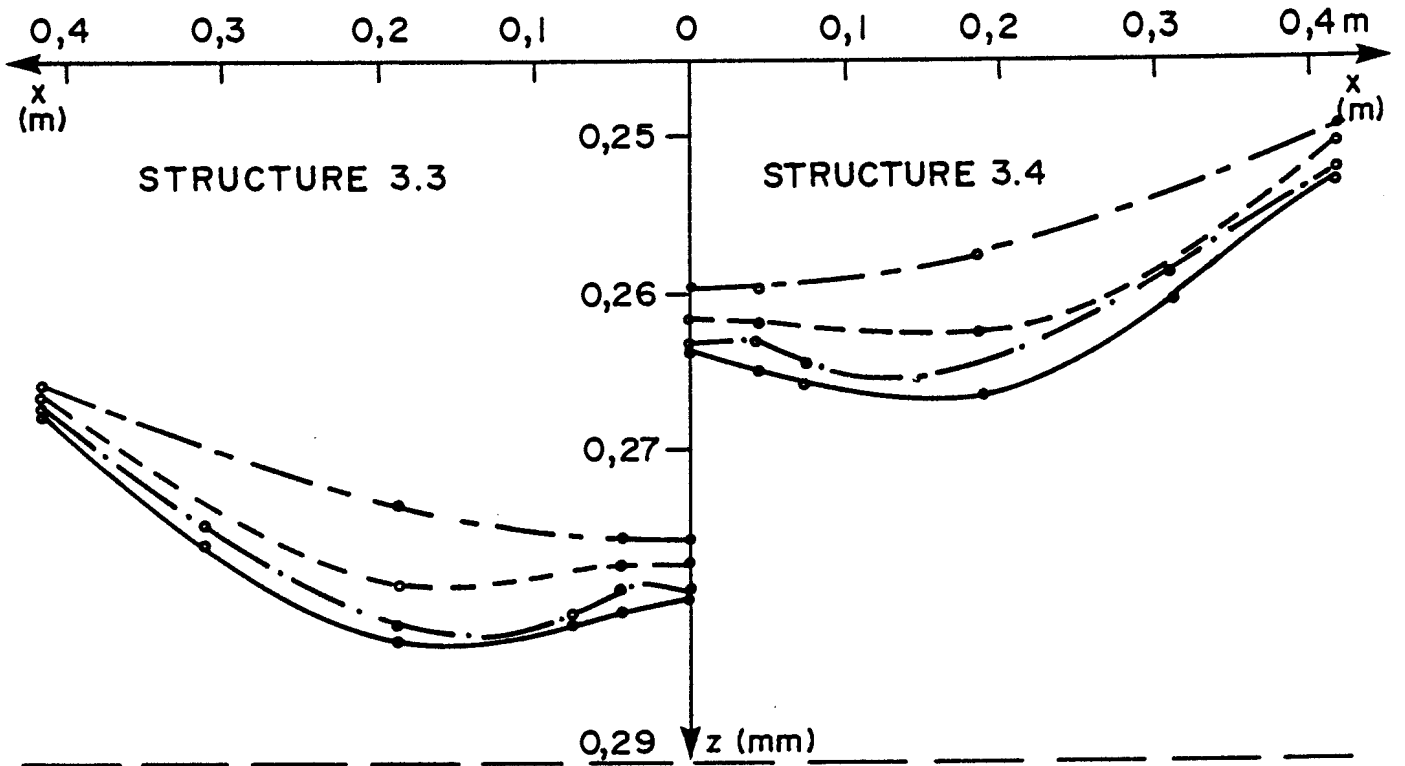
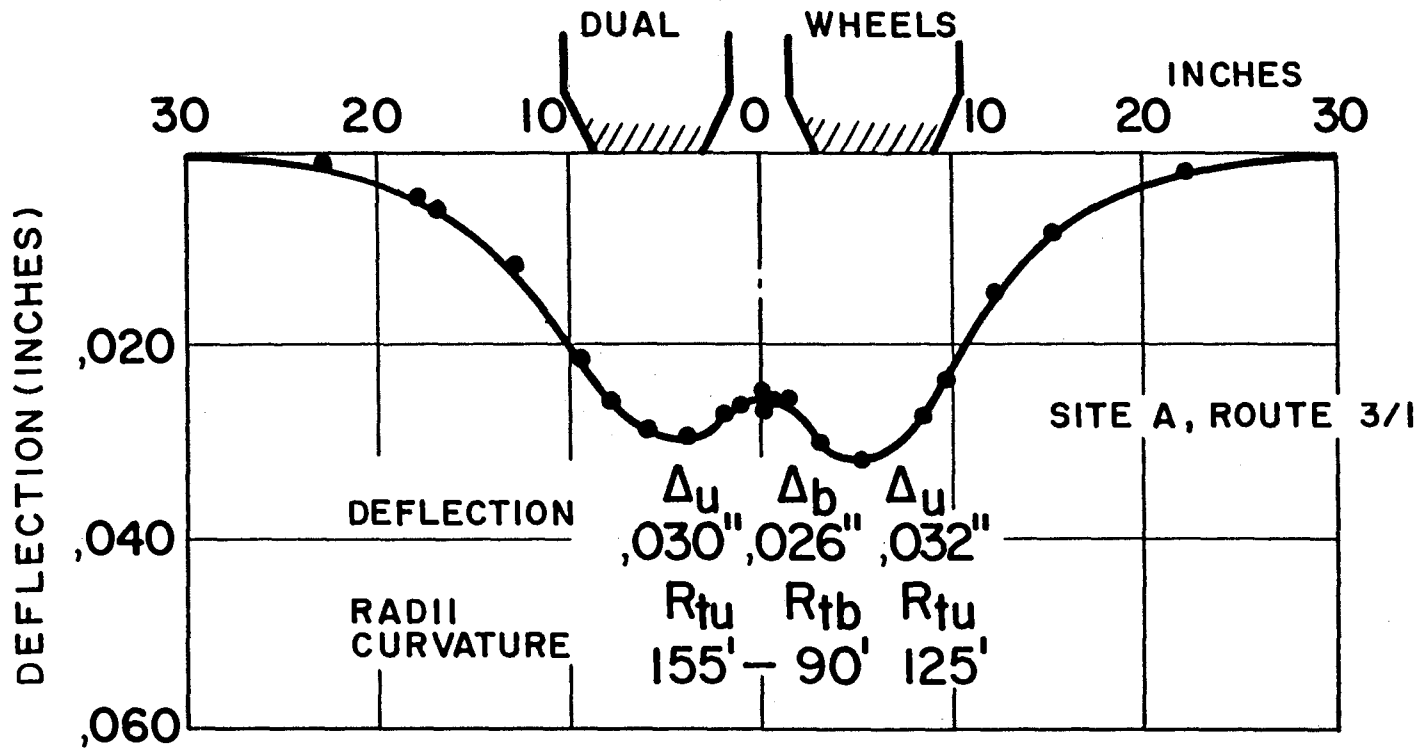


FIGURE I.II  
TRANSVERSE DEFLECTION PROFILES  
(University of Dundee, 1980)

40-4-4919/3 JT



1.30

FIGURE 1.12  
TYPICAL EXAMPLE OF TRANSVERSE DEFLECTION  
PATTERN BENEATH DUAL WHEELS (Dehlen, 1962 b)

Lacroix deflectograph is more suitable for routine evaluations than the FWD. The RSD developed in South Africa overcomes the normal problems experienced with a standard Benkelman beam concerning poor sampling frequency and testing in adverse weather conditions. Owing to the limited length of any such beam device the problem of the beam supports being inside the deflection basin will not be eliminated completely. This is particularly true of stiffer pavements where the deflection basin is broad. The Technical Committee Report on flexible Roads of the XVII World Road Congress (Permanent International Association of Road Congresses, 1983) also concludes that; "Precision of measurement can be difficult when testing stiff pavements containing cemented layers and cracking in those layers can reduce the significance of measurements of the deflected shape."

### 3.3 Correlations between Devices

There are numerous references in the literature to the correlation of deflections obtained with the different devices. Generally the newer generation measuring devices are correlated with the older generation devices like the Benkelman beam. Whitcomb (1982) records relationships between the Road rater, Dynaflect and Benkelman beam or travelling deflectometer. Hoyinck, et al. (1982) even correlate Lacroix deflectograph and Benkelman beam deflections measured with different techniques.

The reason for the correlations is that one type of deflection measurement may be translated into another, so that empirical or established interpretation graphs can be used without the measurement having to be repeated in the prescribed manner. In addition to the reason noted above, Whitcomb (1982) notes that the newer generation vibrating measuring devices offer significant advantages of ease and speed of operation over the Benkelman beam and California deflectometer.

Moore et al. (1978) make the following statement on the quality of such correlations: "All of the steady state dynamic deflection devices can be expected to correlate reasonably well with

static deflection measurements. Many evaluation procedures employ these dynamic deflection devices for estimating the anticipated useful life (or load-carrying capacity) of pavements based upon correlation of the measurements with static deflection measurements".

It is obvious though, from the discussion on deflection parameters (see 1.3.2) that the correlation of a single deflection point, like a Benkelman beam deflection, with a highly complicated deflection basin description will not necessarily be a good one. For this reason Whitcomb (1982) cautions about the use of applying published correlations without some knowledge of the degree to which the two variables have been correlated. It is more desirable to avoid the need to make the correlations at all.

The following is quoted from the FHWA study (1984): On the correlations between NDT deflection devices "In general, a different correlation should be developed for each major pavement type and for different pavement thicknesses within particular types of pavement because the correlation is not unique, ....". Regarding the interchangeability of data the following is also quoted: "The source, testing procedure and equipment configuration used in developing the data must be fully understood before data collected by another agency can be used."

#### 4 CONCLUSIONS AND RECOMMENDATIONS

Ideally deflection basin measuring equipment should:

- (a) realistically simulate moving traffic loads in terms of magnitude of load, shape and equivalent time of loading
- (b) accurately measure the whole deflection basin with high levels of reproducibility
- (c) be simple to operate, so that it is possible to use it with competence in the field; but it should also be applicable to research



- (d) be capable of attaining high levels of productivity, which must reduce the cost of testing.

Considering these prerequisites, it seems that the FWD is the most appropriate of the devices discussed. As far as cost and ease of operation in particular are concerned, the vibratory devices such as Dynaflect and Road Raters are also considered appropriate. The main advantage of these newer generation deflection measuring devices lies in the fact that they normally measure at least four points on the deflection basin. The modified RSD or Benkelman beam and a modernized Lacroix deflectograph are able to monitor the deflection basin at frequent intervals in spite of there being only one measuring point. The Lacroix deflectograph is used by the road authorities in South Africa on a network basis with a proven level of efficiency. A vast amount of information is available on various pavement structures from HVS testing and on full structural lives measured with the RSD and MDD on the same location. The information gained from these devices may be used to determine suitable deflection basin parameters accurately or to perform realistic correlation studies between these parameters. It is possible to use deflection basin measurements obtained from a modernized Lacroix deflectograph for more detailed analysis. To date only the maximum deflection ( $\delta_0$ ) has been used to distinguish between various uniform sections of road statistically. By the use of deflection basin parameters related to specific pavement structure type and state a higher level of engineering interpretation and effective service can be provided for the purpose of pavement management, rehabilitation and overlay design. It is suggested though, that tests be done with the FWD and vibratory deflection basin measuring devices in South Africa in view of their advantages mentioned above. These devices will have to be correlated with the above-mentioned data bank on deflection measurements from HVS sites in order to ensure uniform standards of deflection interpretation.

The parameters of the deflection basin must -

- (a) represent the full characteristics of the whole deflection basin (not only maximum deflection ( $\delta_0$ ), but rather a combi-

nation of parameters like SCI and BCI covering the whole deflection basin);

(b) be simple to calculate and interpret, and

(c) be able to relate to the structural characteristics of the full depth of pavement structures.

From the survey it is obvious that in the past at least two deflection points on the deflection basin are normally needed in an analytical procedure. One such point is the point of maximum deflection ( $\delta_0$ ). The other point should preferably be varied in distance relative to the centroid of the loaded area ( $\delta_r$ ) in accordance with prescribed requirements. Examples of such parameters are Q and ST, which still require other points measured on the deflection basin in order to select a value of  $\delta_r$ . Another alternative is to use fixed values of radius for deflection points, for example  $\delta_0$ ,  $\delta_{305}$ ,  $\delta_{610}$ , etc. It is suggested that the parameters that use these deflection values, for example SCI, ST, BDI, BCI, etc., be investigated in view of the guidelines described above and the equipment available in South Africa. A further suggestion, which will be discussed in more detail in a later section, is that these selected parameters be related to the pavement structure classification used in TRH4 (NITRR, 1985a) and to pavement performance models. A parameter like SCI will then be determined differently for a granular base than, for example, from for a cemented base pavement, reflecting its different deflection basin characteristics and structural performance.



## **CHAPTER 2**

### **MEASUREMENT AND DATA PROSESSING OF DEFLECTION BASINS IN SOUTH AFRICA**

## CHAPTER 2: CONTENTS

	PAGE
1. INTRODUCTION	2.2
2. THE MEASURING EQUIPMENT AND PROCEDURE	2.2
2.1 Measuring equipment	2.2
2.2 The procedure	2.3
2.2.1 Site selection and preparation	2.3
2.2.2 Measuring procedure	2.6
3. EXISTING PROCEDURES TO EVALUATE DEFLECTION MEASUREMENTS	2.9
3.1 Pre-automation data evaluation (Rebound procedure)	2.9
3.2 Automated data evaluation (WASHO procedure)	2.14
4. THE NEED FOR CURVE FITTING PROCEDURES	2.17
5. PROPOSED DEFLECTION BASIN MEASURING EVALUATION PROCEDURE	2.19
5.1 Data manipulation and preparation	2.19
5.2 Higher level deflection basin data manipulation	2.20
6. CONCLUSIONS AND RECOMMENDATIONS	2.25

## 1. INTRODUCTION

In South Africa the use of the full deflection basin was generally neglected in the analysis of deflection basin parameters. In the past the analyses were mostly concentrated on the small area of the deflection basin in the vicinity of maximum deflection. In the program of accelerated testing with the Heavy Vehicle Simulator (HVS) fleet in South Africa, the whole deflection basin is measured on the surface and in depth of the pavements. The same limitation of data analysis was concentrated on the small area of the deflection basin near the vicinity of the maximum deflection for these depth deflection basins measured. In this chapter a brief description is given of how the surface deflection basin is measured in South Africa by means of the automated Benkelman beam or also called the road surface deflectometer (RSD). The procedure and equipment to measure the deflection basin at various levels in the depth of a pavement by means of a multi-depth deflectometer (MDD) are also briefly discussed.

The present data analysis procedure is discussed. Based on this and a discussion of the whole deflection basin and related parameters, the author suggests changes to this data analysis procedure. Specific reference is made of the need for a better description of the full deflection basin. Curve fitting models are discussed briefly and recommendations are made for practical use with the road surface deflectometer (RSD) and the deflectograph..

## 2. THE MEASURING EQUIPMENT AND PROCEDURE

### 2.1 Measuring Equipment

HVS testing is done by repeated application of a chosen wheel load to the road structure. Several sophisticated instruments are used

to monitor the response of the road. In the field, a micro-processor system is used to record the measured data on a magnetic disc. The data on the magnetic disc is then transported to the central laboratory in Pretoria for processing by the main computers (Freeme, et al., 1981). During an HVS test the measurements of the surface deflection and curvature of the pavement with an automated Benkelman Beam, also called the Road Surface Deflectometer (RSD) (Basson, 1985), are collected as data. Elastic deflection and permanent deformation measurements are taken at different depths within the pavement using the multi-depth deflectometer (MDD). (Basson, et al. 1980.)

The MDD is a device that can simultaneously measure the vertical deflections and permanent deformations of up to six points on a vertical line in any pavement. The methods of site preparation and illustration of the MDD is shown in Figure 2.1. The RSD is an electronically instrumented deflection beam which can measure dynamic resilient deformations to an accuracy of  $\pm 0,01$  mm. (Shackel, 1980.) This modified Benkelman Beam (the RSD) and the use of the RSD and MDD plus other related instruments are illustrated in Figure 2.2. The modules of the MDD and the measuring point of the RSD make use of a linear variable differential transformer (LVDT) to measure pavement deflections. This discussion serves only as a brief description of the equipment used to measure deflections in depth and on the surface of a pavement structure being tested with the HVS.

## 2.2 The procedure

### 2.2.1 Site selection and preparation.

A typical HVS test section is selected after a deflectograph survey of the road length was done. Uniform sections of the road are then identified which differ significantly statistically. A decision is made whether to select a section that represents for example the 85th percentile, 15th percentile or average of the road in terms of the deflectograph survey. A detail survey of each meter of normally a 100 meter section is

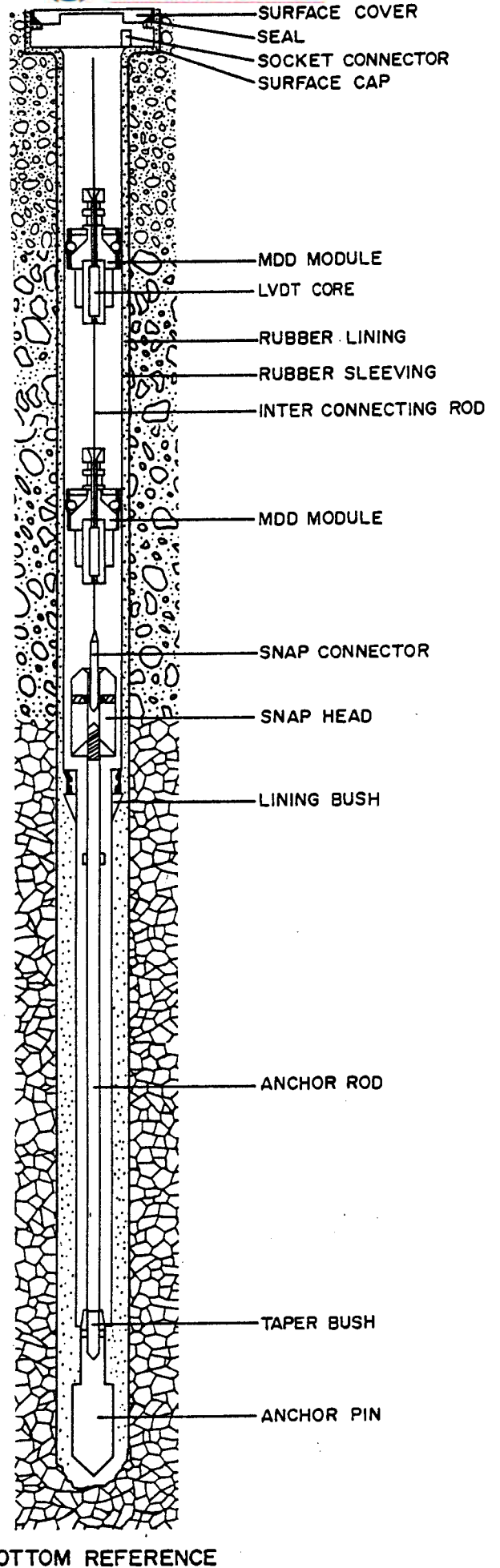
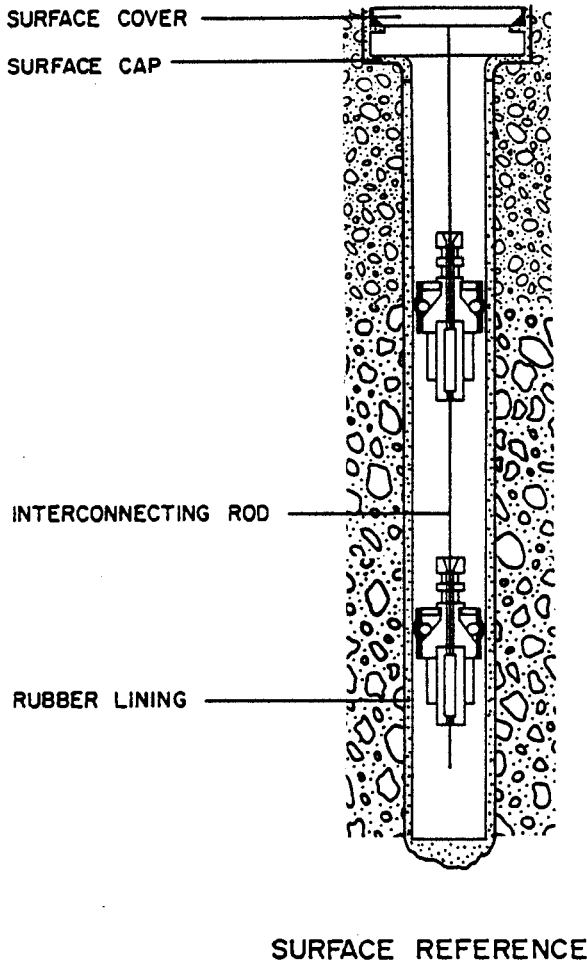


FIGURE 2.1  
METHODS OF SITE  
PREPARATION OF THE  
MULTI-DEPTH-DEFLECTOMETER

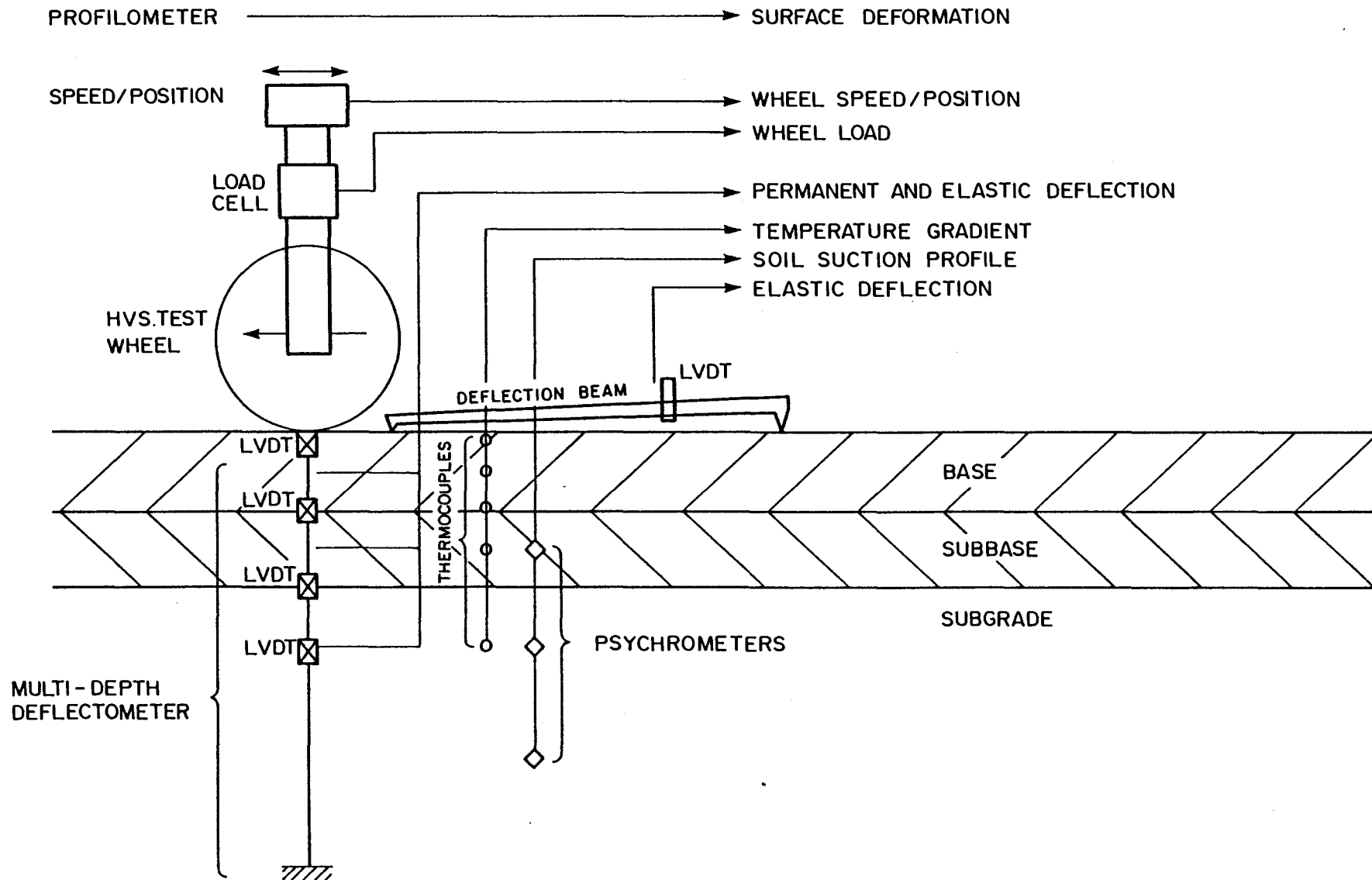


FIGURE 2.2  
THE HVS SECTION INSTRUMENTATION



then carried out with the standard Benkelman Beam. Based on these results a 8 meter section of road is selected which is uniform in terms of its maximum deflection measurements.

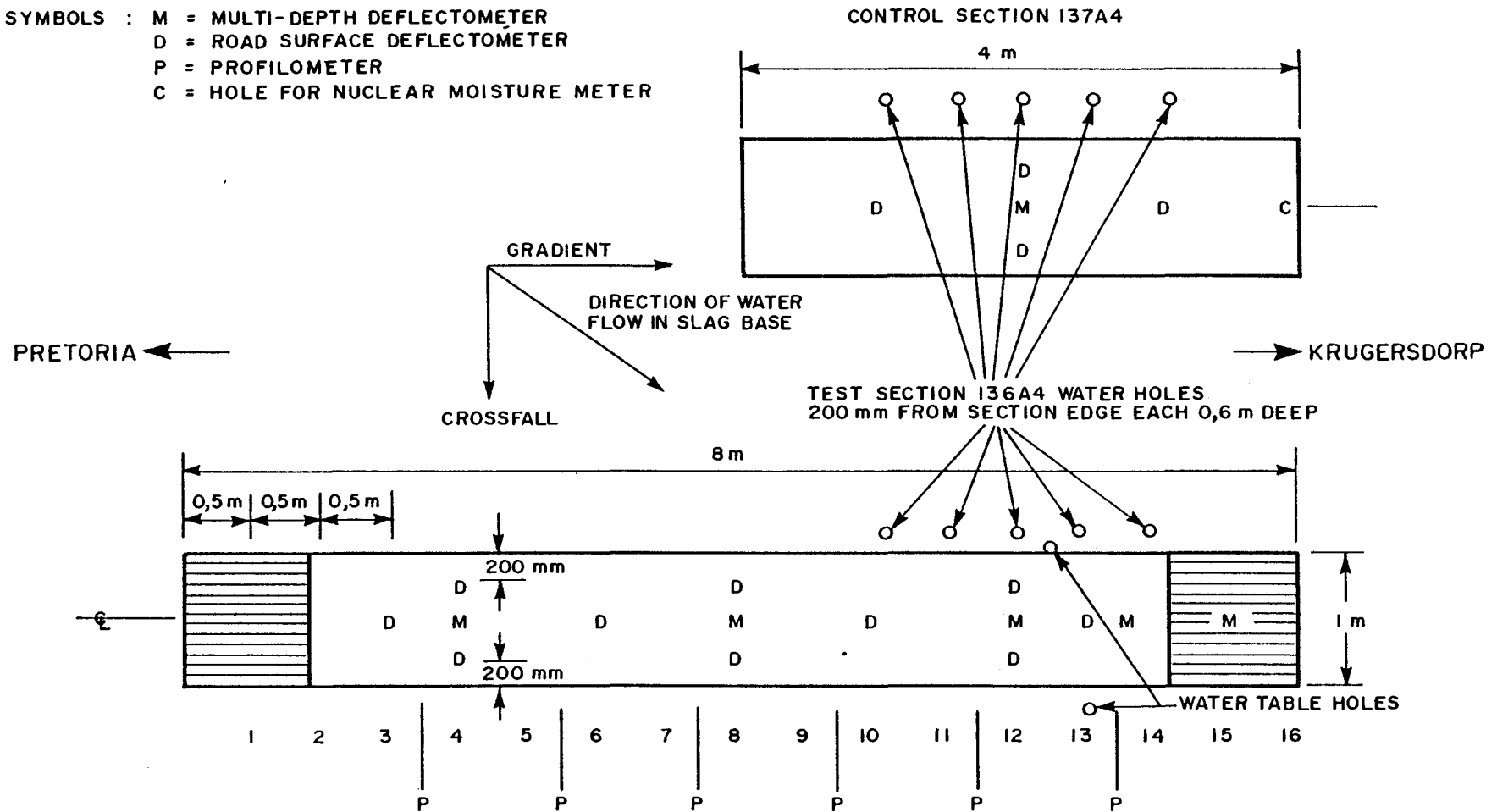
Other factors such as road safety, gradient etc. are also considered in the selection of such an HVS test section. (Shackel, 1980.) In some cases, particularly short experimental sections, the selection of a site may follow a different procedure, but the aim is normally to have at least an HVS test section that is uniform over its 8 meter length in terms of Benkelman Beam deflections.

The instrumentation and marking of such a selected test section is as shown in Figure 2.3. As can be seen, normally at least two MDD holes are installed while the RSD measuring points are marked on the surface in order to represent the whole section and enhance repeatability.

#### 2.2.2 Measuring procedure

The dual wheel with the specified tyre pressure and load is moved  $\pm 3$  meters away from the measuring point. The deflection produced by the load approaching the measuring point of either the RSD or MDD is recorded on a chart as a continuous trace, while switches, at measured distances along the road, record the passage of the load passing them. A typical trace is shown in Figure 2.4. The square waves of the switches reflect the variance in speed at which the wheel load approaches the measuring point in order to facilitate the correction to relate distance to deflection accurately. The loaded wheel moves past the measuring point for a distance of about 1,2 meter whereafter pulses simulating measurements are generated automatically to complete the standard set of 256 measurements of a deflection basin. Each measured point on this set is a standard distance apart, usually 22,07 mm, depending on the switch characteristics. Usually measurement sets with the MDD are taken only on the centre line and with the RSD in line with the measurement point. Off-centre measurements can be taken with the MDD. At

SYMBOLS : M = MULTI-DEPTH DEFLECTOMETER  
D = ROAD SURFACE DEFLECTOMETER  
P = PROFILOMETER  
C = HOLE FOR NUCLEAR MOISTURE METER



2.7

FIGURE 2.3  
TYPICAL LAYOUT OF TEST AND CONTROL SECTION

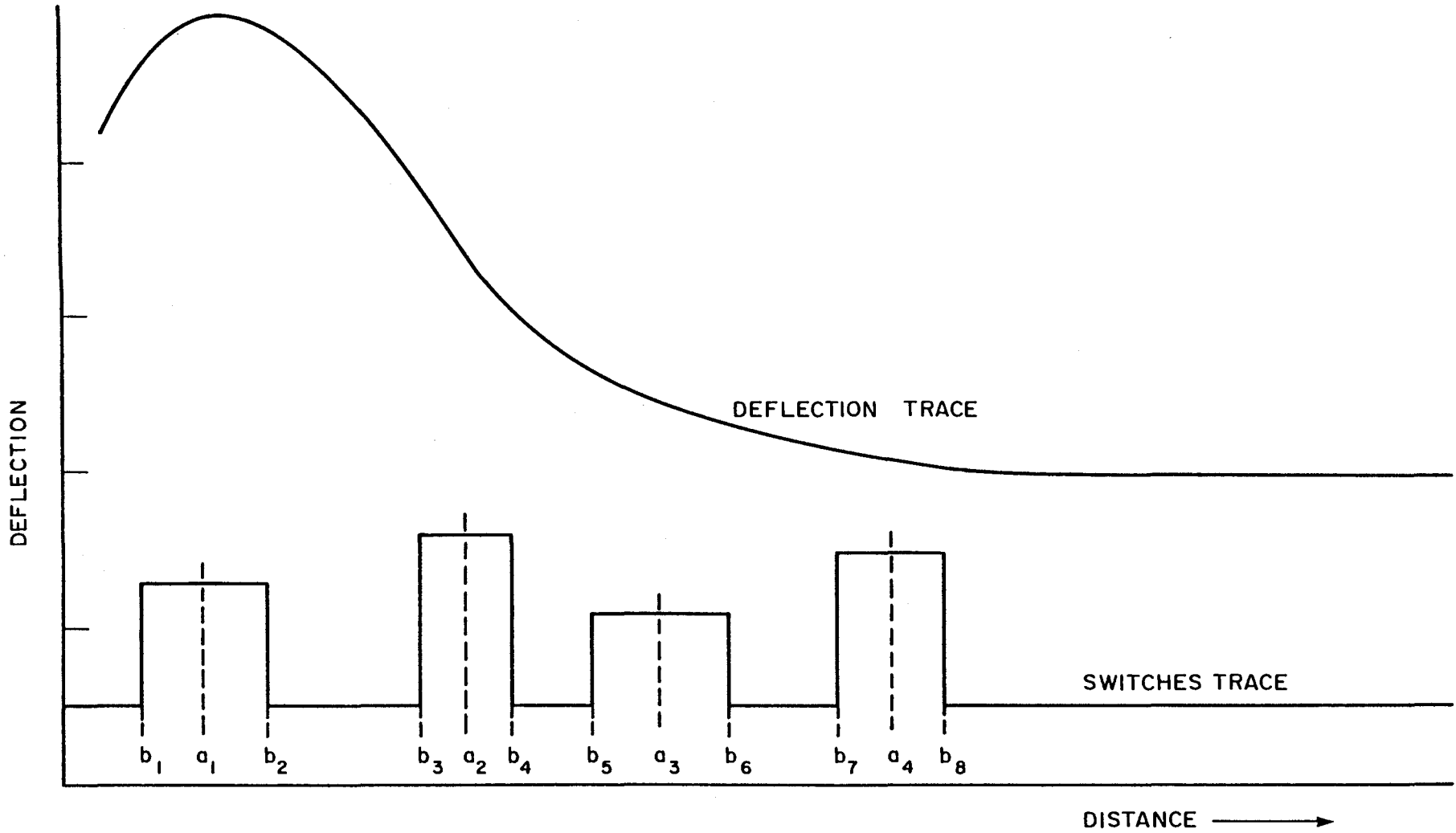


FIGURE 2.4  
TYPICAL RECORDED CHART FROM RSD MEASUREMENT SHOWING DEFLECTION AND SQUARE WAVE PRODUCED

least 2 measurement sets are taken as control at each measuring point of the RSD and MDD at a specific time during the testing. Various wheel load and tyre pressure combinations are used during measurements.

It is important to note that the method of measurement of the standard Benkelman Beam and that of the RSD and MDD under HVS conditions differ. The RSD and MDD measurements use the WASHO procedure (Monismith, 1979) while with the standard Benkelman Beam the rebound procedure is used. In the WASHO procedure the load approaches the end of the probe or measuring point and the deflection is observed. In the rebound procedure the wheel moves away from the measuring point and rebound of the pavement is measured. Rebound deflection is about two times the deflection measured with the WASHO procedure. This may vary with the type of pavement measured. This is probably due to plastic deformation.

### 3. **EXISTING PROCEDURES TO EVALUATE DEFLECTION MEASUREMENTS**

#### 3.1 Pre-automation data evaluation (rebound procedure)

The Benkelman Beam was used very effectively by Dehlen (1961) to measure deflection-distance curves manually. This was done by measuring the deflection basin manually at 3 inch (75 mm) intervals as the wheel load approached the measuring point. Smooth curves were drawn through the plotted points. Particular care was taken over the central 2 feet (610 mm), and any irregular curve rejected. This is illustrated in Figure 2.5. The maximum deflection was obtained directly from the observations. The radius of curvature at the point of maximum deflection was obtained by determining the circle which is the best fit to the curve over the central 6 or 9 inches (150 to 225 mm). The radius of curvature of the road surface was then computed from the radius of the circle of best fit from the formula;

$$R = r \cdot \frac{v}{h^2}$$

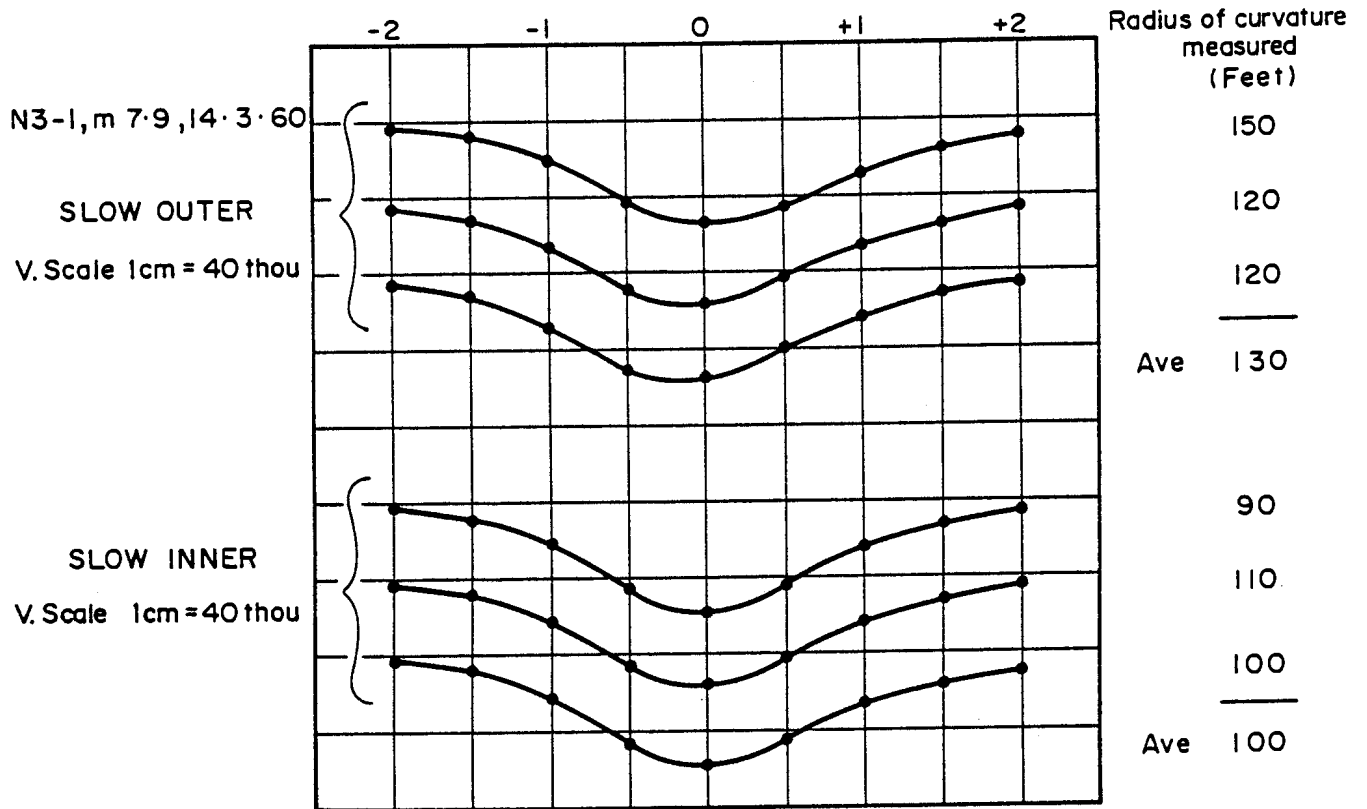


FIGURE 2.5

EXAMPLE OF THE PLOTTING OF DEFLECTION OBSERVATIONS AND MEASUREMENT OF RADIUS OF CURVATURE

where  $R$  = radius of curvature of road surface,  
 $r$  = radius of plotted circle, in the same units as  $R$ ,  
 $v$  = vertical scale of plot expressed as a dimensionless ratio,  
 $h$  = horizontal scale of plot expressed as a dimensionless ratio

Dehlen (1961) noted that a circle fitting the deflected surface in the field became an ellipse when plotted to different horizontal and vertical scales. Thus ideally, determination of radius of curvature from the deflection plot should be made by fitting ellipses. Dehlen (1961) estimated that the error introduced by fitting circles however, was not likely to exceed 5 per cent. It is also observed by Dehlen (1961) that care and experience is necessary for the accurate determination of the radius of curvature from the observations.

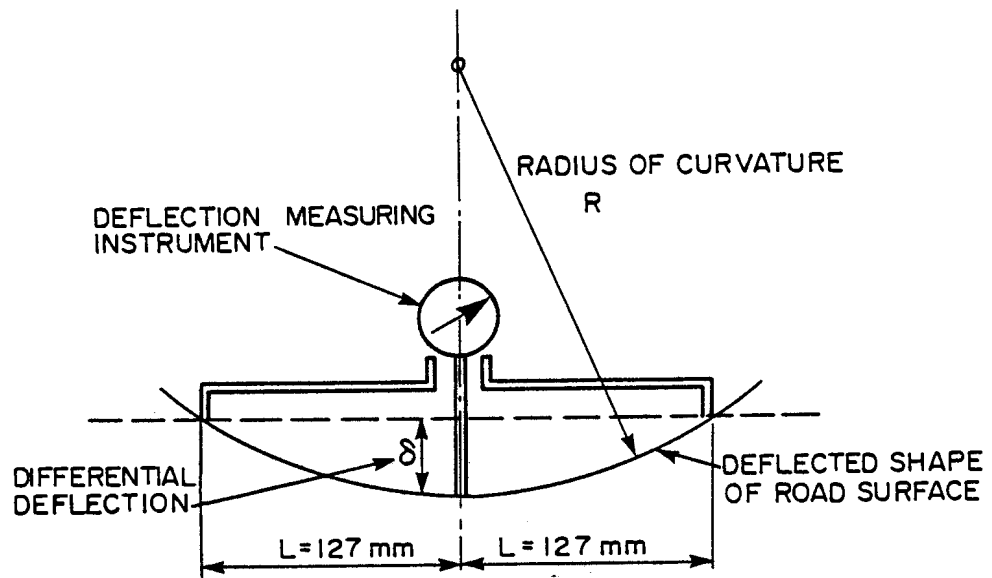
The Dehlen curvature meter developed by Dehlen (1962a), enabled measurement of the curvature directly, as illustrated in Figure 2.6. The relation between curvature and differential deflection may be deduced by simple geometry by fitting an appropriate curve to the three points on the road surface defined by the instrument. Dehlen (1962a) indicated that using a parabola, the radius of curvature is given by

$$R = \frac{L^2}{2\delta}$$

where  $\delta$  is the differential deflection

$L$  is the distance between the deflection gauge and each support

Dehlen (1962b) observed that a study of numerous deflection patterns obtained over a period of time indicated that in the vicinity of the points of maximum deflection the curves are typically of a sine form. It has also been noted that points of inflection (points  $P$  in Figure 2.7, where the curve changes from concave to convex) occur fairly consistently at distances ( $S$ ) of 6 inches (150 mm) on either side of the point of maximum deflection. The



NOT TO SCALE

FIGURE 2.6  
DIAGRAMMATIC SKETCH SHOWING THE PRINCIPLE OF  
THE CURVATURE METER

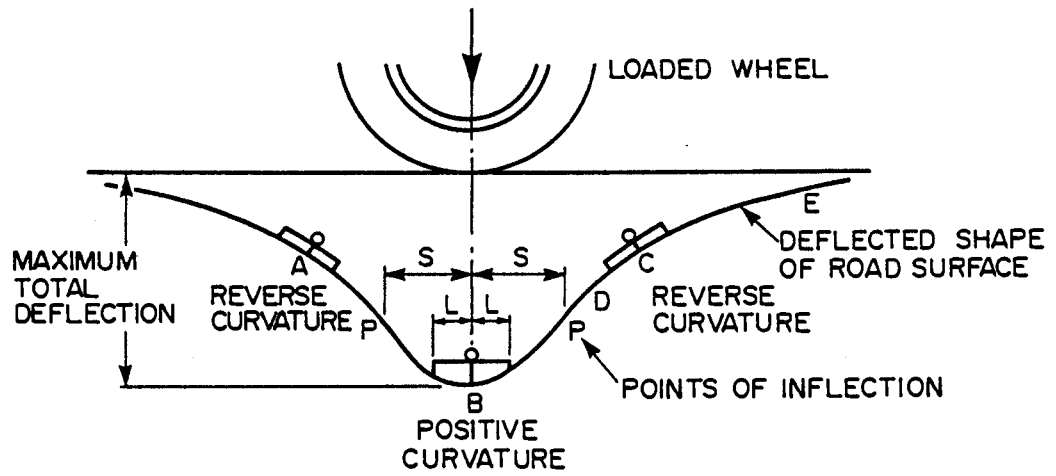


FIGURE 2.7  
 TYPICAL PATTERN OF DEFLECTION OF A ROAD SURFACE  
 BENEATH A LOADED WHEEL



relation between radius of curvature (R) and differential deflection ( $\delta$ ) in the case of a sine curve is

$$R = \frac{L^2}{F\delta} \quad \text{where } F \text{ is a factor which varies between 2 and 2,47.}$$

With  $F = 2,3$  and  $L = 5$  inches (127 mm) the formula is reduced to:

$$R = \frac{7}{\delta}$$

$\delta$  is measured in mm; R in meter.

### 3.2 Automated data evaluation (WASHO procedure)

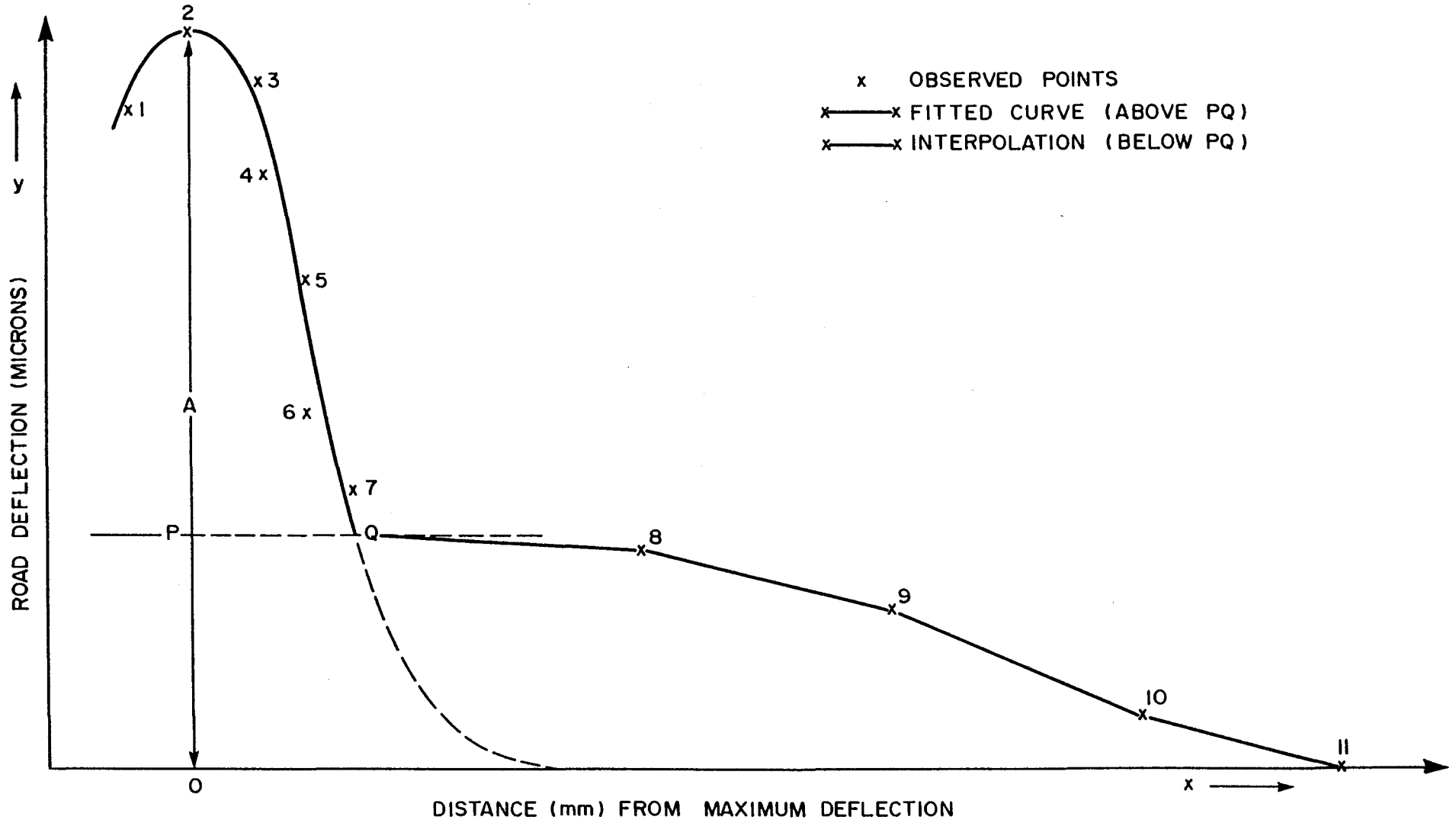
A program BENKI was written by Szendrei (1974) and later updated as BENK5 (Szendrei, 1975(a)) to evaluate the automated Benkelman Beam (RSD) field data on computer. These programs were later updated again by (Szendrei, 1975(b)) to accommodate the processing of the MDD deflection data too.

In these programmes the deflection tracer, as supplied from the field measurements, is defined by 11 points of the original 256 points measured, along the length of the trace. The points on the chart are converted to true road distances and road deflections. The result of these operations is to produce 11 points on a plot of road deflections versus road distances. The 11 points lie on a plot as shown in Figure 2.8 which still follow the basic shape, although somewhat distorted.

Szendrei (1975(a)) noted that the top part of the curve down to some level PQ (Figure 2.8), which is about 30 per cent of the maximum, approaches a probability curve closely. This is represented by the equation;

$y = A \exp(-kx^2)$  in which A is the maximum amplitude occurring at  $x = 0$  and k is an attenuation constant which determines the width of the curve. Below PQ, (see Figure 2.8) a linear interpolation method was followed. The values of k and A are determined by

940- 4- 4 966/6 BS



2.15

FIGURE 2.8  
 FITTING OF EXPONENTIAL CURVE TO MEASURED POINTS OF THE POSITIVE

using the y co-ordinates of the measuring points from point 2 down to level PQ.

The standard error  $e$  of the fitted curve can then be estimated from;

$$e = \sqrt{\frac{\sum d_i^2}{n}}$$

in which  $d_i$  = deviation of observed point from value calculated from the fitted curve ( $y_i - A \exp(-kx_i^2)$ ) and  $\Sigma$  indicates the summation for all  $n$  points observed above level PQ.

The main aim of these programs are to determine the radius of curvature at the point of maximum deflection. By using the general formula of radius of curvature (Szendrei, 1975(a)) at any point along a curve defined by  $y = f(x)$ , radius of curvature is given by;

$$R = \frac{\left| 1 + \left(\frac{dy}{dx}\right)^2 \right|^{3/2}}{\frac{d^2y}{dx^2}}$$

For the curve fitted, Szendrei (1975(a)) derives a radius of curvature at any point along the curve:

$$R = \frac{(1 + 4k^2x^2y^2)^{3/2}}{2ky(2kx^2 - 1)}$$

The minimum radius of curvature, occurs at the point of maximum deflection of the curve. Substituting the values of  $y = A$  and  $x = 0$  into this derived equation, Szendrei (1975(a)) derives;

$$R = \frac{0,5}{kA}$$

Using Dehlen's radius of curvature formula,  $R = \frac{7}{\delta}$  when  $\delta$  is measured in mm and  $L = 127$  mm, Szendrei (1975(a)) made a more direct comparison with the Dehlen radius of curvature. This is done by calculating deflection  $\delta_{127}$  at 127 mm from the deflection basin. Assuming that the curve is symmetrical about the vertical and passing through the maximum, the values of  $\delta_{127}$  will

be the same on both sides. Differential deflection  $\delta$ , as described by Dehlen and corresponding to the measurement of the Dehlen curvature meter instrument is then expressed as follows:

$$\delta = A \left| 1 - \exp(-(127)^2 k) \right|$$

To find the mean radius of curvature between  $x = 127$  mm and  $x = -127$  mm, where  $x = 0$  at the maximum of the curve, a solution for the circle with origin at  $(0, y_0)$  and intersecting the exponential curve (Zendrei, 1975(a) at  $x = \pm 127$  mm is closely approximated by;

$$R = \frac{8,065}{\delta} \quad \text{where } \delta \text{ is in mm and } R \text{ in meter.}$$

Szendrei (1975(a)) noted that this formula gave a discrepancy of 14 per cent if compared to the Dehlen radius of curvature. This does not necessarily reflect the difference in the model used to fit this part of the deflection basin. It must be remembered that the difference in measuring procedure (WASHO versus rebound), for the particular pavement type compared, will also contribute to this difference.

#### 4. THE NEED FOR CURVE FITTING PROCEDURES

In the preceding sections it was illustrated that even with the automated Benkelman Beam or RSD, the emphasis was to measure mainly two deflection basin parameters, namely: maximum deflection ( $\delta_0$ ) and radius of curvature (R). Both these parameters are measured in the area of positive curvature of the deflection basin (see Figure 2.7). This is only a very small part of the whole deflection basin. The fact that these two parameters alone are reflecting only limited information available from any possible deflection basin of any particular pavement is described in full elsewhere. (Horak, 1984.)

In the development of fundamental methods of pavement evaluation by means of deflection basin measurements it is imperative that an

accurate description of the deflection basin is obtained. In Table 1.1 a summary of deflection basin parameters and their respective formula are given (Horak, 1984). The level of description of the deflection basin varies from a singular point to a highly sophisticated polynomial function. It is clear though that there is a move towards incorporating parameters of the deflection basin that attempt to describe the reverse curvature (see Figure 2.7) of the deflection basin too. Horak (1984) clearly indicates that there is reason to believe that deflections measured (and their related parameters) on the outer edges of the reverse curvature of the deflection basin give a clearer indication of the structural value of the subgrade. Deflections measured nearer to the point of maximum deflection (on the positive curvature, Figure 2.7) give a better indication of the structural value of the upper layers. The structural effect of the lower layers are also reflected by these parameters and the need arises therefore to separate these effects by giving more attention to the proper description and measurement of the reverse curvature of the deflection basin.

The preceding sections indicated that the standard procedure at any HVS test section is in fact to measure the whole deflection basin very accurately with the RSD on the pavement surface and the MDD in depth of the pavement. As stated earlier the data evaluation of these curves were traditionally only focused on the related parameters of the positive curvature part. In fact the model for curve fitting used, only attempts to describe the 30 per cent part of maximum deflection while the reverse curvature part is linearly interpolated. Only 7 selected points on the positive curvature are used to do curve fitting with (see Figure 2.8) in the Szendrei model (1975(a)). This can lead to a misrepresentation although a statistically acceptable fit is achieved.

There exists a discrepancy in the interpretation of or calculation of radius of curvature (R) if the Dehlen radius of curvature and the Szendrei radius of curvature is calculated. The Dehlen radius of curvature measurement uses, the rebound method while the Szendrei radius of curvature, from RSD data, is measured with the WASHO procedure. The maximum deflection differs by a factor of two when these two procedures are compared. It is obvious that the radii of curvature will also be influenced. While the circle being fit through points at  $\pm 127$  mm and maximum deflection (through  $\delta_0$ ) in the Dehlen procedure of radius of curvature calculation, the Szendrei procedure only require it to intersect at  $\pm 127$  mm on the deflection basin. Both radii of curvature further do not really comply to the strict definition of radius of curvature as two or three points are intersected. Curvature at a point is the rate at which the curve is turning away from the tangent line at that point and radius of curvature is the reciprocal of curvature. (Bedford et al., 1970) For such calculations, a proper definition of the curve is needed mathematically. Factors such as plastic deformation and reverse curves within the positive curvature centre (Horak, 1984) can remove radius of curvature calculations even further away from a soundly based scientific definition and interpretation.

The standard evaluation of maximum deflection and Dehlen radius of curvature of the RSD and MDD results lacks the freedom or ability to do more sophisticated analysis of the pavement structurally. The need arises therefore to relate deflection basin parameters of the whole deflection basin to specific structural layers or zones or behaviour states.

The vast amount of RSD and MDD measurements available from all the HVS tests and quality of measurements make it imperative that better use of the whole deflection basin measurements must be made. New models and procedures should be investigated to evaluate such deflection basin data.

## 5. PROPOSED DEFLECTION BASIN MEASURING EVALUATION PROCEDURE

### 5.1 Data manipulation and preparation

In Section 3.2 it was described how RSD and MDD deflection basin data are prepared. At the stage before the modelling of the positive curvature (see Figure 2.7) is done, the data is in a standard form where the 256 measurements of deflection are correlated correctly to horizontal distance. In Figure 2.9 a graphical illustration is given of such a typical set of measurements. As can be seen the deflection has, as measured, a negative sign and the origin is not at the point of maximum deflection ( $\delta_0$ ). The possibility of the reference points of the RSD being inside the deflection basin and leading to incorrect deflection measurements increase significantly as the loaded wheel passed the measuring point (point of maximum deflection). Additionally there exists the danger of plastic deformation at particularly higher wheel loads, interfering with the quality of deflection measurements, as the wheel passes the measuring point and slowing down to a halt. For that reason the author decided to work only with the first part of the curve up to the point of maximum deflection. In order to make calculations easier too, the negative sign of the deflection was reversed and the origin was chosen at the point of maximum deflection. The description of the programmes and procedures to do these manipulations on computer are given in detail by Horak and Otte (1985). In some cases "spikes" occur due to interferences like wind, touching wheels, etc., on the original data set (as in Figure 2.9). This is first smoothed out by a standard programme procedure (Horak and Otte, 1985). The final data set, as prepared, is then stored on computer in a format whereby the deflection and horizontal distances are correctly related. A graphical presentation of such a data set is as shown in Figure 2.10. Such a data set of a deflection basin measurement can now be defined as edited for further data manipulation. As will be seen in the next section such data manipulations can be done with various levels of sophistication.

## 5.2 Higher level deflection basin data manipulation.

The form in which a data set of a measured deflection basin is, as described in the preceding section, ideal to calculate all the

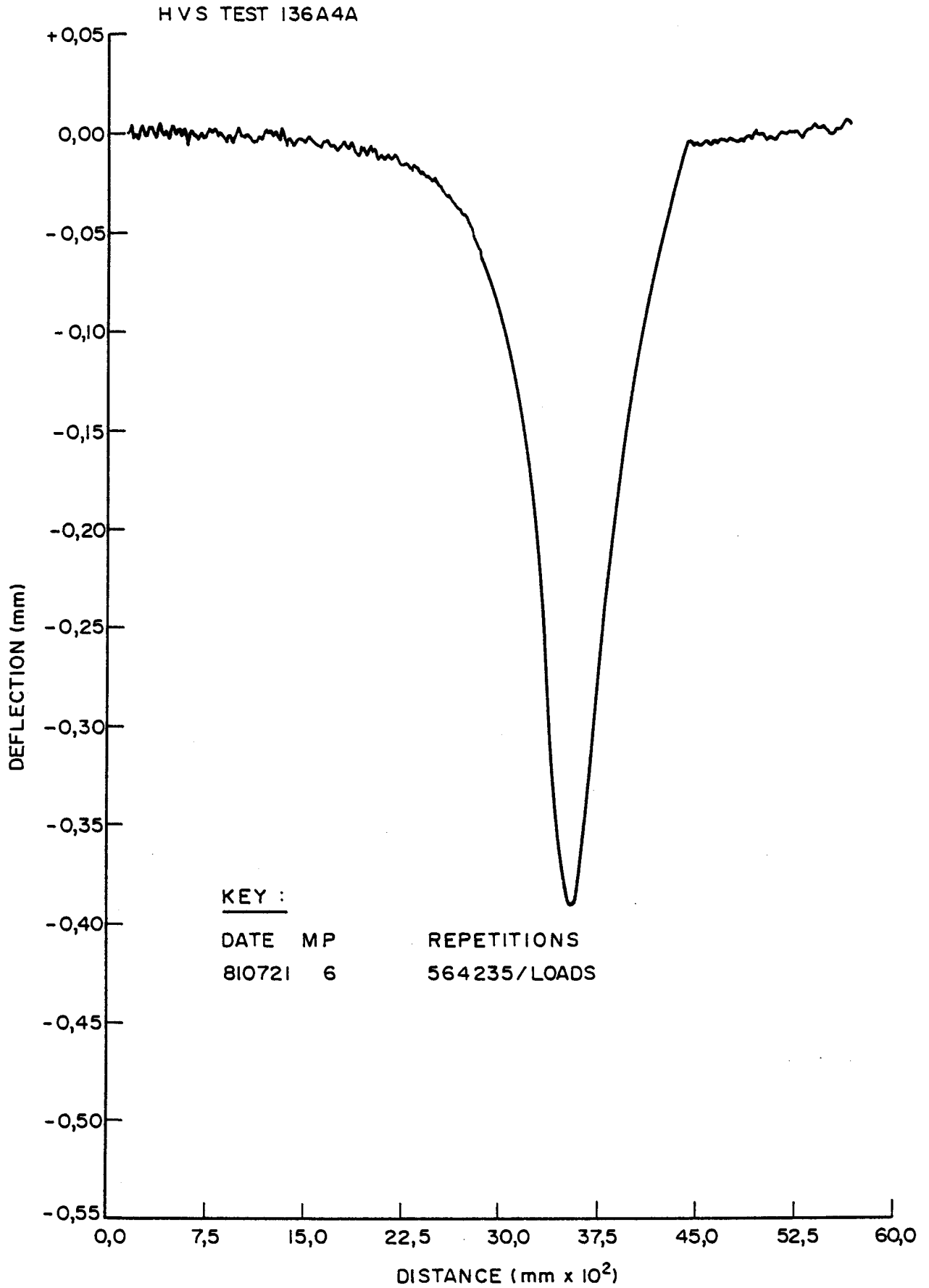


FIGURE 2.9  
TYPICAL RSD RESULTS OF  
DEFLECTION BASIN MEASUREMENTS



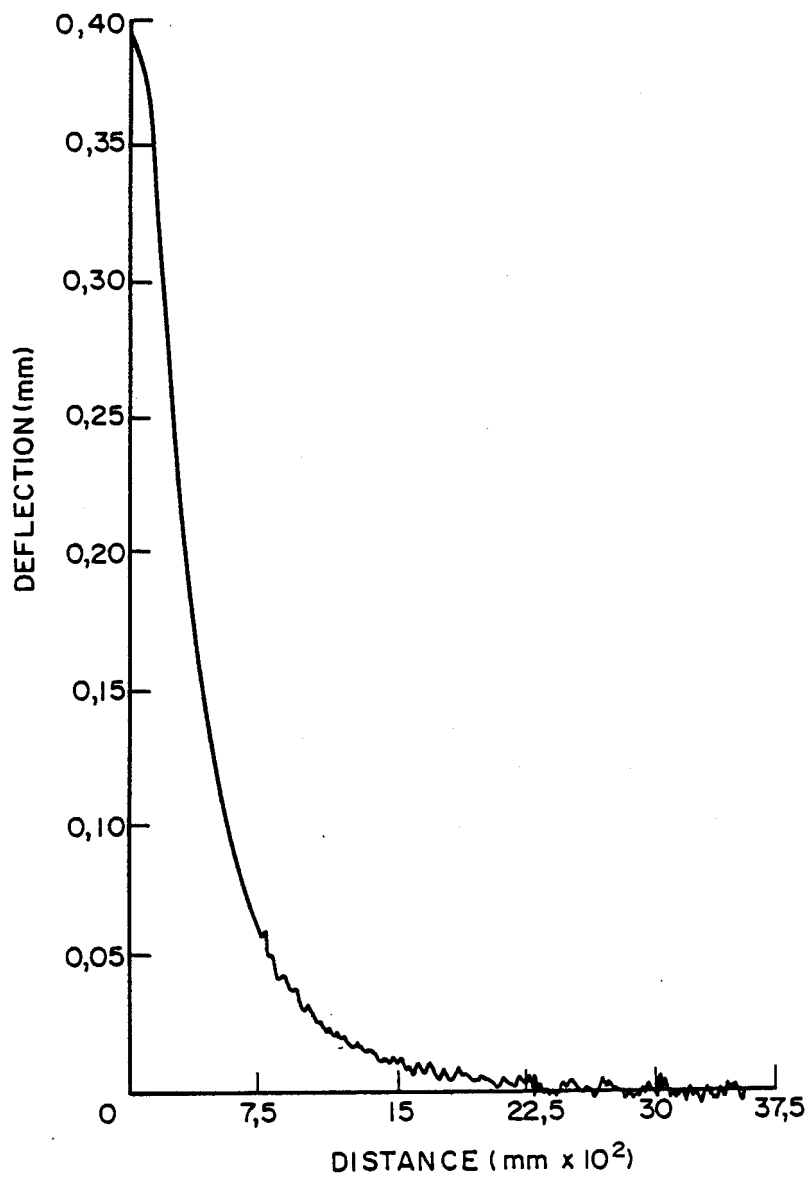


FIGURE 2.10  
TYPICAL MANIPULATED RSD DEFLECTION BASIN HALF  
OF DATA SET

deflection basin parameters as discussed in Chapter 1. The various deflection basin parameters and their respective formula as found in the literature survey are all shown in Table 1.1. In Table 2.1 the number of deflection basin parameters has been reduced to 11. All these deflection basin parameters listed here can be calculated by using deflection points at standard off-sets on a specific deflection basin data set. These deflection points are at the off-sets of 0, 127, 305, 610 and 915mm. These deflection points can easily be determined by a simple interpolation procedure ( Horak and Otte, 1985) on such a prepared data set. This expands the description of the deflection basin considerable if compared to the traditional limited description of the deflection basin by calculating only the first two parameters listed in Table 2.1 ( maximum deflection and radius of curvature).

The author also explored the area of a mathematical expression for the whole deflection basin. The measured deflection basins are discrete points and various mathematical and physical models available , were selected and tested to fit these discrete measuring points. The SPSS Statistical Package for the Social Sciences (Nie et al, 1975; Robinson, 1984) was used to do linear and non-linear regression analyses. This work is described in detail in Appendix A. When linear regression analysis procedures are used mathematical models can either describe the area of positive curvature or that of the negative curvature well, but not both areas simultaneously (see figure 2.7). This regression analysis method also cause a slight distortion in the area of positive curvature.

The use of the non-linear regression analysis procedures does lead to improved fittings of either the positive or negative curvature of the deflection basin (see figure 2.7). The mathematical models still either describe the positive or negative curvature well, but not both.

The physical model of a point load on an unlimited beam on elastic foundations gave the best fit using the non-linear regression analysis procedure. It also gave a better fit of the whole



TABLE 2.1 SUMMARY OF DEFLECTION BASIN PARAMETERS

Parameter	Formula	Measuring device
1. Maximum deflection	$\delta_0$	Benkelman beam Lacroix deflectograph
2. Radius of curvature	$R = \frac{r^2}{2 \delta_0 (\delta_0 / \delta_r - 1)}$ $r = 127 \text{ mm}$	Curvaturemeter
3. Spreadability	$S = \frac{[(\delta_0 + \delta_1 + \delta_2 + \delta_3) / 5] 100}{\delta_0}$ $\delta_1, \dots, \delta_3 \text{ spaced } 305 \text{ mm}$	Dynalect
4. Area	$A = 6 [1 + 2(\delta_1 / \delta_0) + 2 * (\delta_2 / \delta_0) + \delta_3 / \delta_0]$	Falling weight deflectometer (FWD)
5. Shape factors	$F_1 = (\delta_0 - \delta_2) / \delta_1$ $F_2 = (\delta_1 - \delta_3) / \delta_2$	F W D
6. Surface curvature index	SCI = $\delta_0 - \delta_r$ ; where $r = 305 \text{ mm}$ or $r = 500 \text{ mm}$	Benkelman beam Road rater F W D
7. Base curvature index	BCI = $\delta_{610} - \delta_{915}$	Road rater
8. Base damage index	BDI = $\delta_{305} - \delta_{610}$	Road rater
9. Deflection ratio	$Q_r = \delta_r / \delta_0 \text{ where}$ $\delta_r \approx \delta_0 / 2$	F W D
10. Bending index	BI = $\delta / a$ where $a = \text{Deflection basin}$	Benkelman beam
11. Slope of deflection	$SD = \tan^{-1}(\delta_0 - \delta_r) / r$ where $r = 610 \text{ mm}$	Benkelman beam

deflection basin, but still lacked accuracy in the small area of maximum deflection (see figure 2.7 or Appendix a for detail). The combined use of a mathematical model in this area solves the problem. The use of the physical model leaves the opportunity for detailed evaluation on a theoretical basis. This approach was not pursued further in view of the fact that various deflection basin parameters, as described above, can be calculated with ease with a high degree of description of the full deflection basin. The practical and simple approach was therefore selected by this author to be pursued in this thesis rather than such a highly theoretical approach in spite of the challenging possibilities.

## 6. CONCLUSIONS AND RECOMMENDATIONS

- (a) The measuring equipment, RSD and MDD, associated with the accelerated testing of the HVS is highly sophisticated and accurately measure deflection basins on the surface and in depth of pavement structures. The measuring procedure ensures statistically representative deflections of a pavement structure.
- (b) The evaluation procedures of typical Benkelman beam and Dehlen radius of curvature meter measurements are not automated and limited deflection basin information in the vicinity of maximum deflection is gathered and processed. The data evaluation procedures of these rebound measurements are peculiar to the method and equipment.
- (c) The measuring procedures of the RSD and MDD are automated and the whole deflection basin is recorded. The evaluation or data processing procedure make use of model curve fitting, but interest is concentrated on the small area of positive curvature while the large negative curvature of the basin is virtually ignored. The WASHO procedure of measurement is relatively free of plastic deformation effects and is preferred to the rebound method.

- (d) For fundamental methods of pavement evaluation it is imperative that an accurate description of the deflection basin is obtained. Various deflection basin parameters can be used to reflect the whole deflection basin and associated structural relationships.
- (e) Only the elastic side of a typical RSD or MDD deflection basin is processed to ensure that the data is relatively free of plastic deformation and possible interferences of reference points in the deflection basin.
- (f) The data preparation procedure, even before model curve fitting is done, can provide as measured deflections ( $\delta_0$ ,  $\delta_{127}$ ,  $\delta_{305}$ ,  $\delta_{610}$ ,  $\delta_{915}$  and  $\delta_{2000}$ ) which is normally used in the calculation of the majority of deflection basin parameters. It is suggested that this approach should be followed for normal data processing.
- (g) Higher level data manipulation using linear and non-linear curve-fitting procedures were used to express the discrete set of measuring points of a deflection basin mathematically. The most successful model was that of a point load on an elastic foundation using non-linear regression analysis techniques. This shows great promise, but is not pursued further here due to the obvious ease and accuracy of the simpler approach mentioned above.



### **CHAPTER 3**

#### **ANALYSIS OF DEFLECTION BASINS MEASURED DURING ACCELERATED TESTING**

**CHAPTER 3: CONTENTS**

	PAGE
1 INTRODUCTION	3.2
2 MEASURED DEFLECTION BASIN PARAMETERS	3.3
2.1 Behaviour of deflection basin parameters with repetitions	3.3
2.1.1 Bitumen base pavement	3.3
2.1.2 Granular base pavement	3.7
2.1.3 Cemented base pavement (equivalent granular state)	3.10
2.1.4 Light structured granular pavement	3.14
3 BEHAVIOUR STATES	3.16
4 RUT RELATIONSHIPS IN THE FLEXIBLE BEHAVIOUR STATE	3.18
5 SUMMARY AND CONCLUSIONS	3.19

## 1. INTRODUCTION

In the preceding chapters it was described how the deflection basin can be described by means of various deflection basin parameters. The use of these parameters with the road surface deflectometer (RSD) was proposed as a viable analysis technique as the RSD accurately measures the full deflection basin. It was also shown how the analysis of the measured RSD deflection basins can be simplified to calculate all the deflection basin parameters as shown in Table 1.1.

Up to date, the RSD is associated only with the accelerated testing facility, the fleet of heavy vehicle simulators (HVS's). As a vast number of pavement sections have been tested over the years, there exists potentially a vast data bank of information on RSD measured deflection basins. The original data processing of the accelerated tests were however done with other goals in mind. The result is that this RSD data is stored on magnetic tape in an awkward format. Detail background information of specific tests is further needed to acquire the necessary information in the raw data form. Due to this cumbersome process of getting the data it was therefore decided to concentrate the effort on tests on typical representative pavement types tested where there is a high confidence in the knowledge of the detail of the test information. These tests selected would then act as a pointer for possible detailed analyses as a separate project.

Accelerated tests carried out with the Heavy Vehicle Simulator (HVS) fleet on four different pavement structures were selected for a detailed analysis of the deflection basin data measured. The four HVS tests selected are representing pavements with a bituminous base on a cemented subbase (Opperman et al., 1983), a typical granular base on a cemented subbase (Horak and Maree, 1982), a typical light granular pavement structure (granular base and subbase) (de Beer 1982 and Van Zyl and Triebel, 1982) and a cemented base and subbase (Opperman, 1984 and Kleyn et al., 1985). The latter three have thin asphalt surfacings ( $\leq 40$  mm) which is typical of South African roads. The test on the cemented base pavement has particular significance too: it is the only HVS test where, after the



completion of the initial test, the test section was overlaid and the test was continued on the overlaid section.

The curve fitting procedure described elsewhere (Horak, 1985 and Horak and Otte, 1985) was used by this author to calculate the deflection basin parameters from the deflection basins as measured during the HVS tests. Due to the small sample size of the relevant data sets the discussion on the relationships between the structural parameters of each individual layer and the calculated deflection basin parameters mean that no meaningful regression analyses could be done. The discussion on this is therefore more general and directed towards the graphical evidence presented. The behaviour of the various deflection basin parameters related to the behaviour of the various pavement types under accelerated testing is discussed in detail. Suggestions are made as to the usefulness of these deflection basin parameters to describe pavement behaviour states and layers. The fold out at the back (Table 1.1) referring to the various deflection basin parameters should be used for ease of reference.

## 2 MEASURED DEFLECTION BASIN PARAMETERS

### 2.1 Behaviour of deflection basin parameters with repetitions

#### 2.1.1 Bitumen base pavement

The various parameters, as calculated under a 40 kN dual wheel load, were related to the actual number of repetitions of the HVS test at Paradise Valley (Opperman et al., 1983). Parameters were grouped together in terms of units and range and all presented versus actual repetitions as shown in Figure 3.1. Although the actual test consisted of  $2,3 \times 10^6$  actual repetitions, only about  $1,5 \times 10^6$  actual repetitions are shown in Figure 3.1.

In general, deflections ( $\delta_0$  to  $\delta_{915}$ ) show a tendency to increase slightly with number of actual repetitions. This is as expected. What is significant though is that  $\delta_{305}$  and  $\delta_{610}$  show

PARADISE VALLEY: VALUES RECORDED UNDER 40 kN DUAL WHEEL

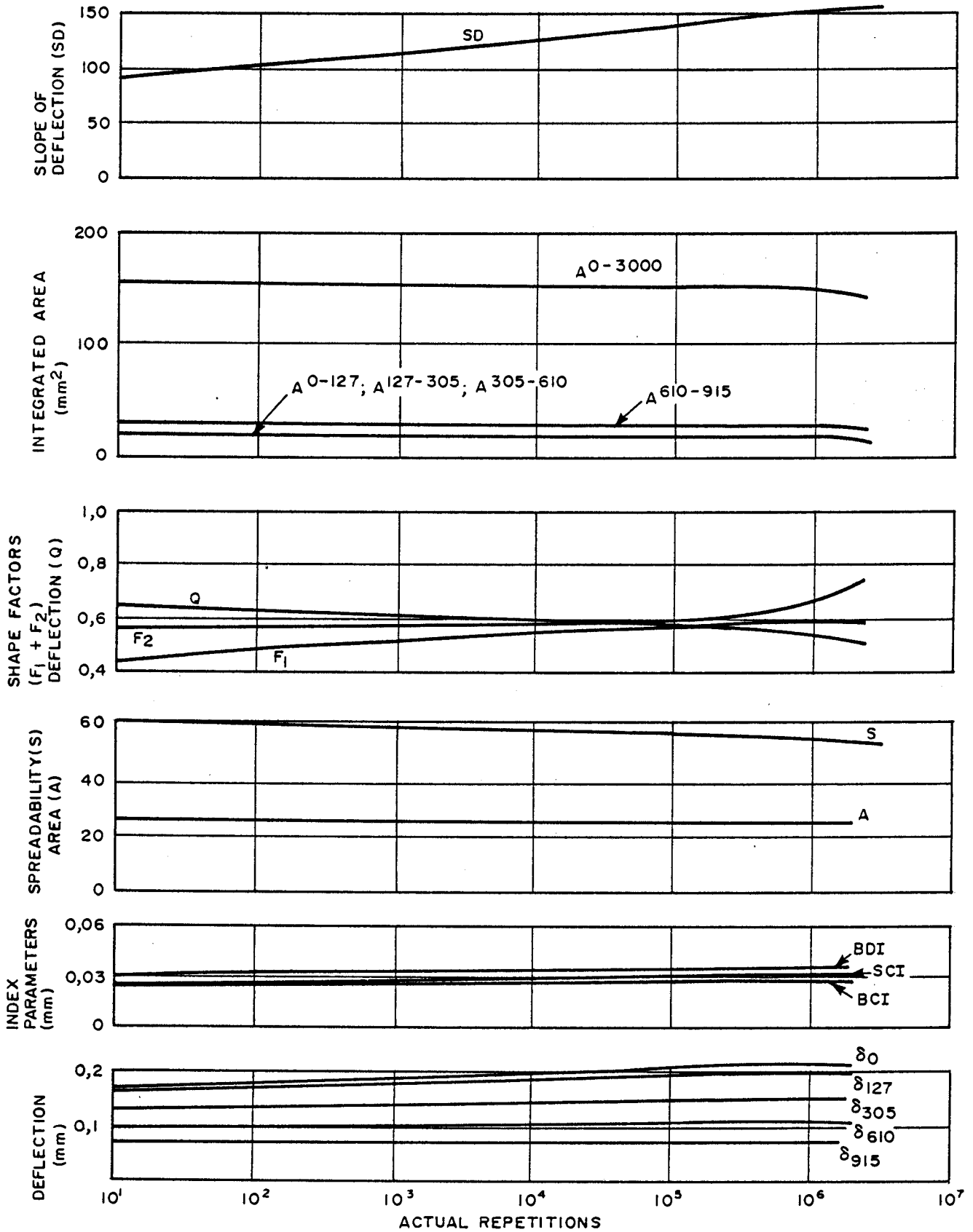


FIGURE 3.1

DEFLECTION BASIN PARAMETERS VERSUS ACTUAL REPETITIONS FOR A BITUMEN BASE PAVEMENT

some relative increase in deflection to  $\delta_{915}$ , which is virtually constant. This may reflect a change in elastic moduli of the subbase and selected layer (Tam, 1985). In the region of  $10^5$  to  $10^6$  actual repetitions all deflections ( $\delta_0$  to  $\delta_{915}$ ) level off. If these results are compared to the change in calculated effective elastic moduli as shown in Figure 3.2, it is confirmed that the subbase, selected layer and subgrade show the greatest change in this region ( $10^5$  to  $10^6$  actual repetitions).

The index parameters, surface curvature index (SCI), base damage index (BDI) and base curvature index (BCI) also reflect the same changes as their calculations are based on the values of  $\delta_0$ ,  $\delta_{305}$ ,  $\delta_{610}$  and  $\delta_{915}$ . SCI shows only a slight increase in value with increase in actual repetitions. This reflects a bitumen base which is structurally strong, with minimal change in effective elastic moduli deeper in the pavement structure (Kilareski et al., 1982). This corresponds with the change in effective elastic moduli as shown in Figure 3.2 for the subbase, selected layer and subgrade over the range where their elastic moduli showed the greatest change. The slightness of change in BDI and BCI are indicative of the scale of change of the effective elastic modulus of the cemented subbase which still had a high residual effective elastic modulus at the end of the test.

Parameters such as spreadability (S) and area (A) reflect the whole of the deflection basin. The major portion of the deflection basin, particularly away from the point of maximum deflection, reflects changes in the lower layers (Tam, 1985). Figure 3.2 indicates that the changes in effective elastic layers were relatively small. This may contribute to S and A being relatively constant.

Shape factors (F1 and F2) and deflection ratio (Q) are not specifically related to any structural layers. In the calculation of these parameters the shape of the deflection bowl, or change thereof (e.g. becoming more peaked), would be reflected. This apparently did not happen.

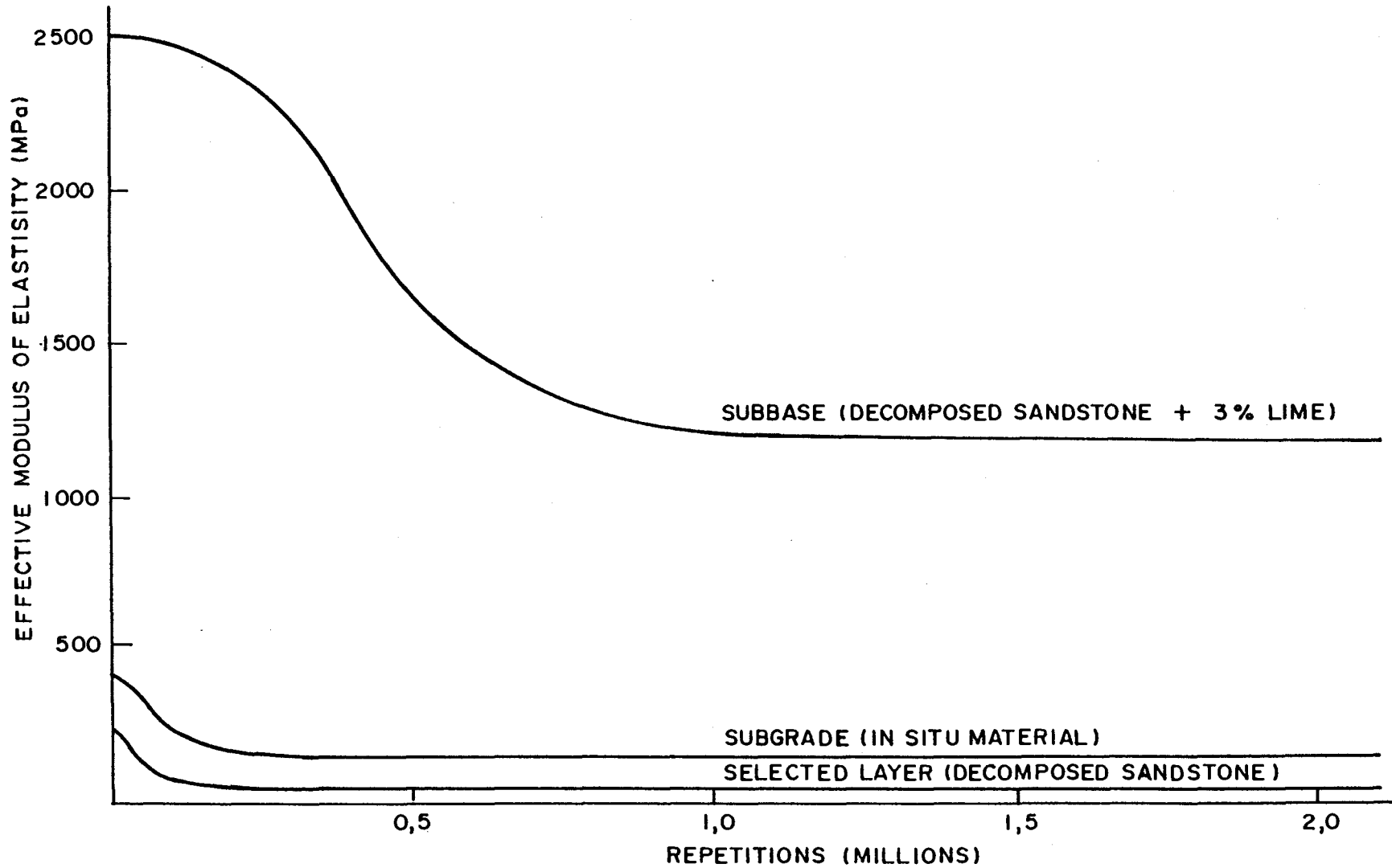


FIGURE 3.2  
CHANGE IN EFFECTIVE E-MODULI OF THE DIFFERENT LAYERS IN THE HVS TEST 162A3  
AT PARADISE VALLEY (OPPERMAN *et al.*, 1983)

The statement above is enhanced when the fitted deflection basin functions (Horak, 1985) are integrated over various segments (e.g. 0 to 127 mm, etc.). Virtually no changes took place until about  $1 \times 10^6$  actual repetitions.  $A^{0-3000}$ , which is the integrated area under the whole deflection basin, shows very clearly only a slight change after  $1 \times 10^6$  actual repetitions.

Slope of deflection (SD) shows a gradual rise in value as actual repetitions increase. This parameter can unfortunately not be related to any change of any particular structural layer. It is however an indication of a deflection basin which is becoming gradually more peaked, but can, due to the low range it is covering, not be defined as peaked.

#### 2.1.2 Granular base pavement

The various parameters, as calculated from deflection basin measurements under a 40 kN wheel load, are presented for the HVS test at Erasmia (Horak and Maree, 1982) in Figure 3.3. The deflection basin showed definite changes with the increase in actual repetitions. Although  $\delta_{915}$  showed virtually no change,  $\delta_{610}$  and  $\delta_{305}$  to  $\delta_0$  in particular showed the greatest changes. This clearly indicates changes in the base and subbase effective elastic moduli (Tam, 1985). In Figure 3.4 it can be shown that the base and the subbase in particular did change considerably in terms of effective elastic moduli up to around  $2 \times 10^5$  actual repetitions.

This change in the base and subbase effective elastic moduli is clearly reflected by the change in surface curvature index (SCI) (Anderson, 1977). The base damage index (BDI) and base curvature index (BCI) changed to a lesser extent, indicating changes in the effective elastic moduli of the selected layer and the subgrade (Kilareski and Anan, 1982). Radius of curvature (R) showed a definite reduction as actual repetitions increased which confirms the indication of the SCI values. Spreadability (S) and area (A) did however not reflect any

ERASMIA: VALUES RECORDED UNDER 40kN DUAL WHEEL

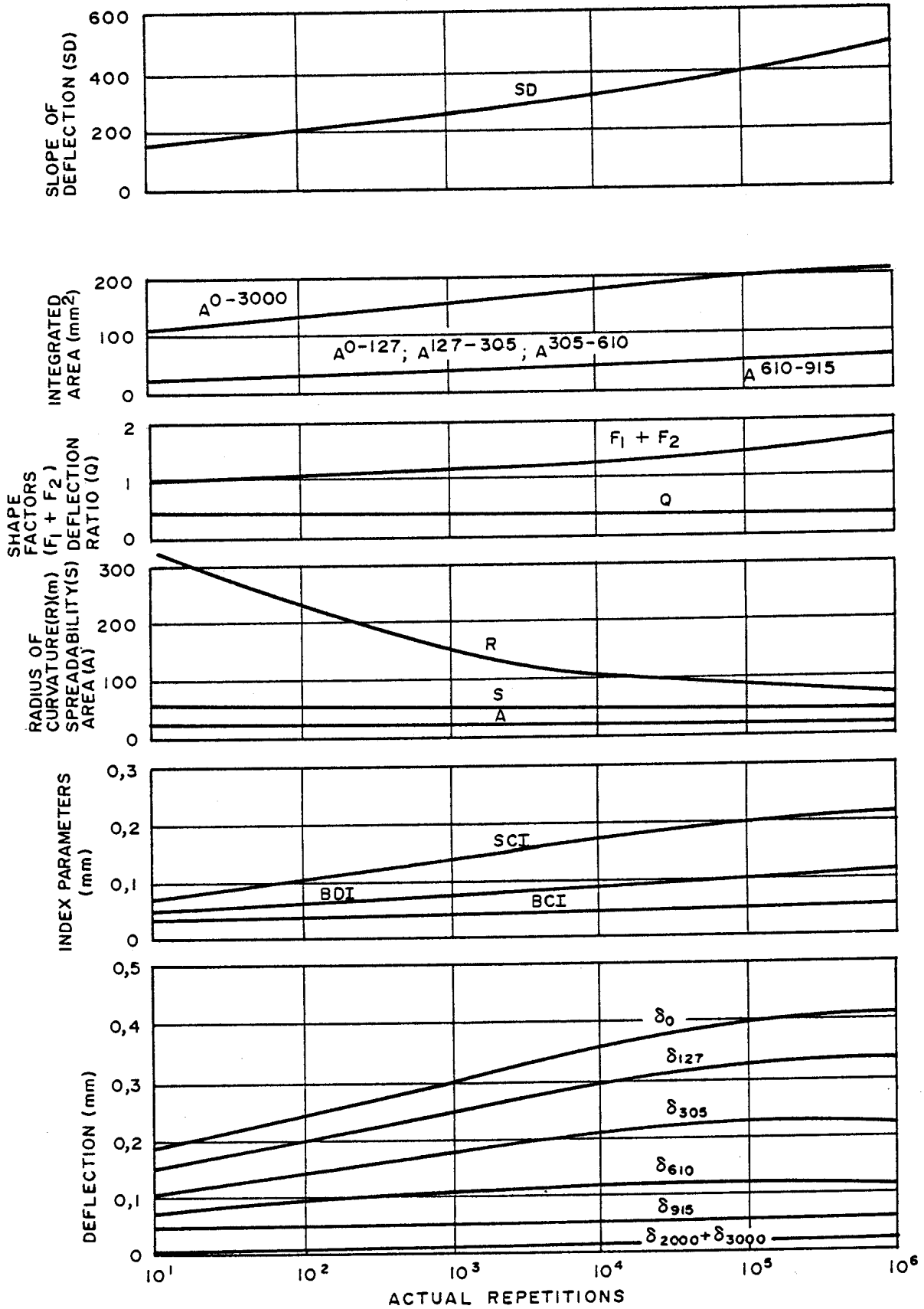


FIGURE 3.3

DEFLECTION BASIN PARAMETERS VERSUS ACTUAL REPETITIONS FOR A TYPICAL GRANULAR BASE PAVEMENT

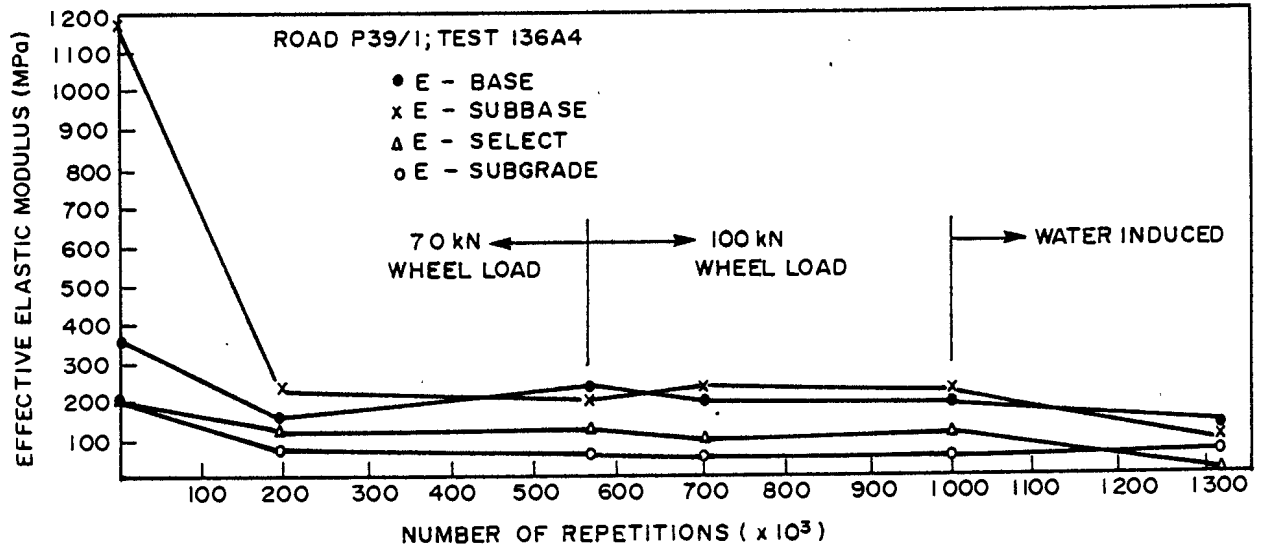


FIGURE 3.4

AVERAGE EFFECTIVE ELASTIC MODULI VALUES FOR A 40 kN DUAL WHEELLOAD (Horak and Maree, 198 )

change. Their values were slightly higher than those of the bitumen pavement but were also constant.

The parameters, shape factors (F1 and F2) were the same and showed a steady increase in value with the increase in actual repetitions. This is generally the same as the behaviour for bitumen base pavements, indicating a more peaked deflection basin developing. Deflection ratio (Q) stayed rather constant, reflecting no particular change of any structural layer.

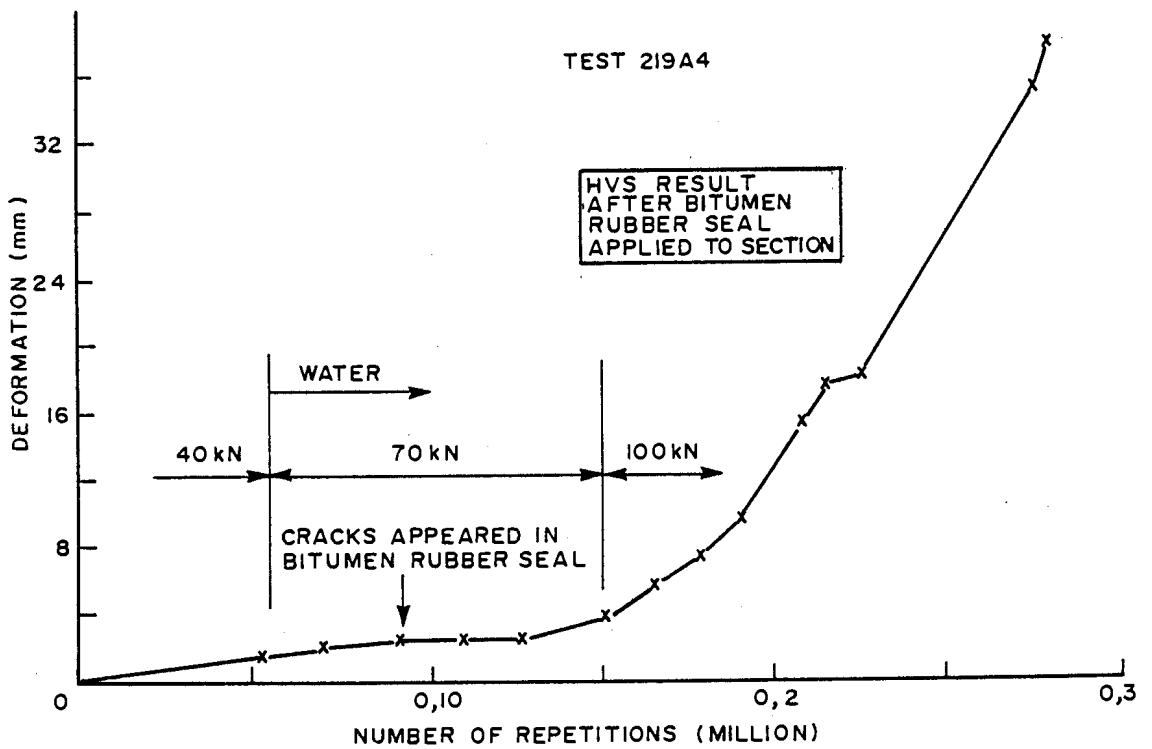
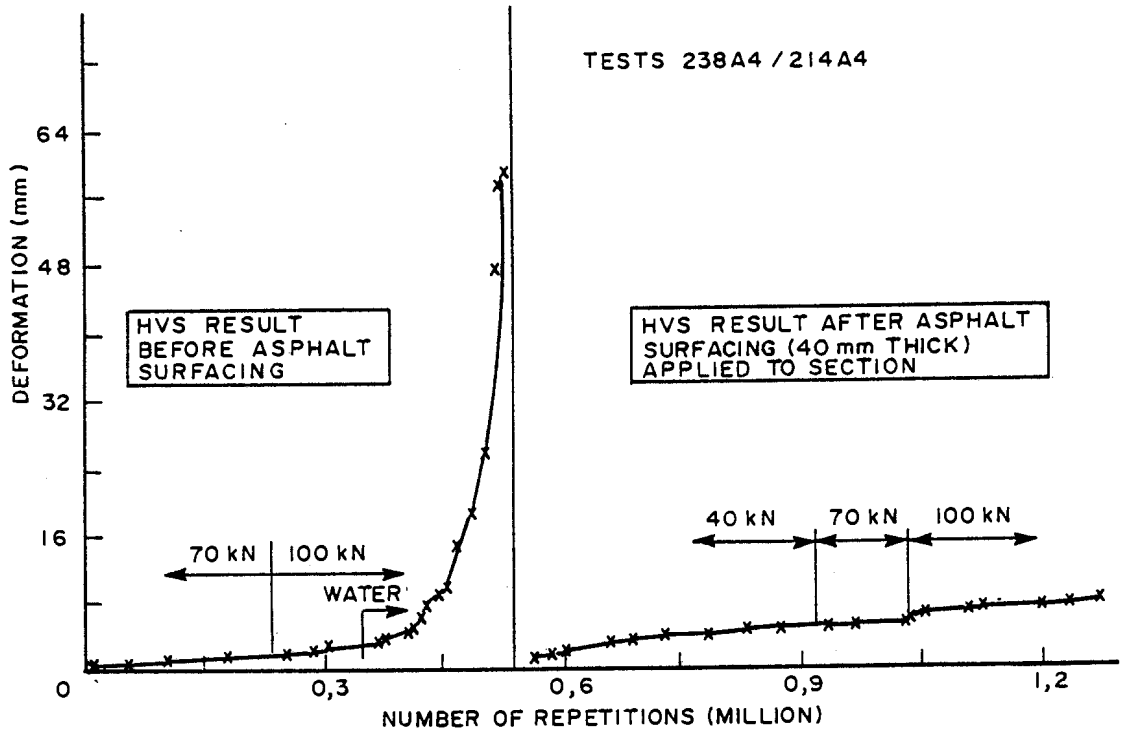
The integrated area under sections of the function of the fitted deflection basin showed a slight increase in values for all the sections. The slope of deflection (SD) indicated by its change that the deflection basin is becoming more peaked. The initial value was higher than that of the bitumen base pavement, which clearly indicates that this granular base pavement had a much more peaked deflection basin from the start. This clearly reflects the lower effective elastic moduli of the granular base too.

### 2.1.3 Cemented base pavement (equivalent granular state)

The deflection basin parameters were determined for the cemented base pavement at Hornsnek (test 214A4) which was in a flexible state, exhibiting equivalent granular behaviour from the start of the test (see Figure 3.5). This is a rehabilitated or overlaid pavement (Opperman, 1984). In Figure 3.6 the deflection basin parameters are shown in relationship to the actual repetitions.

The deflections generally increase as measured at various points on the deflection basin ( $\delta_0$  to  $\delta_{915}$ ). The deflection furthest out ( $\delta_{915}$ ) showed only a slight increase with the increase in actual repetitions. It is however  $\delta_{610}$  and  $\delta_{305}$  which showed the greatest increase, reflecting changes in effective elastic moduli of the deeper layers (Tam, 1985). The  $\delta_{127}$  value actually showed less increase than the  $\delta_{305}$  value. This is typical behaviour of a granular base, as described earlier with a cemented subbase. Opperman (1984) reported that due to the





b) EFFECT OF BITUMEN RUBBER SEAL

FIGURE 3.5  
AVERAGE DEFORMATION OF THE ROAD SURFACE AFTER  
REHABILITATION MEASURES (ROAD 30 HORNSNEK)  
(OPPERMAN, 1984)

HORNSNEK: VALUES RECORDED UNDER 40 kN DUAL WHEEL

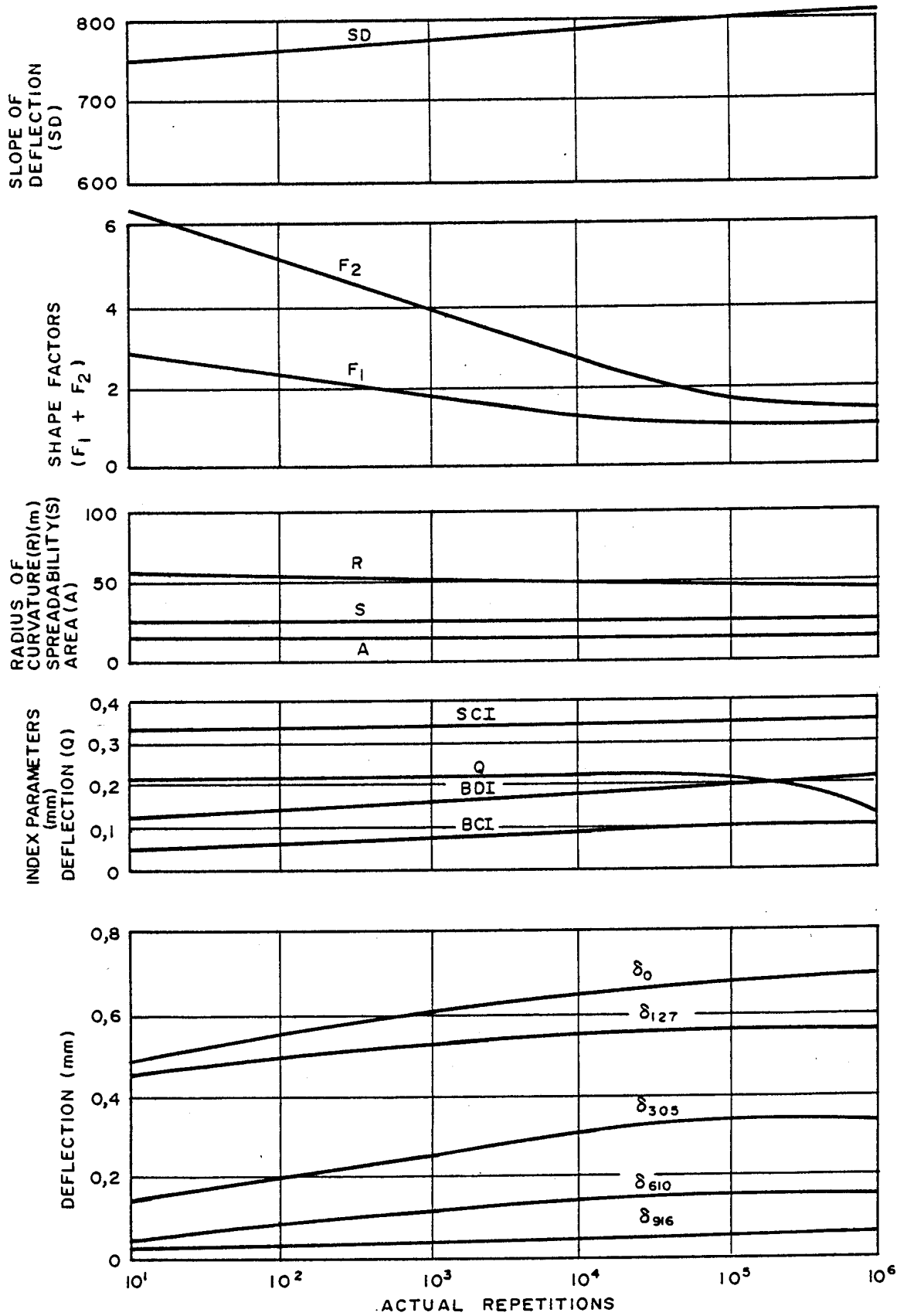


FIGURE 3.6  
DEFLECTION BASIN PARAMETERS VERSUS ACTUAL REPETITIONS FOR A TYPICAL CEMENTED BASE EXHIBITING EQUIVALENT GRANULAR BEHAVIOUR

crushing of the upper cemented base and limited cracking of the cemented subbase layer under the soft interlayer this is exactly the case.

The index parameters (SCI, BDI and BCI) confirm the observation of the change in the lower layers (subbase selected layer and subgrade) while the base is rather stable. The surface curvature index (SCI) stayed virtually constant with the increase in actual repetitions. The initial value is however in the same order where the granular base pavement, discussed earlier, ended. The base damage index (BDI) and base curvature index (BCI) showed a steady increase with the increase in actual repetitions. These values also started off at the level where the typical granular base pavement, discussed earlier, ended. This definitely confirm the changes in effective elastic moduli of the cemented subbase, selected layer and subgrade. The deflection ratio (Q) shown with the index parameters in Figure 3.6 is virtually constant up to  $10^5$  actual repetitions whereafter it declines. Unfortunately it does not indicate any specific relevance to structural change in the various layers.

The parameters, spreadability (S) and area (A), like in the case of the granular base and bitumen base pavement, are constant and more or less in the same range. This again leads to the conclusion that these parameters are not sensitive to change in the various structural layers.

Radius of curvature (R) shows only a very slight increase, which is not unusual. It should be pointed out though that the level at which it starts off in itself is already low. It is interesting though that the shape factors (F1 and F2), contrary to the behaviour of the bitumen base pavement and the granular base pavement in particular, showed a decrease in value with the increase in actual repetitions. The starting values of this pavement in the equivalent granular behaviour state, is more than those of the granular base towards the end though. In line with the reasoning for the other pavement types earlier, the conclusion must be drawn that the deflection basins are becoming

less peaked or more level. This line of reasoning is confirmed by the behaviour of the slope of deflection (SD) too. It started off at a very high value ( $\pm 750$ ), indicating a peaked deflection basin from the start as R indeed indicated. The rate at which SD increased with actual repetitions is even less than that of the bitumen base pavement discussed earlier. This points to the fact that there is some form of remoulding or change in balance of the pavement, becoming a "deep" pavement (Kleyn et al., 1985). This would definitely reflect more of the quality of the subgrade, which controls the outer edges of the deflection basin (Tam, 1985).

#### 2.1.4 Light structured granular pavement

The deflection basin parameters as calculated for the light structured granular pavement on Main Road 18 near Malmesbury, are shown in Figure 3.7 versus the number of actual repetitions. As shown at the top of this figure, water did enter this test section. In general this wet phase leads to quite different behaviour of the deflection parameters as the pavement in this state failed rapidly. Discussion centres on the dry phase in order to correlate the general behaviour with that of the other pavement structures tested and discussed here.

In Figure 3.7 it can be seen that in the dry phase, deflection ( $\delta_0$  to  $\delta_{915}$ ) showed a general increase with the increase in actual repetitions. Even  $\delta_{915}$  showed a definite increase, indicating that this can be termed a "deep" structure reflecting changes of the subgrade (Tam, 1985). Maximum deflection ( $\delta_0$ ) also shows an increase relative to  $\delta_{305}$  indicating changes in the upper layers too. In the wet phase  $\delta_{915}$  was the least affected due to the effect of a clayey subgrade (De Beer, 1983).

The index parameters, base damage index (BDI) and base curvature index (BCI), which reflect the effect of subbase and subgrade layers (Kilareski and Anani, 1982) showed an increase in value with actual repetitions in the dry phase. This indicates a lowering of the effective elastic moduli of these layers. The

MALMESBURY : VALUES RECORDED UNDER 40 kN DUAL WHEEL

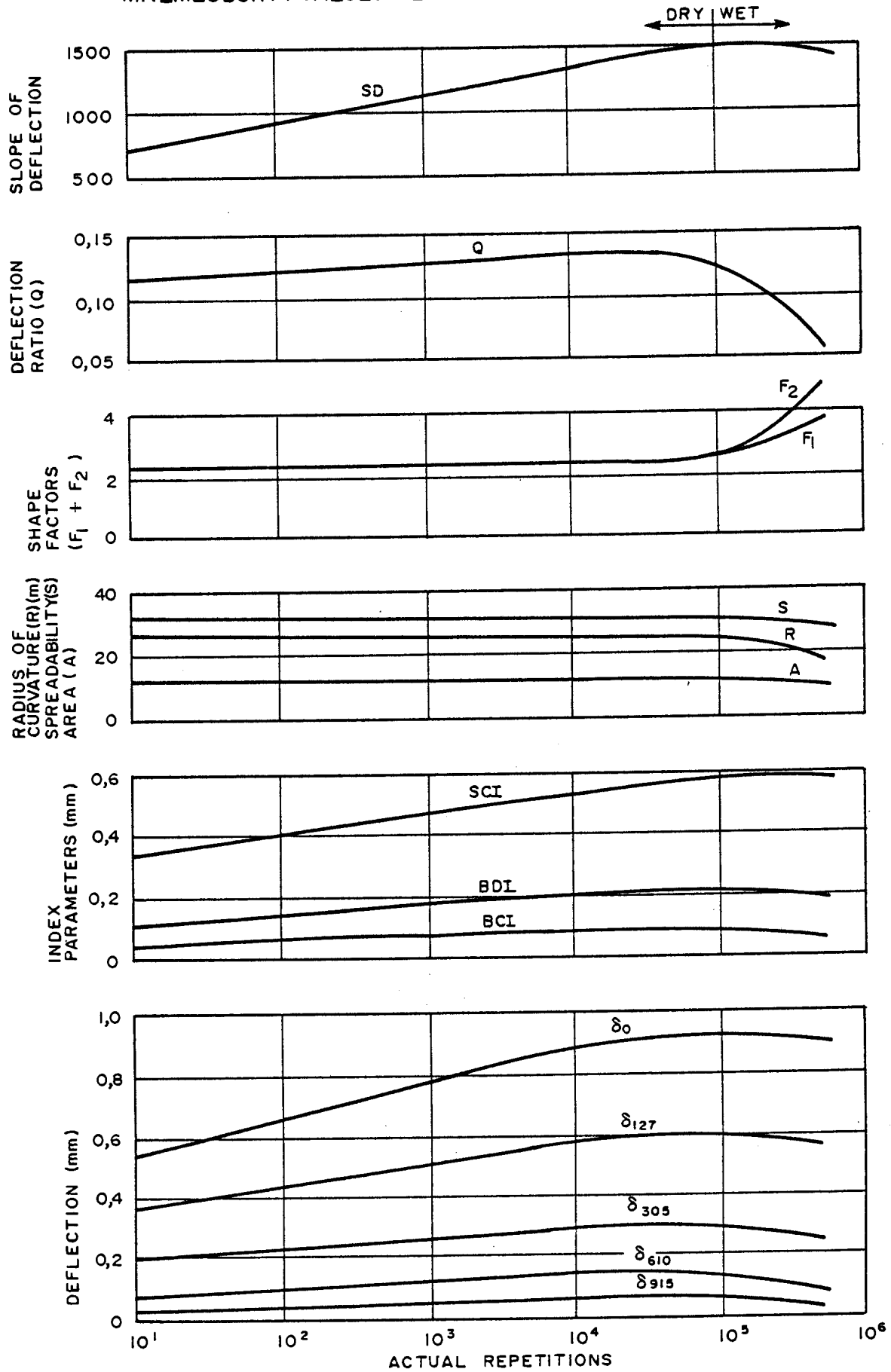


FIGURE 3.7  
DEFLECTION BASIN PARAMETERS VERSUS ACTUAL REPETITIONS FOR A TYPICAL LIGHT STRUCTURED GRANULAR PAVEMENT

surface curvature index (SCI) also indicates a lowering in effective elastic moduli of the base layer by the increase in SCI in the dry phase. In the wet phase the value of SCI levels off while BDI and BCI even show a lowering of their values. This is most probably due to plastic deformation or even shear deformation in the base (Van Zyl and Triebel, 1982) and the effect of the clayey subgrade (De Beer, 1983).

The radius of curvature (R), spreadability (S) and area (A) parameters stayed virtually constant in the dry phase of this test. The low initial value of R, does however indicate a weak base with less support than with a cemented subbase. Shape factors (F1 and F2) and deflection ratio (Q) also either stayed constant during the dry phase of the test or were meaningless in terms of any structural changes. This author believes that the changes in the abovementioned deflection basin parameters only reflect the distressed state of the failing pavement at that stage without any specific reference to structural layers.

The slope of deflection (SD) showed an increase in value during the dry phase of the test. This may indicate a change in the form of the deflection basin, as the SCI values also indicate, in the region of the loaded wheel. Radius of curvature (R) however does not confirm this behaviour but this may be related to measuring problems (Horak, 1984). The initial value of SD is higher than that of the typical granular base pavement which indicates that the deflection basin was indeed rather peaked from the start. This again reflects on the lack of quality of the base and subbase.

### 3. BEHAVIOUR STATES

The behaviour of the different pavement types is controlled by the behaviour of the individual layers and by the interaction between the layers forming the pavement structure (Freeme et al., 1986). The definition of the states of behaviour is given by Freeme (1983). These states range from very stiff to very flexible as can be seen in Table 3.1.

TABLE 3.1 Definition of states of pavement behaviour <sup>3.17</sup>

State	Approximate deflection range (mm)	Comments
Very stiff	< 0,2	Pavement behaviour predominantly controlled by high modulus (> 2 000 MPa) layers acting as slabs
Stiff	0,2 to 0,4	Pavement behaviour controlled by layers with reasonably high moduli (> 500 MPa). Some layers could be cracked but blocks tend to be larger than 2 m in diameter
Flexible	0,4 to 0,6	Pavement behaviour controlled by material in the granular state. Moduli of load-bearing layers in the range of 200 to 500 MPa (excluding thin surfacing moduli). Cementitious layers can be further cracked into smaller blocks
Very	> 0,6	Pavement behaviour controlled by materials flexible in the granular state usually with low moduli (< 200 MPa). Pavements tend to be susceptible to the ingress of water

TABLE 3.2 Ranges for behaviour states

Behaviour	Deflection basin parameter ranges				
	$\delta$	SD(*10 <sup>-6</sup> )	SCI	BDI	BCI
Very stiff	<0,2	<50	<0,01	<0,01	<0,01
Stiff	0,2 to 0,4	50 to 400	0,01 to 0,2	0,01 to 0,1	0,01 to 0,05
Flexible	0,4 to 0,6	400 to 750	0,2 to 0,4	0,1 to 0,15	0,05 to 0,08
Very flexible	>0,6	>750	>0,4	>0,15	>0,08

Using Table 3.1 the various HVS tests described earlier were classified according to their behaviour states. It is clear that the Paradise valley test with the bituminous base is still in the stiff behaviour state at the completion of the test. The granular base test at Erasmia changed from a stiff behaviour state to a

flexible behaviour state after 100 000 actual repetitions. The cemented base in the equivalent granular state at Hornsnek,

changed from a flexible to very flexible behaviour state virtually from the start of the test. The same description holds for the light structured granular pavement tested at Malmesbury.

The ranges of the various deflection basin parameters that were identified as the most reliable indicators earlier were determined for each of the behaviour states. It is believed that by looking at more deflection basin parameters than only maximum deflection that a better definition of the behaviour states is possible. These ranges are shown in Table 3.2 .

#### 4 RUT RELATIONSHIPS IN THE FLEXIBLE BEHAVIOUR STATE

In the previous section it was indicated that the granular base or pavements in the equivalent behaviour states were the only pavements that could be classified as being in either a flexible or very flexible behaviour state. For these pavements identified, the standard relationships between rut and actual repetitions are available.

The rut measurements of these pavements were correlated with the equivalent axle repetitions (E80s) and the measured deflection basin parameters in a stepwise multiple regression analysis. An exponent of  $n = 3$  was used in the calculation of the E80 repetitions (Maree et al., 1982). In the stepwise multiple regression a R-square value of at least 0,75 was set or three variables in the relationship for acceptance. This resulted in a data matrix of 12 by 30, representative values of the granular base pavements in the flexible and very flexible behaviour states.

Two relationships were determined;

$$\text{Relationship 1.... Rut} = -13,696 + 5,698 (F1) + 4,153 (F2)$$
$$R^2 = 0,79$$



Where, Rut is measured in mm, F1, F2 are shape factors.

Relationship 2.

$$\text{Rut} = -15,205 + 6,002 (F1) + 0,444 (F2) + 3,935 (E80s).$$

Where; Rut,  $R^2 = 0,82$ ; F1 and F2 areas described above, E80s are equivalent 80 kN axes in millions ( $10^6$ ) repetitions.

The significance of these relationships is that granular base pavements in the flexible or very flexible behaviour states can be identified and rut can be calculated from deflection basin measurements. It is also significant that the two shape factors F1 and F2 which did not correlate well with changes in state or material state the base layer in particular, does correlate well with the permanent deformation behaviour. Most of the permanent deformation in granular bases originate in the base layer (Maree et al., 1982).

## 5 SUMMARY AND CONCLUSIONS

Four accelerated tests with well documented results were selected to calculate deflection basin parameters. These tests represent typical bitumen base, granular base, cemented base and light pavement structure granular pavements. The latter three pavement types were in the flexible behaviour state while the bitumen base pavement was in the stiff behaviour state.

Due to the limited amount of HVS tests analysed the findings reported earlier in chapter 2 were used as reference in the discussion. It was therefore only investigated to what extent the typical deflection basin parameters confirmed the indications of other researchers.

Considerable more HVS tests needs to be analysed with the proposed deflection basin parameters (Table 1.1). If statistically significant numbers of tests of each pavement type is available it is suggested that a proper regression analysis be done to see which deflection basin parameter correlate the best with important

structural parameters such as effective elastic moduli with the increase in repetitions.

In spite of the limited survey an attempt was made to make statements about the generalised relations between the deflection basin parameters and effective elastic moduli changing with the number of repetitions. In line with findings reported in chapter 2 it can be stated that the index parameters (SCI, BDI and BCI) gave relatively clear indications of their relations with respectively the base, subbase and selected layers and their respective effective elastic moduli changing with the number of repetitions. Other deflection basin parameters gave rather vague relations if any which limits their use at present with this limited survey.

From the results of the various tests and measured deflection basins, it is possible to give a better description of the behaviour states. It is suggested that not only maximum deflection should be used to indicate in which behaviour state a pavement is, but preferably the index parameters (SCI, BDI, BCI) as indicated in the Table 3.2.

Rut can be calculated from deflection basin parameters  $F_1$  and  $F_2$  and optionally the  $E_{80}$ s too. This is true for granular base pavements in the flexible or very flexible behaviour states for this small sample size analysed.

The author strongly recommends that in future a larger sample size of tested pavements be analysed in order to broaden the data base facilitating proper statistical analyses. This will be of particular benefit to possible relationships between deflection basin parameters and structural parameters of individual layers. With the new data manipulation programmes for HVS data this will in future be a relatively simple operation. A dedicated and concerted effort will however be needed for the data retrieval of the past tests. This author only sees his role in this regard as having investigated the possibilities for this present purpose.



## **CHAPTER 4**

### **LITERATURE SURVEY ON MATERIAL CHARACTERIZATION AND STRUCTURAL ANALYSIS USING DEFLECTION BASINS**

**CHAPTER 4: CONTENTS**

	PAGE
1 INTRODUCTION	4.2
2 GENERAL	4.4
3 METHODS INCORPORATING TWO-LAYER LINEAR ELASTIC THEORY	4.5
4 METHODS INCORPORATING THREE OR MORE LAYERS	4.8
4.1 Methods using up to two deflection basin parameters	4.11
4.2 Methods using at least three deflection basin parameters	4.20
5 CONCLUSIONS AND RECOMMENDATIONS	4.34

## 1 INTRODUCTION

The full deflection basin can be measured and the various deflection basin parameters give a better description of it. This was discussed in detail in the previous chapters. The main aim of this thesis is to use such measured deflection basin parameters in the analysis procedure. In Figure 4.1 the South African mechanistic rehabilitation design or analysis procedure is illustrated (Freeme, 1983). The pavement class and pavement type description of steps 1 and 2 will not be discussed here, but detail can be found elsewhere (TRH4, 1985a). In the previous chapter it was shown how the pavement behaviour state can be enhanced by using measured deflection basin parameters. Step 4 where the pavement layer state is described is also discussed in detail elsewhere (Freeme, 1983). In Appendix B a brief summary is given on how condition surveys enhance this identification of pavement layer state.

The main emphasis of this literature survey in this chapter is to indicate how measured deflection basins can also enhance step 5 (see Figure 4.1). The layer thickness of the pavement can be determined from as-built plans or by profile trenching. In the mechanistic design process effective elastic moduli are fundamental inputs in the analysis procedure in order to ensure that the evaluation procedure in step 6 (Figure 4.1) can be executed successfully. In South Africa the material classification as outlined in TRH14 (1985b) and TRH4 (1985a) is based on fundamental behaviour and strength characteristics. This description of materials form the basis for the description of the effective elastic moduli of each material type in a specific behaviour state (Freeme, 1983). Various destructive and non-destructive tests are normally executed to ensure a correct definition of pavement material layers in terms of the effective elastic moduli used in the final non-simplified analysis procedure. Measured deflection basins, as a non-destructive testing means, can enhance the confidence in the assigned effective elastic moduli. In this chapter a detailed description

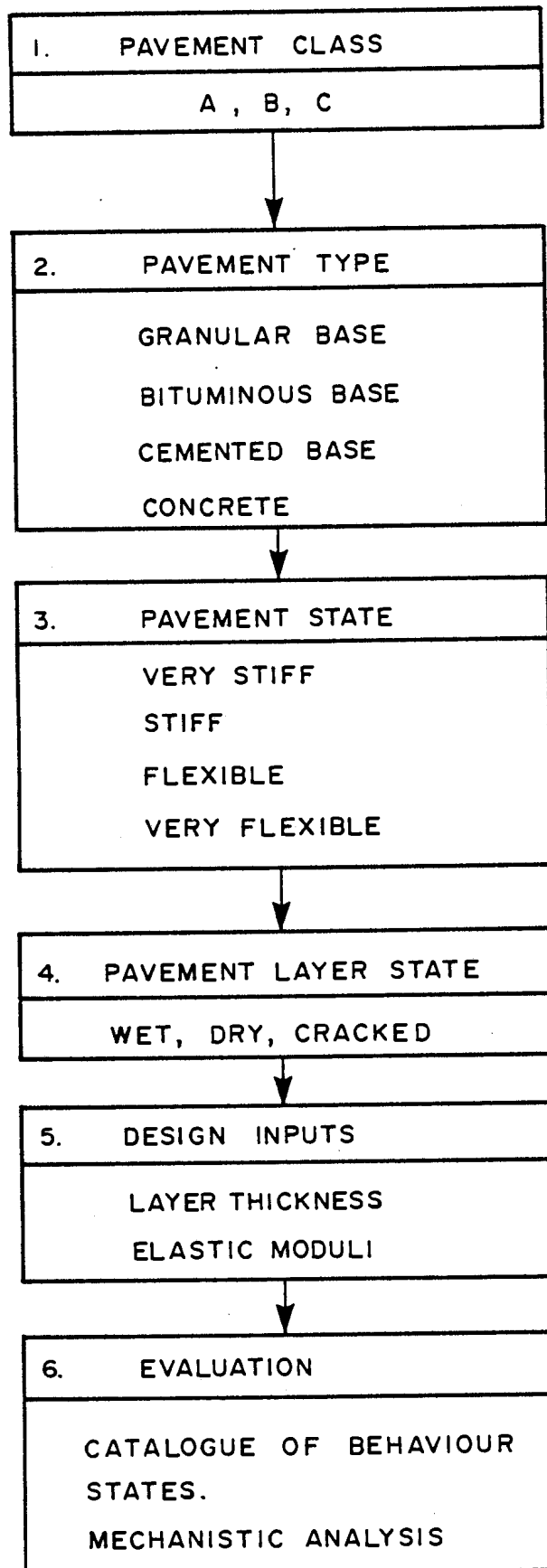


FIGURE 4.1  
*FLOW DIAGRAM OF THE MECHANISTIC  
PAVEMENT REHABILITATION DESIGN  
METHOD (FREEME, 1983)*

is therefore given given of various analytical methods of material characterization using deflection basin measurements as main input as found in literature.

## 2 GENERAL

In the characterization of materials of flexible pavements, various deflection based analysis methods are used. There are two main groups of methods. The first group is empirically based procedures with limited information on the full deflection basin and with limited deflection criteria. The second group uses basic elastic behaviour to determine the material properties. The majority of procedures in this latter group are based on linear elastic layered theory while the non-linear elastic behaviour of pavement materials is approximated by using linear elastic layered pavement models or finite element computer programs. The emphasis in this discussion is on the linear elastic group of methods of analysis. These procedures use computerized iterative, graphical, tabulated or nomograph solutions to analyse the pavement structures.

In a review of methods using layered elastic theory to model pavements Whitcomb (1982) observed the following common characteristics -

- (a) The methods use two to five deflection basin values in the analysis.
- (b) These models have two to five layers corresponding with the number of elastic moduli which are back-calculated.
- (c) Some of the methods are developed for a specific non-destructive testing device.
- (d) There are two basic methods of analysis: computerized iterative solutions and graphical fittings or nomographs.

Whitcomb (1982) also lists the following shortcomings of the layer elastic theory in its application to characterize pavement materials:

- (a) An inability to analyse effects of loads at discontinuities (e.g. cracks and edges)
- (b) The validity of the assumptions with regard to interface conditions
- (c) Their inability to handle inertial forces or vibrations
- (d) Non-linear stress and strain behaviour of materials (granular materials).

Of these limitations the last is considered to be the most restrictive. It is generally accepted that most materials used in pavements, in particular unbound granular materials, exhibit non-linear stress and strain behaviour. This leads to the fact that the elastic modulus of such materials is a function of the stress level and the result is that the elastic moduli will change both with depth and lateral position. Patterson et al. (1974) states that when there are more than two layers in a pavement, the number of unknown variables increases by three per layer and the system is generally insoluble unless the response characteristics can be defined more fully. Patterson et al. (1974) also observed that the theoretical models have an inherent weakness in terms of the accuracy in which it can represent the behaviour of the real pavement. They summarised the expected errors in peak surface deflection to be -30 per cent to +60 per cent when material moduli were measured in the laboratory. In more vigorous studies the errors were generally reduced to approximately 20 per cent. Patterson et al. (1974) noted that another limitation of the deflection influence surface technique is that is not very accurate with regard to the layers very near the surface. The limitations of the modelling of the loaded areas cause some doubt as to the accuracy of the deflections within an area of 0,5 m of the loaded area.

The discussion on techniques or methods for determining elastic moduli will be divided into two groups. The first group looks at two-layer models and the second group at three-layer or multilayer pavement models.

### 3. METHODS INCORPORATING TWO-LAYER LINEAR ELASTIC LAYER THEORY





Two-layer linear elastic layer theory can be used for preliminary analysis and interpretation of generalized trends. This may appear to be an over-simplification of more complex pavement structures, but the fact remains though that most surfaced and unsurfaced (low volume) roads have a typical two-layer pavement structure. This is particularly true in South Africa where surfacings are generally thin (average thickness of 25 mm). Considerable use is also made of chipsealing. In analysis methods this thin asphalt layer is often ignored owing to its limited influence on structural analysis.

The two-layered linear elastic model by Burmister (1945) is usually used as the basis for most of these methods. Yoder and Witczak (1975) state that the stress and deflection values obtained by Burmister are dependent upon the strength ratio of  $E_1/E_2$  of the layers, where  $E_1$  and  $E_2$  are the moduli of the reinforcing and subgrade layers respectively. Maximum deflection values for a flexible plate (which represents a tyre load) are determined as follows (Yoder and Witczak, 1975):

$$\delta_o = \frac{1,5 p a F_2}{E_2}$$

where  $p$  = unit load on circular plate

$a$  = radius of plate

$E_2$  = modulus of elasticity of lower layer

$F_2$  = dimensionless factor depending on the ratio of the moduli of elasticity of the subgrade and pavement as well as the depth to radius ratio

Wiseman et al. (1977) proposed the simplification of pavement structures by using the Burmister (1945) two-layer system or preferably the Hogg (1944) model. The Hogg model is that of an infinite plate on an elastic subgrade. Greenstein (1982) used these models for pavement evaluation of low-cost roads. In Figure 4.2 falling weight deflectometer (FWD) deflection basin measurements are used to arrive at values of  $E_p/E_s$  ( $E_1/E_2$ ) for relative values of pavement thickness to load radius ratio and the specific values of poisson ratio ( $\nu_p$  and  $\nu_s$ ). This nomograph is

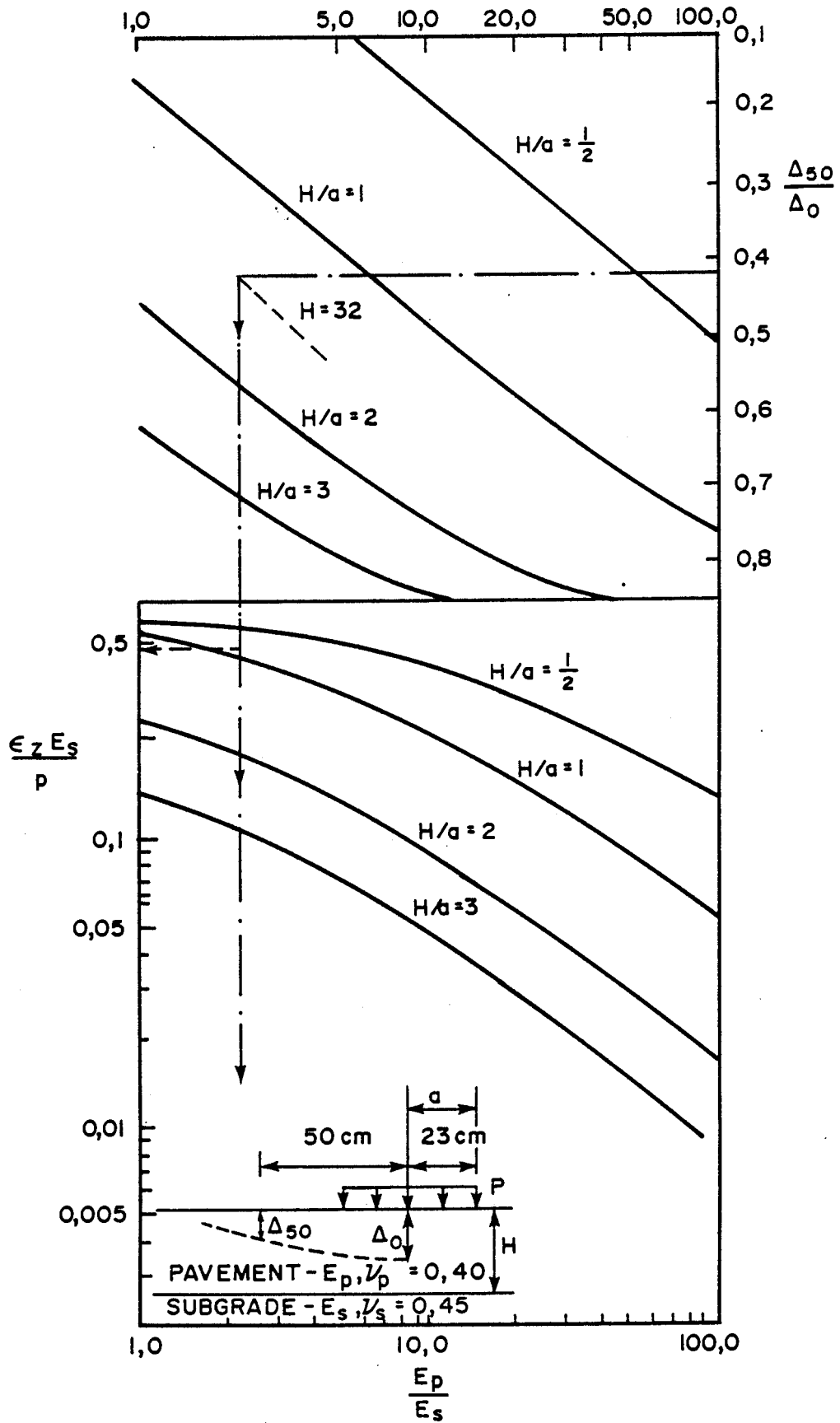


FIGURE 4.2  
TWO-LAYER MODEL USED FOR  
LOW-COST ROADS (Greenstein, 1982)

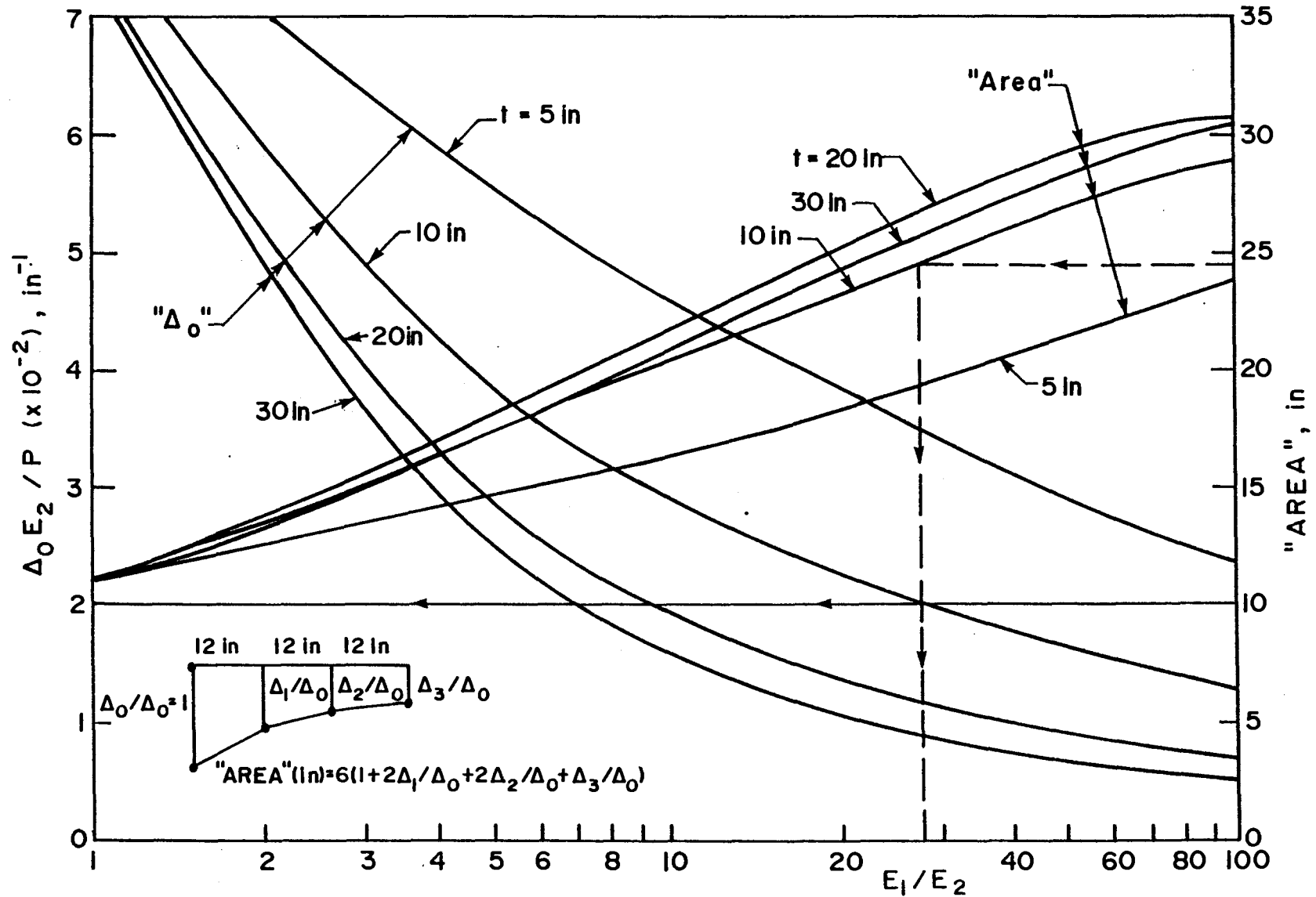
based on that derived by Wiseman et al. (1977). Estimate values of  $E_1$  and  $E_2$  are reached which may be used as a basis for further analysis. Berger and Greenstein (1985) simplified the use of the Hogg model so that it can be used on pocket calculators and deflections as measured with a Benkelman beam.

The general relationship of the ratio  $E_1/E_2$  is used in other graphical or nomographical procedures using the Burmeister model (1945). In Figures 4.3 and 4.4, Hoffman and Thompson (1981) show how four deflection basin parameters,  $\delta_o$ ,  $A$ ,  $F_1$  and  $F_2$ , (see Table 1.1) are related to this basic elastic moduli ratio ( $E_1/E_2$ ). These figures were developed for the Falling Weight Deflectometer (FWD) and Idaho Department of Transportation (IDOT) road raters. Other similar relationships were developed by Swift (1972) and Vaswani (1971) for the use of dynaflect deflection basin measurements.

In conclusion it can be stated that the elastic moduli based on Burmeister's (1945) two-layered linear elastic theory can be back-calculated with confidence using the deflection basin measurements. The specific measuring device and deflection basin parameter selected will result in a specific graphical solution. It is suggested that if this method is used it should preferably be used with granular bases and be treated as a method of estimating effective elastic moduli. The Hogg model (1944) certainly also proved to be a viable method particularly for cemented or bituminous base pavements. It should however also be seen as an approximation procedure of more complex pavement structures.

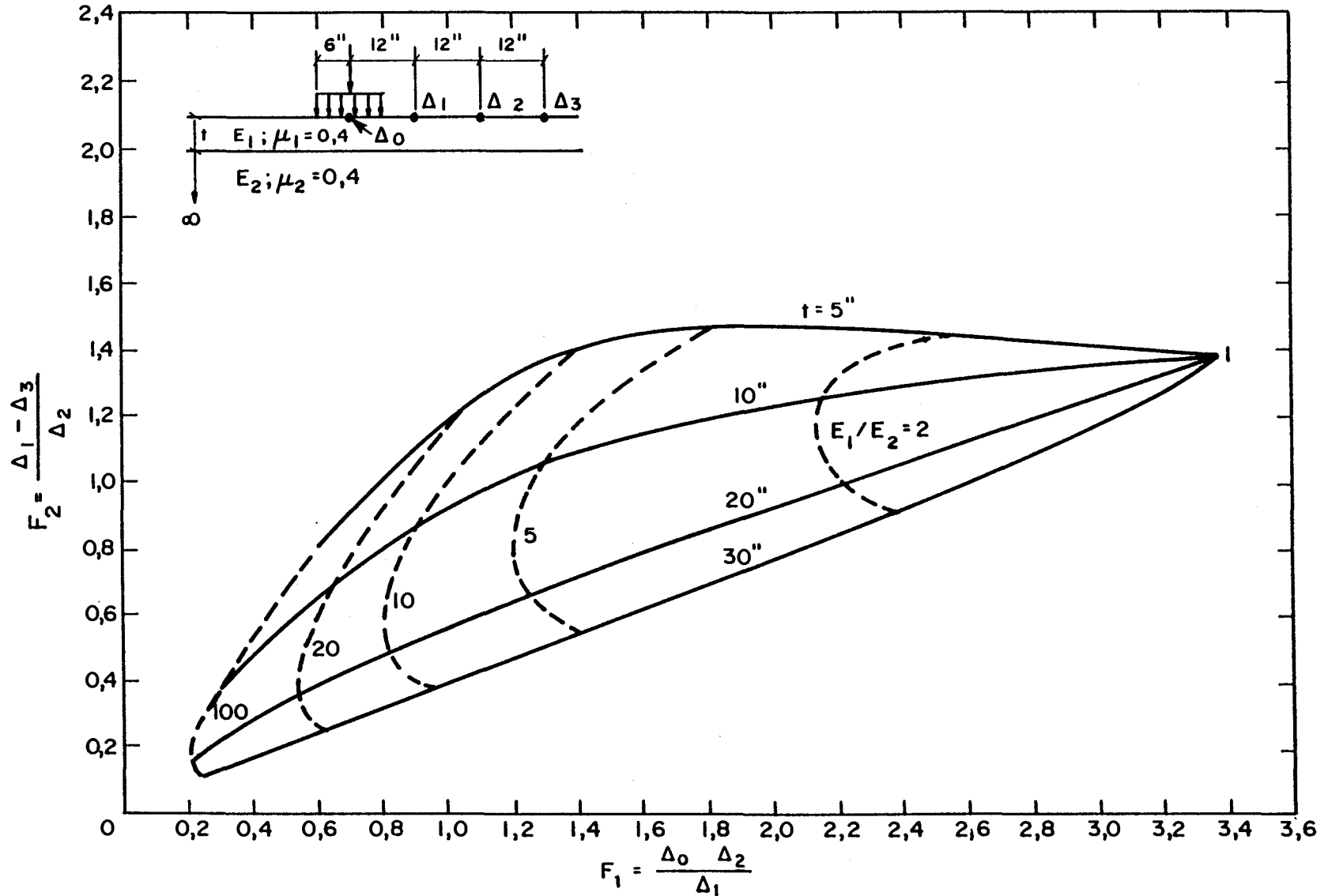
#### 4 METHODS INCORPORATING THREE OR MORE LAYERS

Linear elastic layer theory is widely used to determine effective elastic modulus values of the various layers based on back calculated deflection basin measurements. Although there are a wide variety of such computer models available with varying levels of sophistication only those relevant to the linear elastic theory



NOTE: DEFLECTIONS RESULTING FROM FALLING WEIGHT DEFLECTOMETER LOADING OR IDOT ROAD RATER LOADING MUST BE USED

**FIGURE 4.3**  
**VARIATION OF THE "AREA" AND THE MAXIMUM DEFLECTION FACTOR**  
**IN A TWO-LAYER LINEAR ELASTIC MODEL (DIFFERENT THICKNESSES)**



4.10

FIGURE 4.4  
SHAPE FACTORS OF THE DEFLECTION BASIN IN A TWO-LAYER



will be referred to. Methods using deflection basin measurements or parameters as basic input are discussed briefly below.

#### 4.1 Methods using up to two deflection basin parameters

Grant and Walker (1972) describe a linear elastic layer theory approach to arrive at effective elastic moduli for a three-layered pavement structure. The deflection basin parameters  $\delta_0$  and R are used. Modular ratios of surfacing-over-base and base-over-subgrade are calculated with the CHEVRON computer program and plots in relation to  $\delta_0$  and R are derived, as shown in Figures 4.5 and 4.6. These relationships were developed for thin surfacings with granular bases, which are typical in South Africa. Modular ratios of the base-over-subgrade were defined as varying between two and four and the initial estimates of the subgrade modulus was derived from the relationship:

$$E_{\text{subgr}} = K * \text{CBR}$$

where K is a factor varying between 3,5 and 10,3 with the latter used in most cases.

Typical elastic moduli values are fixed for the asphalt surfacings as shown in Figures 4.5 and 4.6 with typical layer thicknesses for the surfacing and base layers. A Poisson ratio of 0,3 was used for the base and subgrade. Grant and Walker (1972) therefore conclude that "The above method could be used to obtain an estimation of the subgrade and base moduli for roads with thin asphalt surfacings".

The new Shell Pavement Design Manual (Shell, 1978) forms the basis of the method described by Koole (1979). The deflection basin parameters maximum deflection ( $\delta_0$ ) and deflection ratio (Q), determined from Falling Weight Deflectometer (FWD) measurements, are used. A three-layered linear elastic system is modelled. The pavement structure is characterized by eight variables:

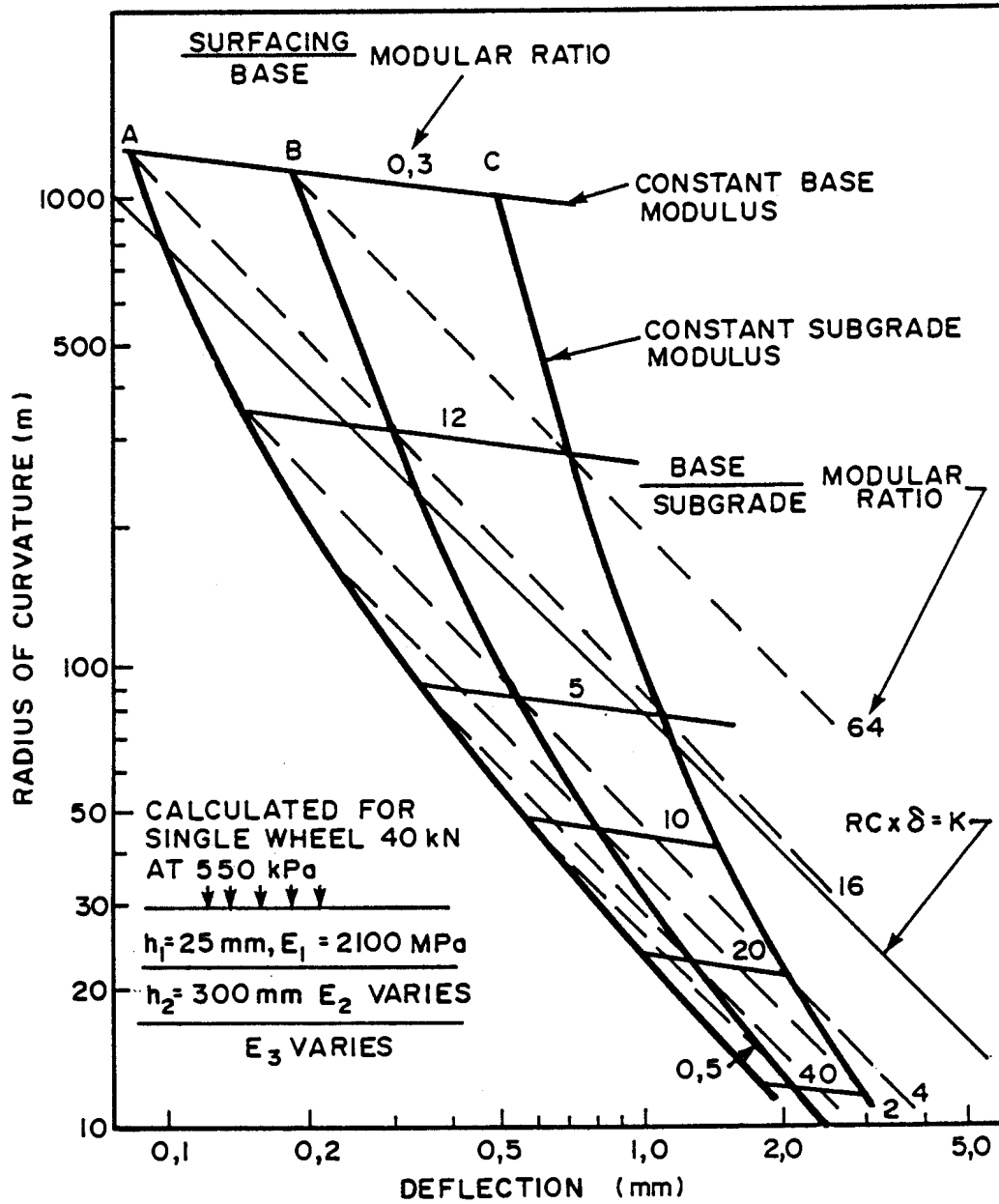


**FIGURE 4.5**  
RELATIONSHIPS BETWEEN DEFLECTION AND RADIUS OF CURVATURE FOR CONSTANT BASE MODULUS, CONSTANT SUBGRADE MODULUS AND CONSTANT BASE/SUBGRADE MODULAR RATIO (SINGLE LOADED AREA (Grant and Walker, 1972))

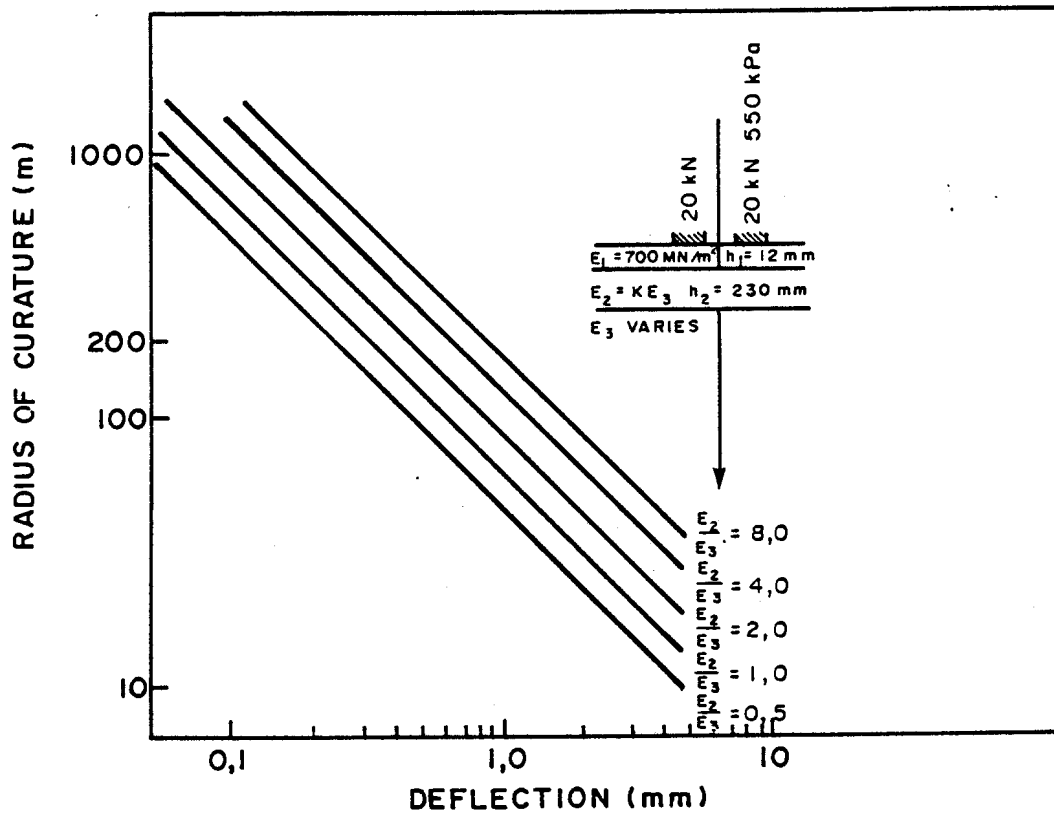


FIGURE 4.6  
PRACTICAL MEASUREMENTS OF DEFLECTION  
AND RADIUS OF CURVATURE RELATED TO  
THEORETICAL BASE/SUBGRADE MODULAR  
RATIOS ( DUAL LOADED AREAS) (Grant and Walker,1972)





$h_1, h_2, E_1, E_2, E_3, \nu_1, \nu_2$  and  $\nu_3$ .

Two assumptions are made: Poisson's ratio is taken as being equal to 0,35 for all the layers and the effective modulus of the unbound base layer is a function of its thickness,  $h_2$ , and the subgrade modulus  $E_3$ . The relationship of Dorman and Metcalf (1963) is used:

$$E_2 = k * E_3$$

where:  $k = 0,2 h_2^{0,45}$ ;  $2 < k < 4$  and  $h_2$  is measured in millimeters.

The computer program BISAR is used to prepare a typical graphical chart such as that shown in Figure 4.7. In this case typical values of  $E_3 = 100$  MPa and  $h_2 = 300$  mm are used. The value of  $h_1$  is determined from coring results or as-built records. By varying these values of  $E_3, E_2$  and a resulting  $E_1$ , deflection basin parameters maximum deflection ( $\delta_0$ ) and deflection ratio ( $Q_r$ ) are matched and values of effective moduli are thus obtained. Koole (1979) states that estimate values of effective moduli for cement-treated bases derived from past experience or measurements should be used as input in the BISAR computer analysis. The nomograph in the Shell Pavement Design Manual (Shell, 1978) is a well-known procedure to determine estimate values of the effective moduli for the asphalt layer.

Snaith et al. (1980) analyse and arrive at effective elastic moduli for a three-layered pavement structure using the familiar relationship between CBR and subgrade elastic modulus and the relationship between the effective moduli of the base layer (granular) and the subgrade. These are the same relationships as those described in the methods proposed by Grant and Walker (1972) and Koole (1979).

Snaith et al. (1980) use the deflection basin parameter,  $\delta_0$ , as measured with a Benkelman beam. A simple method of

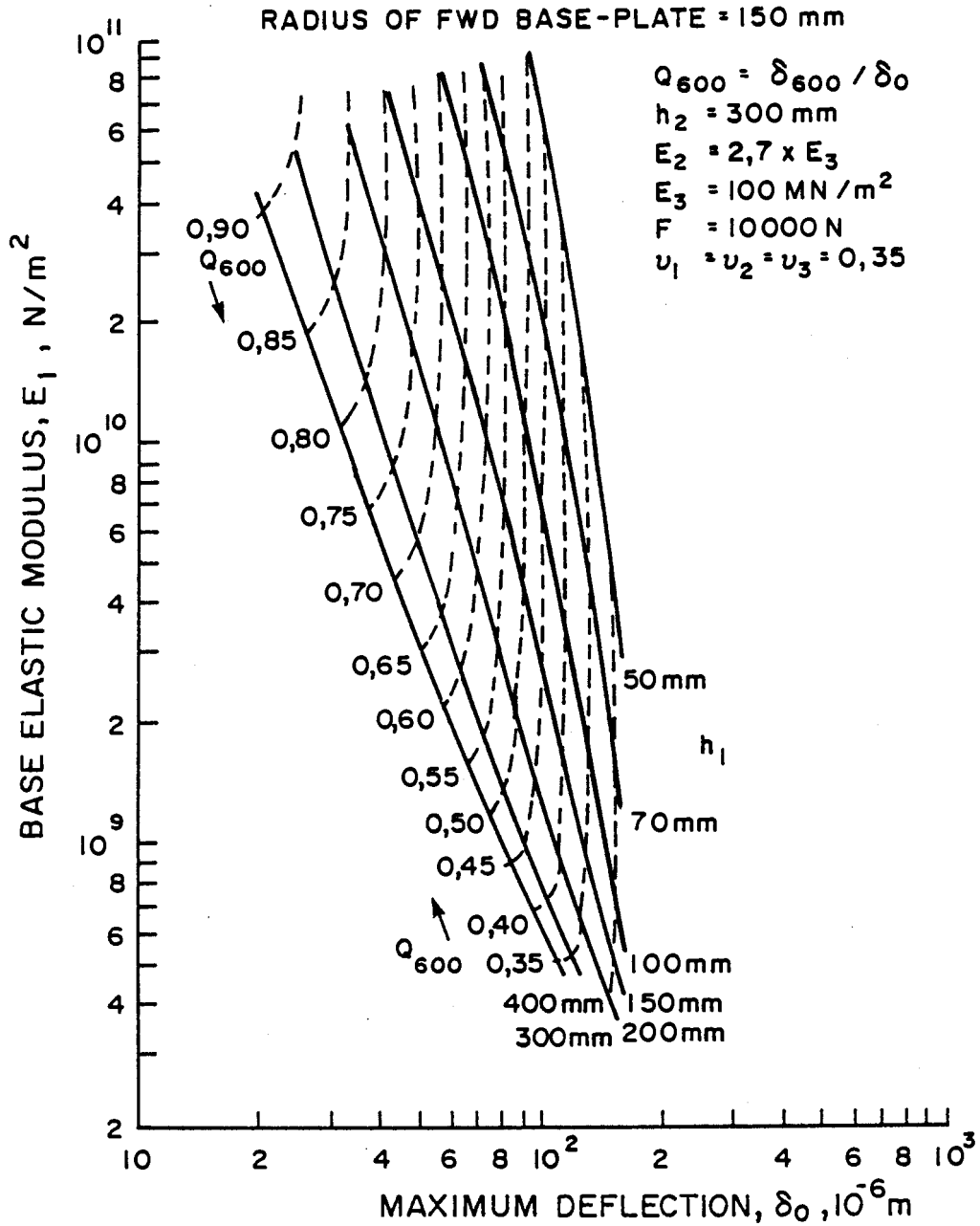


FIGURE 4.7  
DEFLECTION INTERPRETATION CHART  
(Kooie, 1979)



approximating equivalent thicknesses (Odemark, 1949) is used. The solution consists of two steps:

- (a) transformation of the multi-layered system into a single layer with equivalent thickness, and
- (b) use of the solutions for distributed loads on the surface of a linear elastic semi-infinite mass.

In order to change the layered system into an elastic half-space the equivalent thickness ( $H_e$ ) is calculated for each layer. The principle is that the equivalent layer has the same stiffness as the original layer, so as to give the same pressure distribution underneath the layer. This results in the following relationship:

$$H_e = h_1 \left[ \frac{E_1^* (1 - \nu_2^2)}{E_2^* (1 - \nu_1^2)} \right]^{\frac{1}{3}}$$

If the value of the Poisson's ratio is the same for both materials, the expression is reduced to:

$$H_e = h_1 \left[ \frac{E_1}{E_2} \right]^{\frac{1}{3}}$$

For a uniform vertical loading on a circular area, the deflection  $\delta_0$  at any depth  $Z$  at the centre of the loaded area is given by

$$\delta_Z = \frac{(1+\nu)}{E} p a \left[ \frac{1}{(1+(Z/a)^2)^{\frac{1}{2}}} + (1-2\nu)(1+(Z/a)^2)^{\frac{1}{2}} \frac{Z}{a} \right]$$

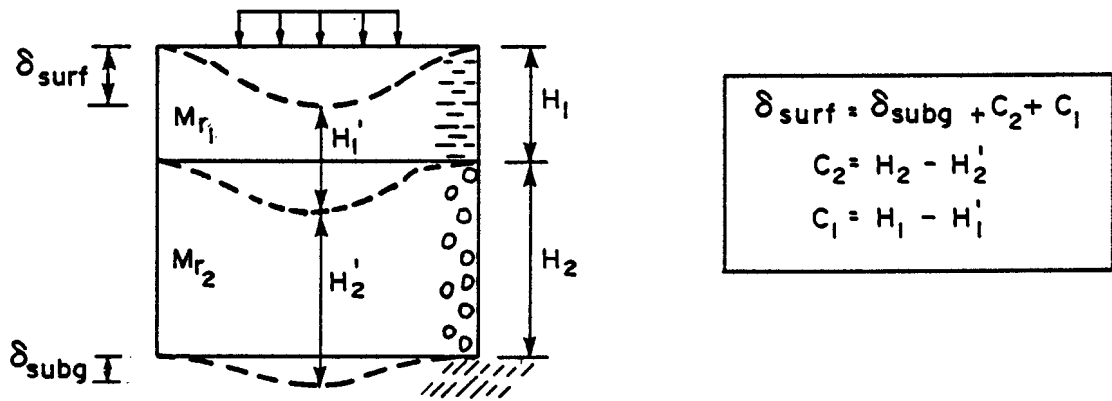


Estimate values of effective elastic moduli are used as input values to determine the value of  $\delta_o$ , which is compared with the measured value. The algorithm to arrive at this value is shown in the sketches in Figure 4.8. Snaith et al. (1980) use an electronic calculator to do the calculations and use the criterion of:

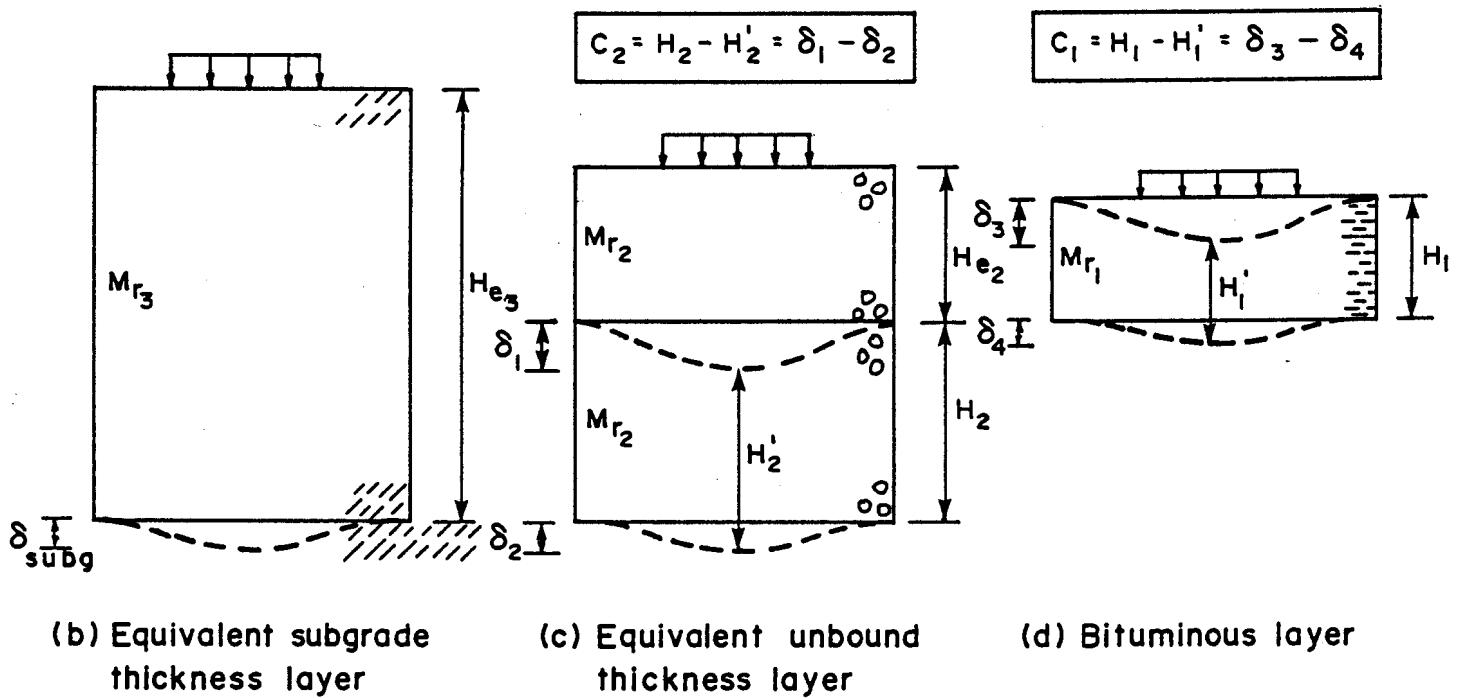
$$|\delta_{\text{surf}} - \delta_o(\text{measured})| < 0,05 (\delta_o(\text{measured})) \text{ for iterations.}$$

After a minimum of three deflection values have been found and plotted on graph paper, it is possible to estimate the required modulus value. It is not clear from the discussion by Snaith, et al. (1980) whether these deflection values refer to  $\delta_o$  alone, but this is assumed to be so owing to lack of indications to the contrary. A check calculation can be done with this estimate value. It is not clear how the load distribution measured under dual tyres is represented in the calculations. Snaith, et al (1980) obviously only consider one loaded area. Dehlen (1962b) also used Odemark's approximate solution for a multi-layered system. Dehlen (1962b) states that; "Because of doubtful validity of Odemark's theory away from the axis of load, no attempt was made to compute deflections or curvatures between dual wheels and, in the case of such tests, computations were made simply for a single circular load of the same area as the dual wheel imprint." The results of such computations are shown in Figure 4.9. Dehlen (1962b) further indicates that differences exist between Elastic Theory and practice, mainly in that deflections are more concentrated about the load than indicated by theory, and that they decrease more rapidly with depth.

Molenaar (1983) analysed a three-layered linear elastic system using measurements taken with a falling weight deflectometer (FWD). Molenaar (1983) also makes use of Odemark's (1949) equivalency theory. He states: "... the equivalent layer thickness is a magnitude which is meaningful and easily understood. A pavement with a high  $H_e$  will last longer than a pavement with a low  $H_e$ ". The equivalent layer thickness ( $H_e$ ) is determined as follows:



(a) Pavement layered system



(b) Equivalent subgrade thickness layer

(c) Equivalent unbound thickness layer

(d) Bituminous layer

FIGURE 4.8  
COMPONENTS OF A SURFACE DEFLECTION  
(Snaith, et al., 1980)

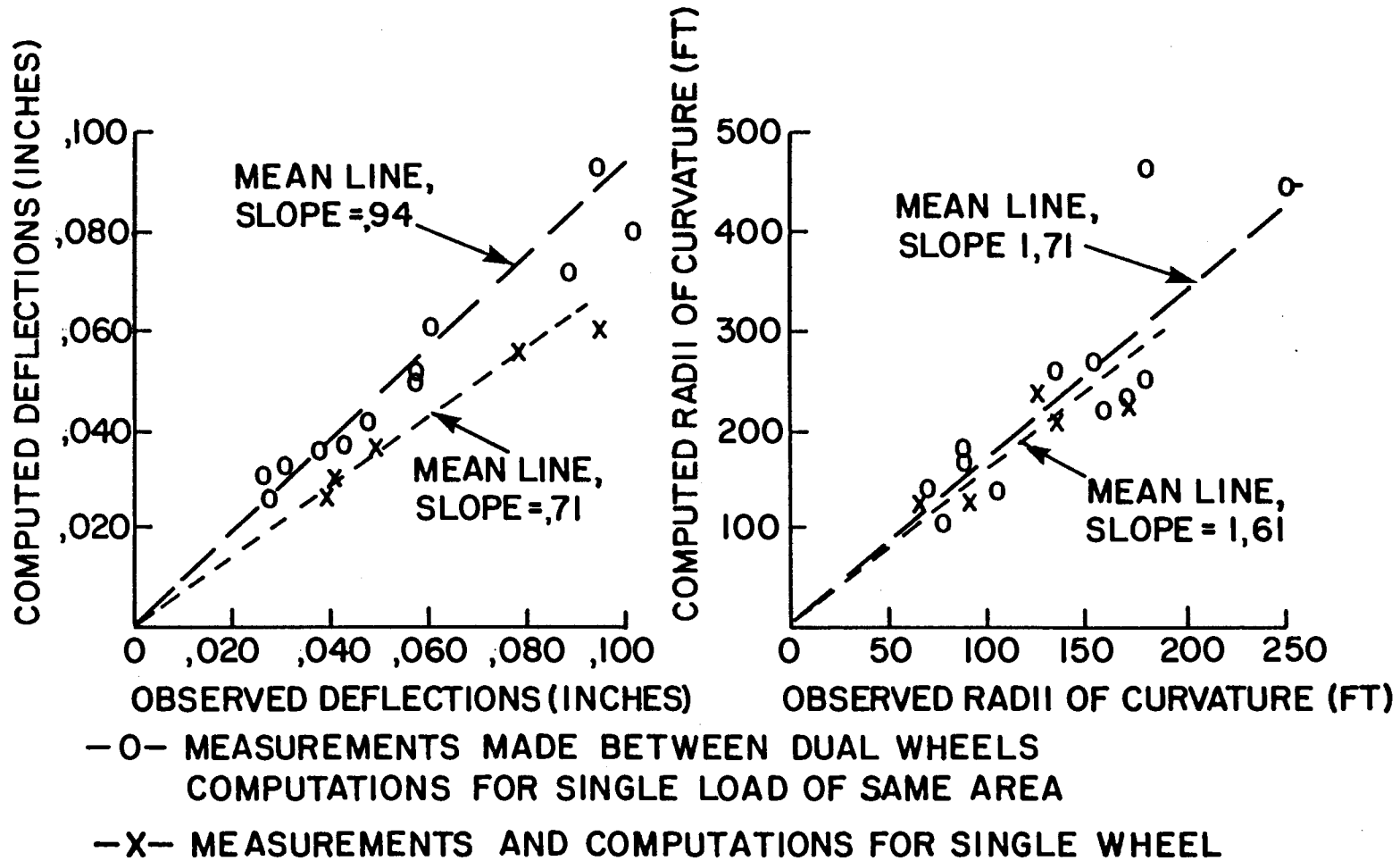


**FIGURE 4.9**  
**COMPARISON OF OBSERVED AND COMPUTED DEFLECTIONS**  
**AND RADII OF CURVATURE (Dehlen, 1962 b)**

$$H_e = 0,9 \sum_{i=1}^{L-1} h_i \left[ \frac{E_i}{E_s} \right]^{\frac{1}{3}}$$

where  $h_i$  = thickness of layer  $i$  in meter

$E_i$  = elastic modulus of layer  $i$  in  $N/m^2$

$E_s$  = elastic modulus of the subgrade in  $N/m^2$

$L$  = number of layers.

Using the deflection basin parameter, surface curvature index (SCI), relationships between the SCI and versus  $H_e$  are determined as shown for various subgrade moduli ( $E_s$ ) in Figure 4.10. This is for a three-layered pavement structure. The subgrade modulus is also calculated directly from the falling weight deflectometer (FWD) deflection basin as follows:

$$\log E_s = 9,87 - \log \delta_r$$

where  $r = 2$  meters from the loading centre and  $\delta_r$  is measured in mm. (The load force is 50 kN, loading time is 0,02 second).

Elastic moduli of the various layers can thus be back-calculated, if the layer thicknesses are known, using a curve similar to that described by Snaith et al. (1980), and using the general moduli relationship between base and subgrade and the Shell nomograph procedure as described by Koole (1979).

#### 4.2 Methods using at least three deflection basin parameters

For a more effective use of the whole measured deflection basin in the determination of effective elastic moduli, at least the same number of deflections should be used as the number of layers in the pavement structure. This general approach is described in a FHWA report (1984). Normally a maximum of five deflection basin measurements extending radially away from the centre of loading are used. In Figure 4.11 a four-layered elastic system is illustrated. When a load of known intensity is applied over a known area, deflections are created at some distance from the centre of the loaded area. It is normally

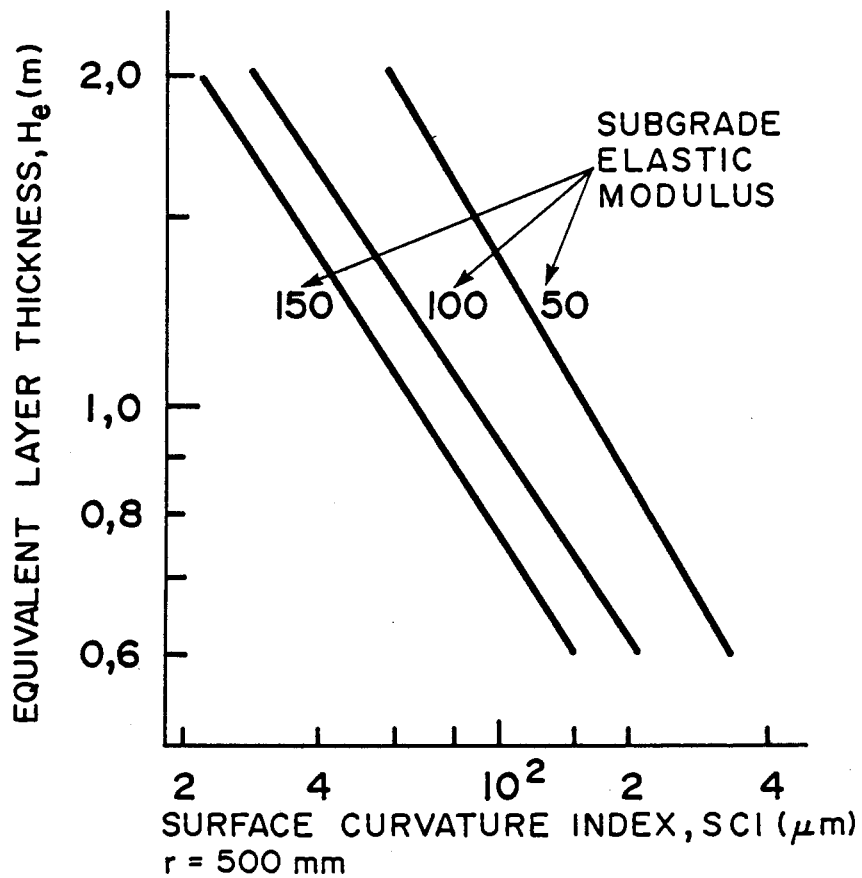


FIGURE 4.10  
 RELATION BETWEEN THE  
 SURFACE CURVATURE INDEX  
 (SCI) AND THE EQUIVALENT  
 LAYER THICKNESS ( $H_e$ )  
 (Molenaar, 1983)



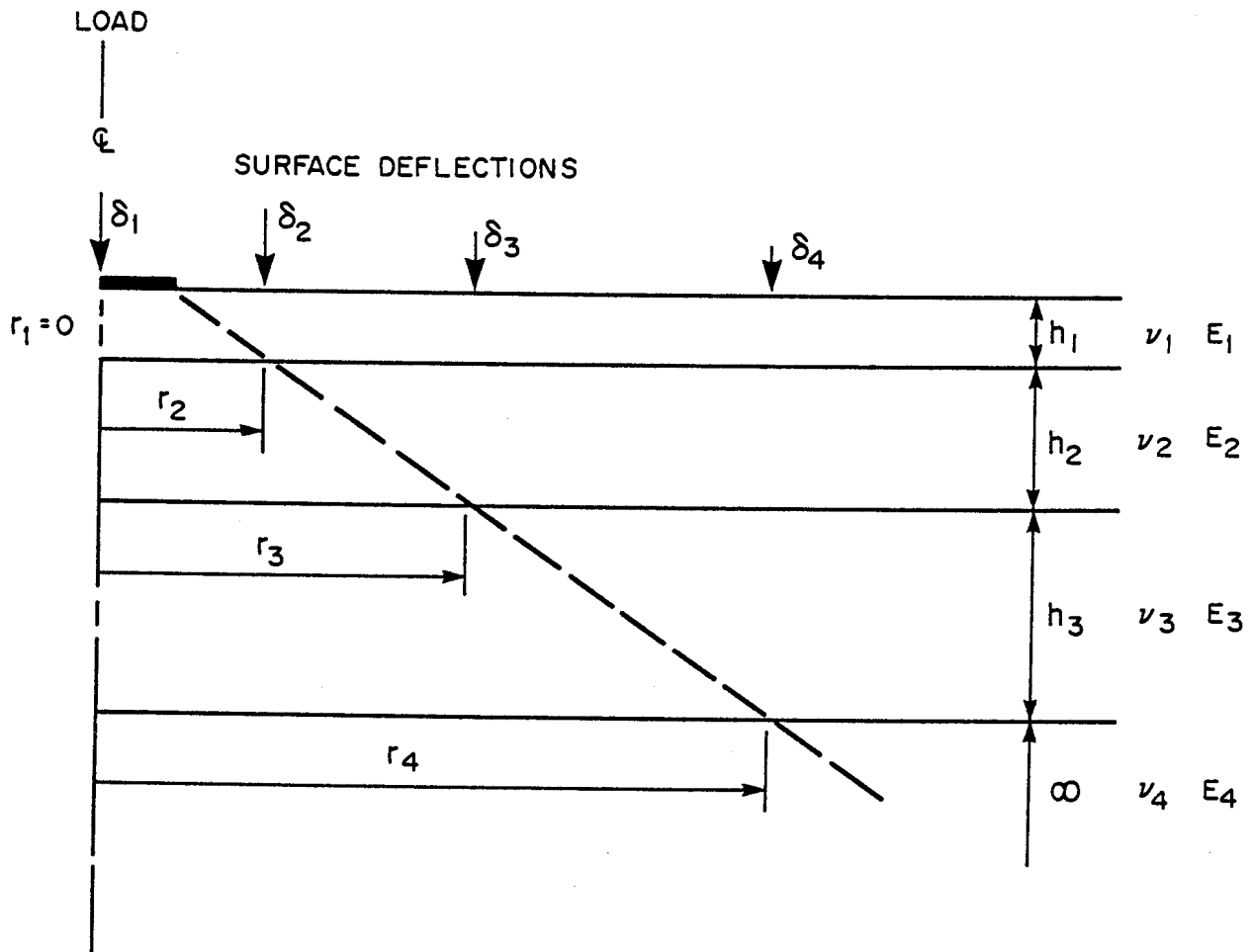


FIGURE 4.11  
FOUR LAYER ELASTIC REPRESENTATION OF A PAVEMENT  
SYSTEM (FHWA, 1984)

assumed that the load is distributed through the pavement system by a truncated cone (as shown by the dashed line in Figure 4.11).

Based on this concept, the deflection  $\delta_4$  at a distance  $r_4$  from the centre of the load is due to the "elastic" compression of layer 4 since layers 1,2 and 3 are outside the influence cone created by the load. Likewise, the deflection  $\delta_3$ , at distance  $r_3$  is due to the compression of layers 3 and 4; the deflection at distance  $r_2$  is due to compression in layers 2,3 and 4 and the deflection  $\delta_1$ , is due to compression in all layers. Thus by back-calculating one should work radially inwards from  $\delta_4$  at  $r_4$  towards the centre of loading in matching calculated deflections with measured deflections. This will result in the determination of effective elastic moduli of deep layers (subgrade) first and then of the other layers progressively upwards to the surface layer.

Using road rater data Kilareski et al. (1982) expressed this as follows:

$$\delta_1 \approx f1 (E_1, E_2, E_3, E_4)$$

$$\delta_2 \approx f2 (E_2, E_3, E_4)$$

$$\delta_3 \approx f3 (E_3, E_4)$$

$$\delta_4 \approx f4 (E_4)$$

This forms the basis of the successive approximation procedure. Estimate or seed values, as discussed previously, are assumed to start the iteration process. Using the BISAR computer program, the deflection values  $\delta_1^1$ ,  $\delta_2^1$ ,  $\delta_3^1$  and  $\delta_4^1$  corresponding to the assumed values of moduli are calculated. These calculated values are compared with the measured deflections,  $\delta_1$ ,  $\delta_2$ ,  $\delta_3$  and  $\delta_4$  at the measuring points as shown in Figure 4.11.

The correction method of the effective elastic moduli  $E_i$  is expressed as follows:

$$E_i \text{ new} = {}^1E_i \text{ old} \left( \frac{\delta_i^1 + \delta_i}{\delta_i^1} \right)$$

2

where  $i = 1$  to 4.



The corrections are made to the subgrade first ( $E_4$  and  $\delta_4^1$ ,  $\delta_4$  values) and a new deflection value is determined after which  $E_3$  is adjusted and then  $E_2$  and lastly  $E_1$  by calculating the new corresponding deflection value ( $\delta_i^1$ ) each time. This completes one iteration after which the process is repeated until the following criterion is met:

$$\text{Error}_i = \left[ \frac{\delta_i - \delta_i^1}{\delta_i^1} \right] * 100$$

where  $\text{Error}_1 = 5$  per cent allowed for  $\delta_1^1$  and  $\text{Error}_2$  and  $\text{Error}_3$   
 and  $\text{Error}_4 = 1$  per cent allowed for  $\delta_2^1$ ,  $\delta_3^1$  and  $\delta_4^1$ .

This is all done by an interactive computer program developed by Anani (1979).

With regard to the uniqueness of solutions, Kilaeski et al. (1982), state that unique values of  $E_4$  can be determined from  $\delta_4$  calculations and similarly unique values of  $E_3$  from  $\delta_3$  calculations. In order to ensure unique values of  $E_2$  and  $E_1$  from  $\delta_2^1$  and  $\delta_1^1$  calculations, a certain range of  $E_1/E_2$  ratios was assumed initially. This value was chosen as 0,7 as determined from laboratory resilient modulus testing on core samples.

MODCOMP I is a computer program developed by Irwin (1981) to interpret the moduli of elasticity of pavement layers from surface deflection data. The program can handle up to eight layers in the pavement using the CHEVRON n-layer code. Up to six surface deflections measured on the deflection basin are used. Measurements with vibration or impact devices are preferred in order to exclude plastic creep associated with Benkelman beam measurements. The principle of this analysis procedure is quoted as follows:

"At large radial distances the surface deflections are primarily the result of deformation in the deeper layers. Thus, the



magnitude of the moduli of shallow layers has very little influence on the surface deflections of the pavement at large distances from the load." The back-calculation procedure is then the same as that described by Kilareski et al. (1982).

Seed values or estimate values of elastic moduli are used as input. An interesting feature of this approach is that the deflection basin measurements are first interpolated with a curve-fitting subroutine (CRVFIT). This is done so that there are measured deflection values, corresponding radially to a 38-degree cone intersecting the pavement layer interfaces as shown in Figure 4.12. No reason for the choice of the 38-degree cone is given. Adjustments to the modulus of the layer underneath the relevant interface are made using the following equation:

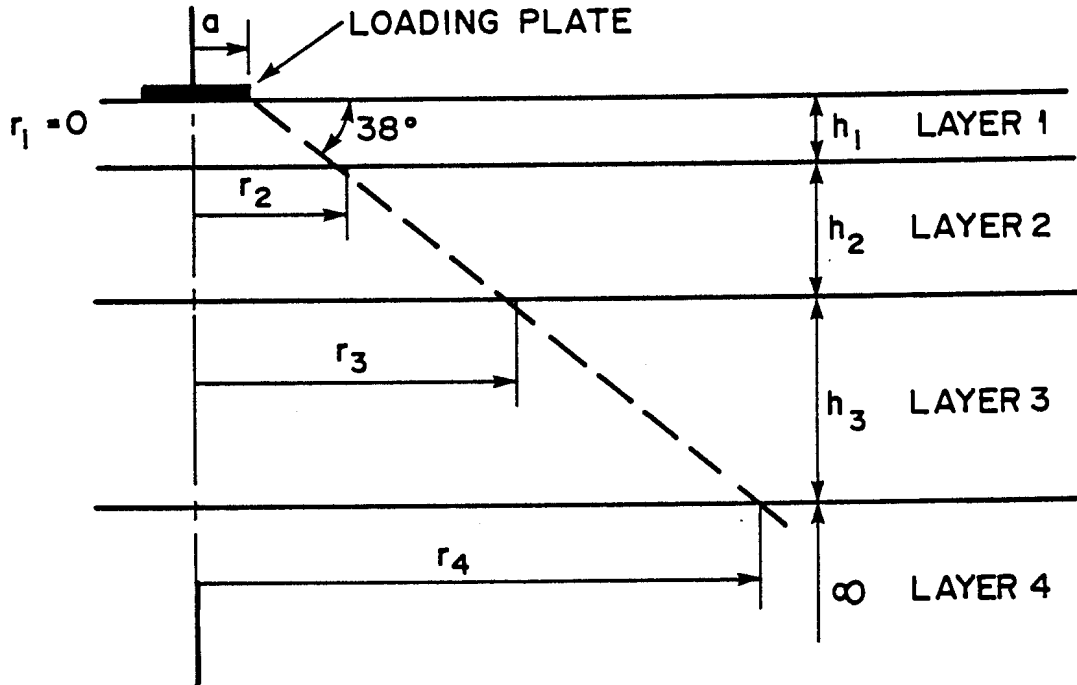
$$E_{\text{new}} = E_{\text{seed}} \left( 1 + 2 \frac{\delta_i^1 + \delta_i}{\delta_i} \right)$$

where  $\delta_i^1$  = calculated deflection at the  $i$ -th radius

$\delta_i$  = measured deflection at the  $i$ -th radius.

The factor 2 is used to accelerate the iteration process, but  $E_{\text{new}}$  is not allowed to become negative. Using the  $E_{\text{new}}$  value (all other values unchanged) the deflection at that point is recalculated. A linear interpolation is then made in log-log space so that a value of the modulus for the layer,  $E_{\text{interp}}$ , is obtained, based upon the measured deflection. From sensitivity analysis data, Irwin (1981) suggests that the tolerance level for computation purposes in MODCOMP I be five to ten times lower than the standard error of the measurement system ( $\pm 0,02$  mm).

The principle of modulus-at-depth as a function of the distance from the loaded area of the deflection basin is also the basis of the method used by Patterson and van Vuuren (1974). The use of the surface deflection basin is seen as a first method of determining effective elastic moduli. Deflection basin measurements were obtained with a modified Benkelman beam with a



CONE/LAYER INTERFACE INTERSECTIONS DEFINE RADII FOR CALCULATIONS

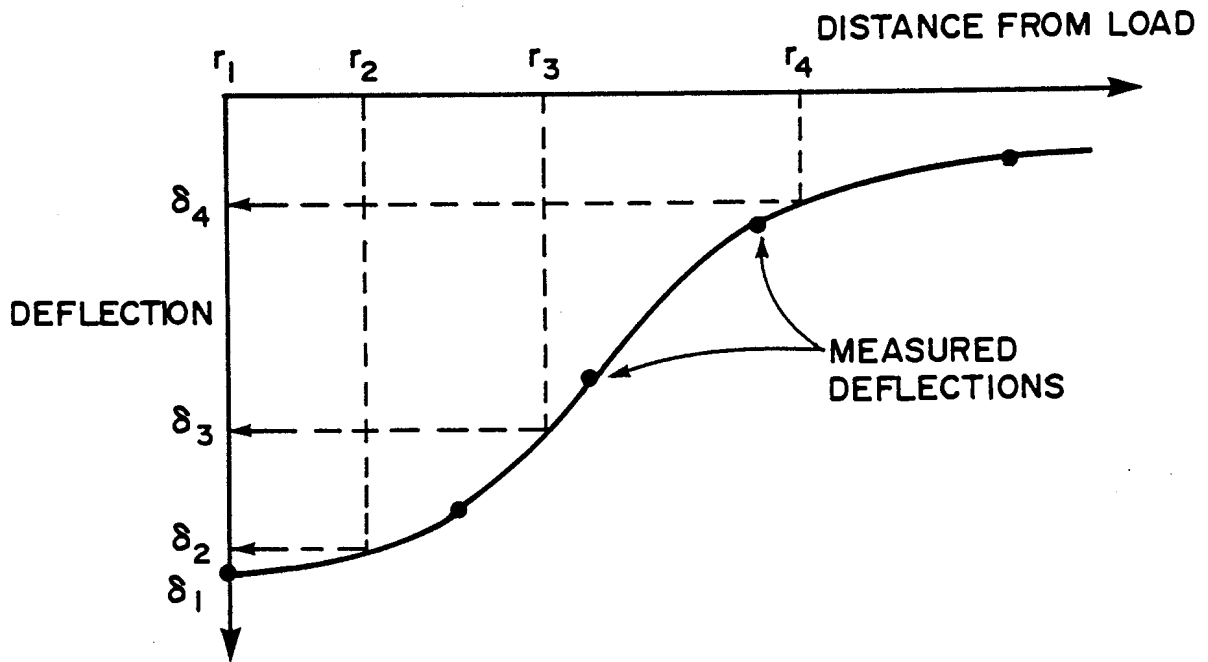


FIGURE 4.12  
DEFLECTION BASIN SHOWING MEASURED DEFLECTIONS AND CRVFIT SUBROUTINE INTERPOLATIONS (Irwin, 1981)

deflection transducer for a "continuous" output. Layer thicknesses and material estimates were used as input in a trial and error process using the CHEVRON and ELSYM programs. The same basic approach as described by Irwin (1981) and Kilareski et al. (1982) was followed to determine and fix effective elastic moduli values by using deflection basin values contracting radially. Figure 4.13 shows a typical result of matching measured and calculated deflection basins and derived effective elastic moduli.

Husain and George (1985) use the CHEVRON program to do deflection matching. The measured deflection basin of either Dynaflect or falling weight deflectometer (FWD) can be used. The deflection equation is inverted by a non-linear pattern search technique to determine the values of the layer moduli that would best fit the observed surface deflections. The elastic modulus of the asphalt concrete layer is corrected for temperature and the base and subbase moduli are corrected for stress dependency. The algorithm used, starts from the surface layer and proceeds to the subgrade. A general gradient technique is used in order to minimize the sum of squared errors.

The principle of deflection at distance from load applied being a function of material characteristics also forms the basis of the model used by Marchionna et al. (1985). In general the model is as follows;

$$\delta_i = f(CM_{1,1}, \dots, CM_{K,J}, \dots, S_1, \dots, S_K, F)$$

where

- $\delta_i$  = deflection relative to the point located at distance  $r_i$
- $CM_{K,J}$  = Jth mechanical characteristic of the material relative to the Kth layer
- $S_K$  = thickness of the Kth layer
- $F$  = load applied

The falling weight deflectometer (FWD) is used with seven measuring positions and an elastic four layered pavement

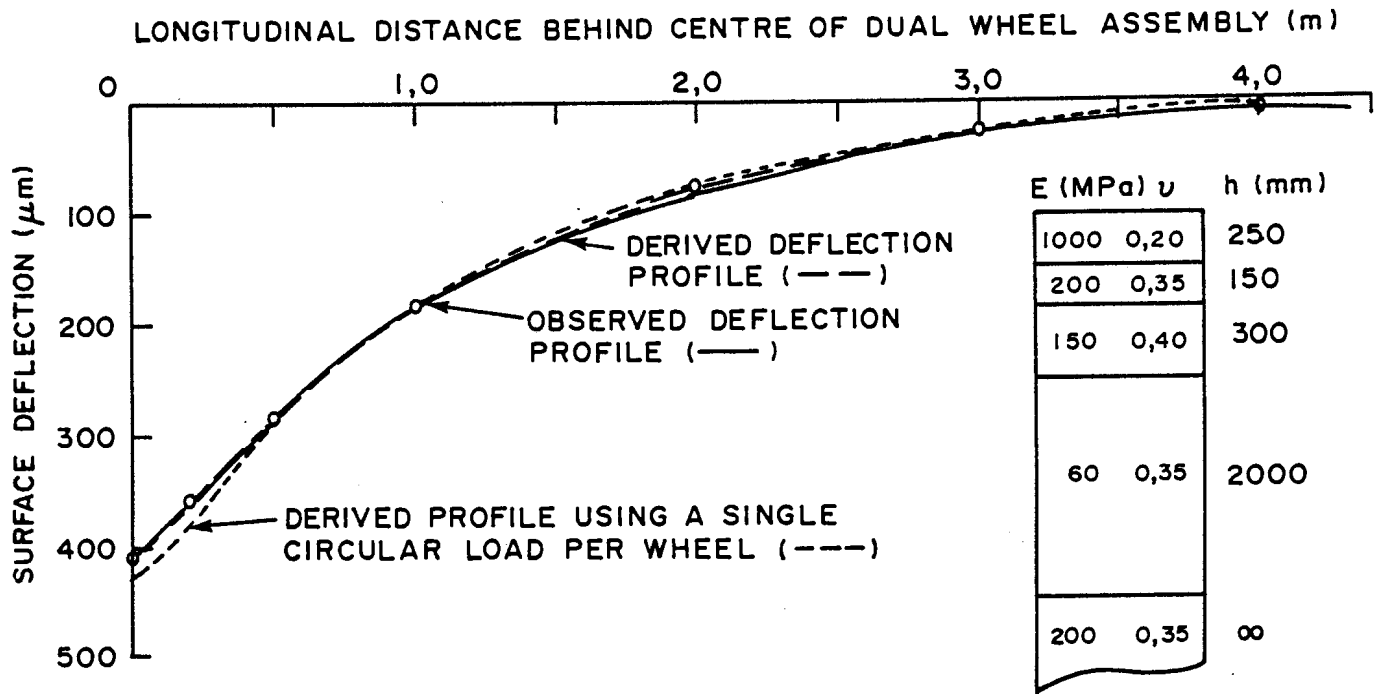


FIGURE 4.13  
SIMULATION OF LONGITUDINAL SURFACE DEFLECTION  
INFLUENCE LINE AND DERIVED MODULI  
(Patterson and van Vuuren, 1974)

structure is used. Bound or treated materials are linear elastic in this model, but granular bases and subbases and subgrade layers are treated as non-linear elastic. The analysis is carried out with the method of finite elements and the Non-linear Structural Analysis Program (NONSAP), developed at the University of California, is used. Various subroutines were added in order to use a technique of multiple regressions to find the expression of the  $\delta_i$  functions that best interpreted the data available and met the conditions described.

The method of equivalent thicknesses described by Odemark (1949) forms the basis of the procedure described by Ullidtz and Peattie (1982). Surface deflections are measured with the FWD at the centre of loading ( $\delta_0$ ) and a minimum of two other positions ( $\delta_1$ , and  $\delta_2$ ). It is specified that  $\delta_2$  be measured at a distance (radially from the load centre) of at least five times the load area radius ( $a$ ); it must also be more than the thickness of the equivalent layer thickness ( $H_e$ ). The latter is calculated in accordance with the description by Koole (1979). He gives the reason for the distance specification is that "at large distances the surface deflections are approximately inversely proportional to the modulus of the subgrade".

Layer thicknesses are determined by coring and estimated values of elastic moduli are assigned to each layer. Values of surface deflections are calculated by using computer programs like BISTRO or CHEVRON, or Finite element method programs. Ullidtz and Peattie (1980) suggest the use of programmable calculators using the equivalent layer thickness approach.

The equivalent surface modulus  $E_0$  (the modulus of the half-space that would give the same surface deflection as the multi-layer structure) is calculated as follows at corresponding distance  $r_2$  where  $\delta_2$  is measured :

$$E_0 = \frac{(1-\nu^2) p a^2}{r_2 \delta_2}$$



where the symbols are as previously described by Snaith et al. (1980) for the two-layered pavement system. For the prescribed value of  $r_2$  the equivalent surface modulus ( $E_0$ ) is approximately equal to the subgrade modulus. The subgrade estimate modulus value is adjusted and the value  $\delta_2^1$  is calculated and compared with the measured value  $\delta_2$ .

The stiffness of the asphalt layer is determined using the ratio of the deflections  $\delta_0^1$ . This ratio is highly dependent on the stiffness of the upper layer. If the calculated value of the ratio is less than the measured value, the estimated value of the stiffness of the asphalt layer must be increased because a high ratio corresponds with a high stiffness in the asphalt layer. The stiffness of the intermediate layer (normally granular) is determined from  $\delta_0$ . Stubstad and Harris (1984) state that the latter is the least accurate value.

Laboratory-derived ratios of  $E_1/E_2$  and  $E_2/E_3$  are used as tolerances or guides. Some of these relationships used by Shell and described by Koole (1979) are also used. In the later versions the program ELMOD on the HP85 microcomputer are used to analyse a four-layered pavement structure. In this program higher precision was reached if the following conditions were met:

- (a) The structure should contain only one stiff layer; if there are more they should be combined into one layer for the purpose of structural evaluation
- (b) Moduli should decrease with depth
- (c) The thickness of the upper (stiff) layer ( $h_1$ ) should be greater than half the radius of the loading plate ( $a/2$ )
- (d) When testing is done near a joint or a large crack or on gravel roads, the structure should be treated as a two-layer system.

Non-linearity of materials was also accommodated for by using a mainframe computer program ISSEM4 which can model a four-layer

pavement. Ullidtz (1982), however, gives guidelines on how to accommodate stress softening (nonlinear) subgrade layers by constructing diagrams based on calculations done with finite element computer programmes. This was done for a two-layer system but formed the basis of the iteration process to determine moduli values for the subgrade.

Adjustments were made for temperature, time of loading and other environmental influences throughout the year. These were built in as standard features of the ELMOD program described above. In conclusion on this method Epps and Hicks (1982) state that: "The method proposed by Ullidtz and Peattie (1980) comes closest to a "universal" technique, but required the use of a computer. As the capabilities of small computers increase and as their use becomes more widespread, this requirement will be less and less of a deterrent to its use."

Stubstad and Corner (1983) made use of this latter method using the FWD to predict damage potential on Alaskan highways during spring thaw. The similarity with stabilized subbases is illustrated by their statement; "... it was immediately noticed that the same tendency toward virtually no deflection at large distances from the FWD load was occurring during the early spring of 1982. Such a phenomenon can only occur if the underlying layers have a high stiffness or modulus of elasticity. It was thus decided to use layered elastic theory to determine the effects of thaw depth and other material characteristics on the seven FWD deflections."

Bush (1980) developed an evaluation procedure for light aircraft pavements based on a layered elastic model. The CHEVDEF program used was developed to determine the set of modulus values that provide the best fit between a measured deflection basin and a computed deflection basin when given an initial estimate of the modulus values, a range of modulus values and a set of measured deflections. Deflections were measured with the Model 2008 Road Rater. Two force levels were used (5 000 and 7 000 lb) in order to predict the non-linear

stress-dependent behaviour of the subgrade material. Results from the CHEVDEF program gave the relationship for the deviator stress and the modulus for the subgrade materials.

Thompson and Hoffman (1983) used the ILLI-PAVE computer programme to develop deflection basin algorithms for conventional flexible pavements and full depth asphalt concrete pavements. The effect of non-linearity of the subgrade of such three layered pavement structures is taken into consideration.

Tam (1985) use the same approach as Kilaeski, et al. (1982) to calculate effective elastic moduli by relating the deeper layers to the outer deflections. Thus by fixing effective elastic moduli from the bottom upwards, deflections are fitted radially inwards. Tam (1985) however make use of the BISAR or BISTRO computer programs rather than CHEVRON. The reason is illustrated in Figure 4.14 where the calculated deflection basins for the specific pavement structure and loading conditions are shown as calculated by BISTRO and CHEVRON. It is clear that the CHEVRON program has a slight discrepancy in the area between the edge of the loaded wheel and + 400 mm from the centre of loading. This tendency was confirmed by Taute et al. (1981) on stiffer pavement types, too. The discrepancy is more pronounced on lighter flexible pavement.

Before the iteration procedure is applied with the typical linear elastic approach, Tam (1985) takes the non-linearity of the subgrade into consideration. This is done by subdividing the subgrade into rather thick layers (0,6 to 1,0 m). The effective elastic modulus of each layer is then calculated as follows:

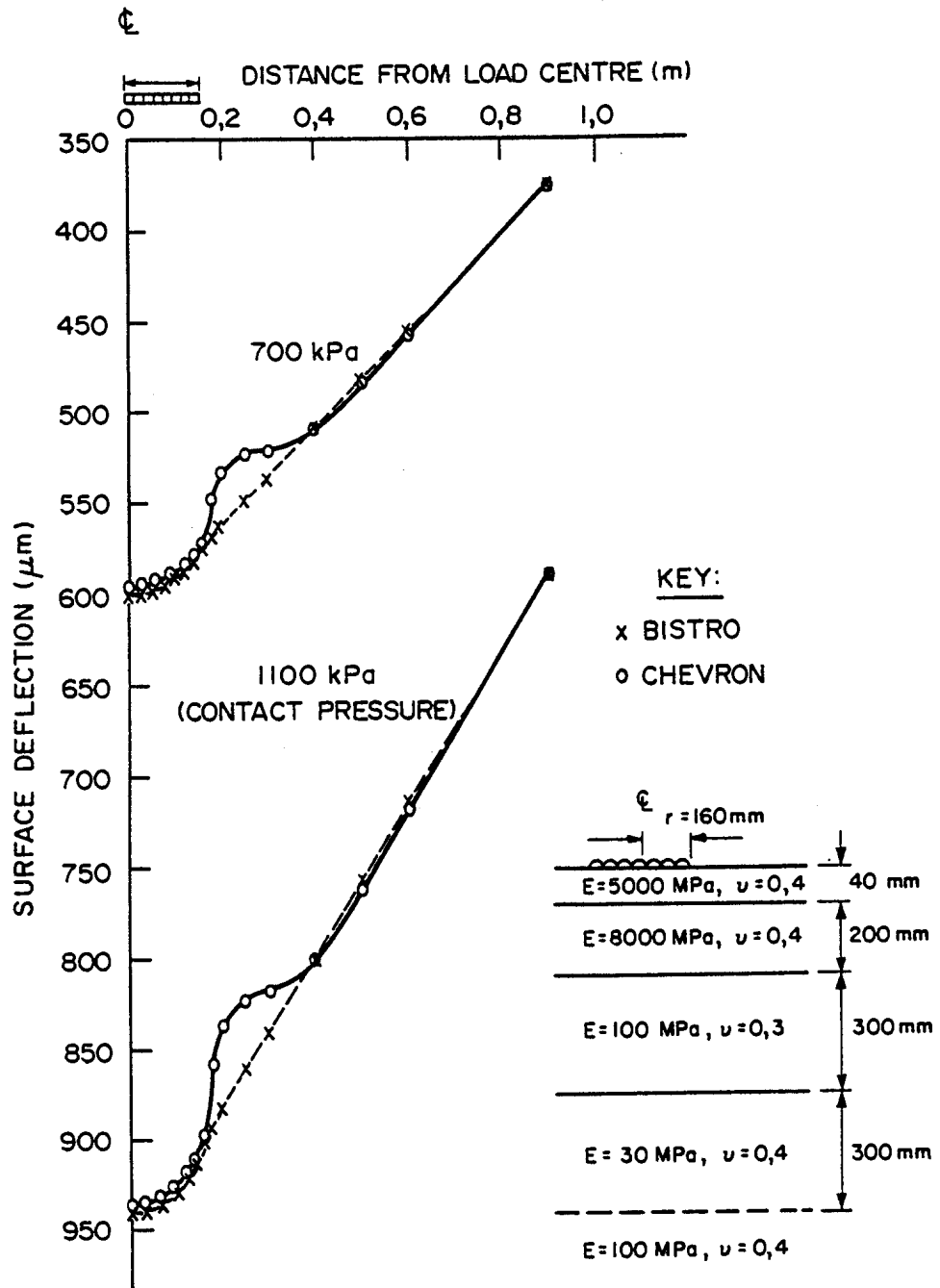


FIGURE 4.14  
COMPARISON OF DEFLECTIONS CALCULATED BY  
BISTRO AND CHEVRON PROGRAMS  
(Tam, 1985)



$$E = A \left| \frac{P_o^1}{q} \right|^B$$

where E is the elastic modulus (MPa)

$P_o^1$  is the initial effective everburden stress (MPa)

q is the deviator stress due to applied load (MPa)

A is the amplification factor (MPa)

B is the nonlinear power coefficient.

The seed values of A and B are selected as 50 MPa and 0,2. By using the deflection measured at a distance of 1,2 m from the load centre, A is first adjusted and then B. When all the subgrade layers have been fixed, the normal iteration procedure, as described earlier, starts.

## 5 CONCLUSIONS AND RECOMMENDATIONS

Estimate values of effective elastic moduli, based on laboratory and field observations, form the basis of the majority of back calculation procedures discussed. The mechanistic procedure used in South Africa forms an excellent basis for these estimate values of effective moduli as discussed. It is believed that by extending the field observations, in particular the HVS tests, this initial estimation procedure can be refined even further.

The analysis procedures have been described at length and for this reason only recommendations related to the South African position will be made. The linear elastic layered computer programs currently in use in South Africa are capable of back-calculating effective elastic moduli values from deflection basin data. Normally there is a maximum of five layers, which require at least five deflection measurements extending radially away from the centre of loading. Various researchers have suggested that the basic relationship of deflection measured radially from the load centre is a function of the various individual layers or combinations thereof. Some have even suggested an angle of intersection

of the interfaces of layers in depth to determine optimal deflection measuring points radially. It is clear from the methods discussed that the re-iterative back-calculation procedure should work radially inwards to match calculated deflections with measured deflections. This would result in the determination of effective elastic moduli for the surface layer. It is evident that this approach focuses on the ideal linear elastic condition and that factors like non-linearity, nonuniformity and stress dependence are mostly ignored. Finite element method computer programs are becoming more readily available and can be used; non-linear models can also be investigated. It is suggested that correlation studies should be done for each type of pavement in order to establish these relationships. Methods to accommodate the non-linearity of the subgrade with the linear elastic computer models available exist and can be investigated.

In none of the methods discussed was much emphasis placed on cementitious bases and subbases and their analysis procedures. It is believed that enough information from HVS tests is available to analyse these pavements accurately with linear elastic layered computer programs. This would include, for example, information on the various stages of cracking of these layers. This also stresses the need for the analysis procedures to be related to the pavement category or class and behaviour state.

As was suggested in Chapter 3 the vast amount of information gained from RSD and MDD results makes it possible to calculate effective elastic moduli by various means for various pavement structures, loading conditions, moisture conditions and equivalent axle repetitions. This may lead to extensive regression analyses done in order to relate deflection basin parameters for the suggested pavement classes to the structural conditions related to structural life and behavioural states.

Serious consideration and analysis should be given to incorporating methods based on Odemark's (1949) equivalent layer thickness theory. It has proved to be a method that can satisfy mechanistic design method criteria. In order to establish this, extensive regression analyses need to be done with the above-mentioned available data.



## CHAPTER 5

### EFFECTIVE ELASTIC MODULI DETERMINED FROM ROAD SURFACE DEFLECTOMETER MEASUREMENTS

**CHAPTER 5 : CONTENTS**

	PAGE
1 INTRODUCTION	5.2
2 EFFECTIVE ELASTIC MODULI CALCULATED FROM DEPTH DEFLECTIONS	5.2
3 EFFECTIVE ELASTIC MODULI CALCULATED FROM SURFACE DEFLECTIONS	5.4
3.1 General	5.4
3.2 The back-calculation procedure	5.6
3.3 Non-linearity of the subgrade	5.9
3.4 Determining effective elastic moduli	5.11
3.4.1 Assuming linearity of the subgrade	5.11
3.4.2 Assuming non-linearity of the subgrade	5.14
4 SUMMARY AND CONCLUSIONS	5.16





## 1 INTRODUCTION

Deflections are measured on the surface and in depth of a pavement when tested with the accelerated testing facilities, the Heavy Vehicle Simulators (HVSs). In the past the deflections as measured in depth with the Multi-Depth Deflectometer (MDD) were used to determine the effective elastic moduli of the various layers with satisfactory results. The whole deflection basin, as measured on the surface with the Road Surface Deflectometer (RSD), was always available for determining effective elastic moduli.

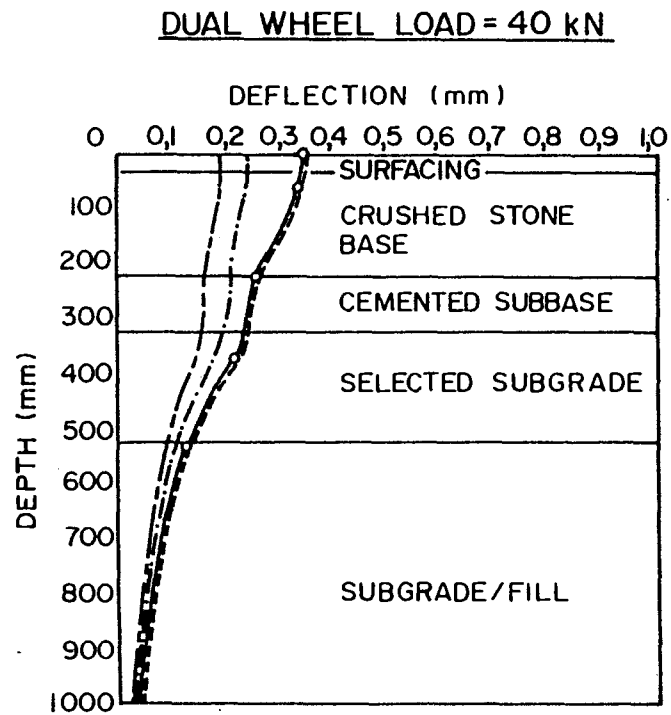
The method whereby effective elastic moduli are determined with the MDD is briefly described. The author proposed a new method for determining effective elastic moduli from measured RSD deflection basins which is described in detail. The effective elastic moduli determined from RSD and MDD deflections from selected accelerated tests are compared and conclusions drawn from that. The non-linearity of the subgrade is investigated by determining the effective elastic modulus by means of the proposed method and comparing the results with the normal linear-elastic approach.

## 2 EFFECTIVE ELASTIC MODULI CALCULATED FROM DEPTH DEFLECTIONS

Deflections are measured at various depths within the pavement structure as a standard procedure (Freeme et al, 1982) on sections tested with the accelerated testing facility, the Heavy Vehicle Simulator (HVS). The deflections are measured with the Multi-Depth Deflectometer (MDD) (Basson et al, 1980). Measurements of resilient deflections with depth are taken throughout the test under various wheel loads and these yield a good record of the change in structural response of the pavement.

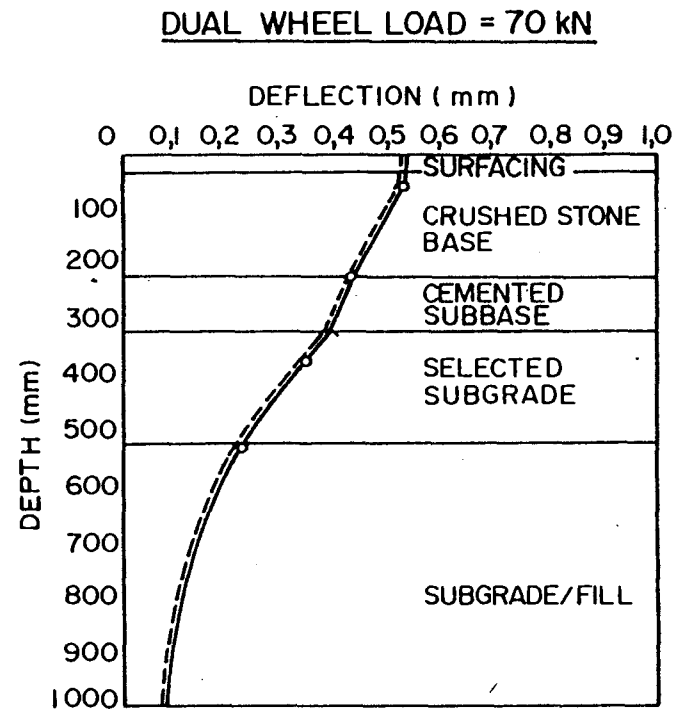
Effective elastic moduli are calculated from these MDD deflections (Maree et al, 1981) by using linear-elastic theory and a linear-elastic layered computer program such as ELSYM5 (University of California, 1972). The iteration procedure whereby moduli values of the various layers are estimated and the measured deflections in depth are matched by the calculated deflections, is illustrated in Figure 5.1 (Maree et al, 1981a). The procedure is illustrated for a 40 and 70 kN wheel load. The slope of the depth deflection curve

940-4-3331 /2 BS



LEGEND:

- MEASURED DEFLECTION
- $E_{BASE} = 450 \text{ MPa}$ ;  $E_{SUBBASE} = 3500 \text{ MPa}$
- $E_{BASE} = 450 \text{ MPa}$ ;  $E_{SUBBASE} = 600 \text{ MPa}$
- $E_{BASE} = 200 \text{ MPa}$ ;  $E_{SUBBASE} = 500 \text{ MPa}$



LEGEND:

- MEASURED DEFLECTION
- $E_{BASE} = 300 \text{ MPa}$ ;  $E_{SUBBASE} = 500 \text{ MPa}$
- $E_{BASE} = 450 \text{ MPa}$ ;  $E_{SUBBASE} = 600 \text{ MPa}$

FIGURE 5.1

MEASURED AND CALCULATED DEPTH DEFLECTIONS (ROAD P157/1)

at any point is an indicator of the modulus of the material at that depth.

This manual method of adjusting moduli values was automated (Coetzee and Horak, 1981) using the CHEV4 computer program (Abbot, 1977). This program was later adjusted to handle up to 15 layers (Coetzee, 1982). The moduli determined from the depth deflections are used as input values for further detailed mechanistic analyses of the pavement structures tested (Maree et al, 1981b).

### 3 EFFECTIVE ELASTIC MODULI CALCULATED FROM SURFACE DEFLECTIONS

#### 3.1 General

The full deflection basin can be measured on the surface of a pavement, using the WASHO procedure (Monismith, 1979). This is measured on HVS test sections with the Road Surface Deflectometer (RSD) (Basson, 1985). In the past only the maximum deflection and radius of curvature were calculated from RSD data. Recently better use was made of the full deflection basin by calculating other deflection basin parameters too (Horak, 1985). In order to make use of the measured deflection basins more effectively, various researchers have used the full deflection basin to calculate effective elastic moduli (Horak, 1984).

In such a procedure to determine effective elastic moduli from surface deflections, at least the same number of deflections should be used as the number of layers in the pavement structure. In Figure 5.2 it is illustrated how the measured deflections, from the surface deflection basin, are used in a typical four-layered elastic system. It is assumed that the load is distributed through the pavement system by a truncated cone intersecting the pavement layers at an angle ( $\alpha$ ). Based on the concept of linear elasticity, deflection  $\delta_4$  at a distance  $r_4$  is due to the elastic compression of layer 4 while deflection  $\delta_3$  at distance  $r_3$  is due to the elastic compression of layer 3 and 4. The result is that maximum deflection  $\delta_1$  in Figure 5.2, is due to the deflection of the effective elastic moduli of all the layers ( $\delta_1 = f(E_1, E_2, E_3, E_4)$ ).

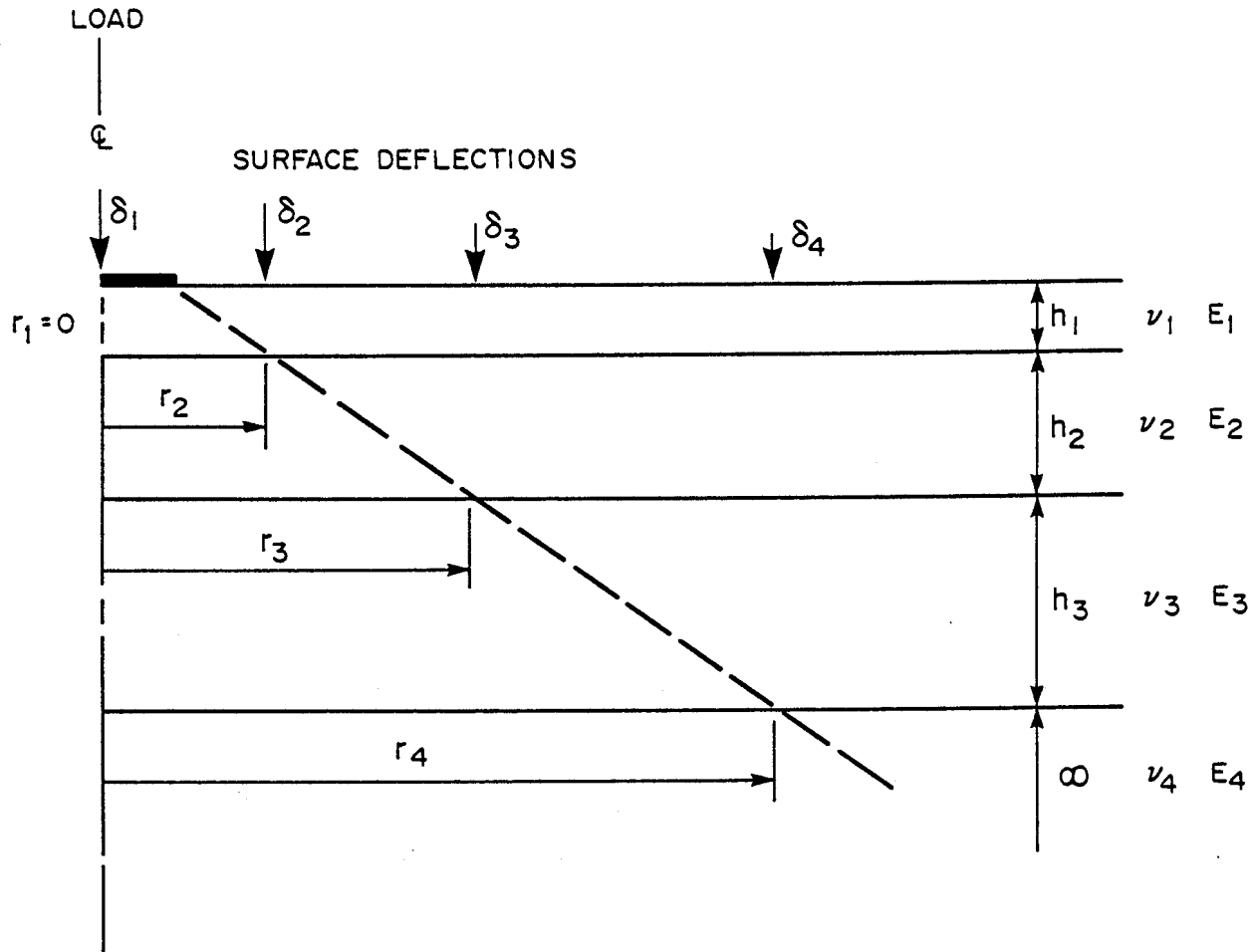


FIGURE 5.2  
FOUR LAYER ELASTIC REPRESENTATION OF A PAVEMENT  
SYSTEM (FHWA, 1984)

### 3.2 The back-calculation procedure

In the back-calculation procedure the effective elastic modulus of the subgrade ( $E_4$ ) is calculated first by fitting the deflection at distance  $r_4$  to the measured deflection  $\delta_4$ . Then follows the calculation of  $E_3$  by calculating and fitting the deflection at distance  $r_3$  to the measured deflection  $\delta_3$ . Effective elastic moduli are therefore calculated from the lower layers upwards by fitting the deflections radially inwards towards maximum deflection.

The BISAR computer program (Horak, 1985) is used in this back-calculation procedure because of its superior accuracy in the vicinity of the loaded wheels (Tam, 1985). Estimate or seed values of elastic moduli are initially assumed for all the layers based on material information, as-built information and material type. These seed values are then adjusted by comparing the calculated deflection with the respective measured deflection at that point considered. This adjustment procedure is done in two phases. The first phase makes use of an interpolation procedure to save computer time. The second phase uses these calculated effective elastic moduli as input or as seed values and calculates the effective elastic moduli more accurately.

In Figure 5.3 the flow diagram of the first phase of adjustment is illustrated. The deflection ( $\delta_i^{\text{seed1}}$ ), as calculated from seed values ( $E_i^{\text{seed1}}$ ), is calculated and compared with the measured deflection ( $\delta_i^{\text{meas.}}$ ). A tolerance of 5  $\mu$ -meter (0,005 mm) is used to decide whether an adjustment is necessary. If there is an adjustment necessary,  $E_i^{\text{Calc.1}}$  is calculated as shown. The factor 2 in the calculation is used to deliberately overcompensate. The BISAR program is run again and now a linear interpolation is used in a log-log space (deflection versus modulus) as indicated in Figure 5.3. The value  $E_i^{\text{interp.}}$  is now used as the new seed value in the calculation and adjustment of the other layers in phase 1 until all the layers are adjusted in such a way.

In phase 2 the seed values of the elastic moduli are those calculated as  $E_i^{\text{interp.}}$  in phase 1. This is illustrated in Figure 5.4.

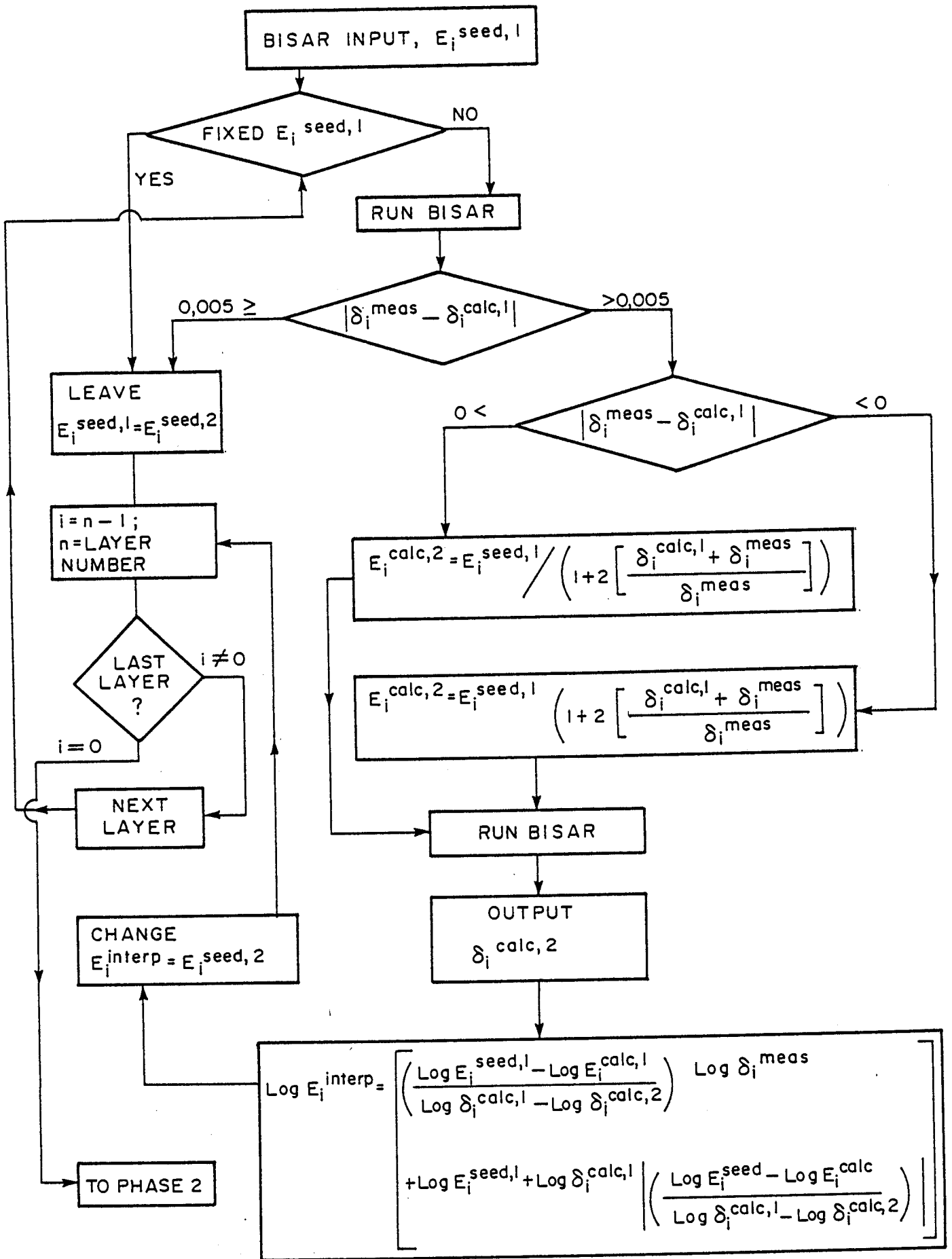


FIGURE 5.3

FLOW DIAGRAM OF PHASE I OF PROGRAM BISFT

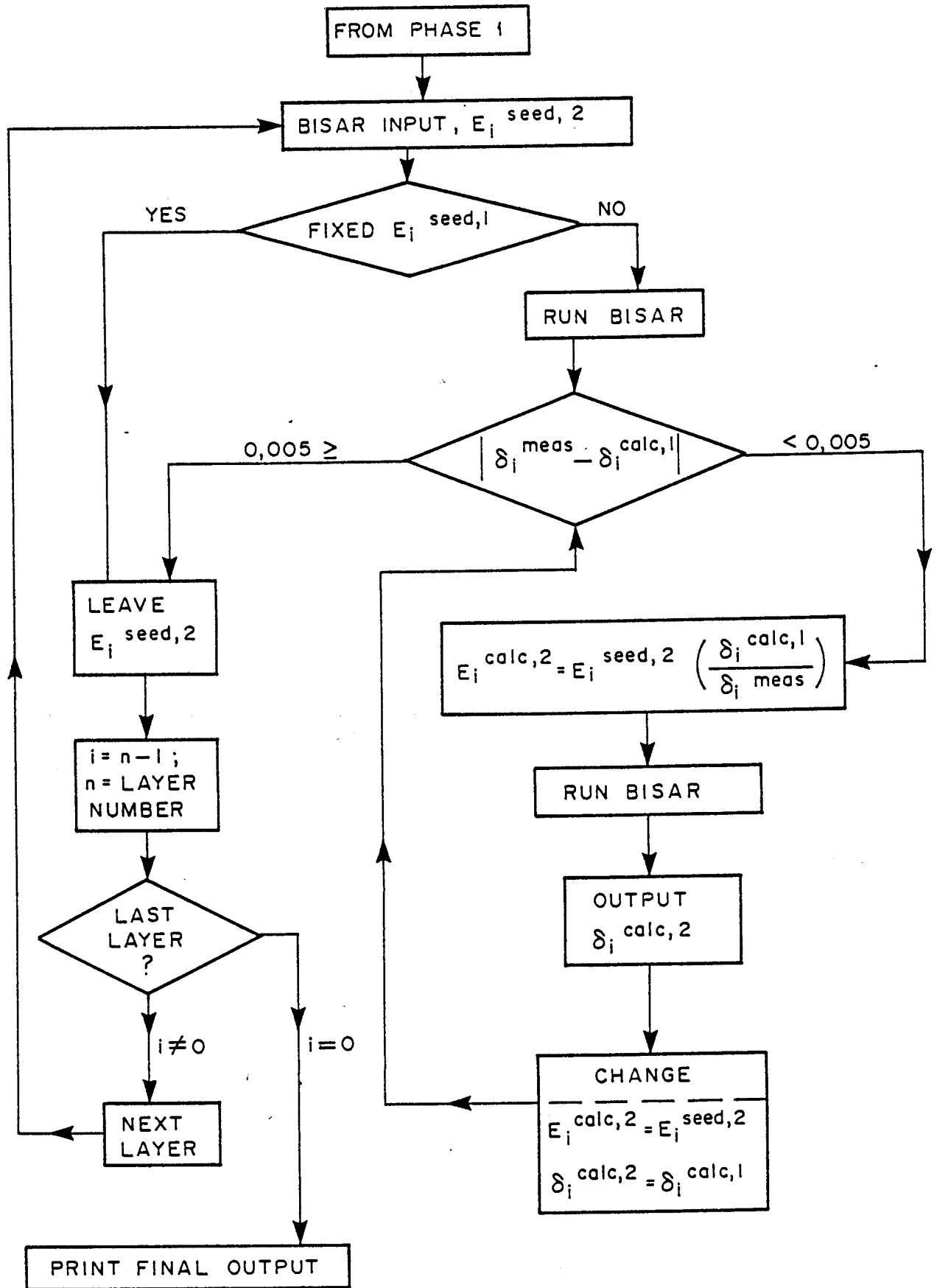


FIGURE 5.4

FLOW DIAGRAM OF PHASE 2 OF PROGRAM BISFT

The deflections calculated ( $\delta_i^{\text{calc},1}$ ) and measured ( $\delta_i^{\text{meas.}}$ ) are checked against the specified tolerance of 5  $\mu$ -meter in order to adjust as indicated. Each layer is adjusted in the sequence as discussed earlier. A maximum of 5 total iteration loops are allowed at this phase to limit computer time. An iteration loop is seen as the adjustment of all the layers.

As the adjustment of effective elastic moduli of the layers near the surface are more difficult to determine and more costly in terms of computer time (Tam, 1985) an option to fix the effective elastic modulus ( $E_i^{\text{Seed, fixed}}$ ) was built into the program. In general the material information, as-built information and knowledge of these layers are such that the material can be classified accurately (Freeme, 1983). The non-linearity of the subgrade is not considered yet in the BSFT back-calculation program. This can however be done manually beforehand.

### 3.3 Non-linearity of the subgrade

The mechanistic design and analysis procedure in South Africa does not yet accommodate the non-linearity of the subgrade. The back-calculation procedure of the MDD inherently makes use of a non-linear approach though. With the assumption that deflection at a depth of 2 meter (where the MDD is anchored) is zero, it is implied in the back-calculation procedure that below 2 meter there exists a semi-infinite rigid layer or a layer with a rather high effective elastic modulus.

The approach that is suggested, is based on the procedure described by Tam (1985). The subgrade is subdivided into four layers with thicknesses of 0,6 m, 1,0 m, 1,0 m and 2,0 m respectively, overlaying a semi-infinite layer. The BISAR computer program is then used to calculate effective elastic moduli at mid-depth of each layer and 2,0 m into the semi-infinite layer. The seed values for the effective elastic moduli as derived by means of BSFT are used as input for the other structural layers. The deflection at distance  $(n-1)305$  mm (where  $n$  is the number of structural layers) from maximum deflection ( $\delta_0$ ) is first checked for non-linearity. This will be 1220 mm for a





a five layered system. If the measured deflection ( $\delta_{1220}^m$ ) differs more than 0,005 mm from the calculated deflection ( $\delta_{1220}^c$ ), non-linearity is assumed in the subgrade. The seed effective elastic moduli of the subgrade layers are then altered by using the equation below as derived by Brown (1979);

$$E_{\text{subg.}} = A \frac{P_o^{1-B}}{q}$$

where E is the subgrade layer effective elastic modulus (MPa)

$P_o^1$  is the initial effective overburden stress (MPa),

$$(P_o = 1/3 (\sigma_1^1 + 2(\sigma_3^1)))$$

q is the deviatoric stress due to applied load (MPa),

$$(q = \sigma_1^1 - \sigma_3^1)$$

A is the amplification factor (MPa)

B is the nonlinear power coefficient

$\sigma_1^1$  and  $\sigma_3^1$  are effective major and minor principle stresses (MPa)

In the iteration procedure, the value of A is taken as the subgrade effective modulus as determined in the linear BSFT program. The value of B is taken as 0,2 as suggested by Tam (1985). In a typical five-layered pavement structure, the deflection at 1220 mm ( $\delta_{1220}$ ) is used to adjust the value of A first, using:

$$A_{i+1} = A_i \left( \frac{\delta_c}{\delta_m} \right)$$

where  $A_i$  and  $A_{i+1}$  are the i-th and (i+1)th iterative value of A  
 $\delta_c$  and  $\delta_m$  are the calculated and measured deflections respectively.

With the new value of A and the same value of B, a new set of subgrade effective elastic moduli are computed. The effective elastic moduli of the other structural layers are kept the same.

This process is repeated until the difference between the measured and calculated deflections at 1220 mm is less than 0,005 mm. The deflection at  $n \times 305$  mm, which is 1525 mm for a 5 layered system, is then used for comparison purposes. The non-linear power coefficient,  $B$ , is then adjusted as follows:

$$B_{i+1} = B_i \left( \frac{\delta_c + \delta_m}{2\delta_c} \right)$$

where  $B_{i+1}$  and  $B_i$  are the  $(i+1)$ th and  $i$ -th iterative values of  $B$  and  $\delta_c$  and  $\delta_m$  are the calculated and measured deflections at 1525 mm from load centre. This process of adjusting  $B$  and the effective elastic moduli of the subgrade layers is repeated until the criterion of 0,005 mm deflection difference is satisfied.

### 3.4 Determining effective elastic moduli

#### 3.4.1 Assuming linearity of the subgrade

Effective elastic moduli were determined from selected pavement structures as tested with the accelerated testing facility, the HVS. The layer depths are known and the effective elastic moduli had already been determined in some cases using the depth deflections from the MDD. The effective elastic moduli were calculated using the measured surface deflection basin data as described in Section 3.2. The angle  $\alpha$ , shown in Figure 5.2 was taken as  $38^\circ$  as standard after  $\alpha$  was varied between  $30^\circ$ ,  $45^\circ$  and  $60^\circ$ . The value of  $30^\circ$  was found to give effective elastic moduli that were better related to those determined with the MDD measurements. This is however also a function of pavement type and material type.

The wheel load used in the calculations was 40 kN with a 520 kPa tyre pressure. In Table 5.1 the calculated effective elastic moduli are shown for a typical granular base pavement tested at Erasmia (Horak, 1986a). The effective elastic moduli as determined from MDD and RSD measurements are shown for each structural layer at various repetitions. In order to compare the effective elastic moduli determined with the two measurements, the modular ratios (RSD method/MDD method) are

also shown. A modular ratio of about 1 would indicate nearly the same effective elastic moduli as determined by both measuring techniques.

The BSFT back-calculation program uses increasingly more time to calculate effective elastic moduli nearer to the surface. This is related to the calculation procedure as outlined in Section 3.2 and the difficulty of achieving the specified accuracy. In order to save computer time, the effective elastic moduli of the surfacing and the granular base layer were fixed. The fixing was based on other material information and prior determined effective elastic moduli with MDD deflections.

TABLE 5.1 - Calculated effective elastic moduli (Erasmia)

Actual repetitions	Layer description	Effective elastic moduli (MPa) determined from		Modular ratio**
		MDD*	RSD**	
10	Base	390	400	1,03
	Subbase	1 180	499	0,42
	Selected	210	210	1,00
	Subgrade	200	230	1,15
196 000	Base	150	150	1,00
	Subbase	230	163	0,71
	Selected	125	43	0,34
	Subgrade	85	194	2,28
564 000	Base	235	240	1,02
	Subbase	220	145	0,66
	Selected	130	58	0,45
	Subgrade	85	220	2,59
700 000	Base	205	210	1,02
	Subbase	230	151	0,66
	Selected	100	23	0,23
	Subgrade	55	210	3,82
1 009 000	Base	195	200	1,03
	Subbase	220	155	0,71
	Selected	120	37	0,31
	Subgrade	55	270	4,91

\* MDD measured depth deflections and RSD surface deflections

\*\* Ratio of RSD/MDD effective elastic moduli

For that reason the modular ratio of the base layer is constantly in the region of 1 in Table 5.1.

In the pre-cracked phase of the cemented subbase, the effective elastic moduli determined from RSD measurements indicate a lower value than the one determined from MDD measurements. In the cracked phase of the subbase, the modular ratio increases from the initial low 0,42 to a rather constant 0,6 to 0,7. This still indicates an undercalculation with the RSD measurements.

The same tendency of undercalculation by using RSD measurements is also true when the effective elastic moduli of the selected layer are inspected. In this case though, the undercalculation becomes worse with the increase in actual repetitions. The subgrade, in contrast, is however constantly overcalculated when the effective elastic moduli determined with RSD measurements are compared with those determined with MDD measurements. This overcalculation increases with the increase in actual repetitions.

It is therefore obvious from the calculated subgrade effective elastic moduli that the non-linearity of the subgrade is not initially influencing the effective elastic moduli of the subgrade, but at a later stage of trafficking it seems to become more influential. The shift in balance, when the subbase cracks, seems to have an effect on both the subbase and the selected layer underneath. This shift in balance can also be reflected by the effective elastic moduli of the subgrade.

In Table 5.2 the effective elastic moduli as calculated from RSD deflection measurements are shown for a typical light-structured granular pavement at Malmesbury (Horak, 1986a).

In this case no effective elastic moduli were determined with MDD deflections. It is clear though that the pavement balance did change to a much deeper structure as the actual repetitions increased. The base and selected layers showed a steady decrease in effective elastic moduli as actual repetitions increased. The structurally stronger subbase and the subgrade

showed initial decreases in effective elastic moduli, but increased again towards the end. The effective elastic moduli of the base and surfacing were again fixed at values as determined with the aid of other material information.

TABLE 5.2 - Calculated effective elastic moduli (Malmesbury)

Actual repetitions	Layer description	Effective elastic moduli from RSD deflections (MPa)
10	Base	80
	Subbase	200
	Selected	60
	Subgrade	230
50 000	Base	60
	Subbase	138
	Selected	35
	Subgrade	161
200 000	Base	50
	Subbase	100
	Selected	28
	Subgrade	157
350 000	Base	45
	Subbase	123
	Selected	30
	Subgrade	230
496 000	Base	45
	Subbase	107
	Selected	28
	Subgrade	285
591 000	Base	40
	Subbase	143
	Selected	30
	Subgrade	521

#### 3.4.2 Assuming non-linearity of the subgrade

The procedure as set out in Section 3.3 was followed in a few selected cases. This was done to determine whether the subgrades do exhibit non-linear behaviour and whether it affects the calculated effective elastic moduli of the other structural layers. The results are shown in Table 5.3.

In the case of the Erasmus test it is clear at the start of the test that there is no strong evidence of non-linearity of the subgrade in depth of the pavement. The average subgrade effective elastic modulus of 350 MPa is higher than the 230 MPa of the linear approach. That difference is due to the calculation procedure of the non-linear approach further away from the centre of loading. It also illustrates some stress dependency as the calculation point is deeper into the structure in the non-linear approach. In the recalculation with BSFT of the effective elastic moduli of the other structural layers, the subbase did increase to a more realistic figure for a cemented subbase.

TABLE 5.3 - Effective elastic moduli with a linear and non-linear approach

Test	Actual repetitions	Layer description	Effective elastic moduli (MPa)	
			Linear	Non-linear
Erasmia	10	Base	400	400
		Subbase	499	912
		Selected	210	210
		Subgrade	230	359
		Subgrade	-	349
		Subgrade	-	353
		Subgrade	-	353
		Subgrade	-	353
Erasmia	1 009 000	Base	200	200
		Subbase	155	155
		Selected	37	19
		Subgrade	270	466
		Subgrade	-	627
		Subgrade	-	638
		Subgrade	-	640
		Subgrade	-	648
Malmesbury	591 000	Base	40	40
		Subbase	143	177
		Selected	30	25
		Subgrade	521	760
		Subgrade	-	1 004
		Subgrade	-	1 003
		Subgrade	-	1 002
		Subgrade	-	1 001

Towards the end of the test at Erasmia (1 009 000 actual repetitions) stronger evidence of non-linearity was shown by the subgrade. This tendency of non-linearity is true in depth of the subgrade too. In the recalculation with BSFT the selected layer showed a tendency to lower also as for the linear case. It is believed that the structural strength of the selected layers is not reflected correctly. Although there is evidence of stress-softening behaviour this layer is forged into balance with the rest of the pavement structure. This means that the subgrade underneath does not suddenly increase to a value of 466 MPa as a discrete event. It is rather a gradual change from the value of 466 MPa to a lower value, but not necessarily as low as 19 MPa, when moving up towards the subbase.

In the case of the test at Malmesbury there is also definite indications of non-linearity of the subgrade. The effect on the other structural layers when recalculation with BSFT is done, is however minimal.

#### 4 SUMMARY AND CONCLUSIONS

- (a) Effective elastic moduli are calculated very effectively using the Multi-depth Deflectometer (MDD) measurements. The effective elastic moduli calculated in this manner have been correlated very effectively with the mechanistic analysis procedure.
- (b) The procedure to calculate effective elastic moduli from surface deflections was described using the BISAR linear-elastic computer program.
- (c) Effective elastic moduli of the various pavement layers in the stiff behaviour state are correlating well when values determined from surface deflection basin measurements are compared with those determined from depth deflections (MDD).
- (d) In the flexible behaviour states the effective elastic moduli of the subgrade, as determined from surface deflections, are determined 2 to 5 times larger than with the MDD deflections.

- (e) The BSFT back-analysis procedure needs considerable assistance in the calculation of particularly the upper layers, in order to ensure unique results.
- (f) The selected layer in a four or five-layer pavement system is constantly undercalculated compared to the upper layers, in order to ensure unique results.
- (g) Non-linearity of the subgrade can be modelled by the BSFT back-analysis procedure. Non-linearity does feature more strongly in the subgrade effective elastic moduli when the pavement is in the very flexible behaviour state. This is probably due to the stress-softening behaviour accompanying the normal change in balance towards a deeper pavement structure.
- (h) The number of pavement structures that were back-analysed with the aid of the BSFT procedure are limited and results can be used only as mere indicators.





## **CHAPTER 6**

### **RELATIONSHIPS BETWEEN DISTRESS DETERMINANTS AND DEFLECTION BASIN PARAMETERS : A LITERATURE SURVEY**

**CHAPTER 6 : CONTENTS**

	<b>Page</b>
1 INTRODUCTION	6.2
2 FATIGUE CRACKING	6.2
3 RUTTING	6.11
4 CONCLUSIONS AND RECOMMENDATIONS	6.17

## 1 INTRODUCTION

Material characterization is greatly enhanced by the use of deflection basin measurements. This has been described in the preceding chapters. This forms the basis of detailed analyses with multi-layer linear elastic computer models in order to calculate typical distress determinants. These distress determinants must normally reflect the two distress states, fatigue and rutting of the pavement. In the analysis of flexible pavements the distress determinant for rut is vertical subgrade strain and for fatigue the distress determinant is that of the maximum horizontal asphalt strain. Jordaan (1986) defines the analysis approach outlined above as the non-simplified approach. It is possible to make use of empirical-theoretical relationships between these distress determinants and deflection basin parameters. Jordaan (1986) classifies the latter approach as a design curve approach. These relationships between the distress determinants and deflection basin parameters are pre-calculated or established by empirical relationships. In the discussion in this chapter such relationships between deflection basin parameters and the distress determinants are highlighted as found in literature. A brief discussion on the validity of the use of these distress determinants are given too.

## 2 FATIGUE CRACKING

Fatigue cracking is a major type of distress in bituminous pavements. The three basic types of cracking are: longitudinal, transverse and alligator or crocodile cracking. Longitudinal cracking is mainly due to environmental effects. Transverse and crocodile cracking are usually due to the effect of traffic loading. Shrinkage cracking (transverse) is mostly kerbed by proper material specification and construction control.

The traditional distress parameter relating to the fatigue life of the asphalt layer is described by Snaith et al. (1980) as follows:

$$N = c \left( \frac{1}{\epsilon_{HA}} \right)^m$$

where:

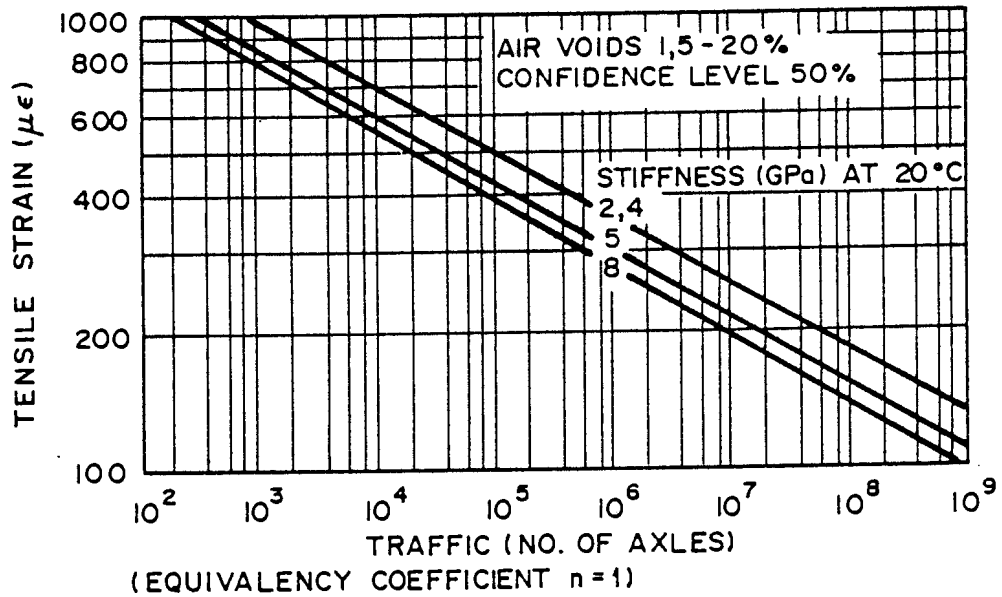
$N$  = number of applications to failure

$\epsilon_{HA}$  = tensile strain repeatedly applied

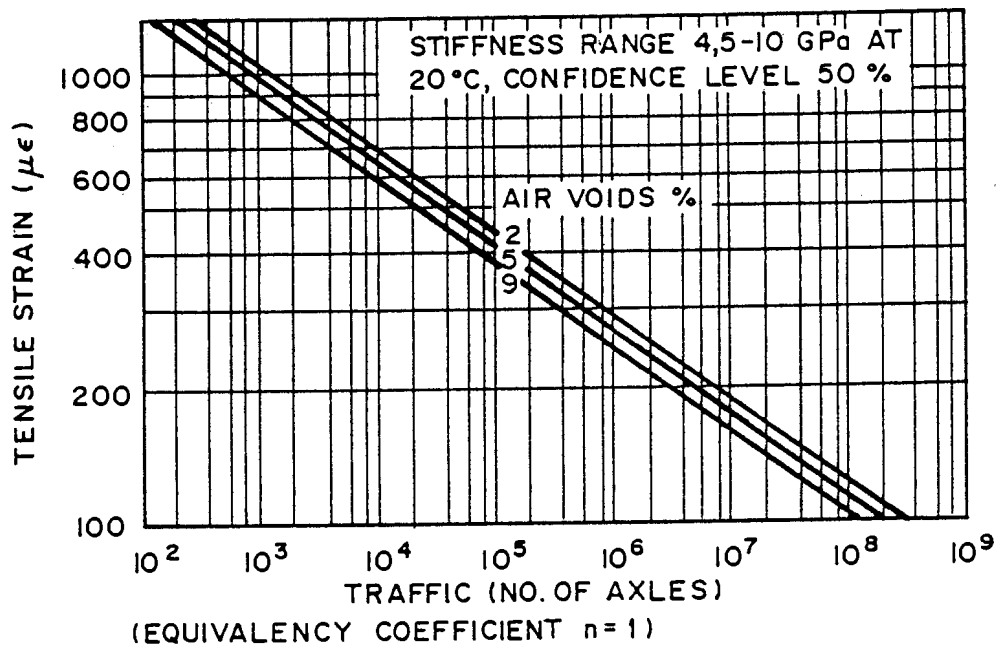
$c, m$  = material coefficients.

Normally researchers use the radial or horizontal strain ( $\epsilon_{HA}$ ) at the bottom of the asphalt concrete layer as the criterion. This is also used for the mechanistic design procedure in South Africa. Freeme et al. (1982a) however, refer to recent research indicating that the maximum tensile strain does not necessarily occur at the bottom of the asphalt layer. Under certain conditions of low stiffness in the asphalt layer, the principle tensile strain at depths 0,8 to 1 times the radius of the load area exceeds the magnitude of the strain at the bottom of the layer. Typical relationships determined for horizontal strain ( $\epsilon_{HA}$ ) are shown for thin and thick asphalt layers in Figures 6.1 and 6.2 for typical South African asphalt mixes. Shift factors are used to compensate for the crack growth until the cracking is clearly visible. For the South African condition these shift factors range from 2 to 10.

Although the maximum horizontal strain is normally calculated at the bottom of the asphalt concrete layer, as described above, the effect of the thickness of this layer is also noted by researchers. Anderson (1977) shows that asphalt concrete layers of 25 to 75 mm reached maximum tensile strain values at thicknesses of 50 to 75 mm for various pavement types as shown in Figure 6.3. Dehlen (1962a) also noted that theory indicates that there may be a critical thickness of surfacing, in the range of 50 to 100 mm, for which flexural stresses are a maximum. This same tendency is illustrated by Grant and Walker (1972) for various combinations of pavement structural strength and radius of curvature ( $R$ ) (See Figure 6.4). They also note: "For the majority of pavements where the asphalt thickness was less than 50 mm the maximum tensile strain in the asphalt layer was at the surface, while invariably being at the bottom of the layer for greater thicknesses." Freeme et al. (1982a) and Patterson (1985) indicate that for such thin asphalt surfacing layers the total number of axles, irrespective



(a) GAP-GRADED ASPHALTS



(b) CONTINUOUSLY GRADED ASPHALTS

FIGURE 6.1

*RECOMMENDED FATIGUE CRITERIA FOR THIN  
BITUMEN SURFACINGS*

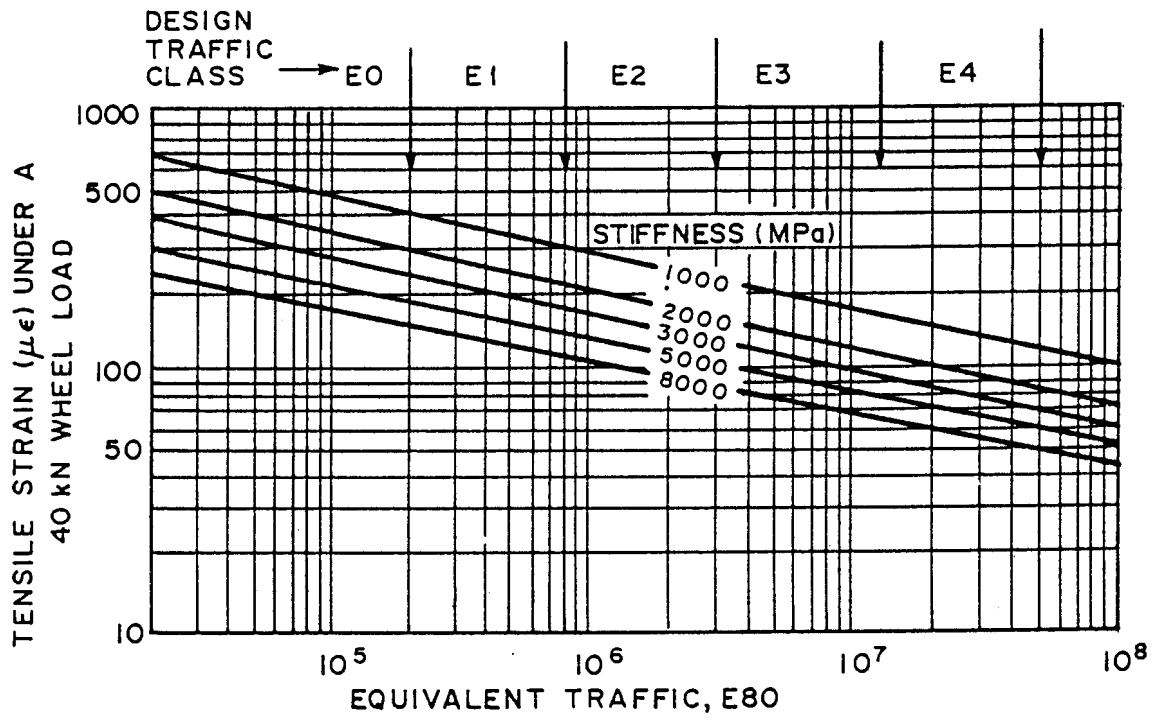


FIGURE 6.2  
RECOMMENDED FATIGUE CRITERIA FOR THICK BITUMEN  
BASES

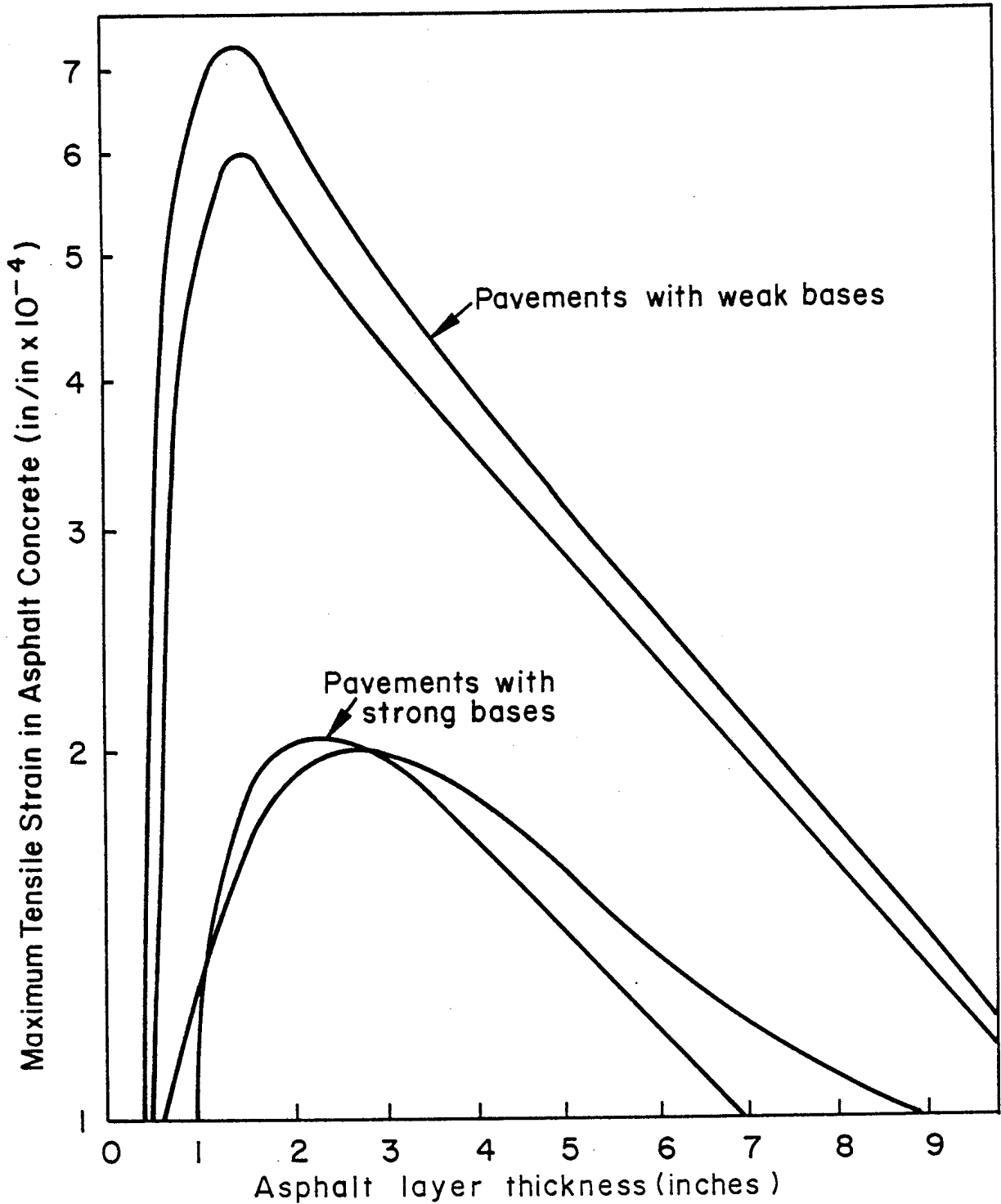
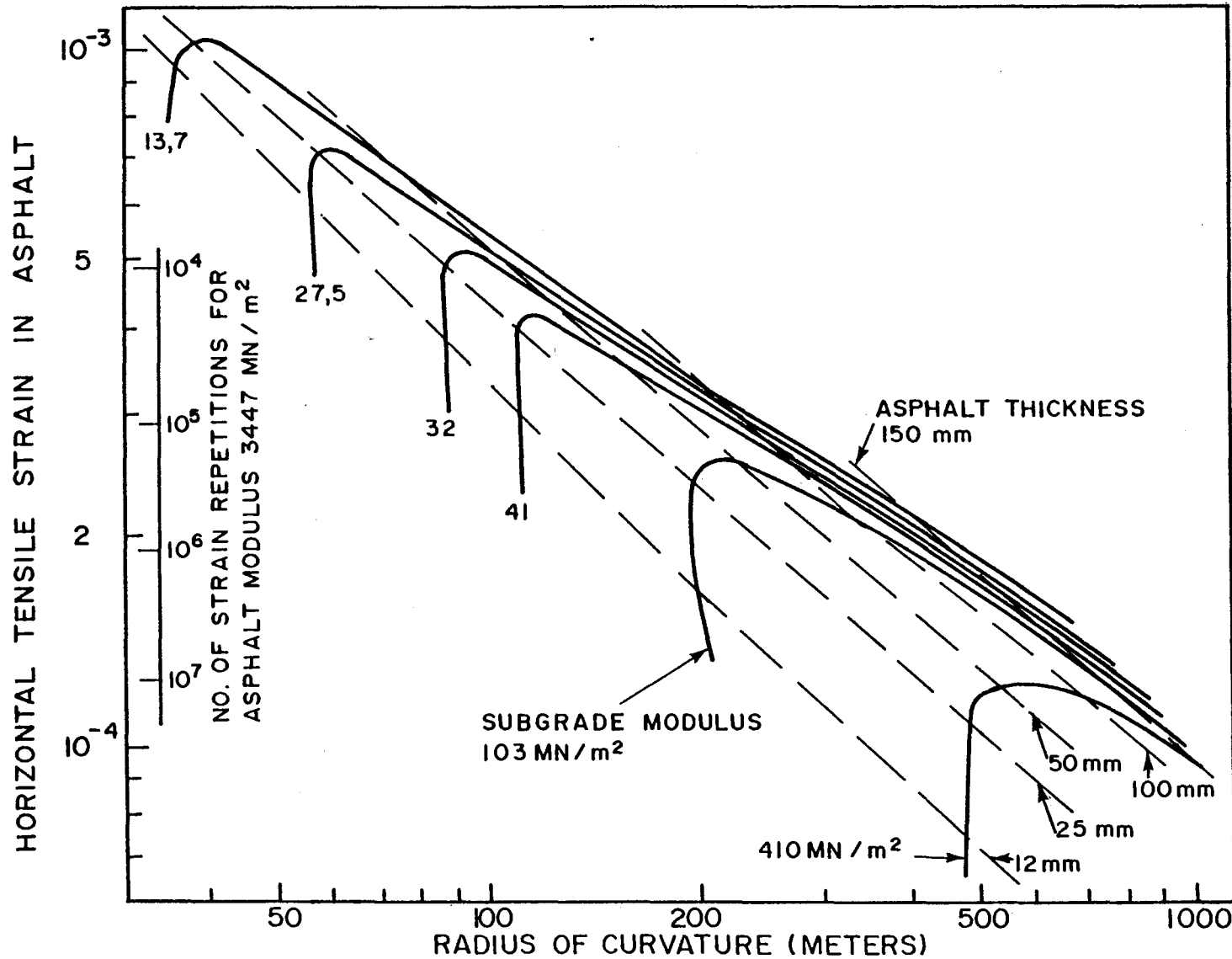


FIGURE 6.3  
 RELATIONSHIP BETWEEN A.C. THICKNESS AND  
 TENSILE STRAIN (Anderson, 1977)



**FIGURE 6.4**  
**CHART FOR DESIGNING AGAINST EXCESSIVE TENSILE STRAIN**  
**IN THE ASPHALT (Grant and Walker, 1972)**





of load, should be considered. Molenaar (1983) refers to various researchers in order to make practical conclusions on cracking behaviour (for example cracking from bottom to top or vice versa), and, in keeping with the recent research trend, also refers to fracture mechanics principles.

Various researchers have done extensive analyses on different pavement structures in order to arrive at regression functions of the deflection basin parameter and the distress determinant for fatigue cracking. The typical relationships between asphalt tensile strain ( $\epsilon_{HA}$ ) and surface curvature index (SCI) for three subgrade conditions are shown in Figure 6.5. This is true for typical three-layered pavements.

Anderson (1977) analysed the typical pavement structures in the State of Victoria, Australia, in order to arrive at a relationship between surface curvature index (SCI), as defined by him versus the asphalt tensile strain ( $\epsilon_{HA}$ ) as shown in Figure 6.6. All these pavement structures have asphalt concrete layers of 50 mm or less. In this figure values are recorded for strains up to  $2 \times 10^{-4}$  (inch/inch). Anderson (1977) concludes that this function can be used to estimate asphalt tensile strains in an overlay design method. In general these relationships have been determined for a granular based, three-layered pavement structure. Monismith and Markevich (1983) expanded this work by analysing 300 different cases of this typical pavement structure. Their resulting relationship was:

$$\epsilon_t = 1,794 \times 10^{-2} (D_o - D_{12})^{0,828}$$

where:

$\epsilon_t$  = maximum tensile strain

$D_o - D_{12}$  = curvature function or surface curvature index (SCI) (see Table 1.1)

In essence, this is also what was done by Grant and Walker (1972) as shown in Figure 6.4. In this case, though, a specific three-layered pavement structure was analysed (granular base) and the radius of curvature (R) was correlated with strain ( $\epsilon_{HA}$ ).

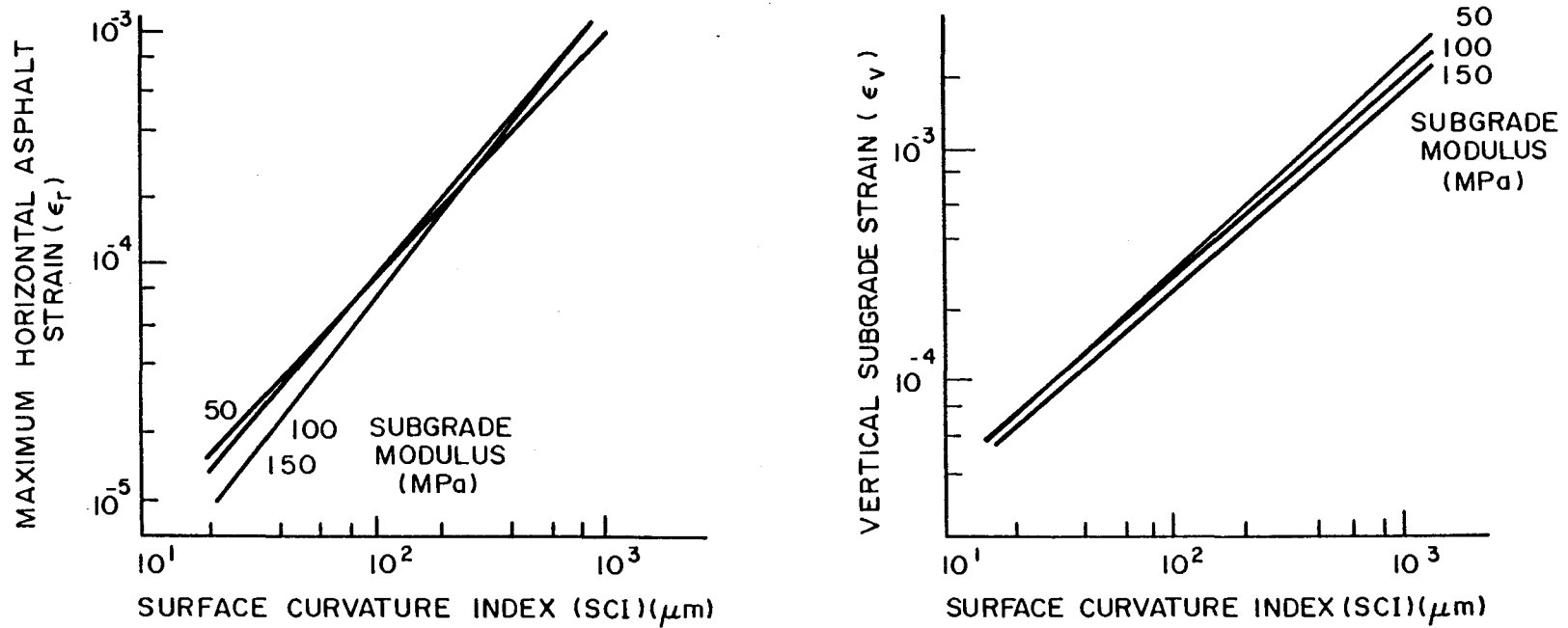


FIGURE 6.5  
RELATIONS BETWEEN SURFACE CURVATURE INDEX AND HORIZONTAL ASPHALT STRAIN OR VERTICAL SUBGRADE STRAIN. (Molenaar, 1983)

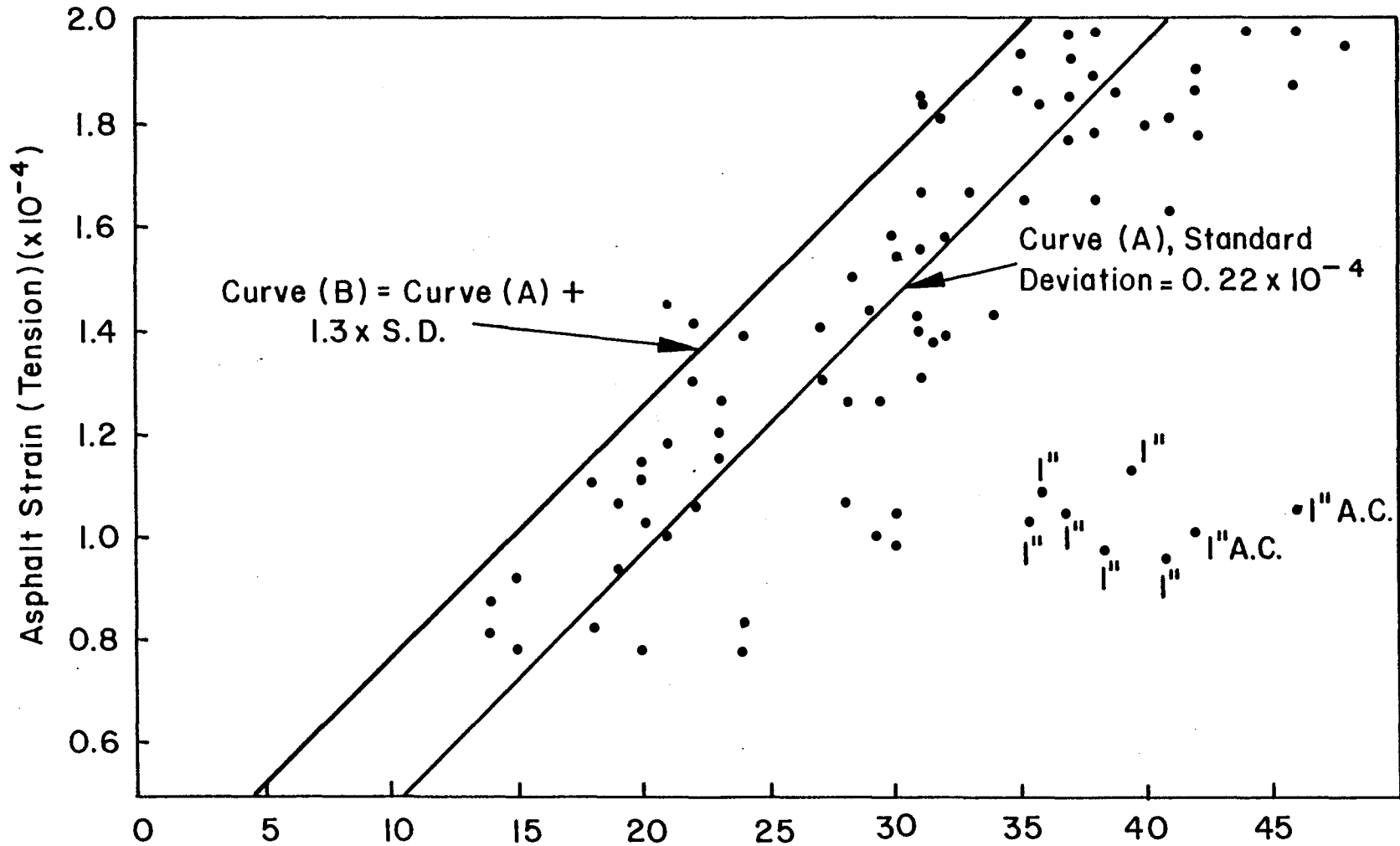


FIGURE 6.6  
SURFACE CURVATURE INDEX vs ASPHALT TENSILE STRAIN  
(Anderson, 1977)

Kilareski, et al 1982) conclude from their analysis that the deflection basin parameters surface curvature index (SCI) and the base damage index (BDI) give better defined relationships with  $\epsilon_{HA}$  than the parameter base curvature index (BCI). The function of surface curvature index (SCI) versus maximum asphalt strain ( $\epsilon_{HA}$ ), as shown in Figure 6.7, is the preferred relationship. In this Figure it is also indicated that the relationship is not linear, but at low strain levels a linear relationship may be used.

### 3 RUTTING

Permanent deformation of the individual layers resulting in permanent deformation of the total pavement structure is a major distress state to be considered in overlay design. The nature and classification of rutting in asphalt concrete pavements are discussed in Appendix B. As mentioned there, the distress determinant most often used is vertical subgrade strain ( $\epsilon_{vs}$ ). As was noted this approach is more historical in the sense that it does not focus on the prevention of deformation, but on the results thereof.

The emphasis in this section is on the analysis and prevention of rutting. The basic relationship used as a first approach is thus restated as follows:

$$N = k \left( \frac{1}{\epsilon_{vs}} \right)^n$$

where

N = number of applications to failure

k, n = material coefficients

$\epsilon_{vs}$  = vertical subgrade strain as determined by, for example multi-layer linear elastic computer materials.

Various researchers have analysed different pavement structures to arrive at regression functions of  $\epsilon_{vs}$  and the deflection basin parameters. Such typical relationships are shown in Figure 6.8. Anderson (1977) established a relationship between maximum deflection ( $\delta_0$ ) and vertical subgrade strain ( $\epsilon_{vs}$ ). This is shown in

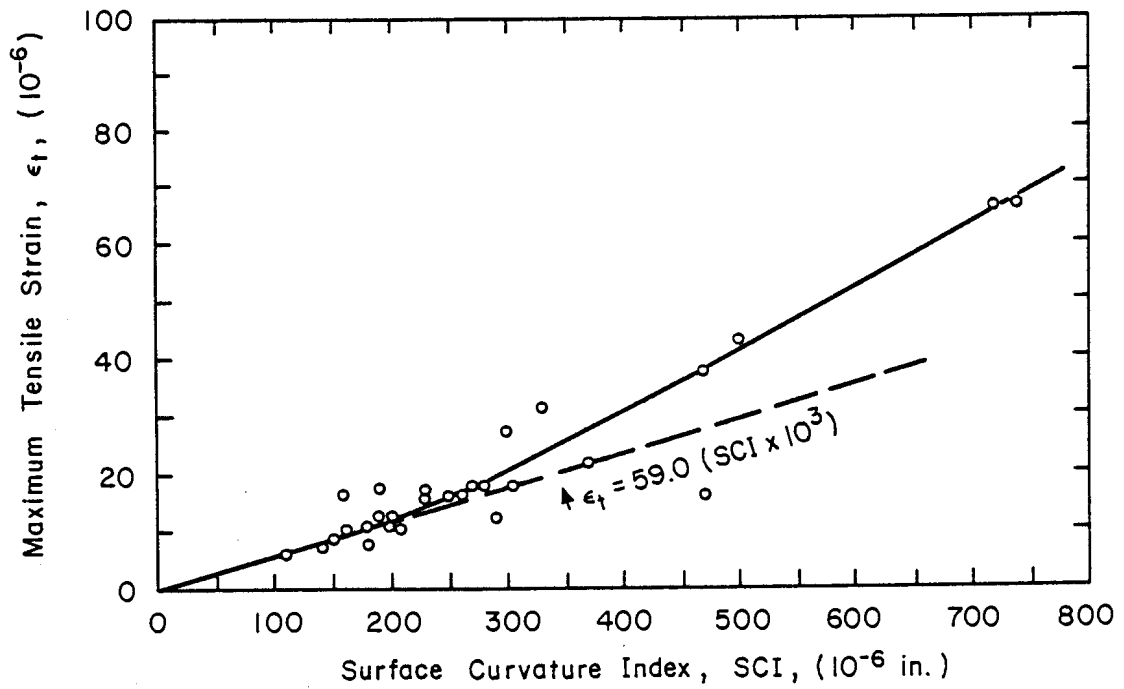
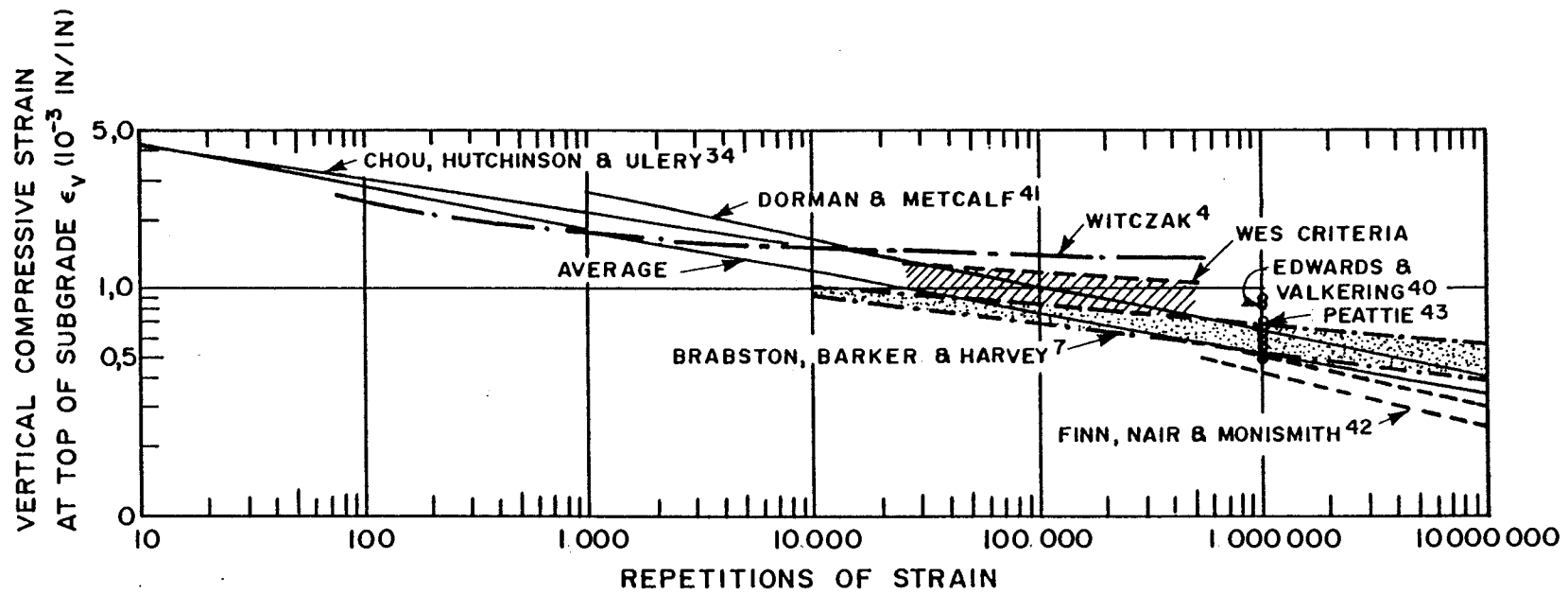


FIGURE 6.7  
 RELATIONSHIP BETWEEN MAXIMUM TENSILE  
 STRAIN AND SURFACE CURVATURE INDEX .  
 (Kilareski, et al., 1982)

240-4-4/60/30



**FIGURE 6.8**  
**COMPARISON OF SUBGRADE STRAIN CRITERIA**  
(1 in. = 2,54 cm (Yoder and Witzak, 1975))

Figure 6.9 with two possible curves fitting the results of granular based three layered pavements analysed. Monismith and Markevich (1983) also used  $\delta_0$  as the deflection basin parameter in their analysis of similar pavement structures. That relationship is:

$$\epsilon_{vs} = 6,3 \times 10^{-4} (\delta_0)^2 (E_s)^{0,8}$$

where:

$\delta_0$  is measured in inches

$E_s$  = subgrade modulus expressed in psi.

A high correlation coefficient was established, for the pavement structures analysed, allowing confidence in this method of estimating vertical subgrade strain ( $\epsilon_{vs}$ ) for this type of pavement structure.

In the light of what was discussed in chapter 4 it is clear that maximum deflection ( $\delta_0$ ) is not necessarily the most ideal deflection basin parameter to correlate with vertical subgrade strain ( $\epsilon_{vs}$ ). Wang et al. (1978) established a relationship incorporating maximum deflection ( $\delta_0$ ) and base damage index BCI for measurements with the Road Rater Model 400. This is shown in Figure 6.10.

On the use of vertical subgrade strain ( $\epsilon_{vs}$ ) as the distress determinant, Molenaar (1983) notes: "Although these simple subgrade strain criteria are very easy to use and therefore very attractive, they are nevertheless thought to cover only a part of the permanent deformation of the pavement structure because each layer can exhibit some permanent deformation itself". In Figure 6.5 it was shown how he relates subgrade strain to surface curvature index (SCI) as he did for maximum asphalt strain. This should be kept in mind, since Grant and Curtayne (1982) also indicated that owing to densification of some layers the pavement is often structurally stronger at the time of overlay analysis. This has been repeatedly confirmed by HVS tests.

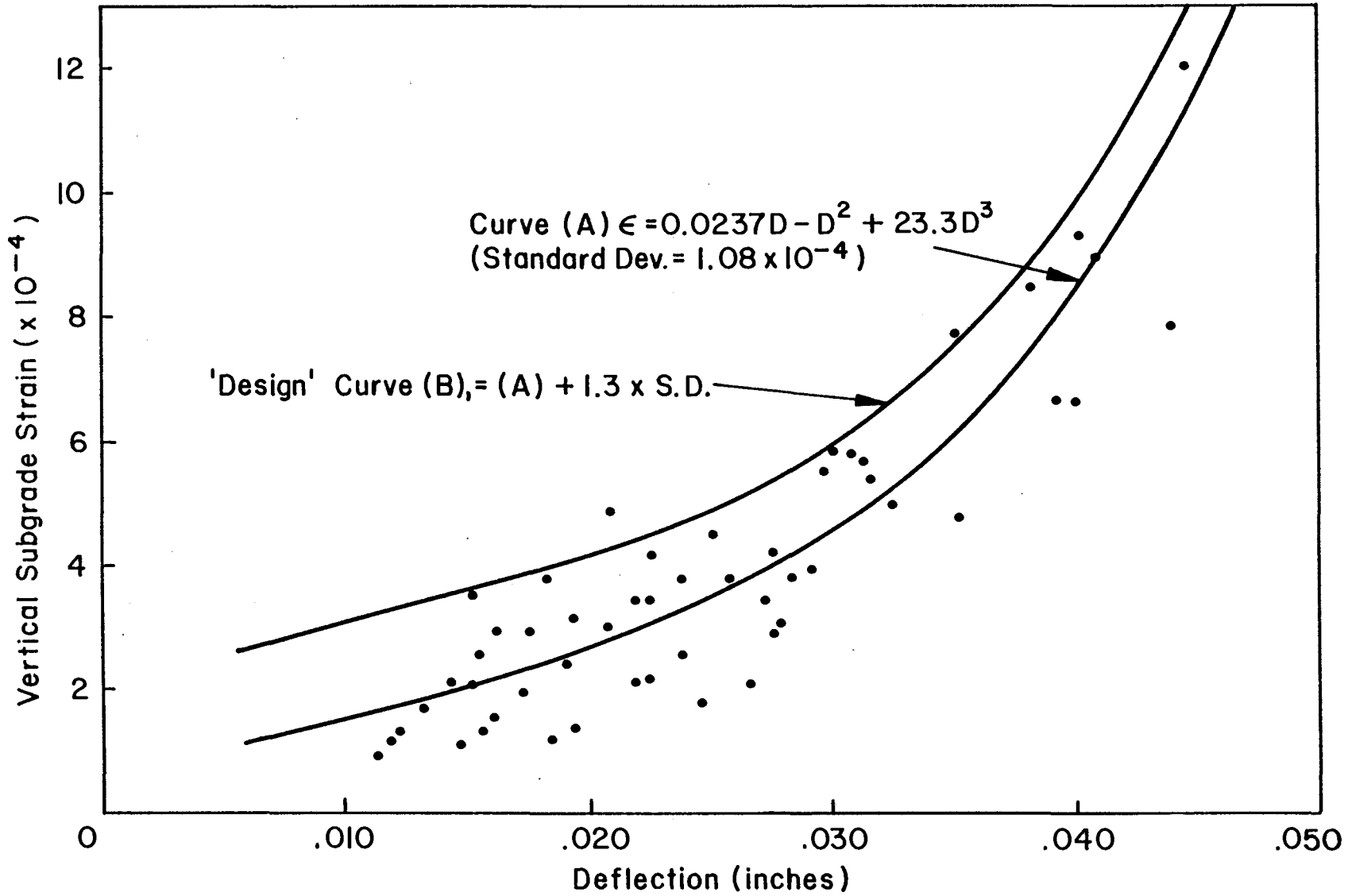


FIGURE 6.9  
DEFLECTION vs SUBGRADE STRAIN (Anderson, 1977)



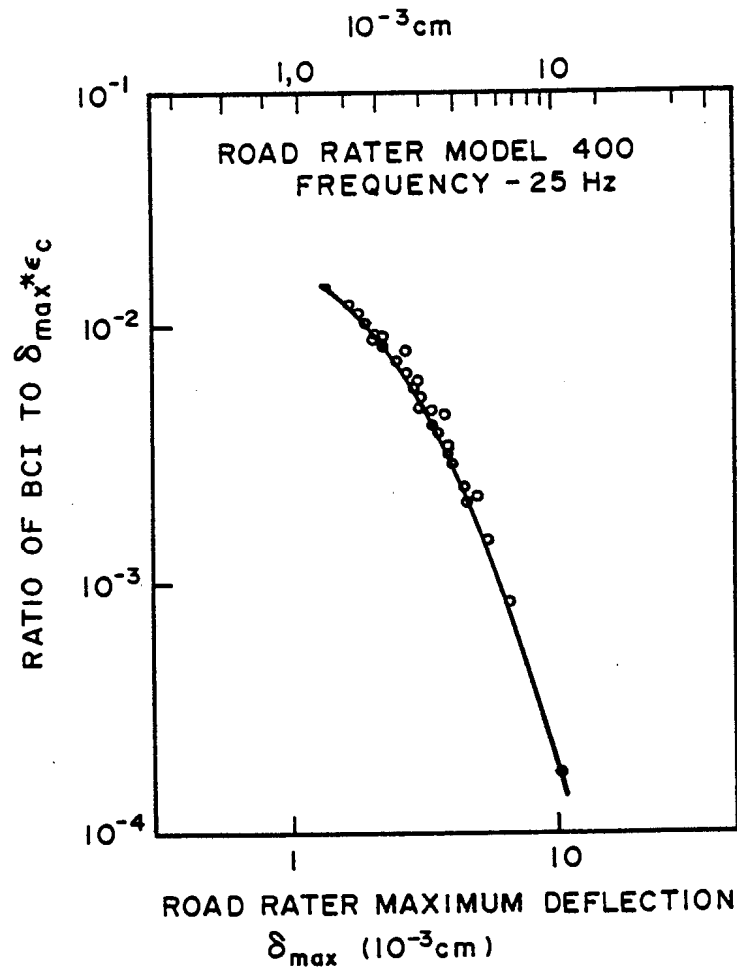


FIGURE 6.10  
 RELATIONSHIP BETWEEN BASE  
 CURVATURE INDEX, MAXIMUM  
 DEFLECTION AND SUBGRADE  
 COMPRESSIVE STRAIN  
 (Wang, et al., 1978)

In an effort to assess the accumulated permanent deformation in all the pavement layers, Treybig et al. (1978) calculate the following stresses and strains:

- (a) vertical strain at the bottom of the top layer
- (b) vertical stress at the bottom of the top layer
- (c) vertical stress at the bottom of the second layer
- (d) horizontal stress, parallel to the load axle, at the bottom of the second layer
- (e) vertical stress at the bottom of the third layer
- (f) vertical strain at the bottom of the fourth layer
- (g) vertical stress at the top of the fifth layer
- (h) vertical strain at the top of the fifth subgrade layer.

These stresses and strains are the largest values, irrespective of their horizontal position under the loaded wheels. The values are correlated to the number of repetitions (N). These correlated functions are derived from the analysis of pavement structures' bound and unbound bases.

The deformation in the bitumen or asphalt concrete layer was referred to in Appendix B. The Shell method of estimating deformation in this layer, as described by Van de Loo (1976) is well established. Work by Viljoen and Meadows (1981) on the creep test provides practical guidelines for South African conditions on the prevention of permanent deformation in the asphalt concrete layer.

#### 4 CONCLUSIONS AND RECOMMENDATIONS

In conclusion it may be stated that the maximum tensile strain in the asphalt layer ( $\epsilon_{HA}$ ) is the distress determinant that is most associated with fatigue cracking due to the ease of calculation. Various research efforts have been reported that characterize and explain the actual cracking behaviour.

It is concluded that, in the South African mechanistic design procedure, the method currently used to determine maximum tensile strain ( $\epsilon_{HA}$ ) at the bottom of the asphalt layer is acceptable. Regression analyses relating  $\epsilon_{HA}$  to the desired deflection basin parameters indicate that this is an acceptable method to be used in overlay design. The majority of analyses though, were done for a basic granular-based three-layered pavement structure. In the light of the previously proposed pavement categories and the behaviour states, (see chapter 4), similar analyses should be done in order to establish possible relationships, for example on bitumen-based and cement-treated base pavements. This will be possible with the available information from the recorded HVS tests and other field observations. The interactions of cement-treated layers and cracks reflected through the upper layers and asphalt concrete layers are well recorded and should also be analysed in this way as they are the cause of cracking in a high percentage of pavements in South Africa.

It can be stated that vertical subgrade strain ( $\epsilon_{vs}$ ) is the distress determinant most often calculated in order to predict rutting. This is the practice in South Africa and multi-layer linear elastic computer programs are usually used to calculate  $\epsilon_{vs}$ . Various deflection basin parameters have been related to  $\epsilon_{vs}$  by regression analysis in order to estimate  $\epsilon_{vs}$  directly from deflection basin measurements. A clear distinction is not always made in regard to the pavement type analysed, although the typical three-layered granular base pavement prevails. As was suggested in the previous section, analyses should be done with the available South African data in order to classify or do regression analyses for each of the aforementioned pavement classes or behaviour states.

From this discussion, HVS tests results and field results it is clear that all the layers contribute to the total permanent deformation. Various other distress determinants are calculated by methods incorporating the stress and strain states in the various layers. It is suggested that on this line, regression



analysis be done too. This in turn should be related to the various pavement categories.



## **CHAPTER 7**

### **RELATIONSHIPS BETWEEN DEFLECTION BASIN PARAMETERS AND DISTRESS DETERMINANTS FOR TYPICAL SOUTH AFRICAN PAVEMENTS**

## CHAPTER 7: CONTENTS

	Page
1 INTRODUCTION	7.2
2 ANALYSIS OF FLEXIBLE PAVEMENT STRUCTURES	7.2
3 DEFLECTION BASIN PARAMETERS VERSUS DISTRESS DETERMINANTS	7.7
3.1 General	7.7
3.2 Vertical subgrade strain	7.7
3.3 Maximum asphalt strain	7.11
4. RELATIONSHIPS WITH OTHER STRUCTURAL PARAMETERS	7.16
4.1 General	7.16
4.2 Granular base pavements	7.16
4.3 Bitumen base pavements	7.20
4.4 Subgrade elastic modulus	
5 THE EFFECT OF OVERLAYS	7.22
5.1 Granular base pavements	7.23
5.2 Bitumen base pavements	7.23
6 CONCLUSIONS AND RECOMMENDATIONS	7.29

## 1. INTRODUCTION

In the analysis of flexible pavements for rehabilitation design the mechanistic rehabilitation design procedure can be used with confidence (Freeme, 1983 and Freeme et al, 1982). It has been explained in chapter 4 how proper material characterization is an important step in this analysis procedure. The normal linear elastic computer programmes are used in such an analysis in order to calculate the distress determinants and relate them to structural life. In chapter 4 and Appendix C and D it was explained how this non-simplified or fundamental approach ( Jordaan, 1986) should function.

In the previous chapter it was shown how it is possible to develop design curves for specific pavement types whereby deflection basin parameters are related to distress determinants. In this chapter it will be shown how this author analysed typical South African flexible pavements in order to relate selected pavement deflection basin parameters to the distress derminants. The broad spectrum of flexible pavements is properly defined and the analysis is further restricted to bitumen, granular and cemented base pavements. The latter type is analysed in the equivalent granular state which means that their analysis is similar to that of the granular base pavements. They have a further common factor in the asphalt surfacing (40 mm average or less).

In the discussion reference is also made to the findings of overseas researchers. Overlaying flexible pavements is an important rehabilitation alternative. For that reason the effect of various overlay thicknesses were also investigated in relation to the effect on the deflection basin parameters.

## 2. ANALYSIS OF FLEXIBLE PAVEMENT STRUCTURES

The pavement structures in the Catalogue of designs (NITRR, 1985a) reflect the typical pavement structures used in South Africa. The pavement types can be subdivided into pavements having granular, bituminous, cemented and concrete bases. Typical granular base



pavement structures analysed, are shown in Figure 7.1. Only the subbase, base and surfacing layers are shown; the selected layer and subgrade are excluded. The latter two layers are, however, prepared in the standard prescribed way (NITRR, 1985a) and are common to all these pavement structures.

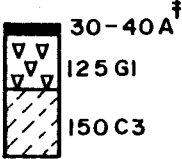
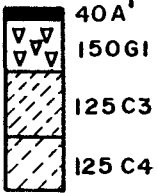
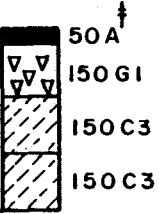
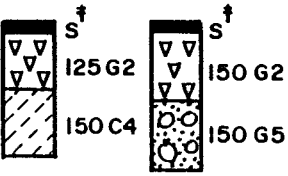
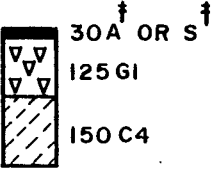
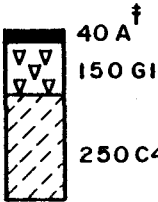
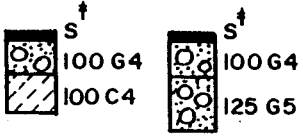
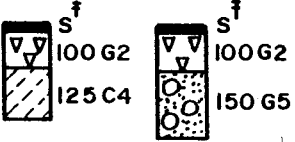
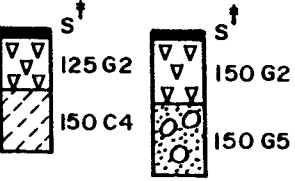
The different pavement types behave differently. Their behaviour is time-dependent; generally pavements become more flexible with time. This necessitates the proper definition of the current state of the pavement in order to determine the most appropriate analysis or design method of predicting future behaviour. The definition of the states of pavement behaviour is given by Freeme (1983); these states range from very stiff to very flexible (See chapter 3 and 4). A flexible pavement is defined as a pavement structure of which the behaviour is controlled by material in the granular state. In chapter 3 it was shown how the various deflection basin parameters can enhance such accurate definition of behaviour state.

The analysis of flexible pavements therefore includes granular, bitumen and cemented base pavements. Pavements with cemented bases or subbases were considered to be in the cracked phase, exhibiting equivalent granular behaviour (Freeme, 1983). All such standard TRH4 (NITRR, 1985a) flexible pavements were analysed first by means of the multi-layered linear elastic program, MECD3 (Maree and Freeme, 1981a). A second level of analysis was done on granular base pavements or bases in the equivalent granular state with the computer program ELSYM5 (University of California, 1972). The ELSYM 5 program (University of California, 1972) tends to be inaccurate in calculating surface deflections between 100 mm and 250 mm from the point of maximum deflection. This is true for bituminous base pavements (Tam, 1985). This tendency is more pronounced when five-layered pavement structures are analysed and when the pavement structure is more rigid, for example a concrete base pavement (Taute, McCullough and Hudson, 1981). For that reason the detailed analysis of the bituminous base pavements were done with the BISAR program (Horak, 1985).

In the analysis of the typical flexible pavement structures of the



## GRANULAR BASES

DESIGN TRAFFIC CLASS E80/LANE OVER STRUCTURAL DESIGN PERIOD					
ROAD CATEGORY	E0 $<0,2 \times 10^6$	E1 $0,2-0,8 \times 10^6$	E2 $0,8-3 \times 10^6$	E3 $3-12 \times 10^6$	E4 $12-50 \times 10^6$
A					
B					
C					

†SYMBOL A DENOTES AG, AC OR AS. SYMBOL S DENOTES S2 OR S4

**FIGURE 7.1**  
Typical granular base pavements from the Catalogue of designs

Catalogue of designs (NITRR, 1985a), surface deflections were calculated at various offsets perpendicular to the axle of the wheels.

The structural integrity of a pavement is reflected in varying degrees of accuracy by various deflection basin parameters. The deflection basin parameters that were investigated in this study are listed in Table 1.1 (for ease of reference use the fold out at the back). The formulae and measuring devices normally associated with them are also listed (Horak, 1984). The deflection parameters vary from the traditional singular point, maximum deflection, to deflection basin parameters such as spreadability and area, which are highly descriptive of the deflection basin as a whole. In the ELSYM5 analysis of the granular base pavements, deflection basin pavements calculated in this region carried less weight in the analysis.

In all of these analyses the wheel load used was a 40 kN dual wheel load with a standard tyre pressure of 520 kPa. A Poisson ratio of 0,44 was assumed for bituminous materials and 0,35 for all other types of material. The elastic moduli values of the materials used in the MECD3 analysis were the average values as defined and verified with HVS test results (Freeme et al., 1982a and Freeme, 1983). The value for thin asphalt surfacings (mostly granular base pavements) was set at 2 000 MPa. The selected subgrade's elastic modulus was set at 120 MPa and the subgrade modulus was varied with 50,70 and 150 MPa.

In the ELSYM5 analysis of granular base pavements (and equivalent granular states) the base elastic modulus and thickness were identified as the most influential structural components in terms of the deflection basin parameters (Tam, 1985). These values were varied over a range commonly found in practice (Freeme, 1983). The base thicknesses were varied in steps of 25 mm between 100 and 250 mm. The effective elastic modulus of the granular base was varied in steps of 15 MPa between 100 and 450 MPa. Also, in order to determine the effect of overlays on granular base pavements, the surfacing thickness was increased in steps of 10 mm (up to 100mm thick) over a basic surfacing thickness of either 20 mm or 40 mm.

In the detail analysis (Horak, 1985) of bitumen base pavements the BISAR computer program was used. In Table 7.1 the various structural components are listed.

TABLE 7.1 - BISAR analysis of bitumen base pavements

Parameter	Range
Overlay elastic modulus (MPa)	3 000*
Overlay thickness (mm)	5, 10, 40, 60
Surfacing elastic modulus (MPa)	2 000, 4 000
Surfacing thickness (mm)	10, 40
Base elastic modulus (MPa)	3 000, 5 000, 7 000
Base thickness (mm)	80, 150, 220
Subbase elastic modulus (MPa)	150, 500
Subbase thickness (mm)	300*
Selected subgrade modulus (MPa)	120*
Selected subgrade thickness (mm)	150*
Subgrade elastic modulus (MPa)	50, 70, 150

\* These values were typical representative values and their variance has a minor influence (Tam, 1985) on deflection basins.

### 3. DEFLECTION BASIN PARAMETERS VERSUS DISTRESS DETERMINANTS

#### 3.1 General

The deflection basin parameters listed in Table 1.1 (see the fold out for ease of reference) were calculated for each flexible pavement structure in these analyses. As pointed out in the introduction the intention is to determine which parameters can be related to the typical distress determinants ( $\epsilon_{HA}$  and  $\epsilon_{VS}$ ) accurately. Only those deflection basin parameters that have a clear and meaningful relationship with the distress determinants are reported here.

#### 3.2 Vertical subgrade strain

The calculated vertical subgrade strain ( $\epsilon_{VS}$ ) was correlated with the various deflection basin parameters of bitumen bases and granular bases separately. This relationship is not possible for flexible pavements in general. The reason for this is shown in Figure 7.2. Both base types show a relationship between SCI and  $\epsilon_{VS}$  and discern the variance in subgrade elastic modulus. As in the relationships between equivalent layer thickness ( $H_e$ ) and SCI (see Appendix F), there is a difference in gradient between the relationships for bitumen and granular base pavements. Additionally, in the case of the granular base pavements these relationships shown in Figure 7.2, are only valid for average values of elastic moduli and layer thickness of the base. In Figure 7.3 the relationship between BDI and  $\epsilon_{VS}$  for granular bases, shows that no discernment is made between subgrade elastic moduli being varied. This is however also true only for average values of base elastic moduli and layer thicknesses. In Figure 7.4 the relationships between R, F1, Q and SD versus  $\epsilon_{VS}$  are shown for bitumen base pavements. It seems that these relationships are not influenced by the variance in the structural input values, as granular base pavements seem to show a tendency for. Of all these relationships shown in Figure 7.4 the deflection basin parameter SD has the most significant relationship.

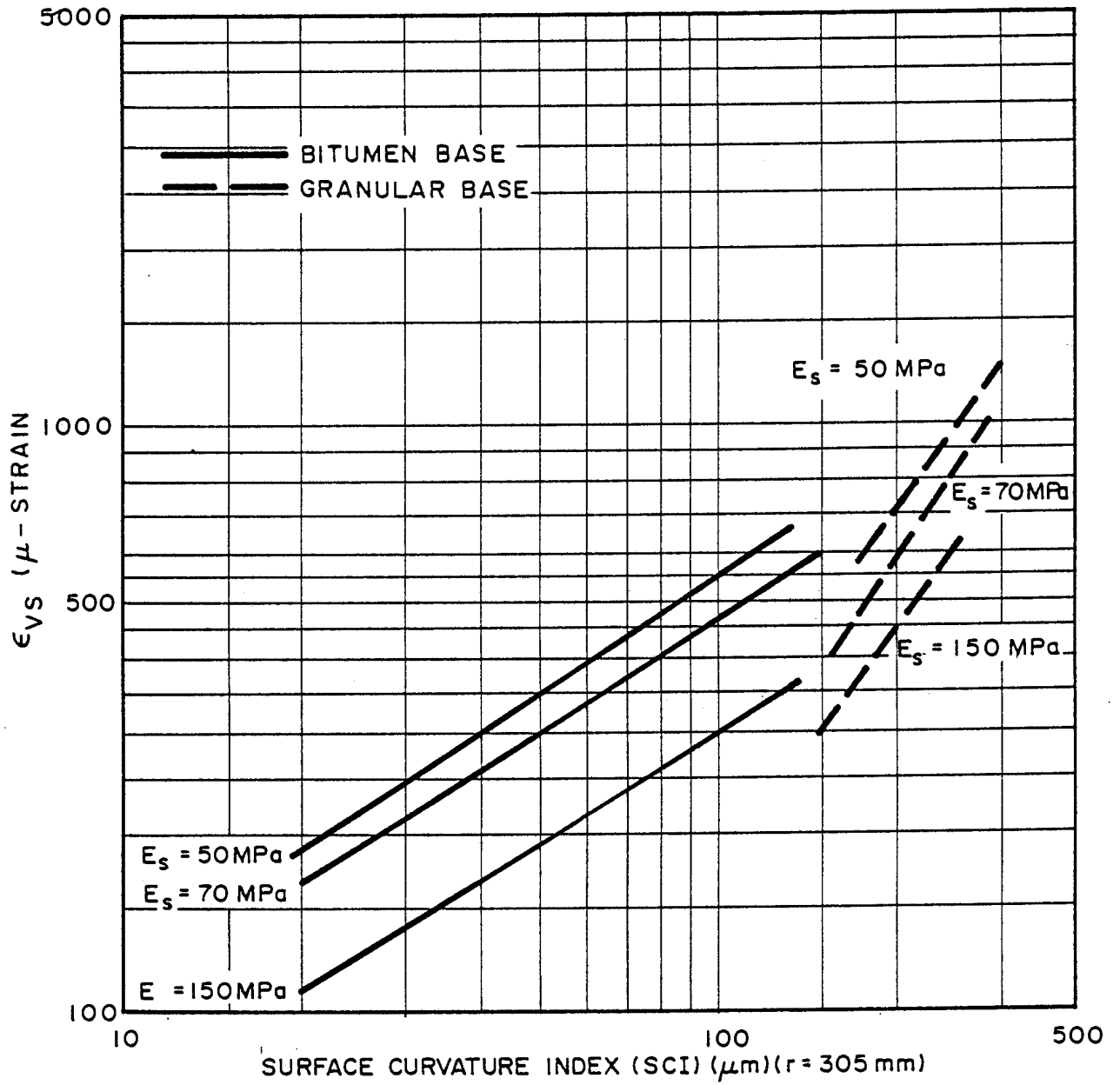


FIGURE 7.2  
Surface curvature index versus vertical subgrade strain

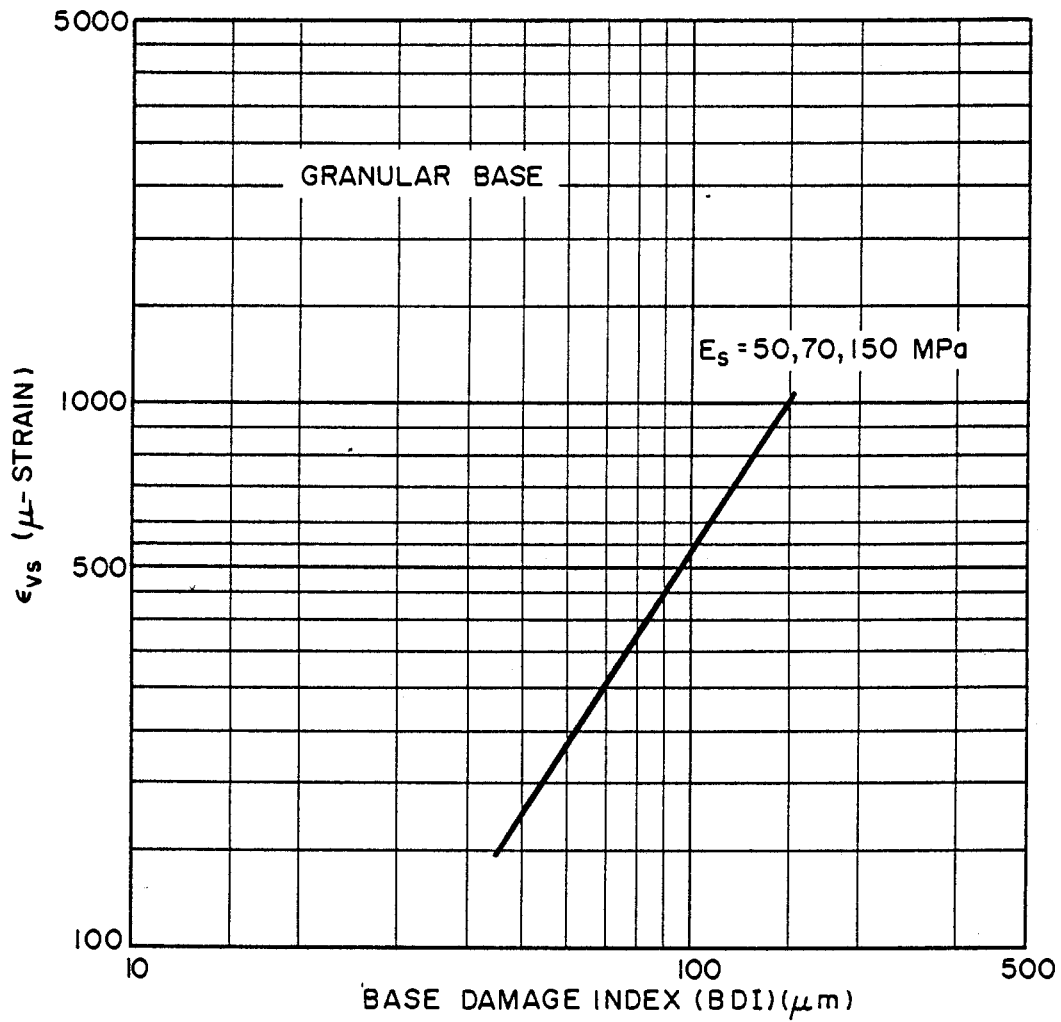


FIGURE 7.3  
 BASE DAMAGE INDEX VERSUS VERTICAL SUBGRADE  
 STRAIN

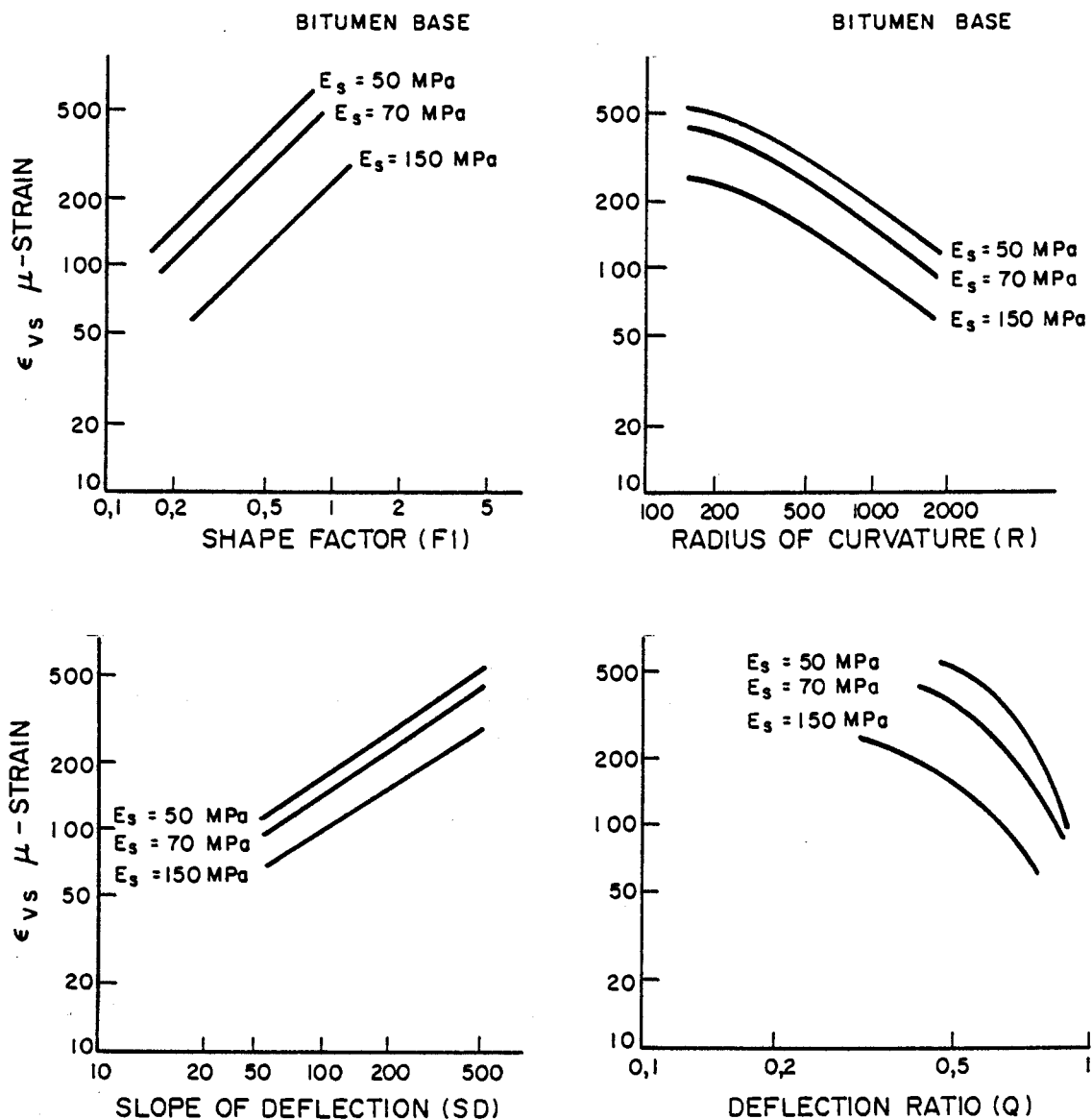


FIGURE 7.4  
BITUMEN BASE DEFLECTION BASIN PARAMETERS VERSUS  
VERTICAL SUBGRADE STRAIN

### 3.3 Maximum asphalt strain

The calculated maximum asphalt strains, ( $\epsilon_{HA}$ , at the bottom of the base) of typical bitumen base pavements were related to the various deflection basin parameters separately. In Figure 7.5 it can be seen that a typical value such as SCI ( $r = 500$  mm) correlated well with  $\epsilon_{HA}$ , but, as Molenaar and Van Gurp (1980) indicated, there is no clear discernment between the various subgrade elastic moduli. In Figure 7.6, deflection basin parameters S, A, F1 and BCI proved to be better in that respect by discerning the variance in subgrade elastic modulus. In this figure the relationship with BCI is the most significant and usefull. When the maximum asphalt strains ( $\epsilon_{HA}$ , under the surfacing) of bitumen base pavements were related to deflection basin parameters, clear, simple relationships became limited to those as shown in Figure 7.7. Area (A) and spreadability (S) can discern the effect of variance in subgrade elastic modulus, but both seem to be rather insensitive to changes in their respective values. As the  $\epsilon_{HA}$  values are compressive, the significance for fatigue calculation of the surfacing is further nullified.

The thickness of the asphalt surfacing layer of a typical granular base pavement has a marked effect on the calculated value of the maximum asphalt strain ( $\epsilon_{HA}$ ). Grant and Walker (1972) showed that for three-layered pavement structures there is a sharp increase in maximum asphalt strain ( $\epsilon_{HA}$ ) values when surfacing thickness is increased to 25 mm . Thereafter the strain increased slowly to reach a maximum strain value between surfaces with 40 and 100 mm thickness. In Figure 7.8 this effect is verified when radius of curvature (R) is correlated with  $\epsilon_{HA}$  for various thicknesses of the surfacing. The subgrade elastic modulus was kept at a standard 70 MPa, but the base elastic modulus and thickness were varied for the granular base pavements. For bitumen base pavements the subgrade elastic modulus was varied though. Figure 7.8 clearly shows that for a normal granular base there is a definite difference in the relationships between R and  $\epsilon_{HA}$  for various thicknesses of asphalt surfacing. At a thickness of 80 mm and above, such a pavement is according to definition (Freeme et



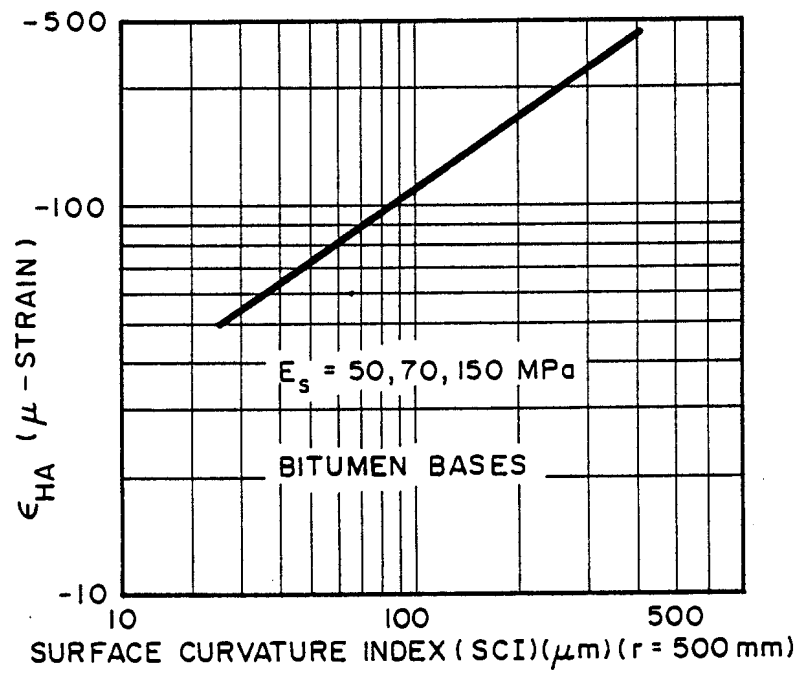


FIGURE 7.5

Surface curvature index versus maximum asphalt strain for bituminous base pavement structures

BITUMEN BASE

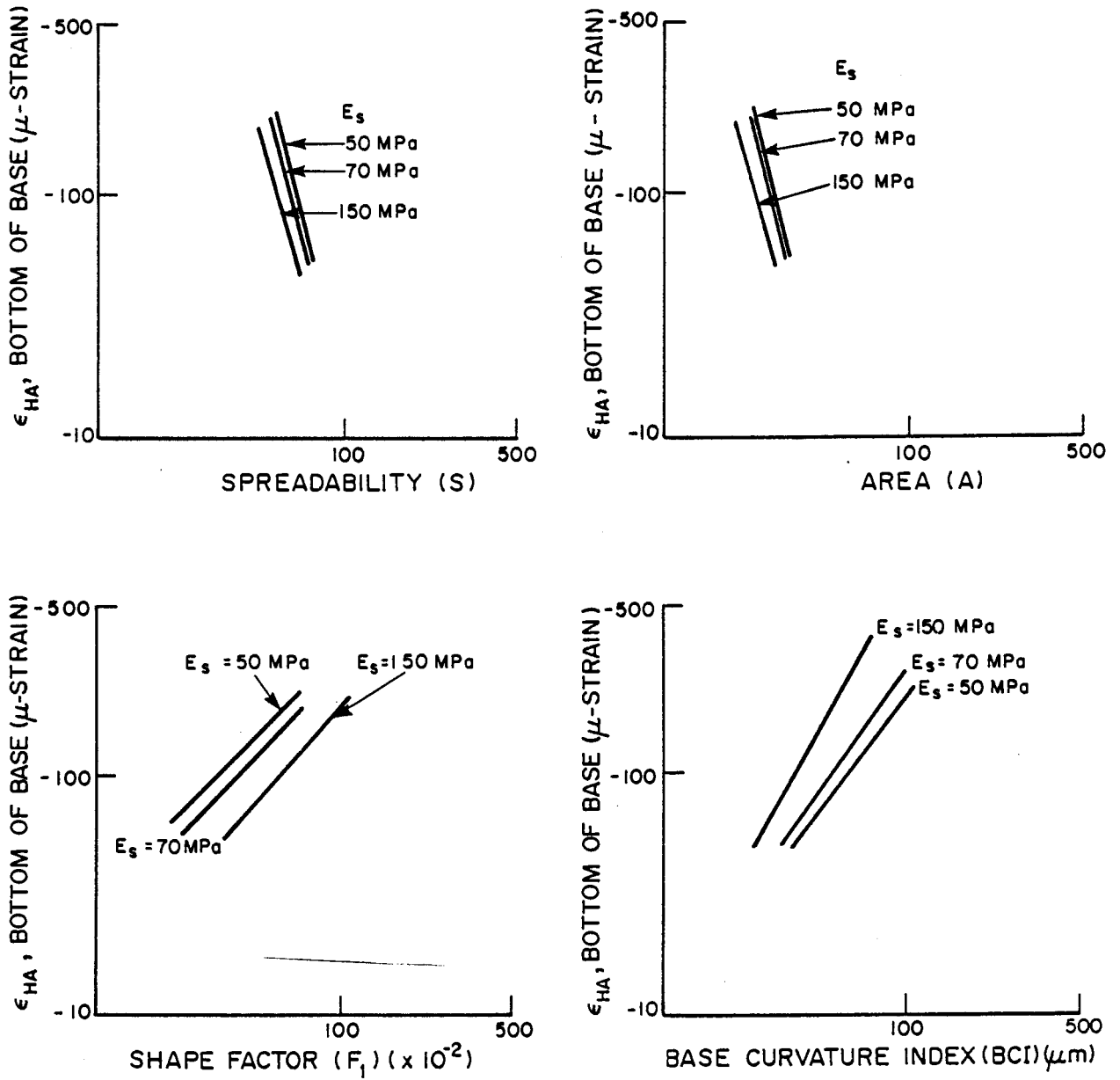


FIGURE 7.6  
BITUMEN BASE DEFLECTION BASIN PARAMETERS VERSUS  
MAXIMUM ASPHALT STRAIN UNDER THE BASE

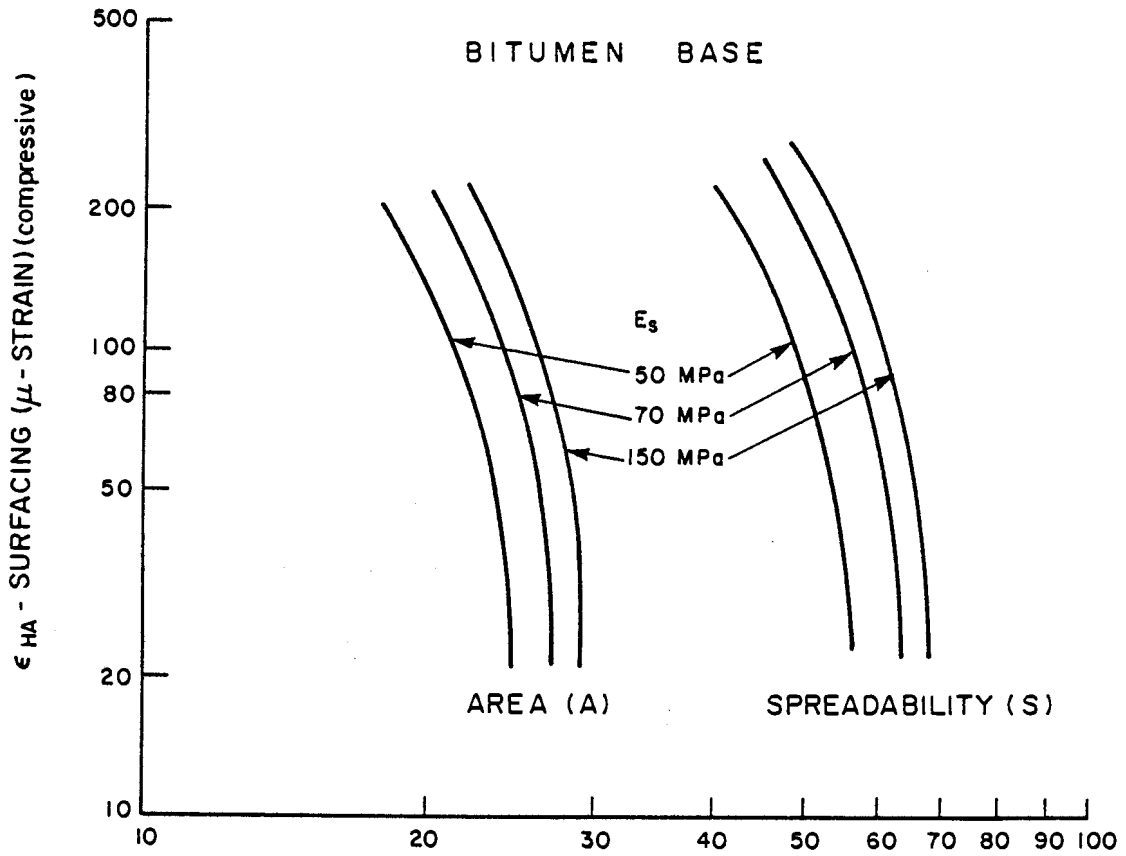


FIGURE 7.7  
MAXIMUM ASPHALT STRAIN UNDER SURFACING  
VERSUS AREA AND SPREADABILITY

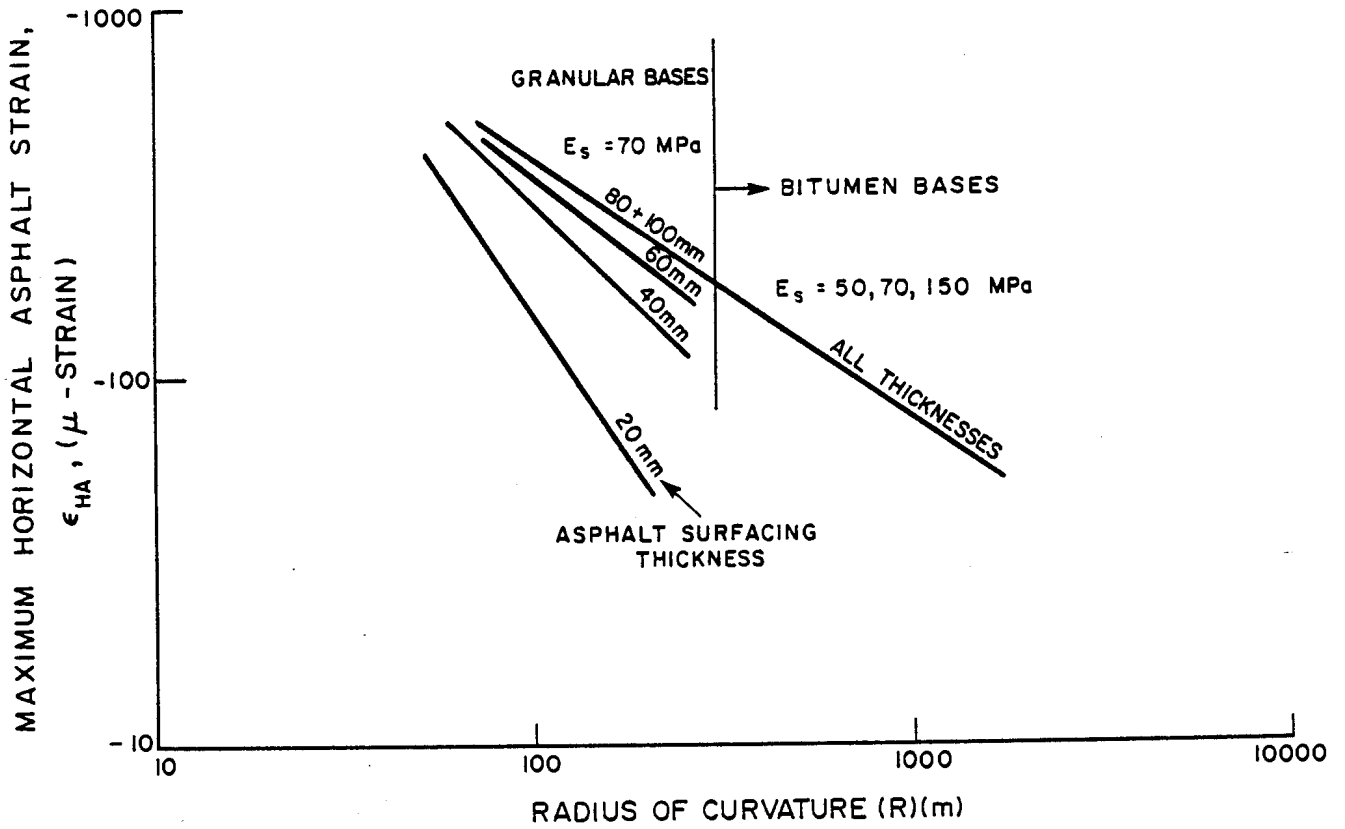


FIGURE 7.8  
RADIUS OF CURVATURE VERSUS MAXIMUM ASPHALT STRAIN

al., 1982a) and (NITRR, 1985a) rather classified as a bitumen base pavement. Proof of the latter is that this relationship (80 mm and 100 mm surfacing) extrapolates to the relationship established for bitumen base pavements. In Figure 7.9 it can be seen that other deflection basin parameters such as S, SCI, F1 and Q tend to group surfacing thicknesses of 40 mm to 100 mm together, while those with thicknesses of up to 20 mm is apart. This reaffirms the observation by Grant and Walker (1972) discussed earlier. Of these relationships that with SCI can be termed the most significant.

#### 4 RELATIONSHIPS WITH OTHER STRUCTURAL PARAMETERS

##### 4.1 General

It is clear from the results of the previous section, that it is not always possible to form clear, simple relationships between distress determinants and deflection basin parameters. The reason for this seems to be the conflicting influences that other structural input parameters being varied, have on the calculated distress determinants. This is more pronounced in the case of the granular base pavements than with bitumen base pavements. The literature survey in the previous chapter and chapter 4 already indicated there are peculiarities with the linear elastic layered programmes used (in the vicinity of the loaded wheel).

##### 4.2 Granular base pavements

In the case of granular bases in particular the variance of elastic modulus of the base and asphalt surfacing thickness had a significant effect on the calculated deflection basin parameters. The effect of the variance of the elastic modulus of the granular base is best illustrated in Figure 7.10 where SCI, BCI, Q and R are related to the base elastic modulus. Surfacing thickness ( $H_{SF}$ ) is however not being discerned by parameters BCI and Q.

A very useful relationship was developed between maximum horizontal asphalt strain ( $\epsilon_{HA}$ ) and easily measurable parameters



GRANULAR BASES  
 $E_s = 70 \text{ MPa}$

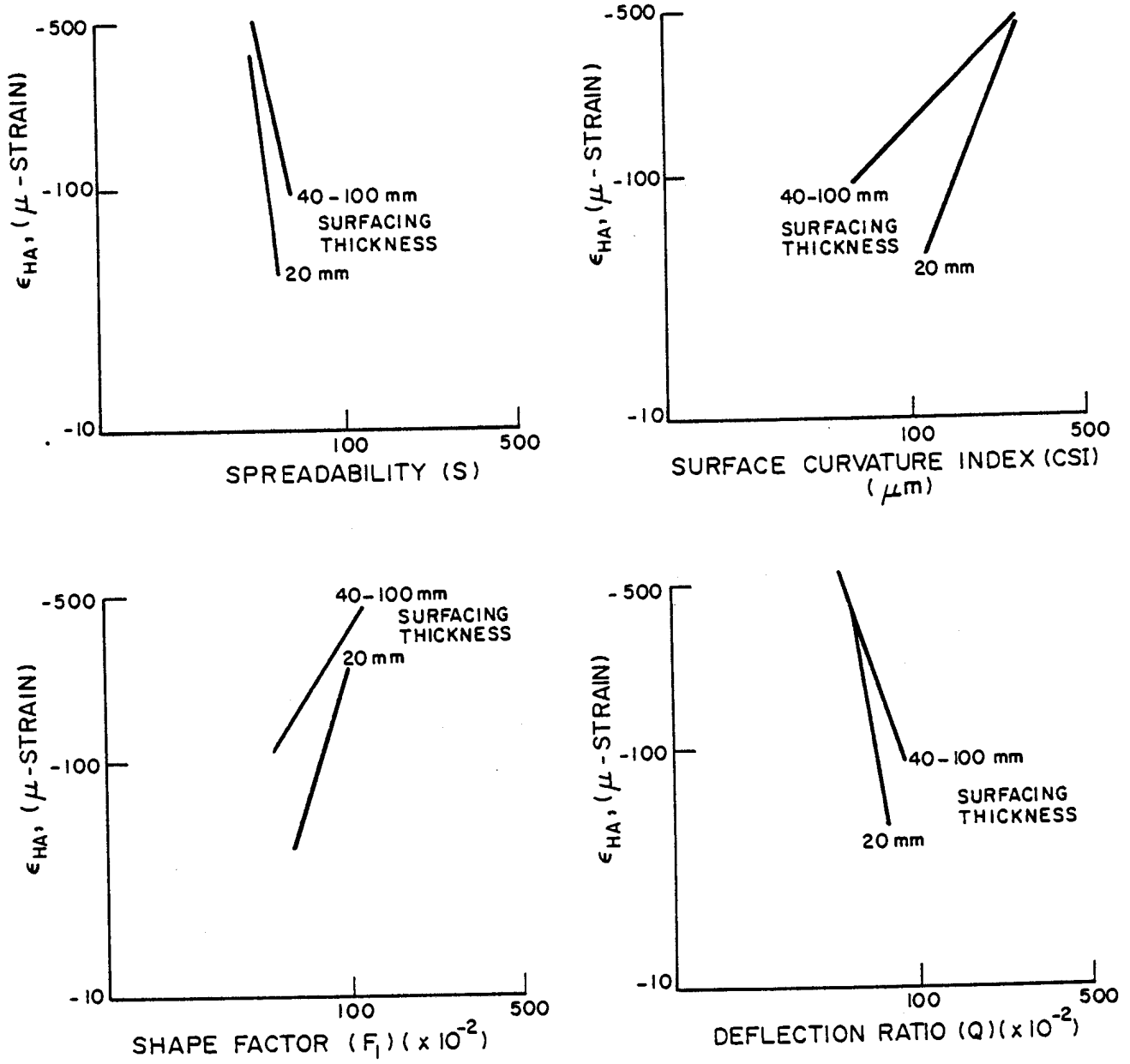


FIGURE 7.9  
GRANULAR BASE DEFLECTION BASIN PARAMETERS VERSUS  
MAXIMUM ASPHALT STRAIN

GRANULAR BASES  
E = 70 MPa

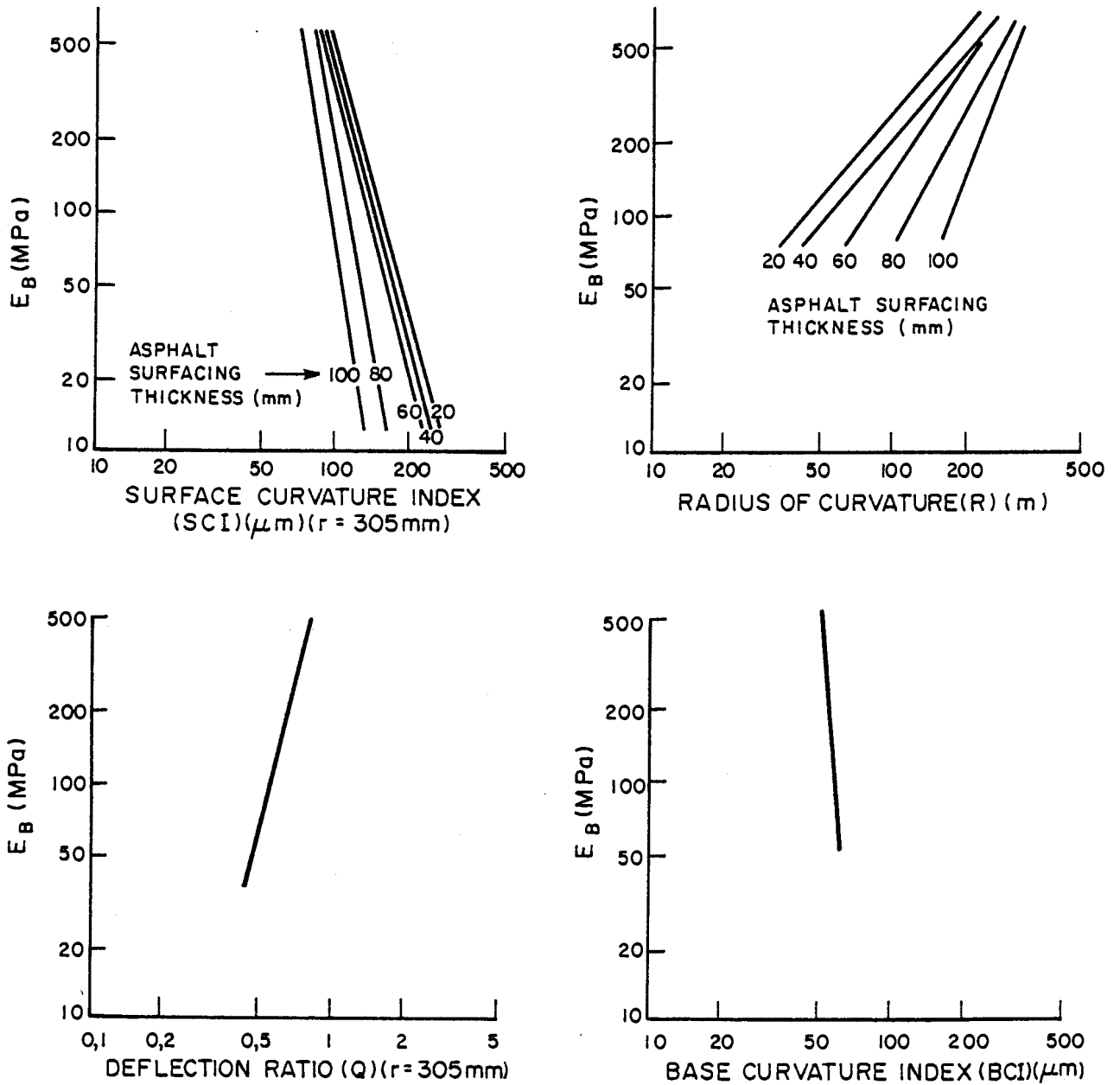


FIGURE 7.10  
GRANULAR BASE ELASTIC MODULUS VERSUS DEFLECTION  
BASIN PARAMETERS

for granular base pavements, by means of stepwise multiple regression. The relationship is as follows:

$$\epsilon_{HA} = 1360,03 F_1 + 4,54 H_{SF} - 2,10 R + 3806,29 Q - 2563,82$$

where:  $\epsilon_{HA}$  = maximum asphalt strain ( $\mu$ -strain)

$F_1$  = shape factor

$H_{SF}$  = asphalt surfacing thickness (mm)

$R$  = radius of curvature (m)

$Q$  = deflection ration ( $r=610$  mm)

This relationship has a R-square value of 92,4 per cent and a coefficient of variability of 9,7 per cent.

Maree et al. (1982a) have shown that for granular base pavements, permanent deformation originates mostly within the base itself. In order to limit or indicate the potential for permanent deformation in a granular layer, Maree (1978) suggested the use of a safety factor,

$$f = \frac{k\{3 \tan^2(45 + \phi/2) - 1 - 2C \tan(45 + \phi/2)\}}{\sigma_1 - \sigma_3}$$

where  $C$  = Apparent cohesion

$\phi$  = angle of internal friction

$\sigma_1$ ;  $\sigma_3$  = major and minor principle stresses

$K$  = constant, depending on the moisture condition.

The safety factor will therefore vary depending on the typical shear parameters ( $C$  and  $\phi$ ) and the moisture condition. Typical shear parameter values and moisture conditions (wet or dry) as suggested by Freeme (1983) were used to calculate safety factors for the wet condition ( $F_{wet}$ ) and for the dry condition ( $F_{dry}$ ). These calculations were done for typical granular base material (G1 to G4). Additionally the deviator stress ( $\sigma_d$ ) for each situation was calculated too.





The safety factors ( $F_{wet}$  and  $F_{dry}$ ) and the deviator stress ( $\sigma_d$ ) were correlated with the calculated deflection base parameters by means of a stepwise multiple regression analysis. The number of variables in the final equation was limited to three or the R-squared value had to exceed 0,75. The results of these regression analysis are shown in Table 7.2.

The deflection basin parameters that correlated the best with  $F_{wet}$  and  $F_{dry}$ , were the shape factor  $F_2$  and the index parameter  $BCI$ . The deviator stress  $\sigma_d$  correlated very well with the surfacing thickness and the index parameter  $BCI$ . The other deflection basin parameters that occurred in the relationships were;  $F_1$ ,  $Q_{610}$ ,  $SD$ ,  $BDI$  and  $S$ . (See Table 1.1 for definitions.)

The significance of these relationships are that for a granular base type, the potential for permanent deformation can be determined by calculating either  $F_{wet}$ ,  $F_{dry}$  or  $\sigma_d$  from deflection basin parameters.

#### 4.3 Bitumen base pavements

The same type of relationship was developed for bitumen base pavements by means of a stepwise multiple regression analysis. The relationship before overlay is as follows:

TABLE 7.2 REGRESSION FUNCTIONS FOR GRANULAR BASES

MATERIAL CODE	DEPENDENT VARIABLE	REGRESSION FUNCTION	R <sup>2</sup>
G1	F <sub>WET</sub>	$-5,80 + 15,84 (F_2) - 45,25 (BCI) + 4,85 \times 10^{-3} (H_{SF})$	0,77
	F <sub>DRY</sub>	$-8,07 + 28,06 (F_2) - 116,30 (BCI) + 9,56 \times 10^{-3} (H_{SF})$	0,78
	$\sigma_d$	$240,73 - 1,93 (H_{SF}) + 3704,43 (F_1) - 197,51 (BCI)$	0,97
G2	F <sub>WET</sub>	$10,04 + 3,77 (F_2) - 19,01 (Q_{610}) - 4,00 (F_1)$	0,77
	F <sub>DRY</sub>	$-6,03 + 13,74 (F_2) + 2,48 (BCI) - 55,79 (SD)$	0,80
	$\sigma_d$	$-72,58 - 2,40 (H_{SF}) + 6848,40 (BCI)$	0,95
G3	F <sub>WET</sub>	$-3,68 + 6,23 (F_2)$	0,80
	F <sub>DRY</sub>	$-7,41 + 12,67 (F_2)$	0,81
	$\sigma_d$	$-43,38 - 2,55 (H_{SF}) + 6329,04 (BCI)$	0,95
G4	F <sub>WET</sub>	$-0,14 + 21,19 (BDI) - 3,08 (Q_{610})$	0,77
	F <sub>DRY</sub>	$-2,46 + 8,09 (F_2) - 4,50 (Q_{610})$	0,77
	$\sigma_d$	$-1,18 - 2,45 (H_{SF}) + 5447,25 (BCI)$	0,84
G1 TO G3	F <sub>WET</sub>	$-0,971 - 0,048 (S) + 38,96 (BDI) + 9,76 \times 10^{-3} (F_2)$	0,77
	F <sub>DRY</sub>	$-1,78 + 2,25 \times 10^{-2} (F_2) + 66,31 (BDI) - 0,07 (S)$	0,78
	$\sigma_d$	$-85,09 + 12703,27 (BCI) - 4003,98 (BDI) - 1,16 (F_2)$	0,81

ELASTIC MODULUS OF SUBGRADE = 70 MPa

DEFLECTION BASIN PARAMETERS AS DEFINED IN TABLE 1.1

$$\log_{10} \epsilon_{HA} = - 0,996 (\log_{10} SCI) - 0,352 (\log_{10} S) \\ - 0,298 (\log_{10} Q) + 2,521$$

where:  $\epsilon_{HA}$  = maximum (tensile) asphalt strain ( $\mu$ -strain)

SCI = surface curvature index (mm)

S = spreadability

Q = deflection ration (r=305 mm)

This relationship has an R-square value of 0,99 and a coefficient of variability of 16,5 per cent.

When this relationship is determined for bitumen bases with overlays it looks as follows:

$$\log_{10} \epsilon_{HA} = - 0,623 (\log_{10} A) - 0,619 (\log_{10} Q) \\ - 0,365 (\log_{10} SCI) + 3,470$$

where: A = area and the rest are as defined earlier.

This relationship has an R-square value of 0,61 and a coefficient of variability of 80,1 per cent. The effect of the overlay is such that this relationship with only three independent variables reduces the R-square value considerably and increases the coefficient of variability to unacceptable limits and the use thereof is not recommended.

#### 4.4 Subgrade elastic modulus

A relationship between deflection at 2 m and subgrade elastic modulus was derived similar to that derived by Molenaar and Van Gurp (1980). In this case though, it is applicable to all types of flexible pavements with four or five layers. This relationship is:



$$\log E_s = 9,727 - 0,989 \log \delta_{2000}$$

where:

$E_s$  = subgrade elastic modulus (Pa)

$\delta_{2000}$  = deflection at a distance of 2 m  
from the centre of loading ( $\mu\text{m}$ ).

This relationship is shown in Figure 7.11 where the subgrade moduli had been correlated with deflections at 500, 610 and 915 mm, too. It is obvious that the gradient of the relationships change from deflection at 500 mm ( $\delta_{500}$ ) to deflection at 915 mm ( $\delta_{915}$ ), but from the latter deflection up to deflection at 2 000 mm ( $\delta_{2\ 000}$ ) the gradient of the relationships stays virtually the same. It is the general feeling (Tam, 1985) that deflections nearer than 500 mm ( $\delta_{500}$ ) to the centre of loading, would increasingly reflect the influence of the other structural layers. nearer to the surface ( base and subbase).

## 5 THE EFFECT OF OVERLAYS

### 5.1 Granular base pavements

Granular base pavements in the dry regions of South Africa have typical surfacing thicknesses of 30 to 50 mm (40 mm average) thick. Alternatively surface treatments typically have thicknesses of 20 mm for double surface treatments. As shown in Appendix F, these thin asphalt surfacings have relatively little influence on the value of equivalent layer thickness ( $H_e$ ) and therefore also on vertical subgrade strain ( $\epsilon_{VS}$ ), as the thickness of the overlay is increased. In the wetter regions of South Africa thicker asphalt surfacings and overlays may be applicable.

The effect of overlay thickness on  $\epsilon_{VS}$  is illustrated; in Figure 7.12. The greater the overlay thickness, the more  $\epsilon_{VS}$  is reduced. An elastic modulus of 3000 MPa was assumed typical for the asphalt overlay and an elastic modulus of

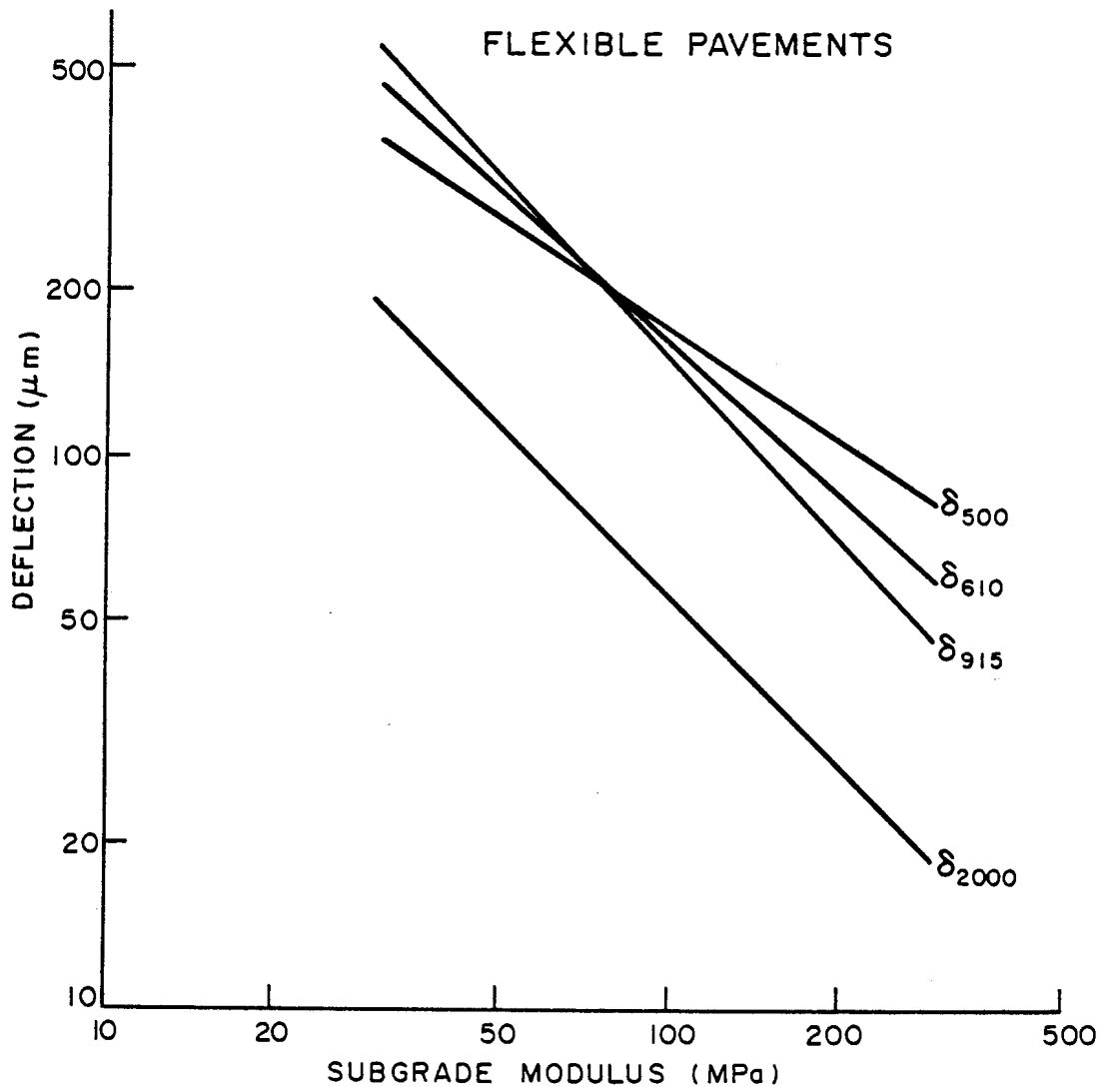


FIGURE 7.11  
SUBGRADE ELASTIC MODULUS VERSUS DEFLECTION

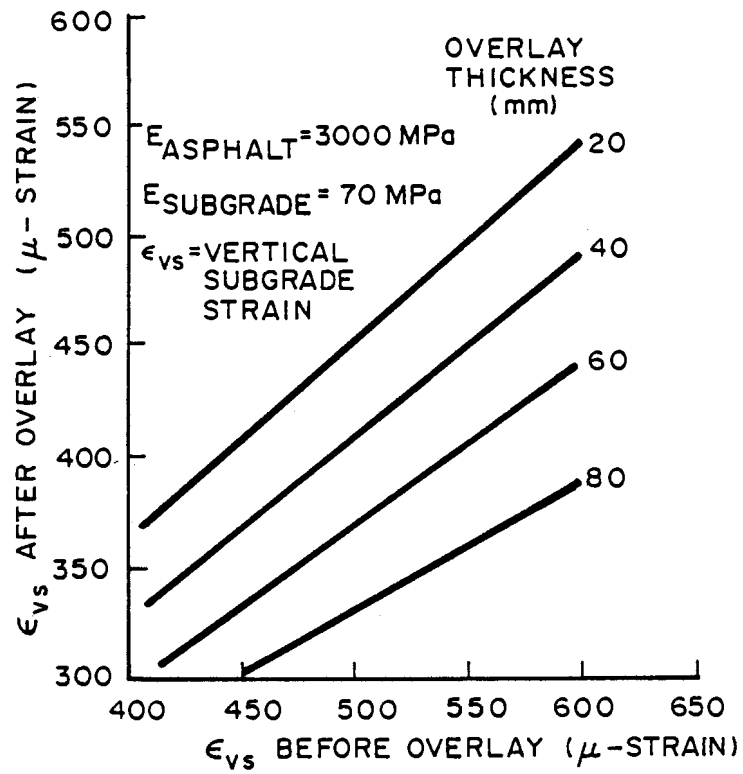


FIGURE 7.12  
 Effect of overlay thickness on  
 subgrade strain of granular  
 base pavements



70 MPa for the subgrade layer. Overlay thicknesses of 60 mm or more would substantially reduce  $\epsilon_{vs}$ , but asphalt layers of such total thickness (surfacing plus overlay) are classified as bitumen base pavements (Freeme et al., 1982a). Such overlay thickness would therefore rarely be applicable. Possibly as levelling courses to correct excessive rut irregularities.

In the discussion of the selection of overlay thicknesses, it is assumed that granular base pavements have either an existing surface treatment with maximum thickness of 20 mm or a premix asphalt surfacing layer with a typical thickness of 40 mm. This original asphalt surfacing thickness has a deciding influence on the deflection basin in the vicinity of the wheel load. This is best reflected in Figure 7.13 which shows surface curvature index (SCI) values before and after overlays of various thicknesses. It can be seen that for granular base pavements with a maximum original surfacing thickness of 20 mm, an overlay of at least 40 mm will be needed to reduce SCI values. For a granular base pavement with an original surfacing thickness of 40 mm, a 20 mm overlay will lead to a reduction in SCI values. This means that there is a reduction in SCI values, only after a total thickness of 60 mm.

The influence of the original asphalt thickness is even more pronounced when the effect of overlays of various thicknesses on the reduction in maximum horizontal asphalt strain ( $\epsilon_{HA}$ ) is considered. In Figure 7.14 the values of  $\epsilon_{HA}$  before and after overlays are shown for original surfacing thicknesses of both 20 mm and 40 mm and for various overlay thicknesses. For a granular base pavement with an original surfacing thickness of 20 mm, an overlay of over 80 mm would clearly be needed to reduce  $\epsilon_{HA}$  values, and this is seen as impractical and costly. A granular base pavement with an original asphalt thickness of 40 mm may only require an overlay of 20 mm to reduce  $\epsilon_{HA}$  if the value of  $\epsilon_{HA}$  before overlay was more than 250  $\mu$ -strain.





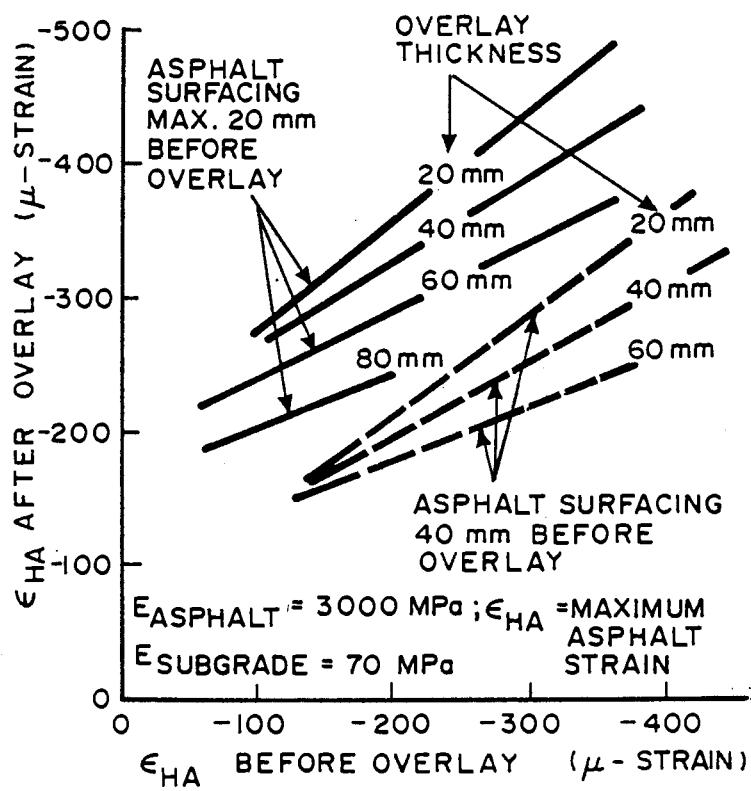


FIGURE 7.14  
 Effect of overlay thickness  
 on maximum asphalt  
 strain of granular base  
 pavements



## 5.2 Bitumen base pavements

Overlay thicknesses have the same effect on bitumen base pavements as on granular base pavements in general, concerning the effect of reducing subgrade strain ( $\epsilon_{VS}$ ). In Figure 7.15 it can be seen that the thicker the overlay, the more the reduction in  $\epsilon_{VS}$ .

The subgrade, as varied in terms of elastic moduli, also has an influence in terms of a difference in gradient for the thicker overlays (40 and 60 mm). Each subgrade condition has a definite range over which they are applicable too. For the overlay of 10 mm, subgrade moduli variance does not have an influence. This thickness would normally not be considered for such a purpose.

Deflection basin parameters calculated before and after an overlay reflect a change with various degrees of significance. In Figure 7.16, deflection basin parameters, S, F1, SCI and SD clearly show the effect of overlay thicknesses on values before and after overlays. In general F1, SCI and SD show a reduction in values while S shows an increase in values when overlaid. The indications are not the same though in terms of a structural improvement as SCI and SD are insensitive to changes in elastic moduli of the subgrade (50, 70 and 150 MPa). The relationships determined for S and F1 are true only for a subgrade modulus of 70 MPa.

Overlays reduce the asphalt strain under the base ( $\epsilon_{HA}$ ) as can be expected. The thicker the overlay, the more the reduction. In Figure 7.17 it is shown how this is true for bitumen base pavements of which the subgrade elastic moduli were varied from 50 to 150 MPa. In the whole analysis it was assumed that no existing cracks occurred in the base, as this would definitely need a different analysis procedure.

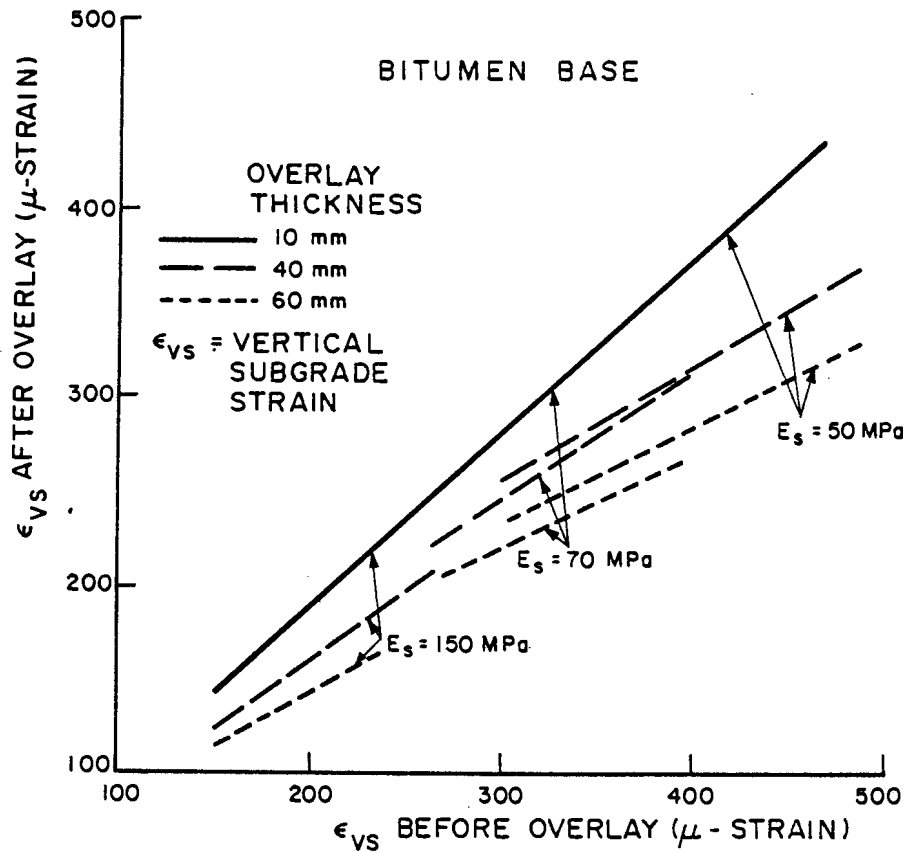


FIGURE 7.15  
 EFFECT OF OVERLAY THICKNESS ON SUBGRADE STRAIN FOR BITUMEN BASE PAVEMENTS

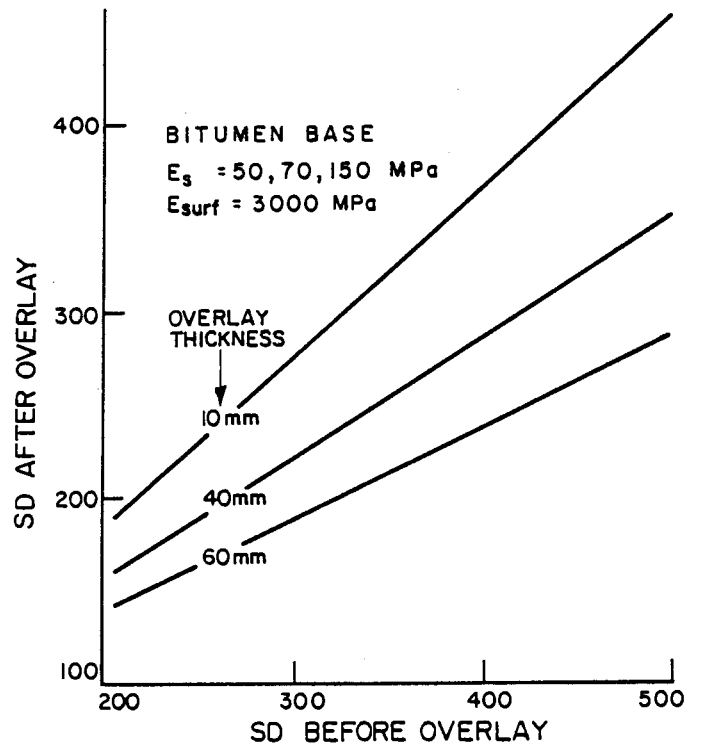
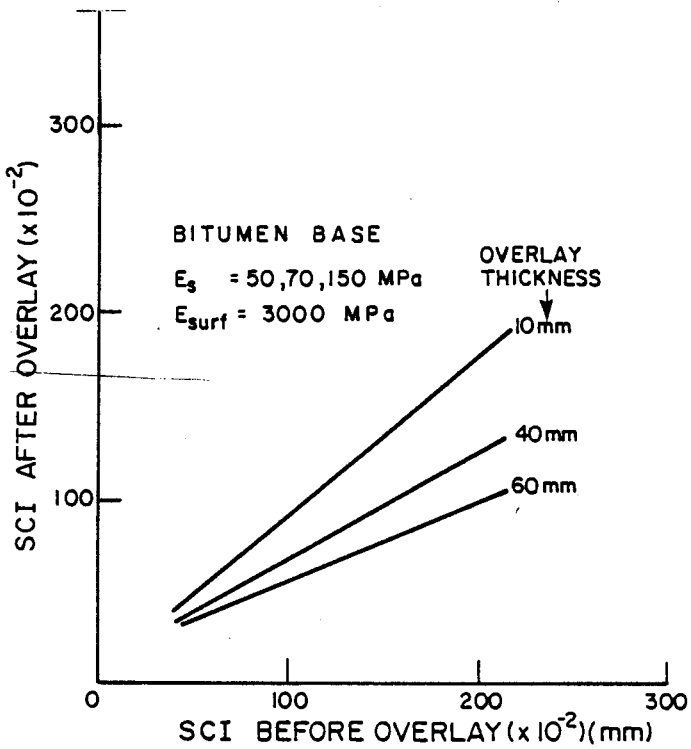
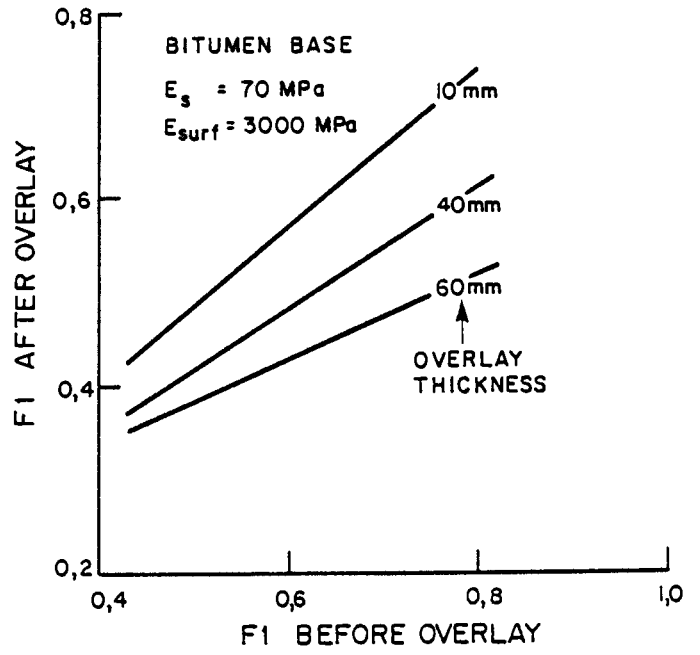
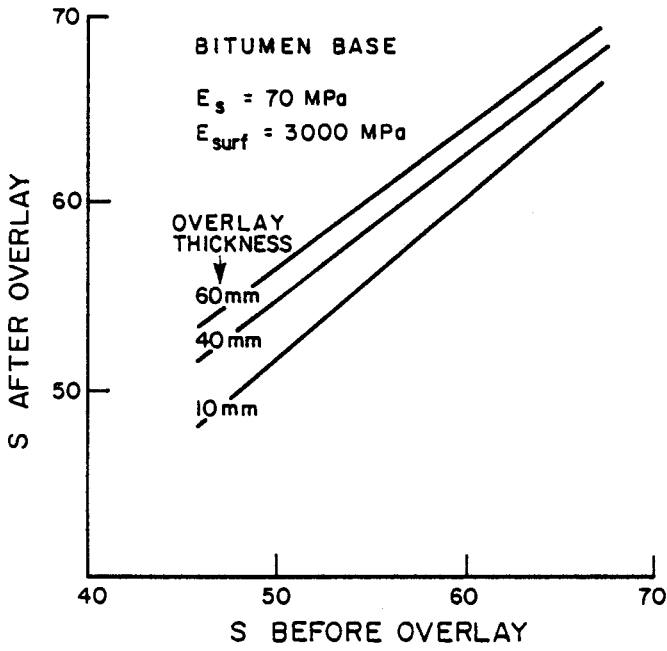


FIGURE 7.16

INFLUENCE OF OVERLAYS OF BITUMEN BASES ON DEFLECTION BASIN PARAMETERS

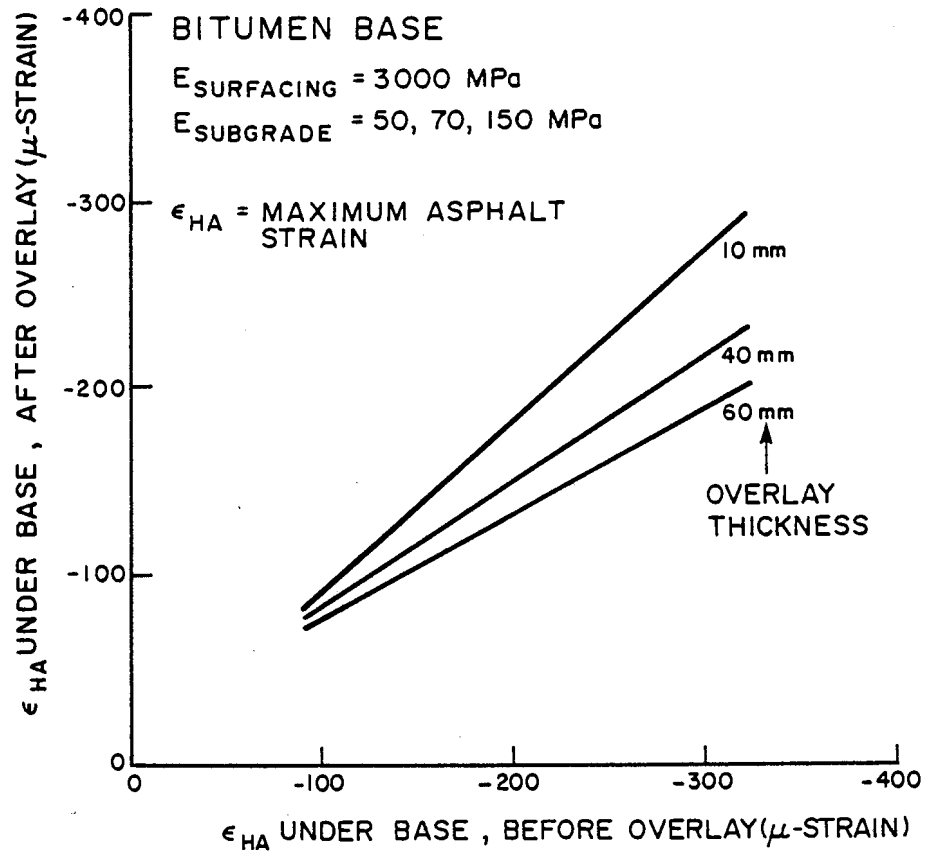


FIGURE 7.17  
 EFFECT OF OVERLAY THICKNESS ON MAXIMUM  
 ASPHALT TENSILE STRAIN OF BITUMEN BASE  
 PAVEMENTS



## 6 CONCLUSIONS

Some deflection basin parameters can be related to distress determinants ( $\epsilon_{VS}$  and  $\epsilon_{HA}$ ) in meaningful and clear relationships. In some cases though no discernment can be made with a variance in subgrade elastic moduli. This is not a great concern as simple and clear relationships are still possible. The simultaneous variance of other structural parameters such as surfacing thickness and base elastic modulus and thickness, lead to a lack of simple meaningful relationships for granular base pavements in particular.

The calculated value of surface curvature index (SCI) versus vertical subgrade strain ( $\epsilon_{VS}$ ) is a useful relationship for granular and bitumen base pavements. There is a clear discernment when subgrade elastic moduli are varied. The gradients of the relationships also differentiate between the two base types (granular and bitumen). Bitumen base pavements seem to be less influenced by the simultaneously varied structural input parameters referred to earlier. Clear relationships between deflection basin parameters  $F_1$ ,  $R$ ,  $SD$  and  $Q$  versus vertical subgrade strain ( $\epsilon_{VS}$ ) are examples.

The maximum asphalt strain ( $\epsilon_{HA}$ ) calculated under the base of bitumen base pavements, correlates well with deflection basin parameters such as  $S$ ,  $A$ ,  $F_1$ , and  $BCI$ . When maximum horizontal asphalt strain ( $\epsilon_{HA}$ ) is calculated under the surfacing of such bitumen base pavements, the values are compressive which reduces its significance for fatigue calculation. The effect of varying the subgrade elastic modulus was discerned by the above-mentioned deflection basin parameters. The thickness of surfacing of granular bases has a definite effect on relationships between deflection basin parameters and  $\epsilon_{HA}$ . The difference in the effect of asphalt thickness is clearly illustrated in the relationships between radius of curvature ( $R$ ) and maximum horizontal asphalt strain ( $\epsilon_{HA}$ ) for granular and bitumen bases. The tendency for

deflection basin parameters, such as S, SCI, F1 and Q, to group together granular base surfacing thicknesses, of 40 mm to 100 mm differing from the effect of thicknesses of up to 20 mm, is in line with work previously done in this regard.

Overlays of flexible pavements reduce subgrade strain ( $\epsilon_{VS}$ ) increasingly as thicknesses of overlays increase. This does not mean though that it is a viable and economic procedure to reduce subgrade strain ( $\epsilon_{VS}$ ). For granular base pavements the overlay thicknesses required to reduce  $\epsilon_{VS}$  is more than that normally applied in practice. Such thick overlays could in some cases be applicable to levelling courses on granular base pavements in order to correct excessive rut irregularities.

Overlay thickness of granular bases does have an effect on the calculated values of deflection basin parameters. Surface curvature index (SCI) values reflect a reduction when granular base pavements are overlaid. The thickness of the original surfacing does have a major effect on SCI values. Even better relationships were found for bitumen base pavements for S, F1, SCI and SD. It is even possible to show that SCI and SD reflect changes due to overlay thicknesses, irrespective of subgrade elastic moduli.

The original thickness of a granular base surfacing influences the required thickness of overlay for a reduction in asphalt strain ( $\epsilon_{HA}$ ). Thin original surfacing layers (less than 20 mm) require impractical thick overlays (80 mm and more) to reduce ( $\epsilon_{HA}$ ). Original surfacing thicknesses of 40 mm require overlays as thin as 20 mm to reduce  $\epsilon_{HA}$ . The base thickness of bitumen bases (more than 80 mm) is sufficient to require normal practice overlay thicknesses to reduce asphalt strain ( $\epsilon_{HA}$ ). Overlay thicknesses as low as 10 mm reduce  $\epsilon_{HA}$  at the underside of the base. Such thin overlays are however also impractical.



## CHAPTER 8

### PROPOSED USE OF DEFLECTION BASIN MEASUREMENTS IN THE MECHANISTIC ANALYSIS AND REHABILITATION OF FLEXIBLE PAVEMENTS





## CHAPTER 8: CONTENTS

	PAGE
1 INTRODUCTION	8.2
2 DEFLECTION BASIN MEASUREMENTS	8.2
2.1 Deflection basin parameters	8.2
2.2 Equipment and measurement	8.4
2.2.1 Network level	8.4
2.2.2 Project level	8.5
3 ENHANCEMENT OF THE MECHANISTIC REHABILITATION DESIGN PROCEDURE WITH DEFLECTION BASIN MEASUREMENTS	8.6
3.1 General	8.6
3.2 Identification of pavement behaviour states	8.7
3.3 Material characterization	8.9
3.3.1 General	8.9
3.3.2 Normal material characterization	8.9
3.3.3 Material characterization with deflection basin measurements	8.12
3.3.4 Back-analysis of effective elastic moduli	8.12
3.4 Analysis of flexible pavement structures	8.13
3.4.1 General	8.13
3.4.2 Rutting	8.13
3.4.3 Cracking	8.16
3.5 Rehabilitation design	8.17
3.5.1 General	8.17
3.5.2 Granular base pavements	8.17
3.5.3 Bitumen base pavements	8.20
3.5.4 Practical considerations	8.21
4 FUTURE RESEARCH	8.21
4.1 General	8.21
4.2 Measuring equipment	8.22
4.3 Material characterization	8.22
4.4 Analysis procedures	8.23

## 1 INTRODUCTION

In this chapter this author endeavours to summarise this study on deflection basin measurements by presenting it in a format that would enhance the present mechanistic rehabilitation design procedure. The discussion summarises the proposed measurement of deflection basins on a network and a project level. Deflection basin parameters that describes the full deflection basin, are suggested for general use. It is shown how the selected deflection basin parameters can enhance the accurate description of the pavement behaviour states. Better material characterization is facilitated by using the relationships established between material properties and deflection basin parameters. In the analysis of typical flexible pavements the relationships between deflection basin parameters and distress determinants are discussed to show how such a design curve approach can enhance the non-simplified approach. Although mention is made of rehabilitation design, the reference only applies to the mechanistic rehabilitation design procedure. Overlay design as an option is highlighted in this chapter. Finally this author indicates what future research needs to be done on deflection basins.

## 2. DEFLECTION BASIN MEASUREMENTS

### 2.1 Deflection basin parameters

In chapter 1 the deflection basin was discussed in great detail. Various deflection basin parameters were defined as listed in Table 1.1. In summary it can be stated that deflection basin parameters must:

- (a) Represent the full range of characteristics of the whole deflection basin (not only maximum deflection, but rather a combination of parameters covering the whole deflection basin)
- (b) Be simple to calculate and interpret, and
- (c) Be able to relate to the structural characteristics of the full depth of pavement structures.

In chapter 2 it was shown that irrespective of the measuring equipment the majority of these deflection basin parameters can be calculated fairly easily. It was shown that the full deflection basin as such does not have to be measured. It was suggested that only deflections on the deflection basin be measured at selected off-sets. The off-sets that are suggested are at 0, 127, 305, 610 and 915mm (the off-set at 127mm is seen as optional as it is only related to radius of curvature). As can be seen from Table 1.1 the majority of the deflection basin parameters can be calculated using the deflections measured at these points. In the discussion in chapter 3 it was shown that the deflection basin parameters that are the most significant in terms of their description of pavement behaviour state and material identification are the index parameters. They are ;

Surface curvature index ( SCI)

Base damage index (BDI)

Base curvature index (BCI).

These deflection basin parameters describe the deflection basin in full. Surface curvature index (SCI) describe the area of positive curvature in the immediate vicinity of the load (see Figure 2.7). This reflects on the structural capacity of the base and surfacing layer. Base damage index (BDI) describes the transitional zone of the deflection basin where the positive curvature changes over to that of the reverse curvature. This reflects on the structural capacity of the base and subbase layers. Base curvature index (BCI) describes the area of the reverse curvature. This reflects strongly on the structural capacity of the lower layers such as the selected layer or subgrade.

Other deflection basin parameters that can be used as assistance in the analysis procedure is that of slope of deflection (SD) or maximum deflection or radius of curvature (R). The latter two are included purely to ensure the change over from the traditional deflection basin parameters and their related relationships with pavement

analysis can be used as an enhancement with the proposed index parameters.

## 2.2 Equipment and measurement

The various measuring devices are discussed in detail in Chapter 1. In general the ideal measuring device should:

- (a) Realistically simulate moving traffic loads in terms of magnitude of load, shape and equivalent time of loading
- (b) Accurately measure the whole deflection basin with high levels of reproducibility
- (c) Be simple to operate, so that it could be used with confidence in the field, but it should also be applicable to research
- (d) Be capable of attaining high levels of productivity, which must reduce the cost of testing.

### 2.2.1 Network level

The NITRR Deflectograph (previously the Lacroix deflectograph) is used on a network basis in South Africa by the road authorities, with a proven level of efficiency. It is believed that this will still be the primary function of this measuring device. In the discussion in chapter 1 it was shown that no other non-destructive measuring equipment can compete with this apparatus in terms of productivity and cost per measuring point. With the old Lacroix deflectograph only the maximum deflection was used to distinguish between various uniform sections of road. This author instigated the change with the new NITRR deflectograph whereby amongst others deflections are measured on the full deflection basin at the off-sets as suggested in the preceding section. This means that the most significant deflection basin parameters can be calculated (eg. index parameters). The IBM computer on board the NITRR deflectograph accumulates the data and from that level data manipulation becomes a standard procedure with other personal

computers in the data processing unit. The ease of the data manipulation of the NITRR deflectograph enables the engineer to give a more fundamental evaluation of the pavement condition even at the network level which previously was not possible. This will be explained in more detail later in this chapter.

### 2.2.2 Project level

On a project level detailed assessment of a pavement section is required. The requirements listed above narrows the list of possible non-destructive deflection basin measuring equipment down to only two. The falling weight deflectometer (FWD) seems to be the most appropriate device when measured against these prerequisites. The FWD is a system which has proven its reliability in environments overseas. The ease and speed of operation and transportability gives it the edge over the road surface deflectometer (RSD). It will take a considerable time before such an apparatus can be commissioned for general use in South Africa. It is suggested that, should such a system become available in South Africa, it be properly calibrated against the road surface deflectometer (RSD). This should preferably be done on various pavement types and behaviour states. Accelerated tests with the Heavy Vehicle Simulator (HVS) would provide the ideal situation for such calibration.

The RSD, as used during accelerated tests under the HVS, is however, still the main reference device for non-destructive deflection measurements of pavements in South Africa. The vast extent of the information recorded on various pavement types under various testing conditions, behaviour states and material states, makes it possible to do extensive modelling of pavement behaviour. The deflection basins of the pavement, as measured with the Multi-Depth-Deflectometer (MDD), are also available for further comparative studies on the same pavement structures and loading conditions. The RSD measures the full deflection basin and therefore does not confine the analysis to specific deflection basin parameters. The WASHO procedure of measuring, as is used

under the HVS, limits the effects of plastic deformation. The wheel approaches the measuring point while the typical rebound procedure, as is still used with the standard Benkelman beam truck, measures plastic deformation too. The RSD can therefore be used with the same standard Benkelman beam truck, but with a different measuring procedure.

The set-up for measuring the deflection basin with the RSD already exists, as used in combination with the Crack Activity Meter (CAM) (see Appendix E). The procedure of data management and analysis for the RSD is well established and is described in detail in chapters 2 and 3. The relationships developed during accelerated tests with the RSD will make it a powerful tool in the hands of the engineer during the detailed assessment phase. In the rest of the chapter this will be discussed in more detail.

### **3 ENHANCEMENT OF THE MECHANISTIC REHABILITATION DESIGN PROCEDURE WITH DEFLECTION BASIN MEASUREMENTS**

#### **3.1 General**

In chapter 4 and 6 reference are made to the mechanistic design procedure. The mechanistic rehabilitation design procedure as used in South Africa is well established and verified with the fleet of accelerated testing facilities, the Heavy Vehicle Simulators (HVSs) (Freeme, et al., 1982b and Freeme, 1983). However, where this rehabilitation design method is lacking, is in making better use of non-destructive measurements to make this rehabilitation and design process more effective. Deflection basin measurements have been under-utilized in South Africa as they were mostly limited to the use of maximum deflection and radius of curvature measurements. This has resulted in empirical relationships which reflected little information on fundamental material and pavement type behaviour.

The use of deflection basin parameters in the rehabilitation and analysis of flexible pavements was investigated and the suggested

incorporation thereof in the existing mechanistic rehabilitation design procedure is described in the sections to follow.

### 3.2 Identification of pavement behaviour states

The behaviour catalogue is an extension of the existing design method, the TRH4 (NITRR, 1985a) which also has a catalogue of designs. The basic philosophy followed in the catalogue of rehabilitation designs and that of the TRH4 (NITRR, 1985a) is therefore similar. This is illustrated in the flow diagram of the mechanistic pavement rehabilitation design method in Figure 4.1. For the reader's convenience this figure is repeated here as Figure 8.1.

The First step is always to identify the pavement class. An in depth discussion of pavement class distinction or selection is given in TRH4 (NITRRa, 1985) and will not be repeated here.

The second phase illustrated in Figure 8.1 is to correctly identify the pavement type. This identification is done in terms of the base layer type. The base types are defined as: Granular, bituminous, cemented or concrete. This subdivision of pavements, based on base types, is clearly described by Freeme (1983) and Freeme et al. (1986) in terms of the difference in the performance or behaviour of these basic pavement types and the resultant difference in the behaviour states and catalogue selection.

Deflection measurements are the basis of the definition of the pavement behaviour states. Approximate ranges of maximum deflection ( $\delta_0$ ) are used to subdivide the pavement behaviour types into very stiff, stiff, flexible and very flexible behaviour states. These ranges of maximum deflection ( $\delta_0$ ) and an abbreviated description of the general behaviour are shown in Table 3.1.

Deflection basin parameters that were measured on various pavement types during accelerated tests (see chapter 3) were used to give a better definition of the various pavement states. These deflection basin parameter ranges are listed in Table 3.2 and repeated in

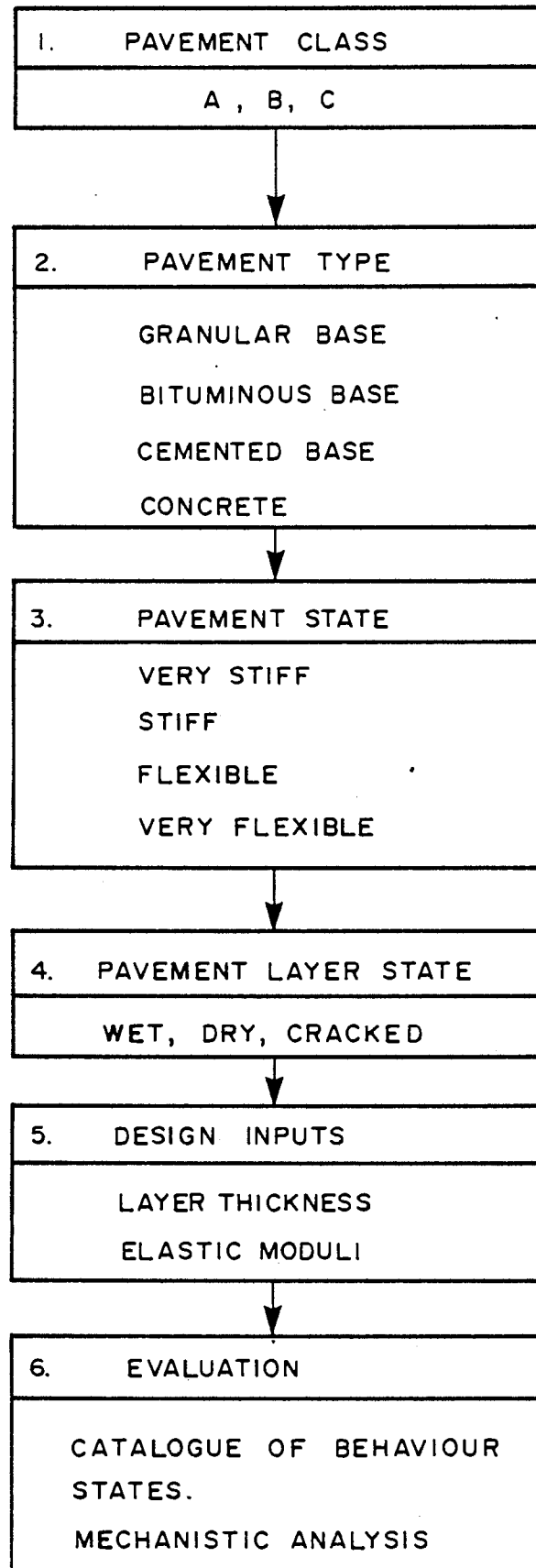


FIGURE 8.1  
FLOW DIAGRAM OF THE MECHANISTIC  
PAVEMENT REHABILITATION DESIGN  
METHOD (FREEME, 1983)



Table 8.1 for the various pavement behaviour states. It is suggested therefore that the index parameters rather than maximum deflection be used in the identification of the pavement behaviour state.

The pavement behaviour states of particular interest in this discussion are the flexible and very flexible behaviour states. In general it will also mean that the pavement types as shown in Figure 8.1 will be narrowed down to granular bases, bitumen bases and cemented bases. As the latter type will mostly be in a cracked layer state, the flexible cemented bases will be analyzed as a granular or equivalent granular base type.

### 3.3 Material characterization

#### 3.3.1 General

For a correct analysis of a pavement in the mechanistic rehabilitation design procedure it is very important that the material of the various layers are identified correctly. In Figure 8.1 it is shown how the class, type, the behaviour state and state of the layer materials are used to characterize the pavement layer materials. This normal approach can be enhanced by the incorporation of deflection basin parameters in the analysis procedure, but such deflection basin parameters can also be used to describe the pavement materials more directly.

#### 3.3.2 Normal material characterization

The normal approach whereby material is characterized is where the principle input for the material properties (layer thickness, effective elastic moduli and Poisson's ratio) is determined from basic pavement and material information. This is best illustrated by referring to Figure B.1 (see Appendix B) where it is shown in the flow diagram that both destructive and non-destructive testing results are used to do effective material characterization. This ties in with the approach outlined earlier for the mechanistic rehabilitation design procedure (Freeme, 1983). Information from

**TABLE 8.1 Behaviour states defined by deflection basin parameters**

Behaviour state	Deflection basin parameter ranges				
	Max. defl. (mm)	SD ( $\times 10^{-6}$ )	SCI (mm)	BDI (mm)	BCI (mm)
Very stiff	< 0,2	< 50	< 0,01	< 0,01	< 0,01
Stiff	0,2 - 0,4	50 - 400	0,01 - 0,2	0,01 - 0,1	0,01 - 0,05
Flexible	0,4 - 0,6	400 - 750	0,2 - 0,4	0,1 - 0,15	0,05 - 0,08
Very flexible	> 0,6	> 750	> 0,4	> 0,15	> 0,08

as-built information, condition surveys, traffic surveys and deflection surveys form the pool of information of the non-destructive testing. Destructive testing like in situ Dynamic Cone Penetrator (DCP) surveys or coring of cemented or treated materials for material sampling and laboratory testing, are normally done during a second phase detailed analysis. Such information is very valuable as even standard laboratory tests can be used to characterize layer material into various material classes as specified in TRH14 (NITRR, 1985b) and abbreviated in TRH4 (NITRR, 1985a). Freeme et al. (1982a) and Freeme (1983) also give a detailed description of the various material classes.

The use of more sophisticated laboratory tests like triaxial tests, repeated loads triaxial tests, repeated loads indirect tensile tests, beam tests, creep tests, etc. can only enhance the correct description of materials. The mechanistic design method in general encourages the use of such sophisticated tests. The effective elastic moduli relationships used in the design method are based on extensive tests of this kind to determine the basic material characteristics. Freeme et al. (1982a) and Freeme (1983) do provide transfer factors for the various pavement classes and pavement layers to relate such sophisticated laboratory results to actual behaviour as measured under accelerated testing. The DCP results enhances not only the proper material characterization, but with the balance curves concept ( de Beer, 1986) the analysis procedure.

Finally it is therefore possible to accurately determine the basic input parameters for the mechanistic analysis, if adequate knowledge and experience concerning such a characterization are available. Freeme, et al. (1982) and Freeme (1983) give a detailed description of each material type, material states and possible configuration in a pavement structure. The effective elastic moduli can therefore be read off such tabulated values. It is believed that, as considerable time and engineering judgement have already gone into the correct material identification up to this stage, any uncertainty can be overcome by doing a sensitivity analysis on such pavement structures during the analysis phase.

### 3.3.3 Material characterization with deflection basin measurements

The subgrade is an important layer in the analysis of a pavement. The effect that this layer has on the general shape of the deflection basin was discussed in detail in chapter 4. In chapter 7, it was shown that there exists a very good correlation between subgrade elastic modulus and deflection measured on the reverse curvature of the deflection basin. These relationships are true for all flexible pavements with up to five structural layers. These relationships are as shown in Figure 7.11. It is suggested that more than one deflection be used in the determination of the subgrade elastic modulus and an average value can be determined. A further refinement can also be added by only using deflection values greater than 0,01 mm to avoid problems with measurement inaccuracies.

The elastic modulus of the base of a granular base pavement can also be determined from Figure 7.10 if the subgrade modulus is 70 MPa. As shown in this figure, various deflection basin parameters can be used to determine the subgrade elastic modulus. The effect of the surfacing thickness is also taken into consideration. Although the subgrade effective elastic modulus is not varied, this figure can be used to determine a first approach to the base elastic modulus value in analyses.

### 3.3.4 Back-analysis of effective elastic moduli

The effective elastic moduli as determined with depth deflections from Multi-depth-deflectometer (MDD) measurements, are the reference values as determined under accelerated testing. These effective elastic moduli were used extensively to verify the tables of effective elastic moduli as proposed by Freeme (1983) and Freeme et al. (1982a).

In Chapter 5, it was described and illustrated how surface deflection basin measurements can be used to back-calculate effective elastic moduli. The linear elastic computer program BISAR was used to back-calculate effective elastic moduli. The



basic procedure is to use deflections on the outer edge of the deflection basin to calculate the effective elastic modulus of the lowest layer (subgrade). Hereafter deflections nearer to the point of loading are used to calculate the effective elastic modulus of the next layer nearer to the surface. By thus each time using deflections nearer to the point of loading, the effective elastic moduli of layers increasingly nearer to the surface are calculated. Although the back-analysis procedure as outlined above can be defined as a standard procedure, considerable manual interference is still needed to arrive at unique layer effective elastic moduli. In conclusion, it can be stated that the confidence in the indirect material classification, as outlined earlier, rates the necessity for such direct approach back-calculation procedure as a confirmative bonus.

### 3.4 Analysis of flexible pavement structures

#### 3.4.1 General

In Figure 8.1 it can be seen that once the material characterization, also called design inputs, is completed, the last phase, namely the evaluation, can be tackled. As shown in Figure 8.1 the catalogue of behaviour states can be used in the analysis, as described by Freeme (1983). The non-simplified approach (Jordaan, 1986) on the other hand is still the standard procedure where the linear elastic computer programmes are used to calculate the various distress determinants. This approach is also described in great detail by Freeme (1983) and will not be repeated here. The deflection basin parameters can however be used in a design curve approach (Jordaan, 1986) whereby the selected deflection basin parameters are related to the various distress parameters. This approach was investigated in detail in chapter 7. The main distress determinants relating to rutting and fatigue cracking are discussed here in the analysis proses.

#### 3.4.2 Rutting

Vertical subgrade strain ( $\epsilon_{vs}$ ) is directly correlated to various deflection basin parameters as described in chapter 7. Only the preferred deflection basin parameters outlined earlier, are used here, but the relationships described elsewhere for these parameters can also be used.

The vertical subgrade strain ( $\epsilon_{vs}$ ) was correlated with the various deflection basin parameters for the basic pavement types, bitumen and granular bases, separately. In Figure 7.2 Surface Curvature Index (SCI) is shown versus vertical subgrade strain ( $\epsilon_{vs}$ ) for granular and bitumen base pavements. In the case of granular bases a relationship between base damage index (BDI) and subgrade vertical strain ( $\epsilon_{vs}$ ) can be used without regard to the subgrade effective elastic moduli. This relationship is shown in Figure 7.3.

In the mechanistic rehabilitation design procedure deformation or rutting is kerbed by the limitation of vertical subgrade strain ( $\epsilon_{vs}$ ). In Figure 8.2 these fatigue life criteria as verified by accelerated testing are shown. The various pavement classes are differentiated as shown. By first determining the vertical subgrade strain with the deflection basin parameters, the remaining life can be determined as outlined in Appendix C.

Although deformation of the whole pavement structure cannot be assessed, the mechanistic rehabilitation design procedure as described by Freeme (1983) does allow for indirect design. In the case of granular bases the calculation of safety factors, based on the basic shear parameters ( $C$  and  $\phi$ ) and the moisture condition of the pavement layers, limit deformation in such a granular layer by set criteria (Maree et al., 1982). Freeme (1983) expanded these criteria for the equivalent granular states of cracked cemented layers and thus limiting deformation in the cemented layers, too. If the quality of the granular base material is known, the safety factor can be determined using the regression functions as determined in Table 7.2 for that specific subgrade condition. The fatigue life criteria as discussed by Freeme (1983) can then be used to determine the remaining life of such a granular base layer.

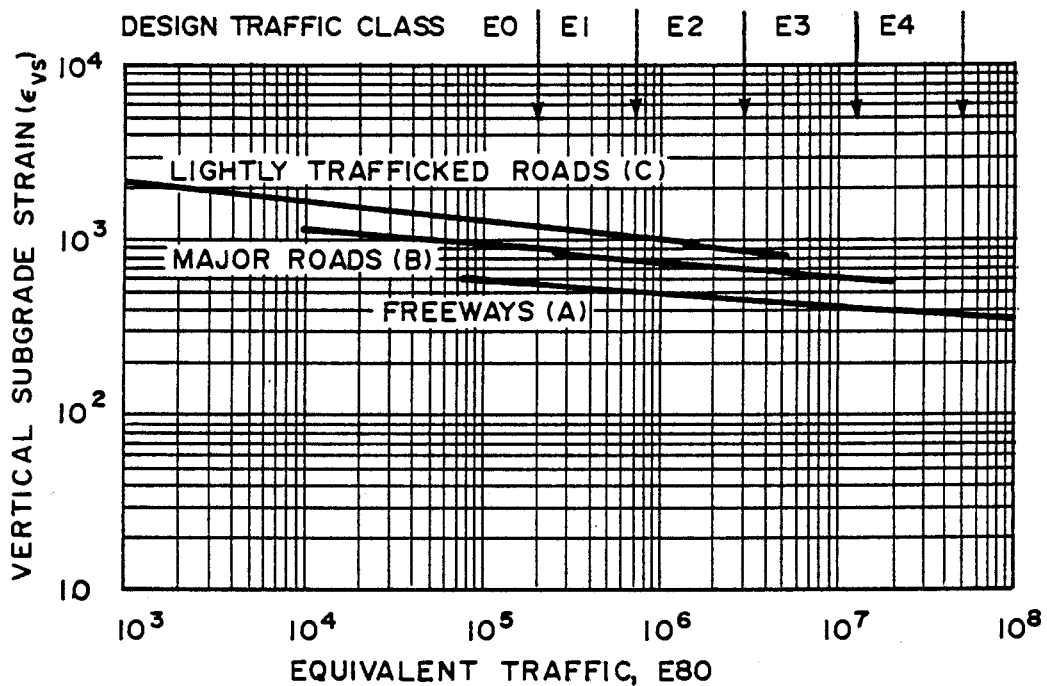


FIGURE 8.2  
Recommended vertical subgrade strain criteria  
for different road categories

Deformation in the bituminous layers are also limited indirectly in mechanistic analysis and rehabilitation design procedures. Thompson et al, (1986) indicate that rut development in such layers are controlled by the proper selection of materials, mix design, and construction control. Freeme et al. (1982a) clearly indicated how this same approach was followed and verified with accelerated testing. Additional criteria developed to kerb creep (Viljoen and Meadows, 1981) indicate the continued development in this direction.

### 3.4.3 Cracking

The critical parameter most commonly used to predict or govern fatigue cracking of bituminous layers, is the maximum horizontal asphalt strain ( $\epsilon_{HA}$ ) at the bottom of the layer. In chapter 6 it was indicated that cognizance is given to the fact that the maximum asphalt strain does not always occur at the bottom of the asphalt layer, but that the criteria as used in the mechanistic rehabilitation design procedure does lead to satisfactory results in the majority of cases.

In Figure 7.8 radius of curvature (R) is related directly to maximum horizontal asphalt strain ( $\epsilon_{HA}$ ). This is true for bitumen base pavements without regard to the subgrade support condition. For the granular base pavements the relationships shown are true only for the effective elastic modulus of 70kN.

The surfacing thickness of granular base pavements has a definite influence on the relationship between maximum horizontal asphalt strain ( $\epsilon_{HA}$ ) and other deflection basin parameters. Other deflection basin parameters, like surface curvature index (SCI), is less sensitive to various surfacing thicknesses, but still sensitive to discern between thin (< 20 mm) and thicker (4) to 100 mm) surfacings. These relationships are shown in Figure 7.9 for a subgrade effective elastic modulus of 70 MPa.

A combination of deflection basin parameters and basic layer thickness information can also be used to determine maximum



horizontal asphalt strain ( $\epsilon_{HA}$ ) by means of the regression relationships developed in chapter 7. Design curves and relationships as discussed above can therefore be used to determine maximum horizontal asphalt strain values for bitumen bases or asphalt surfacings of granular bases.

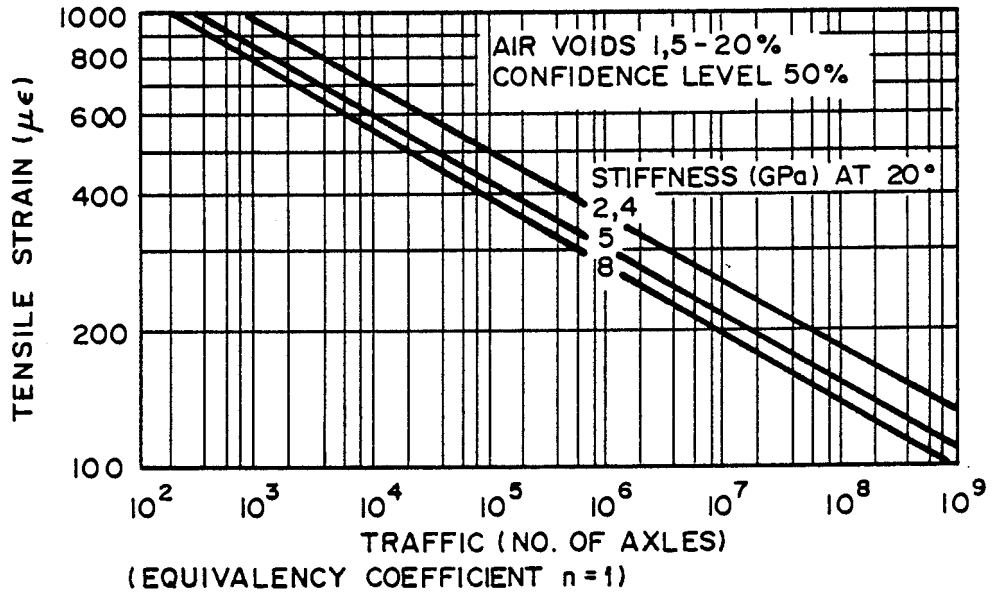
The mechanistic rehabilitation design procedure is unique in the sense that fatigue relationships were developed for thin asphalt layers (< 50 mm) and for thick bituminous base layers (> 80 mm). These relationships are shown in Figures 8.3 and 8.4. In the case of thin asphalt layers, not equivalent 80kN axles (E80's), but actual axle repetitions independent of loading are considered. Remaining life can then be determined as outlined in Appendix D.

### 3.5 Rehabilitation design

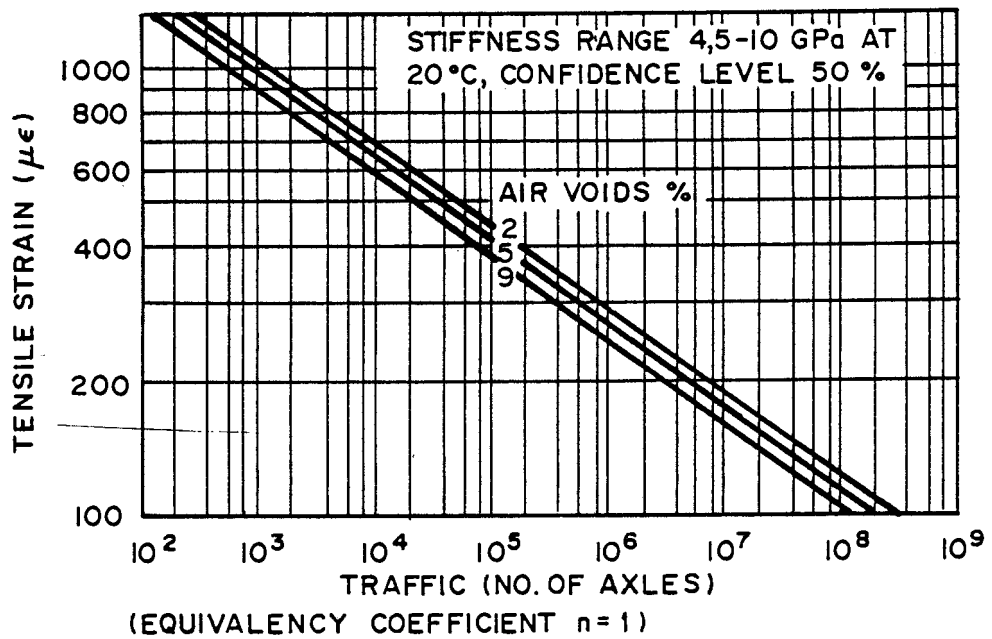
#### 3.5.1 General

The South African mechanistic rehabilitation design procedure (Freeme, 1983) is ideally suited for rehabilitation design. The general tendency would be to determine which distress determinant of which layer does not make the required structural design life. Remedial measures are then applied to lengthen the structural life of such a pavement under consideration. This may constitute various options of which overlays are but one option. As the discussion in this chapter is geared towards the distress criteria, maximum asphalt strain and vertical subgrade strain, overlay design will also be the focus of the deflection basin related rehabilitation design. Deflection basin parameters were used to determine these distress determinants. Overlays of various thicknesses were analyzed for the typical pavement types, granular and bitumen base pavements, in the flexible behaviour state. The results as discussed in Chapter 7 are summarized here.

#### 3.5.2 Granular base pavements



(a) Gap - graded asphalts



(b) Continuously graded asphalts

FIGURE 8.3  
Recommended fatigue criteria for thin  
bitumen surfacings

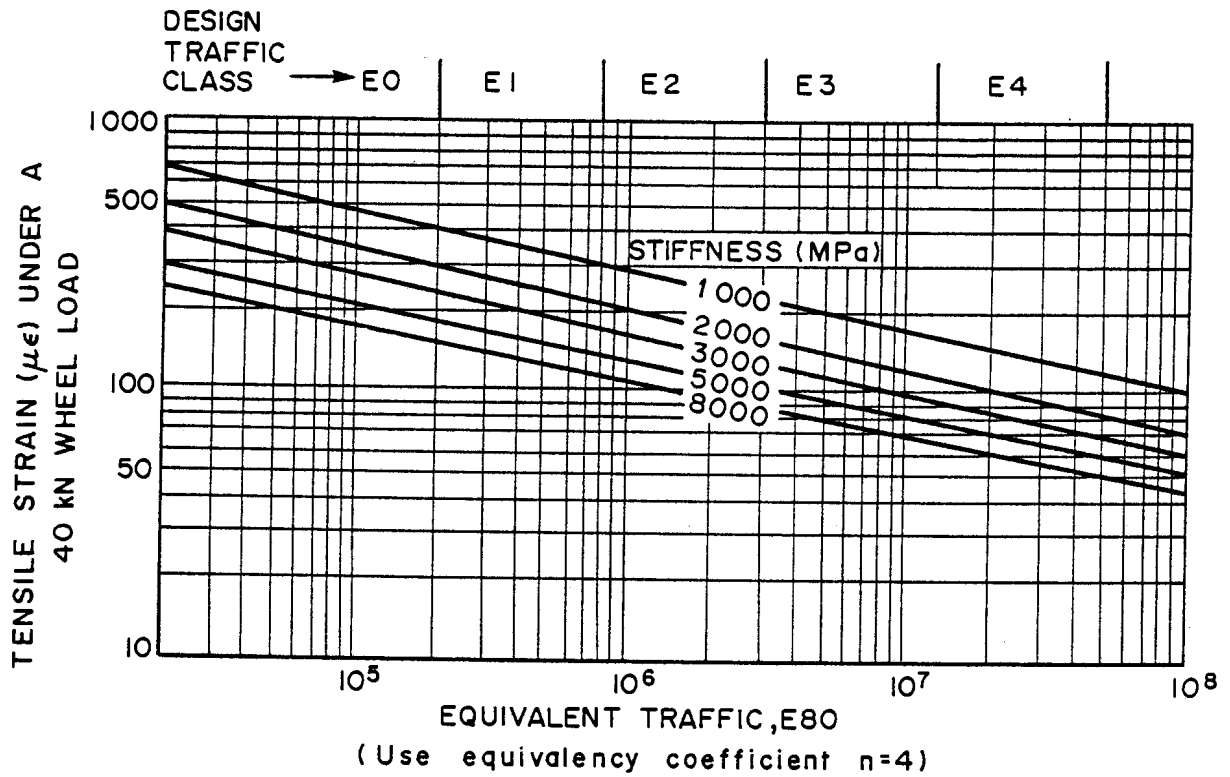


FIGURE 8.4  
RECOMMENDED FATIGUE LIFE CRITERIA FOR THICK  
BITUMEN BASES

Granular base pavements in the larger dry regions of South Africa have surfacing thicknesses in the order of 30 to 50 mm. Thin overlay surfacings (20 mm) cannot be expected to have a significant influence on the reduction of subgrade strain. In Figure 7.12 it is shown that for a subgrade effective elastic modulus of 70 MPa an overlay thickness of 60 mm and more would substantially reduce subgrade strain, but asphalt layers of such total thicknesses are classified as bitumen base pavements. Overlays of such thicknesses would therefore seldom be applied to granular base pavements except in the wetter regions of South Africa.

Existing asphalt surfacings were classified as surface treatments (20 mm and less) or normal thickness surfacings (40 mm average) for overlay purposes to curb fatigue cracking. The effect of this original surface thickness is clearly shown in Figure 7.13 where various thicknesses of overlays (20, 40, 60 and even 80 mm) are shown related to the pre-defined existing surfacing thicknesses. The normal practice with existing surface treatments requiring an overlay is to ignore the thickness of asphalt surface treatment, equate it to the granular base and apply another surface treatment. In normal practice a pavement with an original thickness of 40 mm, however, can receive an overlay of any required thickness in order to reduce the calculated strain values.

### 3.5.3 Bitumen base pavements

Subgrade strain ( $\epsilon_{vs}$ ) can be reduced by overlaying. In Figure 7.15 it is shown that knowledge on the effective elastic moduli of the subgrade is a prerequisite as the variance in subgrade effective elastic moduli lead to different gradients for the various overlay thickness relationships.

As overlay thicknesses are increased, maximum asphalt strain calculated under the base is reduced. In Figure 7.16 it can be seen that this reduction in maximum asphalt strain, by means of overlaying, is true even if the effective elastic modulus of the subgrade is varied as indicated.

#### 3.5.4 Practical considerations

In the design and selection of overlays of flexible pavements, the standard practice should also be considered. Granular base pavements with a double surface treatment (20 mm) would normally receive another surface treatment of about 20 mm. Granular bases with surfacing thicknesses of 30 to 50 mm, can also receive a surface treatment. Overlays of 30 to 40 mm are more typical in the dry regions of South Africa, while thicker overlays may be considered in the wetter regions of South Africa.

As soon as it has been established which of the distress determinants, namely maximum asphalt strain or subgrade strain, would determine the overlay thickness, the situation with the overlay should be checked with the remaining distress determinant. This situation is of particular importance for granular base pavements where a total asphalt surfacing of 40 to 80 mm, in order to curb deformation, may in fact reduce fatigue life drastically (Freeme, et al., 1982a).

## 4 FUTURE RESEARCH

### 4.1 General

This author sees this thesis only as an exploratory exercise on deflection basin measurement and use in the mechanistic rehabilitation design procedure. There is an awareness that in a sense more questions are now asked than answers given to the initial questions asked at the outset of this study. The author nevertheless endeavoured to steer his investigation along the path whereby the new information gained on deflection basins and their use in analysis procedures can be of practical use. For that reason the well proven South African rehabilitation design procedure was used as a main reference in the discussions throughout. This approach also led to the identification of a number of areas in this field that urgently need further attention in future research efforts. The author therefore attempts to identify these needs and motivate the research in the various areas separately.



#### 4.2 Measuring equipment

The RSD as being used in South Africa was specifically developed for the HVS testing system. This apparatus is a natural extension of the Benkelman beam. This is in effect also the problem with this apparatus in the sense that, just like with the standard Benkelman beam, a truck is needed to do the measurements with the equipment and at least 3 persons to operate it. A need for equipment like the FWD which bridges these problems is therefore obvious with the advantages as listed elsewhere in this thesis. As mentioned elsewhere in this thesis, this type of equipment however needs to be properly calibrated and compared to the RSD. The accelerated testing with the HVS provides the unique opportunity to do just that.

The new NITRR deflectograph can measure the deflection at suggested off-sets. This makes this equipment a more effective tool of evaluation on the network level. Considerable work still need to be done in order to relate such measured deflection basin parameters to the specific material and road conditions. The relationship between RSD deflection basins and that of the deflectograph needs proper investigation in order to enable the transfer of relationships developed for the former to be used with the latter.

#### 4.3 Material Characterization

The limited investigation of measured deflection basins with the RSD during accelerated tests enhanced the mechanistic rehabilitation design procedure by enabling more accurate identification of pavement behaviour states. Seen at the back ground of the vast extent of similar information on measured deflection basins being available, the need for an in depth study in this field is glaringly obvious. A larger sample would facilitate the possibility of establishing relationships between deflection basin parameters and specific layer materials in specific behaviour states and for specific pavement types to that of the distress determinants. This semi-empirical approach can greatly enhance the current mechanistic rehabilitation design procedure.

The possibility of back-calculating effective elastic moduli from ASD measured deflection basins is an area that need considerable attention. The procedure as outlined in this thesis, making use of linear elastic computer programmes can be developed much further in spite of the obvious short comings. The possible use of finite element programmes or elasto-plastic computer programmes like the VESYS program warrents a closer look. The possibility of establishing regression relationships between deflection basin parameters as measured with the RSD and MDD may be an avenue to explore too. The effective elastic moduli as calculated with the help of MDD measured deflections are still considered as the most reliable values.

The possibility of establishing relationships between deflection basin parameters and other parameters of other design methods should also be investigated. A typical possible relationship could be between the area (A) parameter and the  $DSN_{800}$  number of the DCP-model.

The analysis of the standard pavement structures being used in South Africa can be expanded considerably to include other typical pavement types and behaviour states. The most influential parameters were identified in the initial analysis, but the small size of the analysis limited the application of the design curves that were established to very specific conditions. It is also believed that other distress determinants relating to fatigue cracking and deformation need to be considered in such an analysis.

#### 4.4 Analysis procedure

The possibility of using the emperical theoretical relationships established between deflection basin parameters and distress determinants were explored. The limited relationships established however has considerable constraints in their application. This confirms the need for a much broader analysis of various pavement types to be analysed as expressed in the previous section. These design curves can then be incorporated in a computer programme which automatically relates the measured deflection basin parameters to these relationships and calculate the life of a pavement type or the rehabilitation design.



**APPENDIX A**

**EVALUATION OF DEFLECTION BASIN CURVE FITTING PROCEDURES**





## 1 MODELS USED FOR CURVE FITTING

Various mathematical and physical models available, were selected and tested using the prepared RSD data sets. The discussion of these models are divided into two subgroups namely; Linear and non-linear models, based on the procedures of regression analysis used. In both cases the SPSS Statistical Package for the Social Sciences (Nie et al., 1975; Robinson, 1984) was used to do linear and non-linear regression analyses. The reason for the choice of the SPSS package was the compatibility with the computer system where the deflection basin data sets are stored. Each of the models used are briefly discussed in terms of the results.

### 1.2 Linear curve fitting model

If a typical set of deflection basin results are plotted on a logarithmic versus linear scale, like in Figure A.1, some guiding observations can be made as to what types of models can be used. There is in general a tendency towards a straight line, although as shown, it is still slightly curved. Based on these observations, the following models as shown in Table A.1, were used. The values of the related parameters are also given as derived from the linear regression model in the SPSS package (Nie et al., 1975) for a typical data set.

The results of these models for typical data sets are shown in Figures A.2 and A.3. Before even considering the statistical evaluation, it can be seen that there are some shortcomings in some of these models.

Figure A.2 illustrates that models 1 and 2 (as defined in Table A.1) are only applicable to the area of positive curvature. Model 2 is however able to be accurate over a wider area (10 to 300 mm). Figure A.3 shows that if model 1 is used over a wider area than that covered by the positive curvature of the deflection basin, it can easily lead to an ill fit. For that reason models 1 and 2

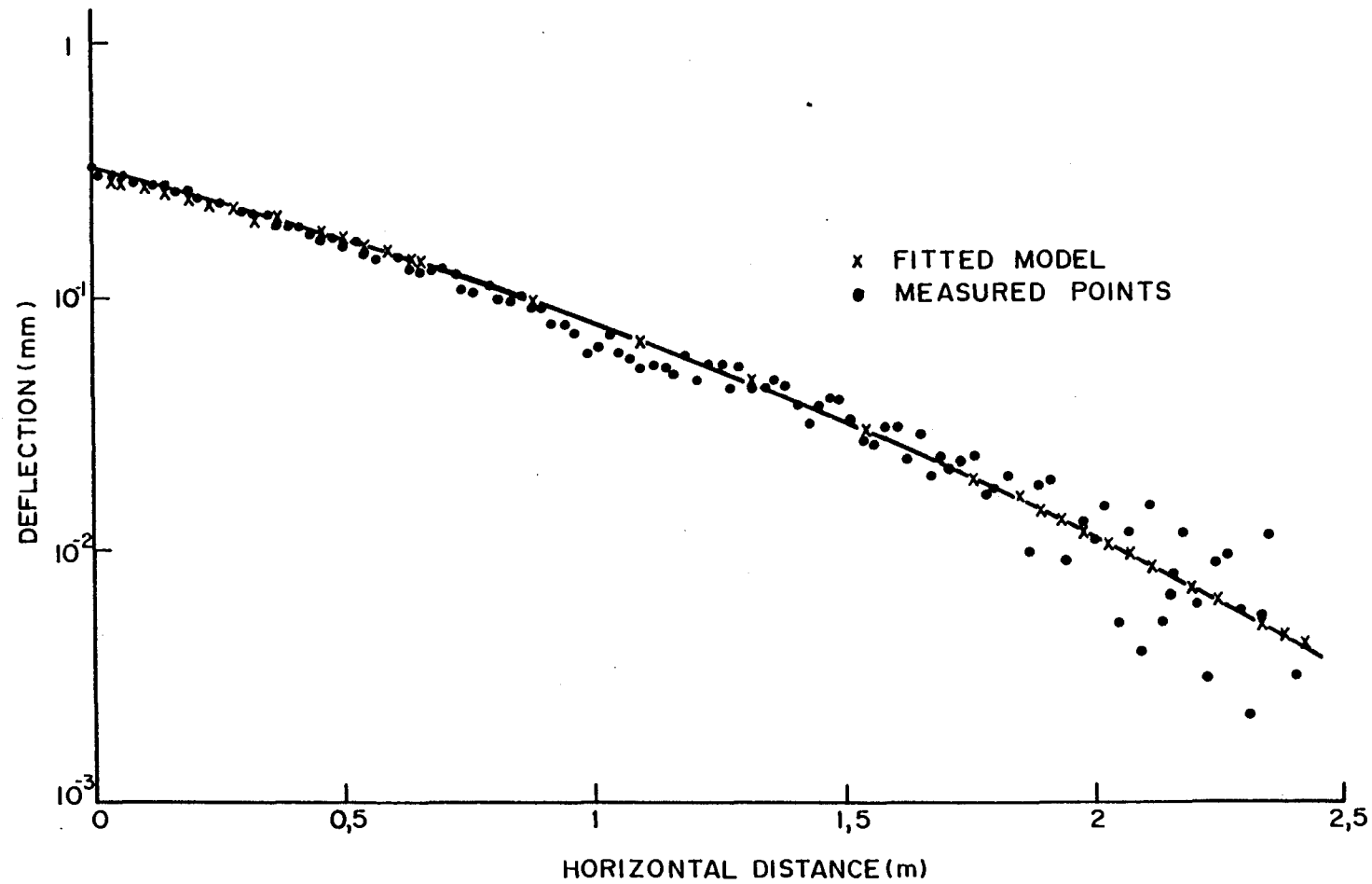


FIGURE A.1  
TYPICAL LOG VERSUS LINEAR PLOT OF RSD DEFLECTION BASIN MEASUREMENTS

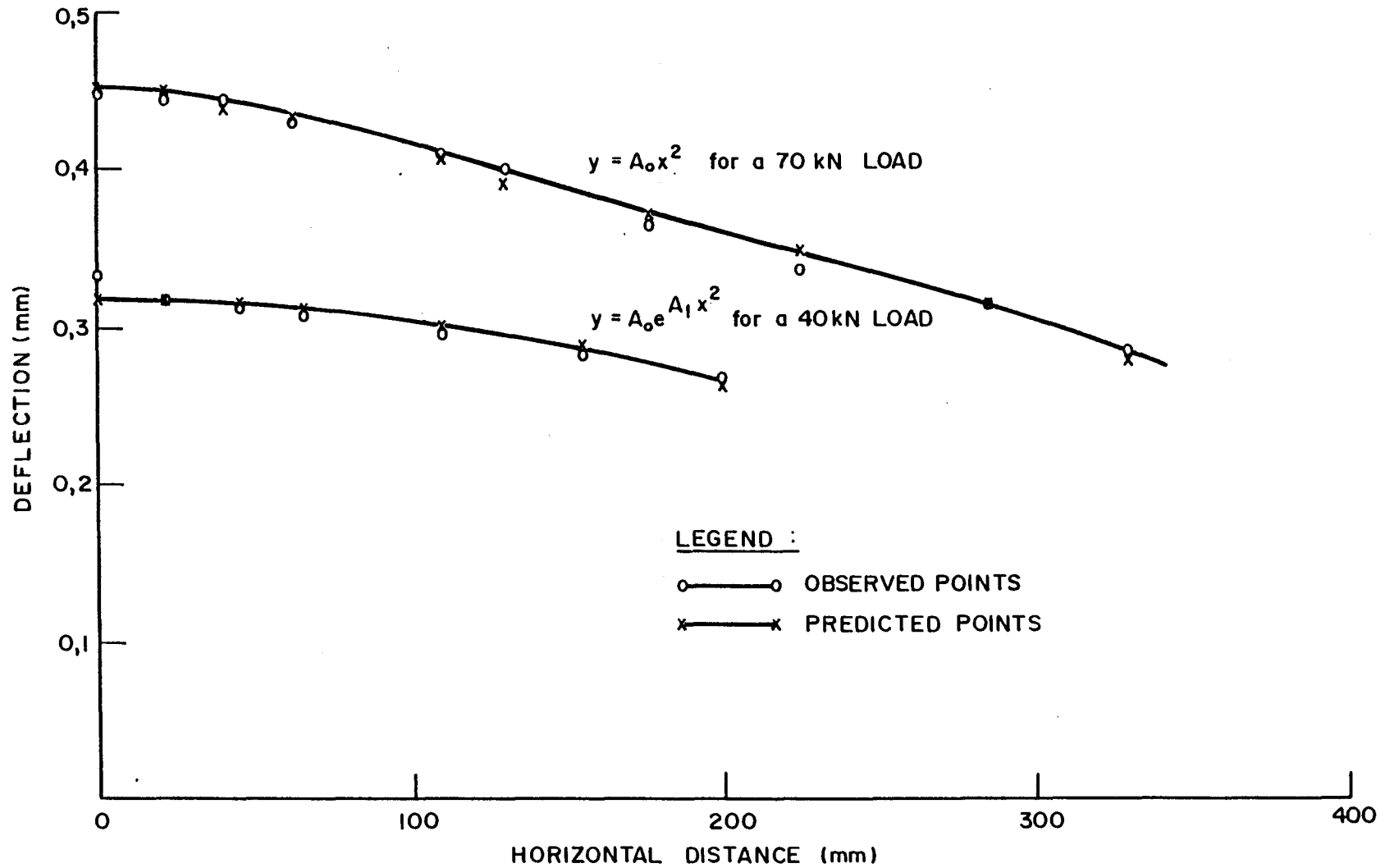


FIGURE A.2

TYPICAL PLOTS OF LINEAR REGRESSION MODELS FITTED TO THE POSITIVE CURVATURE

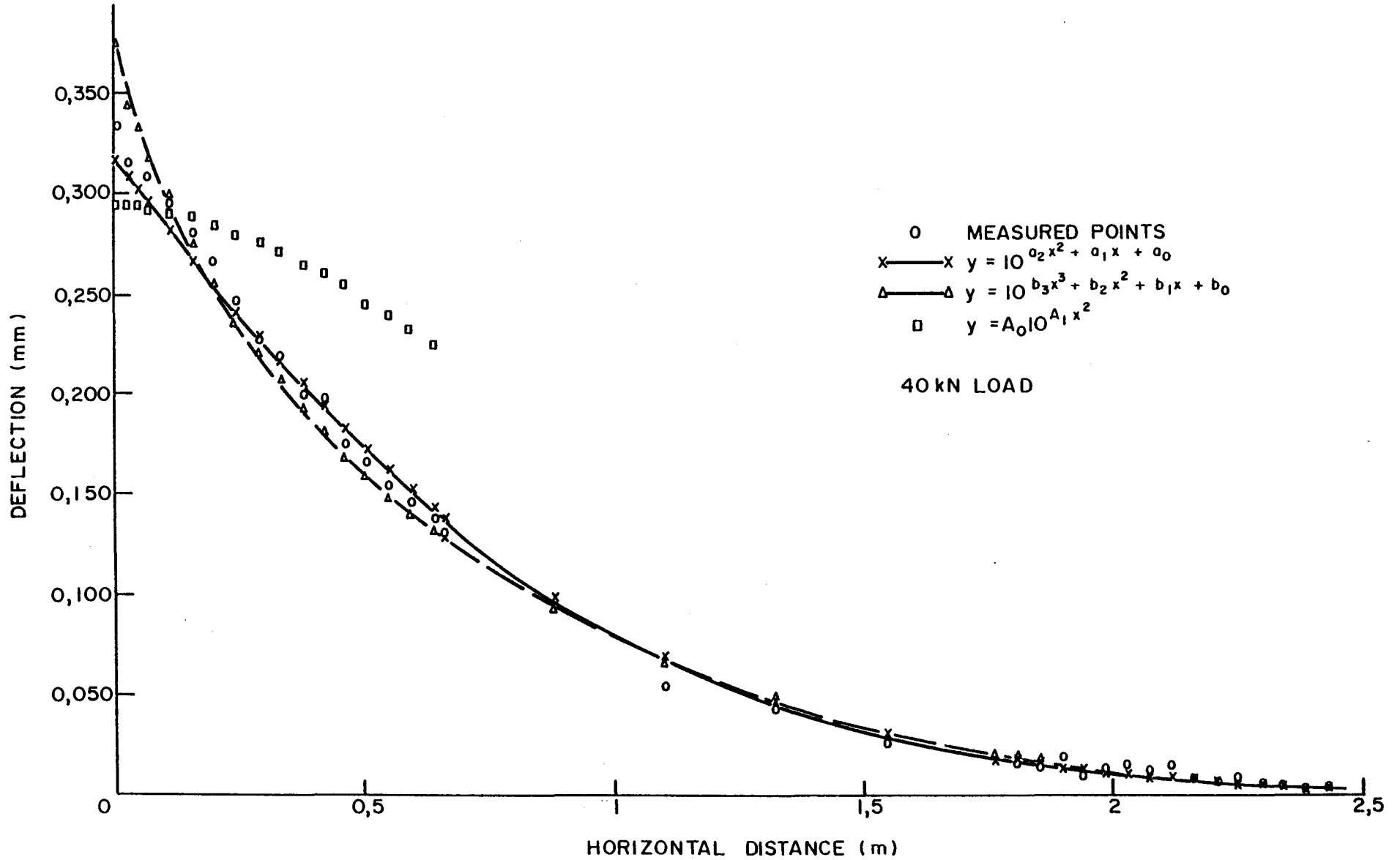


FIGURE A.3  
TYPICAL PLOTS OF LINEAR REGRESSION MODELS FITTED  
TO THE WHOLE DEFLECTION BASIN

TABLE A.1 - Summary of linear model curve fittings

Model	Parameters for a typical data set	R-square
1.	$y = A_0 \exp (A_1 x^2)$ or $y = A_0 10^{(A_1 x^2)}$ or $\log y = \log A_0 + A_1 x^2$	$A_0 = 0,2959$ $A_0 = 0,991 \times 10^{-6}$ 0,99
2.	$y = A_0 x^2$	$A_0 = 0,4578$ 0,99
3.	$y = \exp (a_2 x^2 + a_1 x + a_0)$ or $y = 10^{(a_2 x^2 + a_1 x + a_0)}$ or $\log y = a_2 x^2 + a_1 x + a_0$	$a_0 = -0,4990$ $a_1 = -0,4513 \times 10^{-3}$ 0,98 $a_2 = -0,1330 \times 10^{-6}$
4.	$y = \exp (a_3 x^3 + a_2 x^2 + a_1 x + a_0)$ or $y = 10^{(a_3 x^3 + a_2 x^2 + a_1 x + a_0)}$ or $\log y = a_3 x^3 + a_2 x^2 + a_1 x + a_0$	$a_0 = 0,4467$ $a_1 = 0,7818 \times 10^{-3}$ 0,98 $a_2 = 0,2309 \times 10^{-6}$ $a_3 = -0,1021 \times 10^{-9}$

were only applied to the first 200 mm. This is covering an area wider than the normal width of positive curvature (Dehlen 1962) but it does not lead to ill fits of model 1 (see Figure A.2).

A distinctive feature of the deflection basin curves as shown in Figure A.3, is the peakedness of the area of the area of positive curvature. This area of positive curvature is on average less than 10 per cent of the horizontal distance of the whole deflection basin.

The R-square values of model 1 and 2 are an acceptable 0,99. The goodness of fit was also calculated as follows:

$$T = \sqrt{\frac{1 - \sum_{i=1}^n (Y_i - y_i)^2}{1 - \sum_{i=1}^n (Y_i - A)^2}} * 100 \%$$

where A = Average of measured values

$Y_i$  = Measured data values

$y_i$  = Values from model fitted

The goodness of fit for a typical data set for models 1 and 2 is 95 per cent. Both therefore have acceptable values of R-square and goodness of fit for the positive curvature region.

Models 3 and 4 are polynomial functions of the order 2 and 3. There is no real advantage gained in accuracy when the order of the polynomial is increased above the third order. The computation takes longer and becomes costlier too. The goodness of fit of the second order polynomial (model 3) for a typical set of measurements is 99 per cent. It can be seen in Table A.1 that the R-square values for models 3 and 4 are also an acceptably high 0,98. This is very good, but visually it can be seen in Figure A.3 that the deviance from the observed values in the very small area near the origin (positive curvature) does lead to some concern as to the applicability thereof for the whole deflection basin. This tendency to give equal weight to all data points along the linear horizontal distance (x) is typical of this linear regression model used in the SPSS package. For that reason it was decided to investigate the non-linear regression analysis with available models that would tend to give a better description of the whole deflection basin.

Another point of interest in the vicinity of maximum deflection ( $x=0$ ) is the gradient of the tangent at  $x=0$ . In Table A.2 the

gradient of the curve described by any of the 4 models is given as first order differentials.

TABLE A.2 - First order differentials of curve fitting models

Models	First order differentials
1. $y = A_0 \exp(A_1 x^2)$	$\frac{dy}{dx} = A_0 (\text{Exp}(A_1 x^2)) 2A_1 x$
2. $y = A_0 x^2$	$\frac{dy}{dx} = 2A x_0$
3. $y = \exp(a_2 x^2 + a_1 x + a_0)$	$\frac{dy}{dx} = (a_1 + 2a_2 x) \exp(a_2 x^2 + a_1 x + a_0)$
4. $y = \exp(a_3 x^3 + a_2 x^2 + a_1 x + a_0)$	$\frac{dy}{dx} = (3a_3 x^2 + 2a_2 x + a_1) \exp^*(a_3 x^3 + a_2 x^2 + a_1 x + a_0)$

At the point of maximum deflection ( $x=0$ ) only models 1 and 2 have a horizontal gradient as the first order differentials are equal to zero. The gradient given by Models 3 and 4 are dependent on the values of the constants when  $x=0$ . This is another indication of ill fit of models 3 and 4 at the point of maximum deflection.

## 1.2 Non-linear curve fitting model

### 1.2.1 Mathematical models

As indicated earlier, the non-linear model of regression analysis used in the SPSS package (Robinson, 1984) tends to give equal weight to each measurement on the deflection basin. In using this non-linear regression analysis package the aim is then to minimize the sum of squares. It is the sum squares of the difference between the fitted model and the observed measured points. For this reason it is therefore important that

the unnatural "spikes should be smoothed out before curve fitting is done.

There are two options in the non-linear regression analysis package of SPSS (Robinson, 1984) namely using the Gauss method or the Marquardt method. The latter was selected as superior due to its shorter computing time required. In Table A.3 the two models tested by the two options are shown with the calculated constants and sum of squares values.

TABLE A.3 - Results of non-linear curve fitting procedures

Model	Method	Sum of squares	Parameters for a typical data set
1. $y = A_0 \exp(A_1 x^2)$	Gauss	$8,914 \times 10^{-1}$	$A_0 = 3,321 \times 10^{-1}$ $A_1 = -9,991 \times 10^{-1}$
2. $y = \exp(a_2 x^2 + a_1 x + a_0)$	Marquardt	$3,768 \times 10^{-3}$	$a_0 = -1,066$ $a_1 = -1,134 \times 10^{-3}$ $a_2 = -2,796 \times 10^{-7}$

As can be seen both models had been tested for curve fitting by the linear regression analysis facility of SPSS before. Model 1 was again tested here on an area wider than the positive curvature by selecting the first 350 mm for curve fitting. As could be expected it did lead to a poor fit as reflected in the rather high value of sum of squares.

The residuals (difference between prediction and observation) are also plotted. Apart from giving a visual impression of the goodness of fit, it also serves as a monitor for specific patterns which indicate poor fitting models. In Figure A.4 the residual plot of the model 1 fitting is shown. The definite pattern confirms the ill fit. It re-emphasises the fact that model 1 can only be applied to the area of positive curvature (< 150 mm).

Model 2 (Table A.3) proved to be better suited for the fitting of the whole deflection basin and particularly the large area of



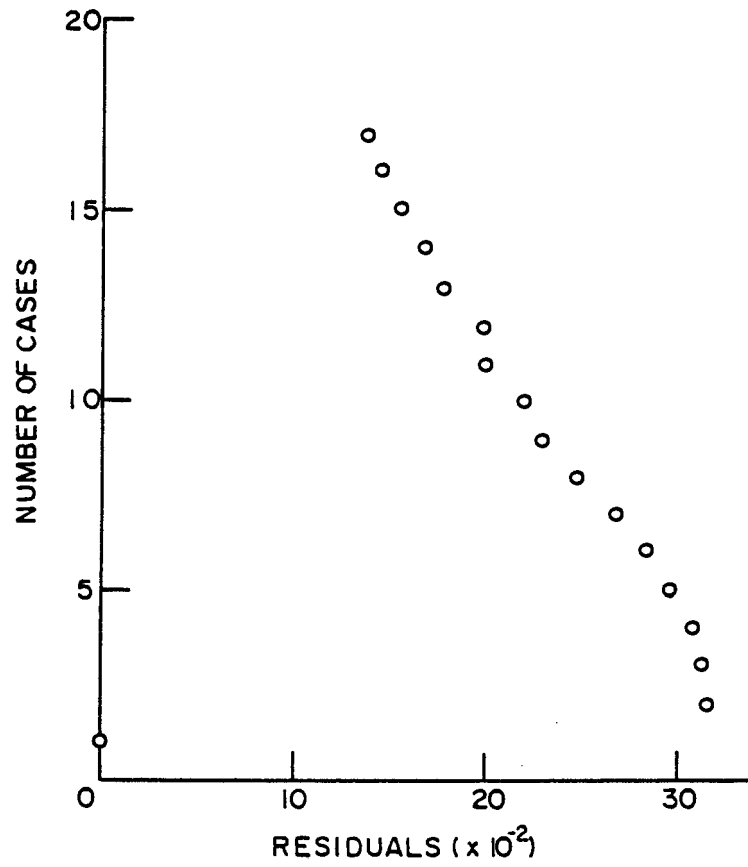


FIGURE A.4  
*RESIDUAL PLOT OF AN ILL FITTING MODEL*

the reverse curvature of the deflection basin. The good fit thereof is reflected by the low value of the sum of squares in table A.3. The plot of residuals in Figure A.5 also reflects no specific patterns indicating a good fit. The lack in fitting the area of positive curvature in the vicinity of maximum deflection still persists as was indicated in the linear regression analysis too. It would be possible though to use these two models of table A.3 and limit the curve fitting of the positive curvature to that by model 1 and the curve fitting of the larger reverse curvature to that of model 2 and achieve satisfactory results.

### 1.2.2 Physical model

The non-linear package of SPSS makes it possible to use relatively complex models in the regression analysis. This gives the opportunity to look at physical models which can be adapted to the observed deflection basin. A promising model is that of beams of unlimited length on elastic foundations with concentrated loading. This model is described in great detail by Hetényi (1971) and Frýba (1967). The intention is not to give a detailed description of this theory here, but rather concentrate on the use and manipulation of the derived solutions in the curve fitting exercise. In the analysis of bending of beams on an elastic foundation Hetényi (1971) states that the assumption is that reaction forces of the foundation are proportional at every point to the deflection of the beam at that point based on the Winkler theory. This theory also states that deformation exists only along the portion directly under loading and was verified in experiments for a variety of soils. Hetényi (1971) is quoted as follows; "... that the Winkler theory, in spite of its simplicity may often more accurately represent the actual conditions existing in soil foundations than do some of the more complicated analysis..."

A short description of the model is as follows; Consider an infinite beam subjected to a single concentrated force  $P$  at the a point  $O$ , which is the origin of the axis system as shown in figure A.6. The general solution for the deflection curve of a

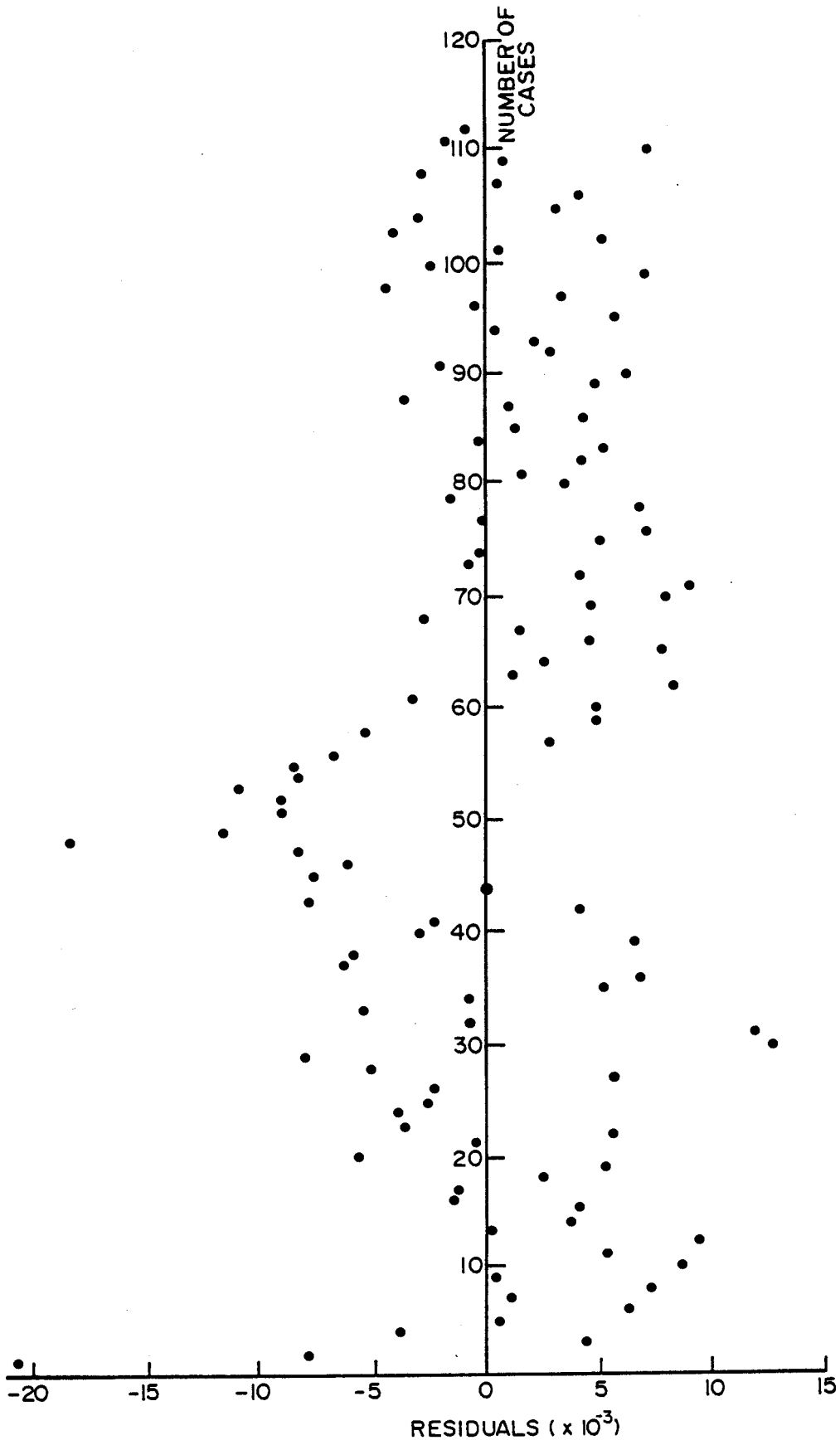


FIGURE A.5  
RESIDUAL PLOT OF GOOD FITTING MODEL

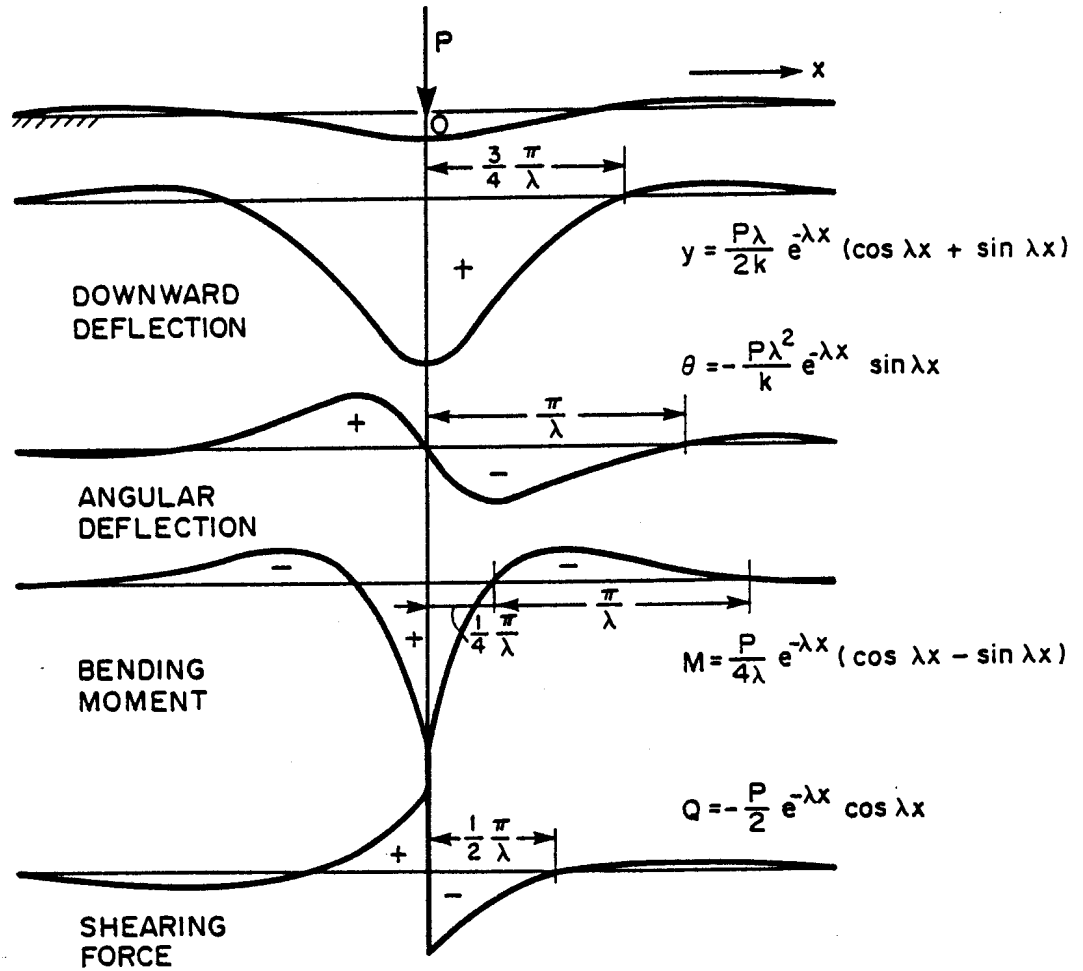


FIGURE A.6  
POINT LOAD ON AN INFINITE BEAM ON AN ELASTIC FOUNDATION

beam subjected to transverse loading is derived by Hetényi (1971) as;

$$y = e^{\lambda x} (C_1 \cos \lambda x + C_2 \sin \lambda x) + e^{-\lambda x} (C_3 \sin \lambda x + C_4 \sin \lambda x)$$

where  $y$  is the deflection taken as positive downwards

$x$  is the horizontal distance from the origin

$C_1, C_2, C_3, C_4$  are constants

$\lambda$  is the damping factor, and

$$\lambda = \sqrt[4]{\frac{k}{4EI}}$$

$k$  is the modulus of the foundation expressed in  $\text{kg/m}^2/\text{m}$

$E$  is the modulus of elasticity in  $\text{kg/mm}$

$I$  is the second moment of area of the beam

Without even going into further detail of the simplification of this model it can be seen in Figure A.6 what the similarities between the modelled deflection curve and the measured deflection basin curves are. When the symmetry of the deflection curve and the equilibrium of the reaction forces are considered this general equation reduces to;

$y = \frac{P}{2k} e^{-\lambda x} (\cos \lambda x + \sin \lambda x)$ , which gives the deflection curve for the right side ( $x \geq 0$ ) of the beam. This correlates well with the data preparations of the deflection basin described in the preceding sections. The form of the curve suggests that the case of no dampening can be considered for this part of the curve analyzed. Frýba (1967) gives the solution as follows for such a situation;

$$y = \frac{1}{ab} e^{-b|x|} (a \cos ax + b \sin a|x|)$$

This form is obviously similar to that derived by Hetényi (1971). In order to simplify the determination process of the constants in these equations, it was decided to use the following curve fitting model;

$$y = B_1 e^{B_2 |x|} (\cos B_3 x + \sin |B_3 x|)$$

In figure A.7 a plot of a typical data set and the curve fitting is shown. Visually it can be seen that this model succeeds in describing the observed deflection basin accurately. The sum of squares value is low ( $4,15 \times 10^{-3}$  for this typical data set) and the plot of the residuals does not indicate any ill fit. The goodness of fit for such a typical data set is above 98 per cent. It was found that this mode is applicable over a wide range of variances in load, load repetitions and structural condition of pavements. It is obvious though that although this model gives the best fit of all models tested it still tends to give an ill fit in the positive curvature area. Although this area is very small and very peaked in relation to the rest of the deflection basin, it was decided to use the parabola of the linear models in this area of possible curvature in order to arrive at a true representation of the whole deflection basin.

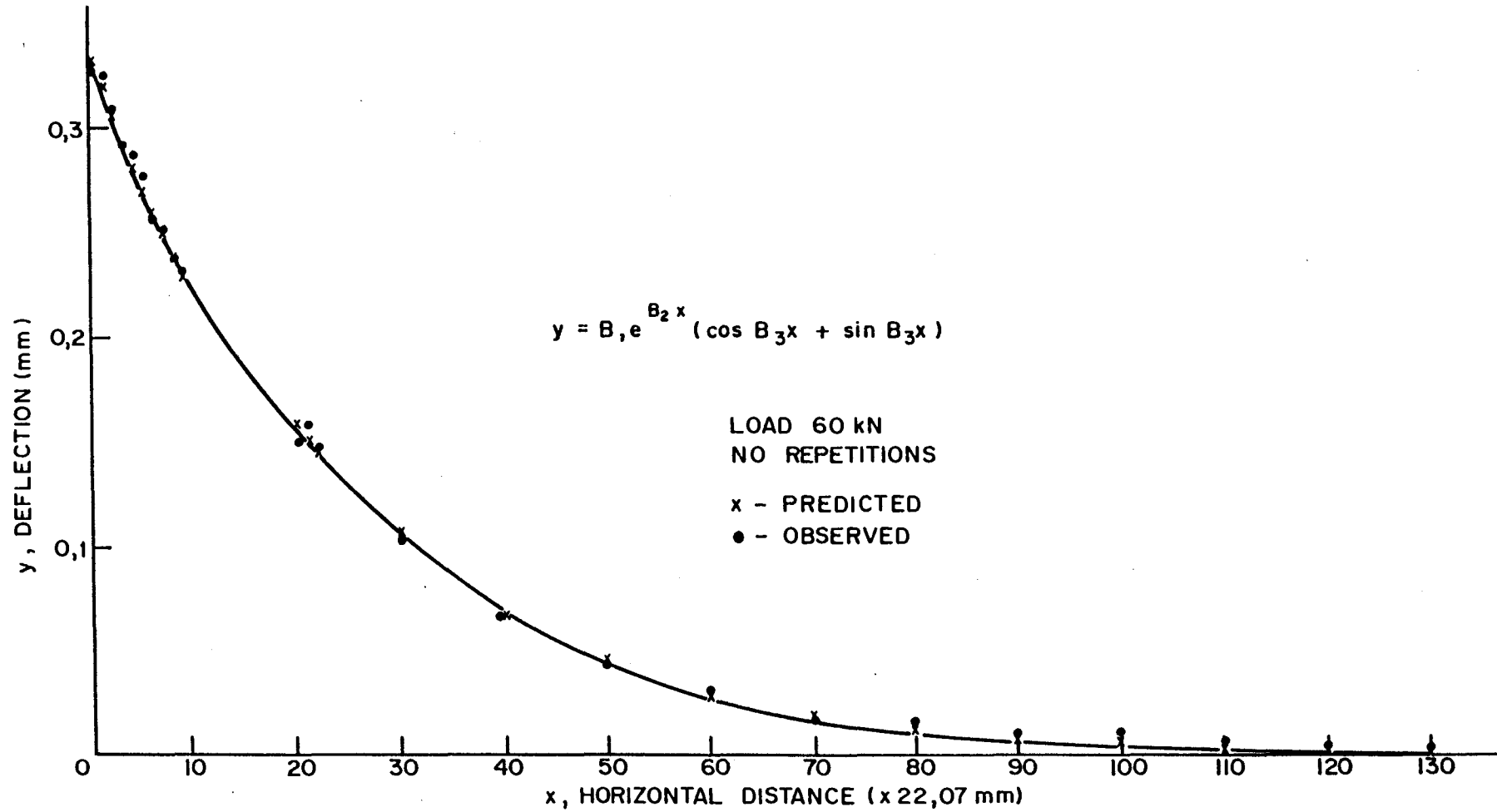


FIGURE A.7  
TYPICAL CURVE FITTING OF PHYSICAL MODEL



**APPENDIX B**

**SUMMARY ON CONDITION SURVEYS ENHANCING  
DEFLECTION BASIN ANALYSIS**



## 1 INTRODUCTION

A condition survey is an important input in the non-destructive testing of an analysis procedure. In Figure B.1 it is shown how this kind of visual survey greatly enhance the understanding of the material characterization in a typical analysis procedure for overlay design. Condition surveys are non-destructive testing procedures enhancing the other non-destructive testing procedures such as deflection basin analysis. In Figure 4.1 it was explained how in the South African mechanistic rehabilitation design procedure (Freeme, 1983) it is important to identify the pavement layer state. The discussion on condition survey will therefore focus on crack and rut classification related to the deflection basin survey (see Figure B.1).

Ullidtz (1982) defines a functional and structural condition in his model on pavement rehabilitation. He states that; "The structural condition is of no immediate interest to the road user but is extremely important to the highway agency because the future functional condition depends on the present structural condition." A visual condition survey can be seen as an aid to a proper structural evaluation.

The standard procedure for conducting a condition survey, as outlined in Draft TRH12 (NITRR, 1983), should be followed. Normally the visual assessment precede the deflection basin survey but it is suggested that the deflection basin survey and visual assessment may be done simultaneously on smaller scale projects. The results of both surveys should be plotted on the same scale. By this means the obvious weak spots can be identified when other relevant information such as drainage, cut or fill transition and soil changes is taken into consideration.

## 2 CRACK CLASSIFICATION

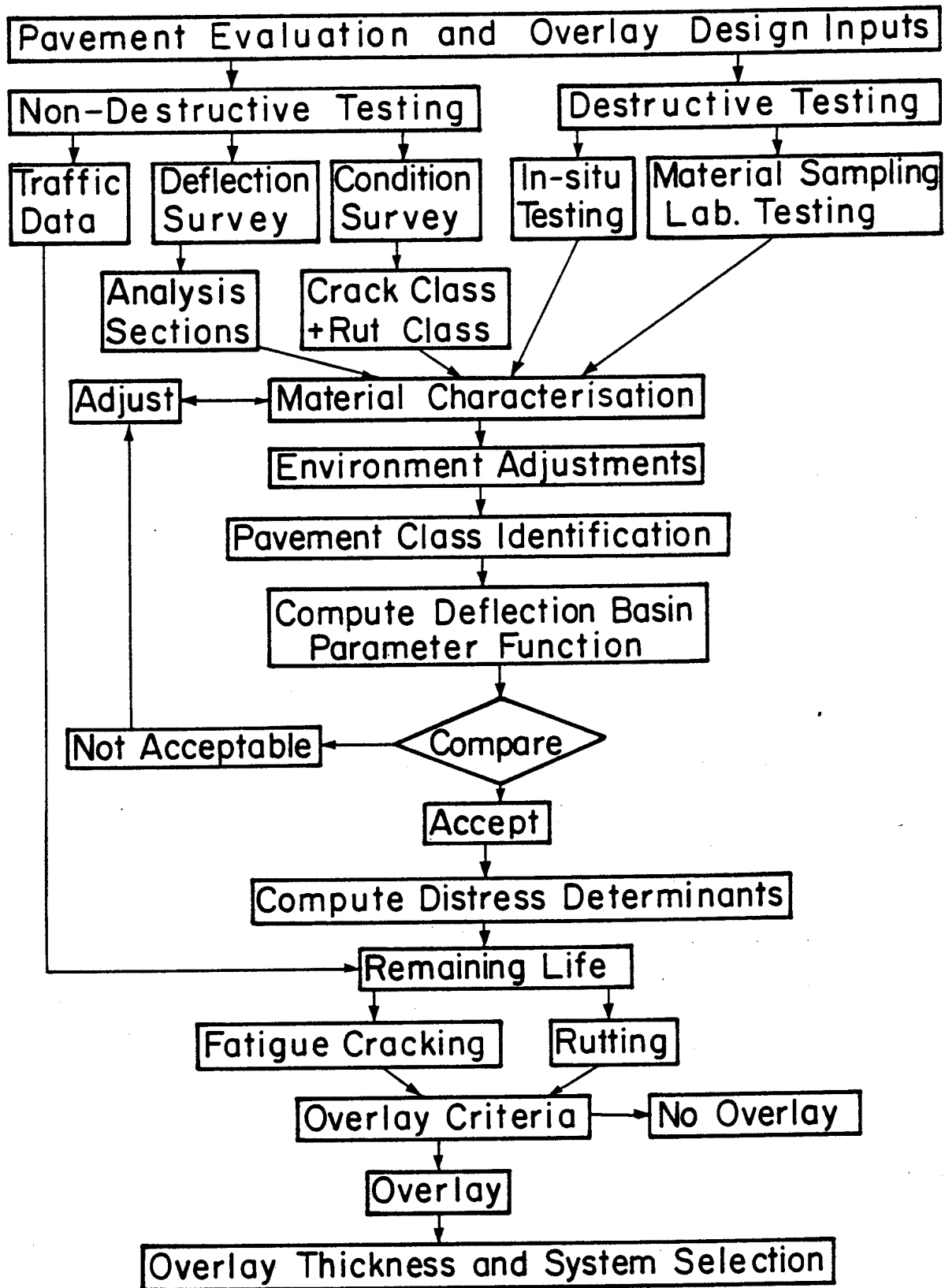


FIGURE B.1  
Mechanistic overlay design flow diagram

Cracks in the existing asphalt concrete layer have a major influence on the overlay design procedure. Normally pavements are classified as either cracked or not cracked. However, the majority of pavements fall somewhere between these extremes. The aim of this section is therefore to establish quantitative procedures to classify cracked pavements in order to improve the rehabilitation design procedure.

Grant and Curtayne (1982) point out that fatigue is not necessarily the cause of cracking in asphaltic concrete layers in South Africa. Other factors, not necessarily traffic-related, should also be considered as being possible causes of premature cracking (Grant, et al (1979). Pronk and Buiters (1982) indicate that with full depth asphalt pavements, even in the Netherlands, cracking does not necessarily begin at the bottom of the asphalt layer. Grant and Curtayne (1982) therefore stress that a study of the past behaviour of the pavements can provide good clues in this respect. The preceding statements are to indicate the complexity of crack mechanisms of asphalt concrete layers. Different reasons for cracking are therefore discussed in order to arrive at a classification for cracked pavements.

The aim of this is purely to simplify the analysis of such a pavement by using the deflection basin parameters in the mechanistic approach.

First it is suggested that the difference in basic crack mechanism, due to the difference in pavement structure be considered. For the South African condition it is suggested that on the grounds of as-built plans or material sampling procedure (Figure B.1), a flexible pavement under survey be classified according to the basic TRH4 (NITRR, 1985a) catalogue, i.e.

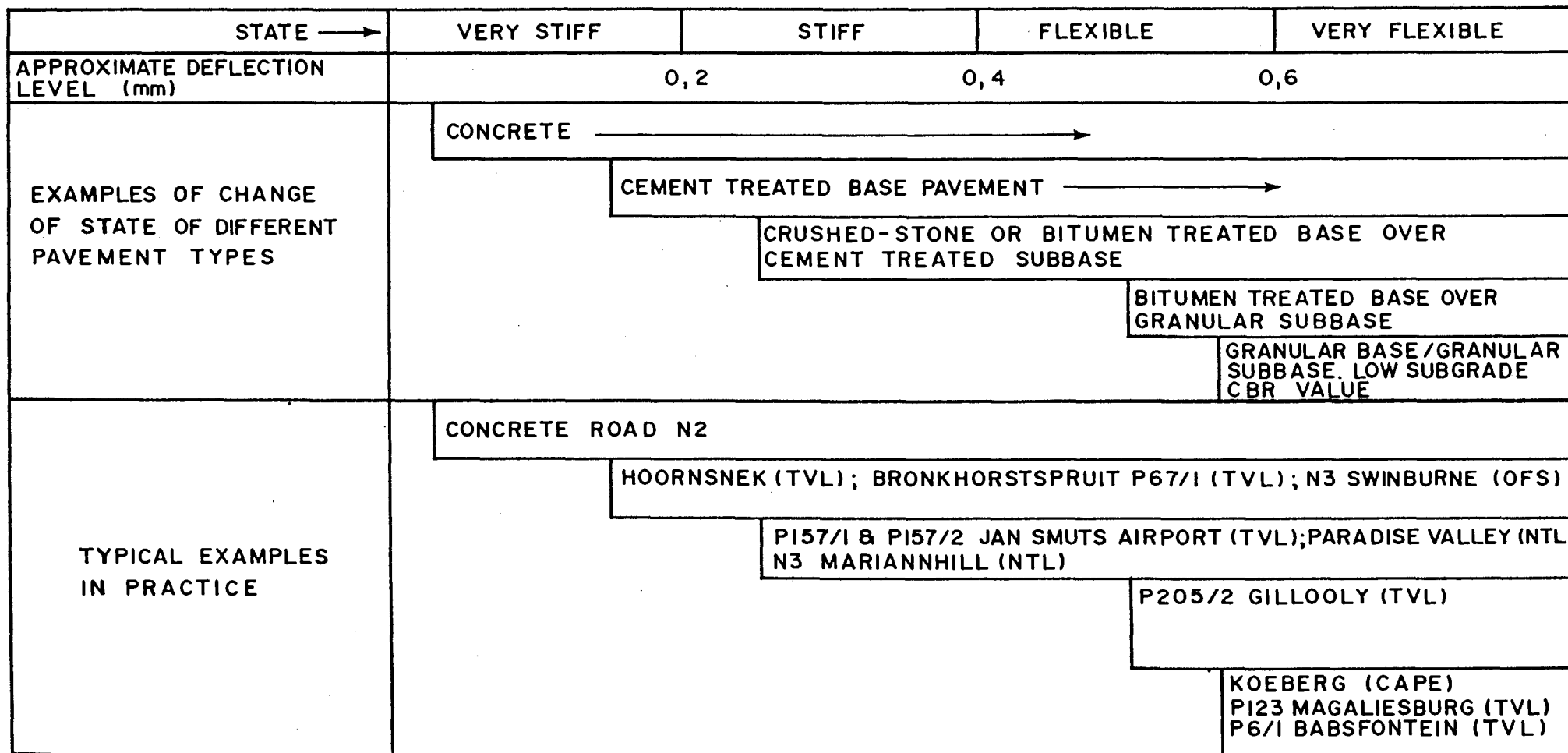
- (a) granular base pavements
- (b) bitumen base pavements (tar as an alternative)
- (c) cemented base pavements.

This basic classification is taken a step further by Freeme (1983) by relating the time-dependent behaviour of different pavement types to the concept of equivalent material state illustrated in Figure B.2. It is explained in Chapter 3 how the measured deflection basin parameters can be used to accurately identify any such pavement behaviour state.

Next, the degree of cracking should be defined. In the light of work done by Kilaeski et al. (1982) and Treybig et al. (1978), it is suggested that the AASHO definition of cracking could be applied. Jordaan and Servas (1983) give a very clear description of three types of cracking and how it should be calculated. These types are crocodile or map or block cracking, longitudinal cracking and other crack patterns or combinations of the preceding types. For these types each 100 m of road length is classified as being in a sound, warning or severe condition. This depends on the percentage of 100 m being cracked and the road category.

Crack conditions can be improved by crack filling and repair of the low percentage of severe cracking of the defined categories or crack types. The decision to repair cracks should be based on economic comparisons, but it is obvious that crack repair will improve possible crack attenuation behaviour in general. Koole (1979) suggests though that an overlay design based on the severe condition of cracking might in some cases be the most economical in the final analysis owing to the expensive nature of procedures to upgrade the pavement in regard to the crack condition outlined above.

In the final level of crack classification more sophisticated methods should be considered. This normally consists of analysis procedures associated with the overlay design analyses. Various researchers, such as Molenaar (1983) and Coetzee and Monismith (1979) suggest the use of fracture mechanics principles and finite element computer programs in the analysis stage. In order to use these procedures though, the previous crack classification would have to be elaborated in order to establish average values of crack width too. Molenaar (1983) states the following:



B.5

FIGURE B.2

DIAGRAMMATIC REPRESENTATION OF THE TIME DEPENDENT BEHAVIOUR OF DIFFERENT PAVEMENT TYPES (Freeme, 1983)

"Although the fracture mechanic's approach has the potential to be an excellent tool in solving the reflection crack problem, it has not gained very much popularity. In fact it can be stated that it is still a research tool and that its practical application is limited to only a few cases."

Recently the monitoring of crack movements, as described by Rust (1984), has become another viable method that may be associated with the classifications outlined above. The Crack Activity Meter (CAM) that was developed can measure amongst others the defined total crack movement. Crack activity or total crack movement normally has the typical peaking behaviour with axle repetitions as shown in Figure B.3. Rust (1985) was able to determine that for a flexible pavement with a cemented base and under specific conditions, there is a good correlation between block size and crack movement. The data indicated that there is a critical block size below which the crack movement increases markedly with further decrease in block size. Typical results are shown in Figure B.4. These concepts can be used effectively to enhance the crack classification as given above.

In Appendix E the good correlation between the measured crack-activity and measured deflection basin parameters is illustrated by means of an example. As will be shown there this greatly enhances the rehabilitation analysis procedure.

### 3 RUT CLASSIFICATION

One of the major aims of a rut survey is to determine the amount of material needed for the levelling of the existing rut before an overlay is applied. This is all related to ride comfort (PSI values) and, in wet conditions in particular, to rider safety. The extent of rutting is generally used in overlay design as a major criterion of permanent deformation and the structural state of the pavement. The general procedure is to limit rutting in overlay designs by limiting the vertical subgrade strain ( $\epsilon_{vs}$ ). This approach was originally developed by Dorman and Metcalf

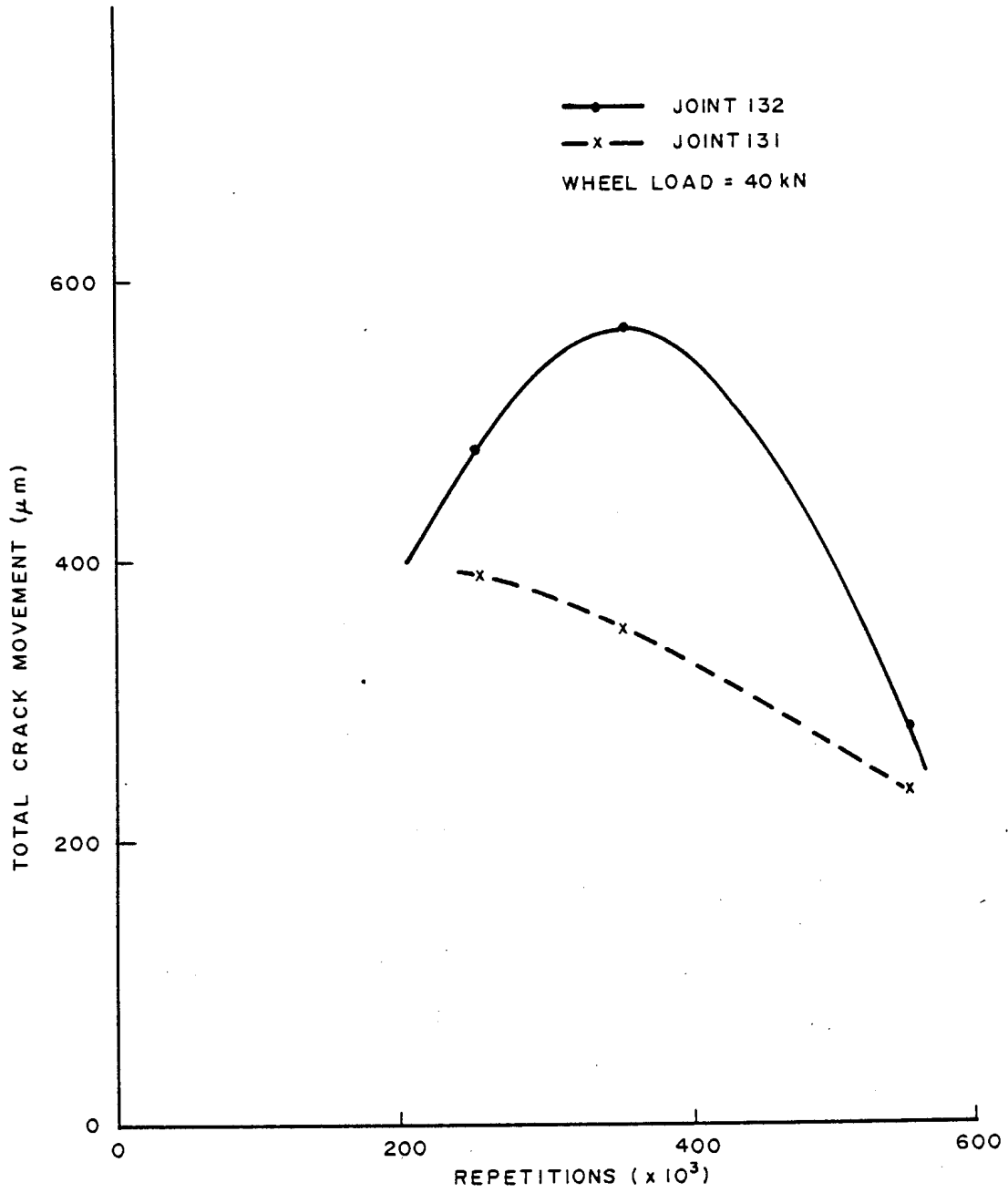


FIGURE B.3

CHANGE IN TOTAL CRACK MOVEMENT DURING HVS TESTING ON THE N2 CONCRETE ROAD-SECTION 258A2 (Rust, 1984)

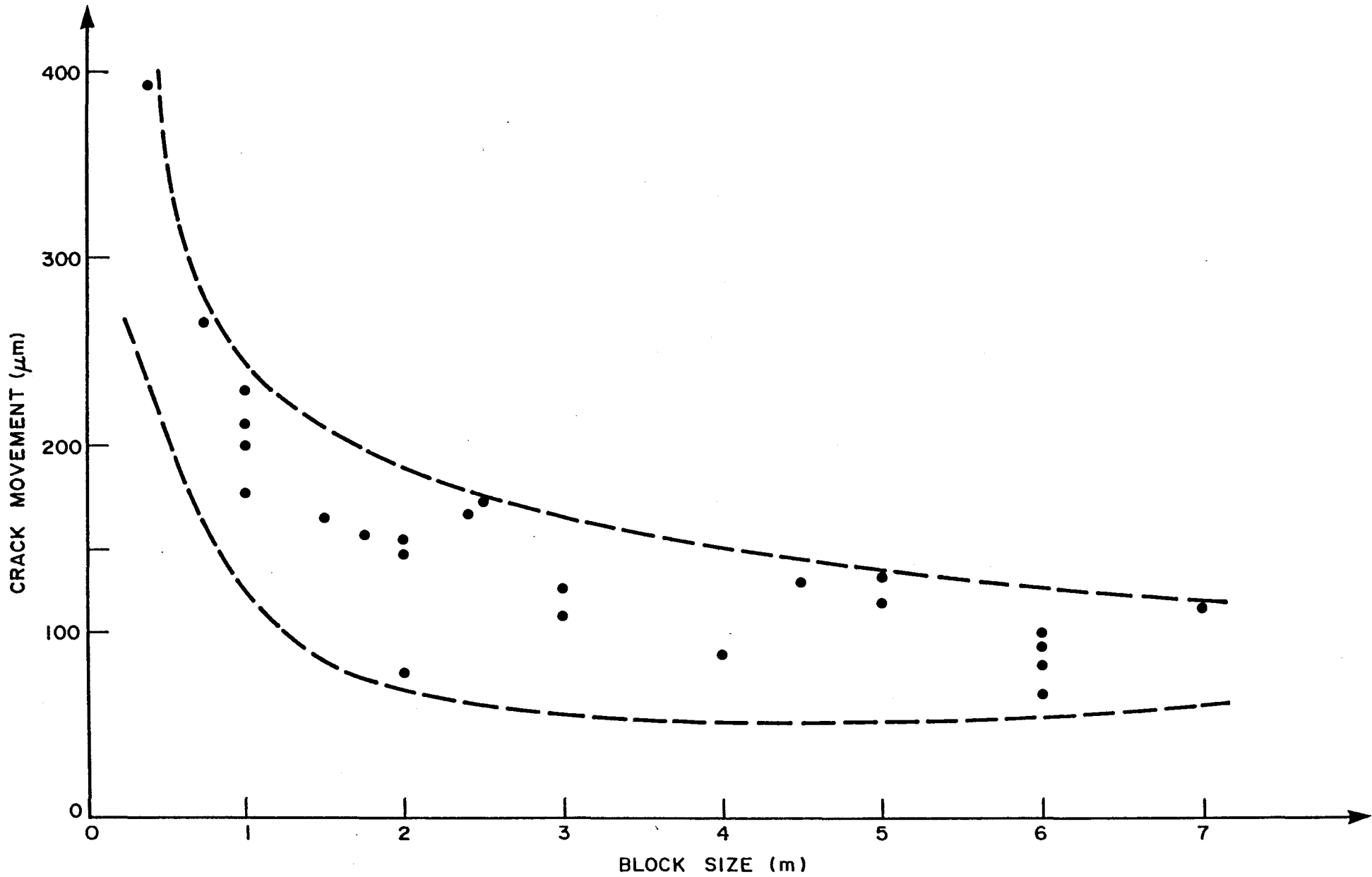


FIGURE B.4

CORRELATION BETWEEN CRACK MOVEMENT AND BLOCK SIZE ON THE MR 27 (Rust, 1985)



(1963) in their analysis of the behaviour of the test sections of the AASHO road test.

It should be noted that rutting is not only related to the subgrade but that contributions also come from the various layers in the pavement. For this reason Koole (1979) mentions that the rut in the asphalt concrete layer should be treated separately. The South African experience also indicates that such a direction should be followed. Freeme et al. (1982a) indicate that better characterization of the bitumen layer in terms of volumetric and shear properties is necessary to accommodate this deformation phenomenon in the bitumen layer. Maree et al. (1982) show that for granular base pavements tested with the Heavy Vehicle Simulator (HVS), most of the permanent deformation took place within the granular base and subbase. The subgrades never meaningfully contributed towards the total deformation and were always well protected. In the same report Maree et al. (1982) illustrate the strong correlation between cracking, excessive rain, moisture intrusion and deformation for typical granular base pavements; this is shown Figure B.5.

The preceding statements make it obvious that a more qualitative classification of rutting is needed than just a report of the average rut. In line with the classification outlined in the previous section on cracking, it is suggested that the pavement structure classification as defined be used also. In fact it is re-emphasized that no indicator like rutting or deflection should be used in isolation. The concept is clearly illustrated by Freeme (1983) in Figure B.6 where various indicators of the behaviour of typical granular layers are shown.

A further practical classification is needed to discriminate between various mechanisms of permanent deformation. Molenaar (1983) classifies two types of rutting (see Figure B.7). The first type is that without lateral displacement due to densification. The second type is that with lateral displacement due to Prandtl type of shear deformation. This ties in with the previous discussion on the South African experience. Grant and

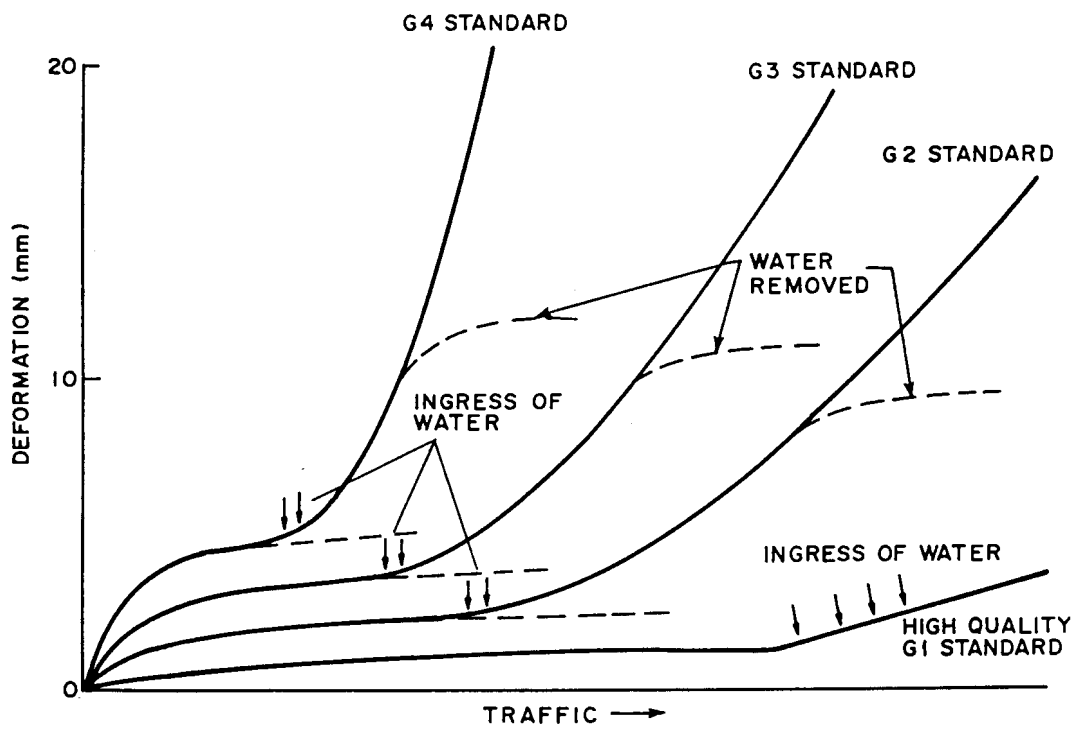


FIGURE B.5

*SCHEMATIC DIAGRAM OF THE RELATIVE BEHAVIOUR OF  
GRANULAR MATERIAL OF DIFFERENT QUALITIES  
(Maree, et al., 1982)*

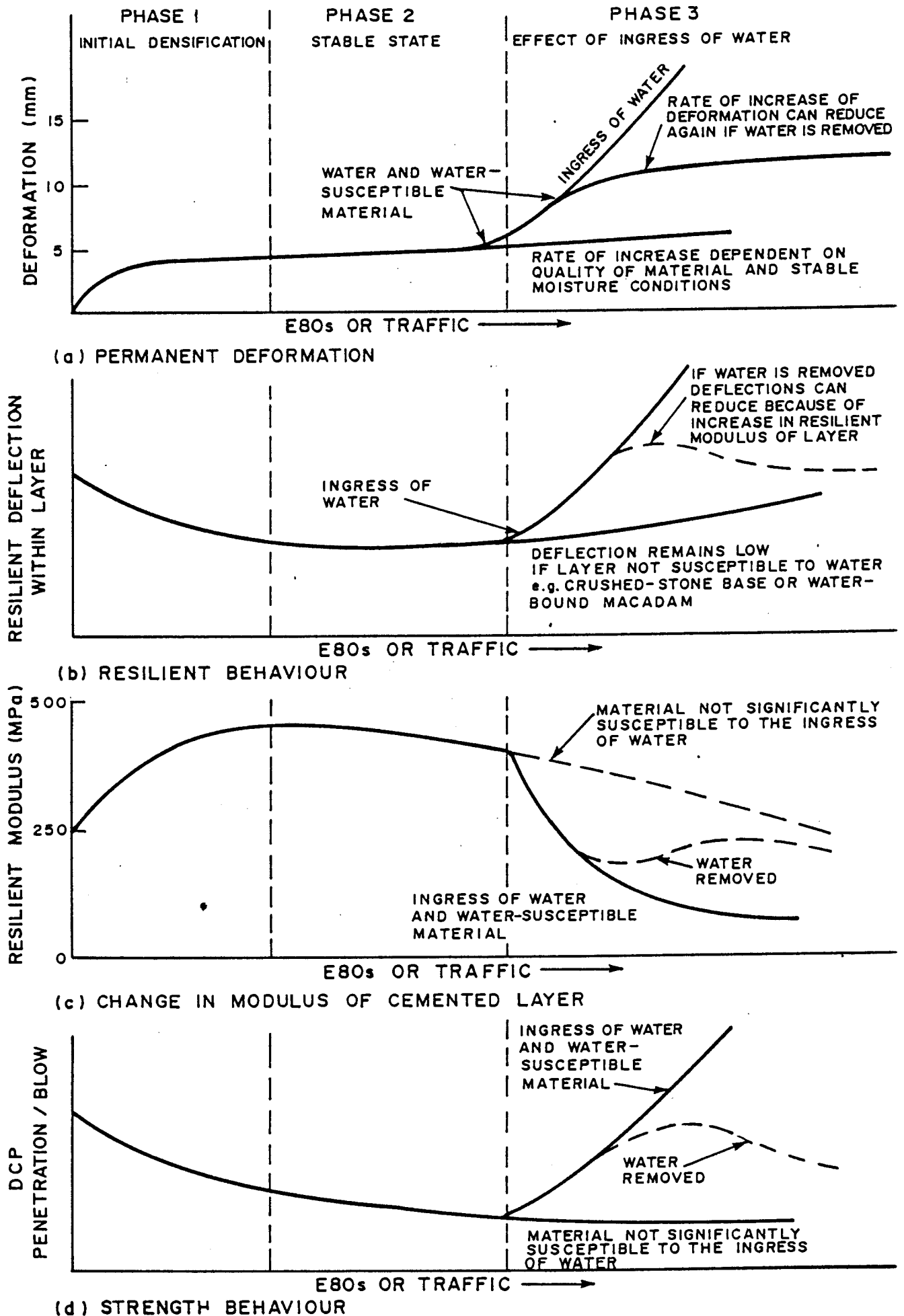
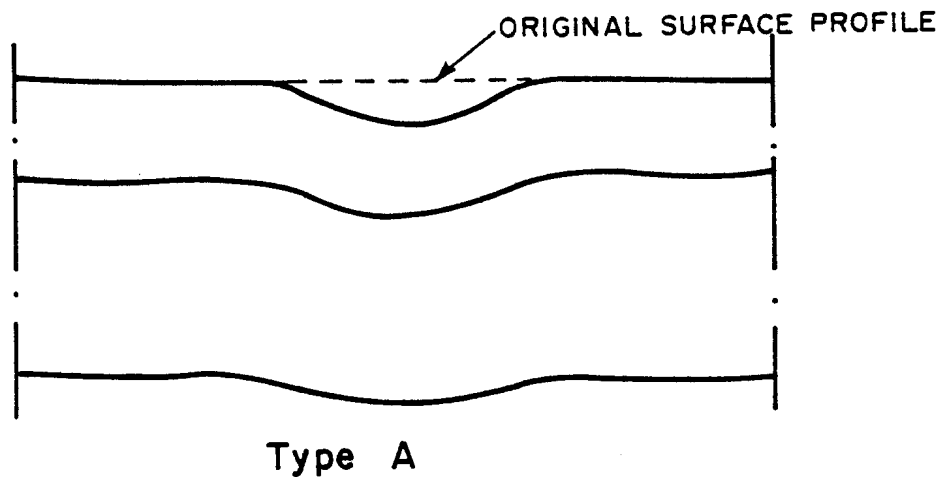


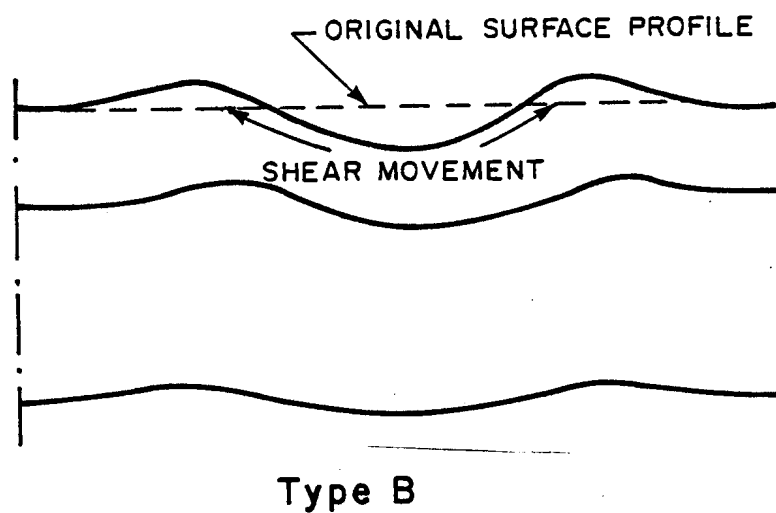
FIGURE B.6

INDICATORS OF THE BEHAVIOUR OF GRANULAR LAYERS

(Freeme, 1983)



Rutting without lateral displacement of the material. This type of rutting is due to densification of the material.



Rutting with lateral displacement of the material. Rutting can be judged to be a Prandtl type of shear deformation.

FIGURE B.7  
 TYPES OF RUTTING WHICH CAN BE DISCERNED  
 (Molenaar, 1983)

Curtayne (1982) note that shear in the subgrade is characterized by wide rutting. Shear in the base layer is characterized by narrow ruts with displaced material appearing like a mound adjacent to the rut.

From the visual survey therefore a classification of the type of rutting that exists may be made, which will strongly influence the overlay design analysis. The Draft TRH12 (NITRR, 1983) give clear indications for rut criteria related to pavement class and pavement type. It is suggested that those criteria and those suggested by Jordaan and Servas(1983) be followed.



## **APPENDIX C**

### **REMAINING LIFE DETERMINATION**

## 1 INTRODUCTION

At any specific moment, an existing pavement has a certain amount of accumulated damage done to it by repeated traffic loading. There is normally also a certain amount of remaining damage which the existing pavement can undergo before failure. The severity of the damage caused by each repeated traffic loading depends on the structural strength of the existing pavement. This is usually expressed in terms of the equivalent number of standard axles (E80s). If the magnitude of the critical strains is reduced, then the existing pavement can carry a larger number of standard axle loads (E80s). The function of an overlay is therefore to reduce the magnitude of these critical load-induced strains or stresses, depending on the distress determinants being used.

Remaining life has two meanings. Without an overlay a pavement normally has remaining life and with an overlay a pavement has a remaining life, that is usually lengthened or prolonged. For this reason "remaining life" will refer to the remaining life of a pavement without an overlay.

In the literature remaining life is usually analysed on the basis of the phenomenological theory of cumulative damage. Attempts to relate the structural condition, based on deflection basin measurements, in a different way to the life of the pavement, will also be discussed.

## 2 THEORY OF CUMULATIVE DAMAGE

The phenomenological theory of cumulative damage is also referred to as the linear summation of cycle ratios. This was advanced by Miner (1945) to predict the fatigue life of metals subjected to fluctuating stress amplitudes. Monismith et al. (1966, 1969) used it to estimate fatigue life of bituminous layers in pavement structures and established it as an acceptable and useful relationship.

This theory is described by Snaith et al. (1980) as follows:

Let  $n_i$  = number of applications at stress or strain level

$N_i$  = number of applications to failure at stress or strain level

$D_i$  = damage due to  $N_i$  number of applications at stress or strain level

Then the damage,  $D_i$ , is defined as the stress or strain cycle ratio, i.e.

$$D_i = \frac{n_i}{N_i}$$

Failure will occur when  $D_i = 1$ .

Let  $r$  = number of different stress or strain levels involved

$D$  = cumulative damage due to number of applications at different stress or strain levels

Then the cumulative damage,  $D$ , is stated as the linear summation of cycle ratios, i.e.

$$\sum_{i=1}^r D_i = \sum_{i=1}^r \frac{n_i}{N_i}$$

Failure occurs when

$$D = 1 \quad \text{or} \quad \sum_{i=1}^r \frac{n_i}{N_i} = 1$$

Snaith et al. (1980) use the distress determinants vertical subgrade strain ( $\epsilon_{vs}$ ), and maximum horizontal asphalt strain ( $\epsilon_{HA}$ ), as discussed in chapter 4 and 6, to determine damage due to rutting deformation and fatigue cracking respectively. For both forms of damage the strain-life relationship is given by the general equation:

$$N = A \left( \frac{1}{\epsilon} \right)^b$$



where A and b are material constants.

It is therefore possible to apply the cumulative damage theory to both forms of damage. The accumulation of damage from repeated applications at various strain levels is illustrated diagrammatically in Figure C.1. In Figure C.1(a) the strain-life diagram is shown with a typical strain-life curve, l-k. On this curve a strain level  $\epsilon_1$ , for example, corresponds to a life  $N_1$ . Lines a-b, c-d, etc., represent  $n_1$  applications at strain level  $\epsilon_1$ , and  $n_2$  applications at strain level  $\epsilon_2$ , etc. These lines, represented by arrows, are called damage paths. The dashed lines, b-c, d-e etc. are called iso-damage lines. If the amounts of damage at b and c are the same, then

$$\frac{n'}{N_2} = \frac{n_1}{N_1} \text{ and thus } n' = N_2 \frac{n_1}{N_1}, \text{ and}$$

similarly  $n''$  and  $n'''$  can be found.

This is represented more simply in a damage-life diagram (see Figure C.1(b)). The damage scale ranges from 0 to 1. The damage paths can be plotted continuously as shown in Figure C.1(c). In this way, the cumulative damage arising from repeated applications is determined in diagrammatic form.

In practice the number of repeated applications ( $n_1$ ) is expressed in terms of the equivalent number of standard axles (E80s). This reduces the analysis to only one strain level to determine remaining life. In Figure C.1(a), therefore, at strain level  $\epsilon_1$  the damaged or consumed life is  $n_1$  and total life is  $N_1$ . Remaining life at this strain level is equal to:

$$N_1 - n_1$$

Alternatively, damage ( $D_1$ ) is often expressed as previously defined and remaining life ( $R_1$ ) is then:

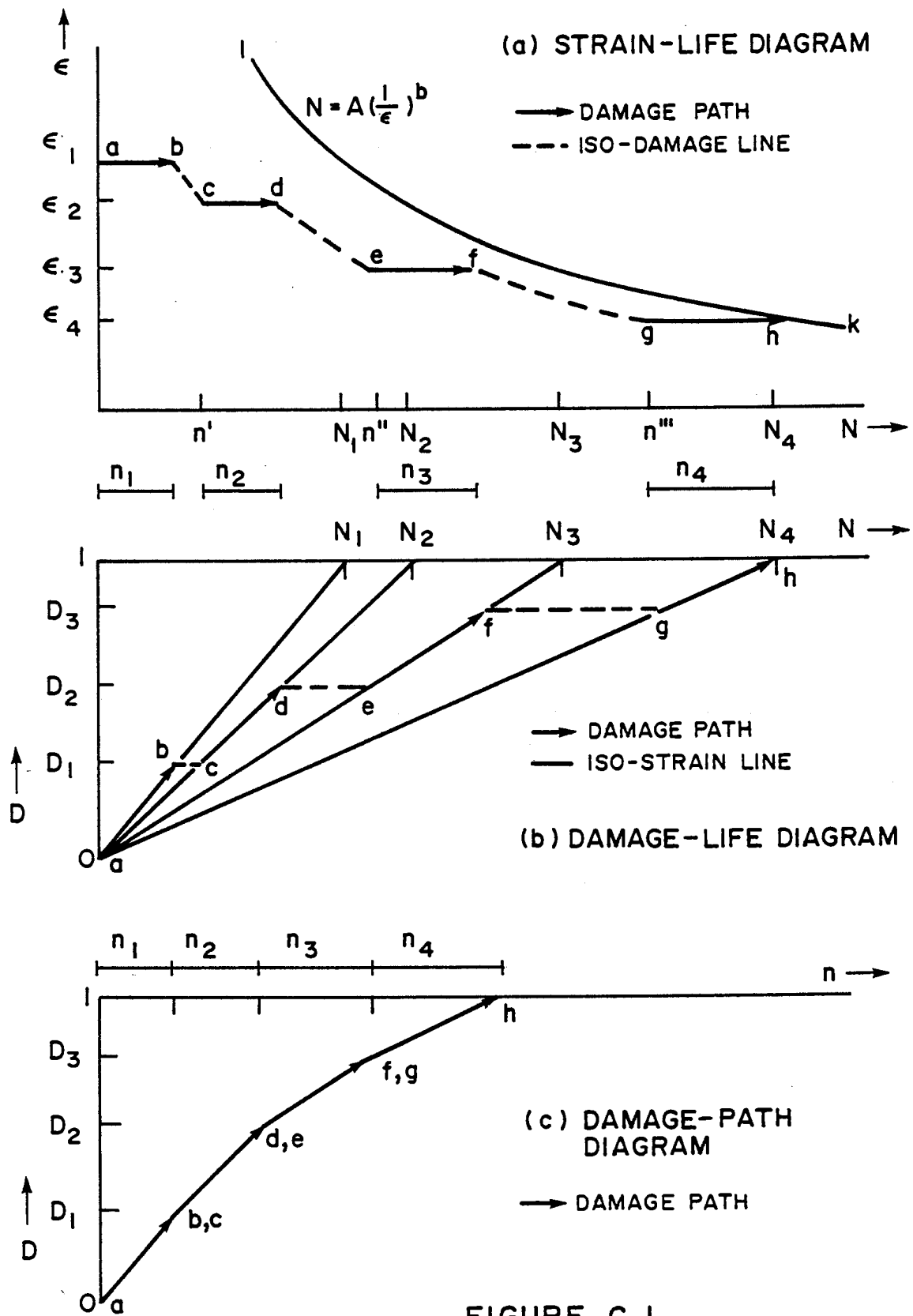


FIGURE C.1  
GRAPHICAL PRESENTATION OF CUMULATIVE  
DAMAGE THEORY (Snaith, et al., 1980)

$$\begin{aligned}
 R_1 &= 1 - D_1 \\
 &= 1 - \frac{n_1}{N_1}
 \end{aligned}$$

Using the same distress criteria, vertical subgrade strain ( $\epsilon_{vs}$ ) and maximum horizontal asphalt strain ( $\epsilon_{HA}$ ), Anderson (1977) also used this theory to determine remaining life. It is pointed out, though, that future environmental or traffic changes cannot usually be foreseen and therefore such a procedure should be seen as a guide only. In considering the remaining life of a pavement with rutting due to permanent deformation, Anderson (1977) reasons that the damaged life or consumed life will be nullified when the surface deformation is removed by an overlay. Koole (1979) supports this view by Anderson (1977) in his description of the Shell overlay design method. The remaining life of a pavement with fatigue cracking is determined in accordance with the description by Snaith et al. (1980).

Treybig et al. (1978) also use the theory of cumulative damage in order to determine remaining life for a pavement with fatigue cracking and rutting due to permanent deformation. As mentioned in Appendix B, however, the cracked state of the existing pavement is taken into consideration in determining the material parameters (E asphalt). Chapter 4 described how these material parameters are used to determine the distress determinants. In a pavement with fatigue cracking the maximum horizontal asphalt strain ( $\epsilon_{HA}$ ) is calculated and used to determine the remaining life in terms of standard axle (E80) repetitions, as described by Snaith et al. (1980). It was shown in Chapter 6, Treybig et al. (1978) consider the contribution of all the structural layers to rutting due to permanent deformation by determining the various stresses and strains of each layer.

It is obvious that Kilaeski et al. (1982) only considered fatigue cracking when determining remaining life. The strain ( $\epsilon_{HA}$ ) need not necessarily be determined, but as shown in Figure C.2 the

deflection basin parameter, surface curvature index (SCI), is related to the number of equivalent single-axle loads (EAL). In this case the structural number has also been determined, based on the AASHO Design Procedure (for the various test sections). The 10 per cent fatigue cracking line is the same form as described above for the general relationship,  $N = A\left(\frac{1}{e}\right)^b$ . The equation for remaining life is as described above, namely  $(N_1 - n_1)$ . Kilaeski et al. (1982) advance this one step further by relating remaining life (in terms of equivalent axle loads) to the SCI for various structural numbers (pavement strengths), as shown in Figure C.3.

### 3 STRUCTURAL PERFORMANCE MODEL

Residual life determined from deflection measurements alone does not lead to satisfactory results. Koole (1979) states: "It is not possible to determine the residual life of a pavement solely from deflection measurements". The reason lies in the fact that the change in a structural parameter, for example elastic modulus (E), with an increase in load repetitions shows a sharp decrease in value initially but thereafter there is a long period during which virtually no change occurs and only at the end of the structural life is there a definite sharp decrease to distress. Deflection measurements also reflect this typical behaviour. However, it is possible to relate early life deflections empirically to the critical life of particular types of pavement structures, as shown in Figure C.4 using work done by Lister and Kennedy (1977). Koole (1979) also mentions that original design life can be determined from FWD deflections. A "crude" test on consumed life is to take FWD deflections between the wheel tracks. If the deflections measured in the wheel tracks, are significantly greater than those measured between the wheel tracks the pavement is approaching the end of its service life.

Pronk and Buiters (1982) mention the procedure in which the decline in effective layer thickness is related to the structural strength. This forms the basis of the structural performance model developed by Molenaar (1983). This principle is shown schematically in Figure C.5 where equivalent layer thickness ( $H_e$ ) decreases in

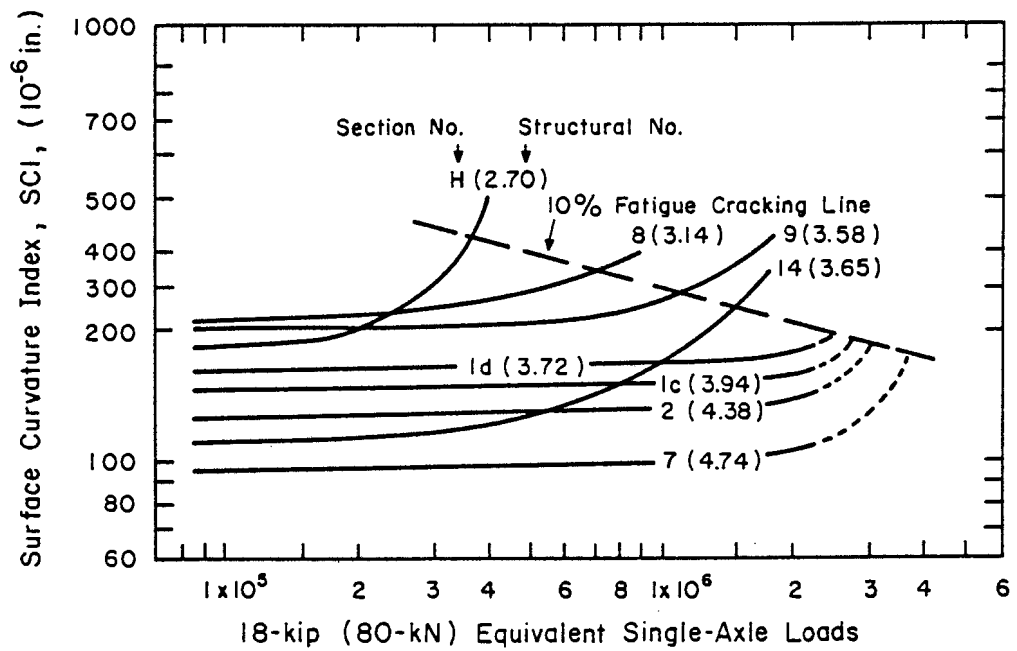


FIGURE C.2  
VARIATION OF SURFACE CURVATURE  
INDEX WITH EAL. (Kilareski, et al., 1982)

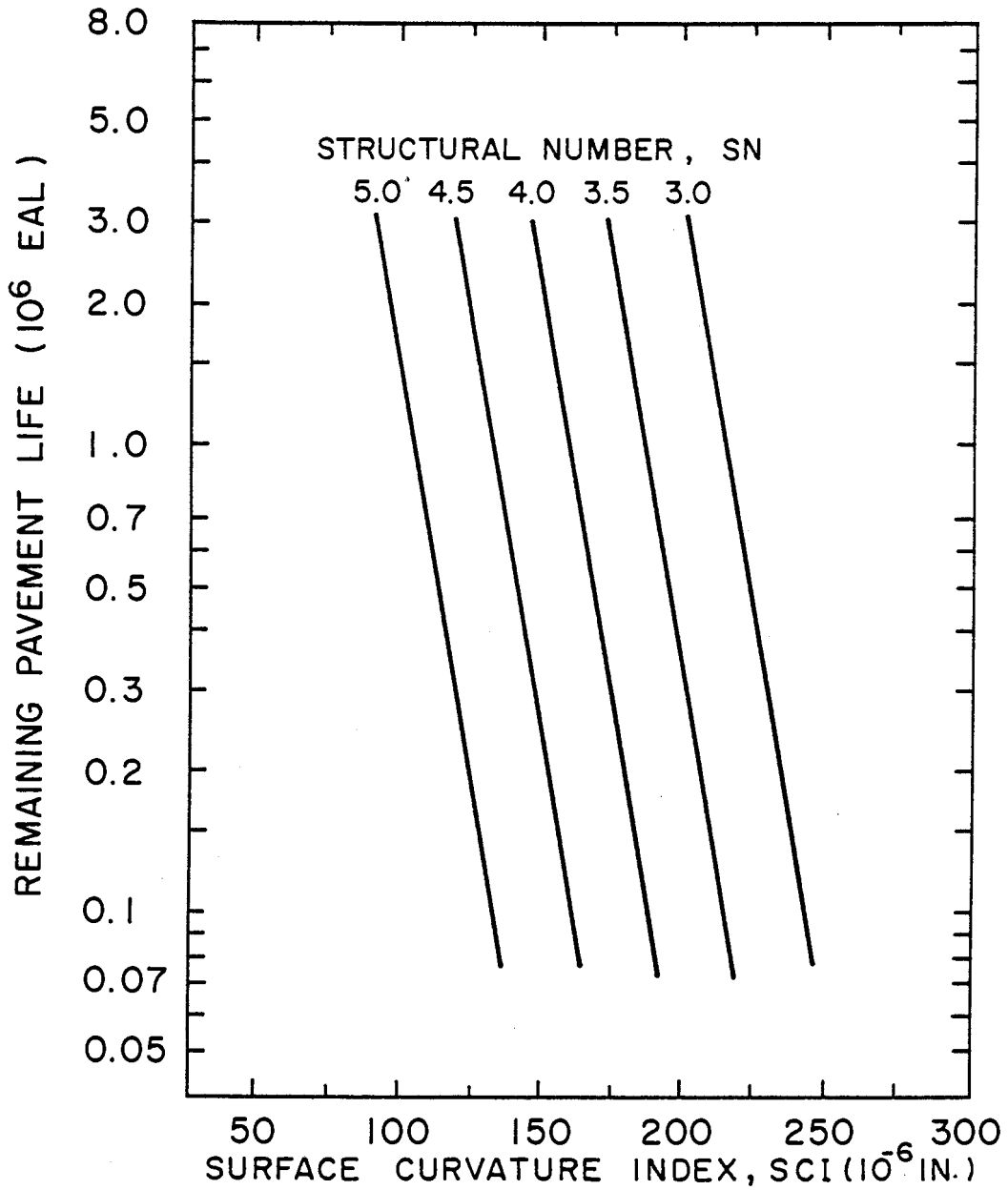
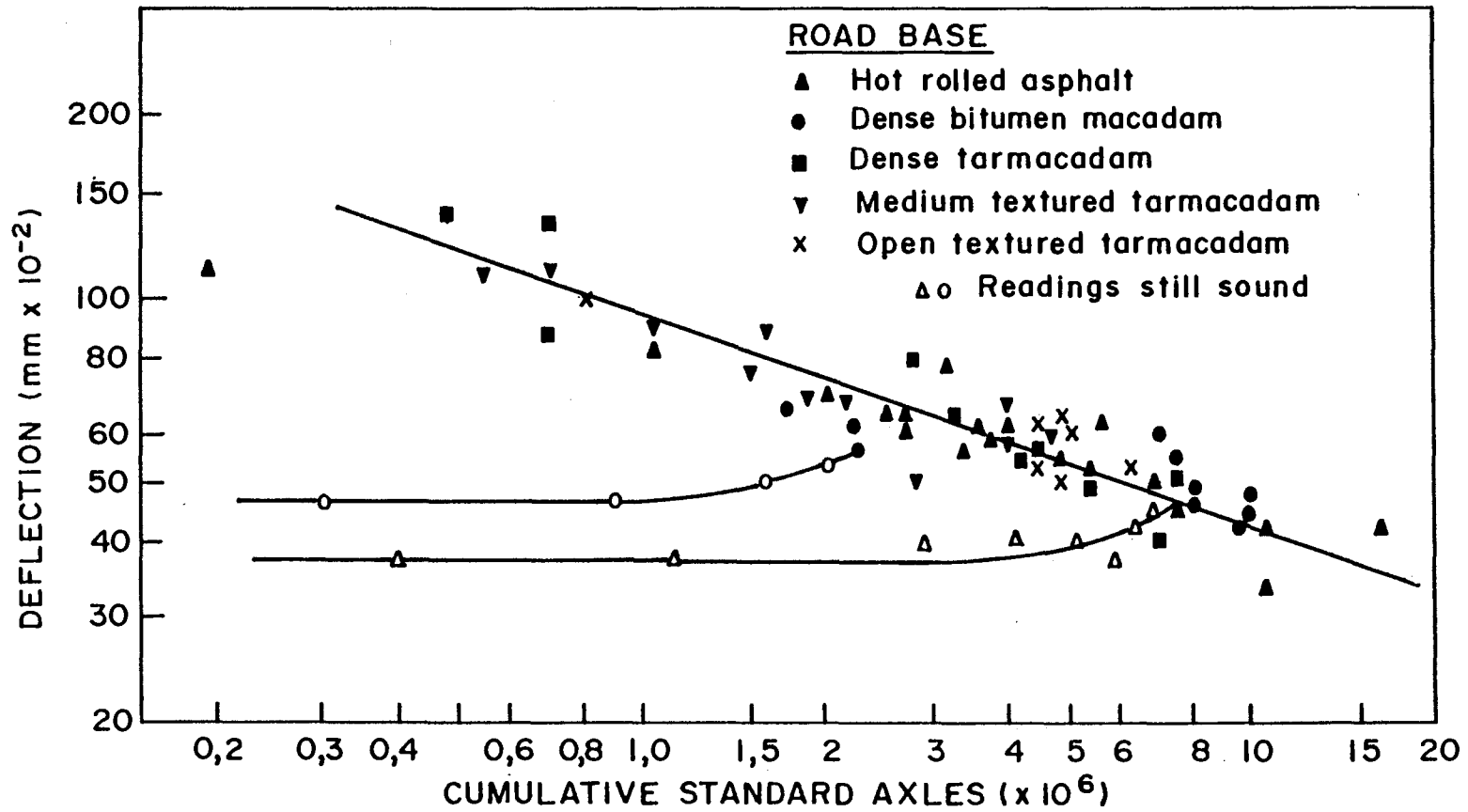


FIGURE C.3  
REMAINING PAVEMENT LIFE BASED ON  
FATIGUE CRACKING FOR BITUMINOUS  
CONCRETE PAVEMENTS WITH SUBBASE.  
(Kilareski, et al., 1982)



**FIGURE C.4**  
RELATION BETWEEN DEFLECTION AND CRITICAL LIFE OF  
PAVEMENTS WITH BITUMINOUS AND TAR BOUND BASES  
(Lister and Kennedy, 1978)

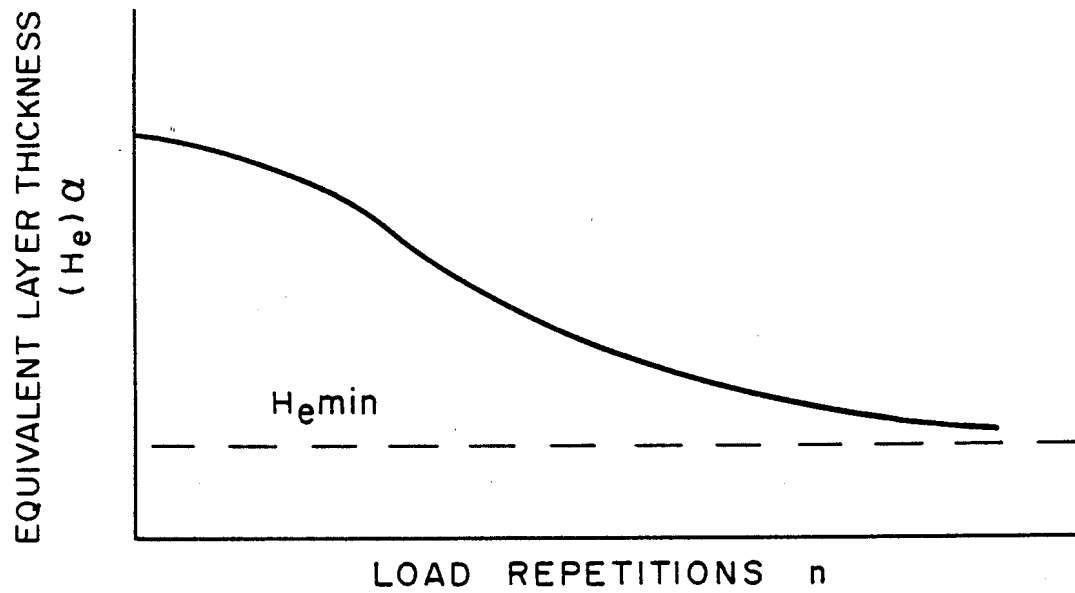


FIGURE C.5  
HYPOTHESIZED DECREASE OF THE EQUIVALENT  
LAYER THICKNESS ( $H_e$ ) WITH RESPECT TO THE  
NUMBER OF LOAD APPLICATIONS ( $n$ ).





relation to the number of load applications(n). The structural condition of the pavement can be characterized by means of the structural condition index P, which is defined as:

$$P = H_{ecn} / H_{eco}$$

where  $H_{ecn}$  = equivalent layer thickness after n load applications corrected for temperature and environmental fluctuations

$H_{eco}$  = equivalent layer thickness just after construction corrected for temperature and environmental fluctuations

In order to determine  $H_{eco}$ , deflection values between the wheel paths are measured as described above. Molenaar (1983) defines  $H_{eco}$  values determined in this way as "candidate"  $H_{eco}$  values since they would have been subjected to some loading between the wheel paths. The amount of future deterioration depends on the expected number of load applications, the structural condition index P and the shape of the deterioration function characterized by  $S_{\log N}$ .

Values for  $S_{\log N}$  should also be determined by means of deflection measurements.  $S_{\log N}$  can be calculated as follows:

$$S_{\log N}^2 = a_1^2 b_1^2 S_{\log H_e}^2 + S_{\text{l.o.f.}}^2 (\log N - \log \epsilon)$$

where  $a_1$  = slope of fatigue relation

$b_1$  = slope of  $H_e$  versus  $\log \epsilon$  relation (=2)

$S_{\text{l.o.f.}}^2$  = lack of fit of the equation used to describe the fatigue relation (=0,16)

In Figure 4.10 the typical relationship between  $H_e$  and surface curvature index (SCI) is shown from results of deflection basin measurements. In Figure C.6 the structural condition index P is

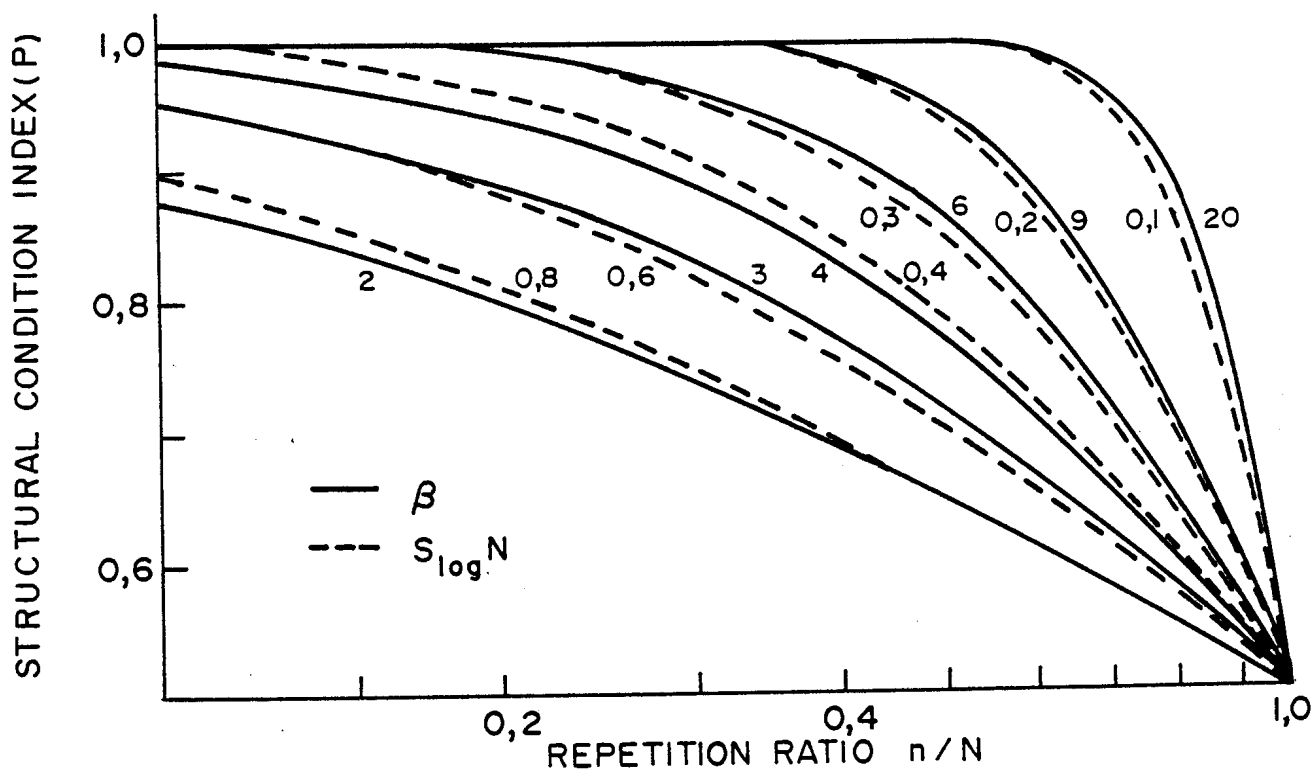


FIGURE C.6  
COMPARISON OF THE THEORETICALLY  
DERIVED STRUCTURAL PERFORMANCE  
MODEL AND THE EQUIVALENT LAYER  
THICKNESS DETERIORATION MODEL  
(Molenaar, 1983)

plotted in relation to deterioration ( $n/N$ ) and the influence of  $S_{\log N}$  can also be seen.

Molenaar (1983) takes this even further by calculating  $P$  and  $S_{\log N}$  directly from deflection basin parameter values such as surface curvature index (SCI) as follows:

$$P = (SCI_o / SCI_n)^d$$

$$\text{and } S_{\log N}^2 = d_1^2 c_1^2 S_{\log SCI}^2 + S_{l.o.f}^2 (\log N - \log \epsilon)$$

where  $SCI_o$  = SCI at time of construction

$SCI_n$  = SCI after  $n$  load applications

$d_1$  = absolute value of the slope of the SCI versus  $H_e$  relation (a reasonable value is 0,53)

$c_1$  = slope of the  $\log(SCI)$  in relation to  $\log N$  (=0,943)

All other variables have been defined before. However, Molenaar (1983) warns as follows:

"Although the procedure to calculate  $P$  seems very simple, one should be aware of the fact that in a number of cases the ratios  $H_{ecn}/H_{eco}$  and  $SCI_o/SCI_n$  might be larger than one.

Remaining life is determined by this procedure as illustrated in Figure C.7.

Molenaar (1983) modified the work done by the Belgian Road Research Centre. He uses the following equation for permanent deformation model:

$$u_p = b_o u_e n^{b_1}$$

where  $u_p$  = permanent deformation (m)

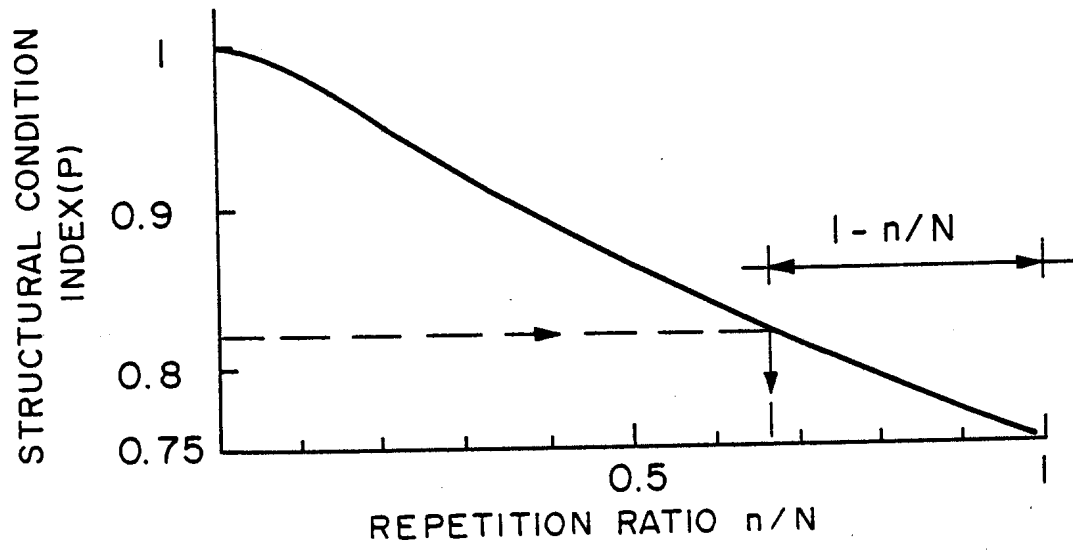


FIGURE C.7  
PROCEDURE TO ASSESS THE REMAINING  
LIFE (Molenaar, 1983)

$u_e$  = elastic deformation (m)

$n$  = number of load repetitions

$b_0, b_1$  = constants

By means of regression analyses of a typical three-layered pavement system Molenaar (1983) used the BISAR computer program to arrive at values of  $b_0$ ,  $b_1$  and  $n$  for the various interfaces between the layers. The elastic deformation at the pavement surface must be known in order to be able to determine the elastic deformation of the top layer. This deformation due to dual wheel loading can be estimated from the maximum deflection ( $\delta_0$ ) value of the falling weight deflectometer (FWD) by using the following equation:

$$\log U_e \text{ surface} = 0,09 + 0,948 \log \delta_{0\text{FWD}}$$

The elastic deformation of each layer can be calculated by subtracting the deformation at the lower interface from the deformation at the upper interface. The permanent deformation can then be calculated by means of the permanent deformation model with constants shown in Table C.1.

A correction factor is applied to relate observed rut depth to these calculated values. By these means rut depth can be related to load applications ( $n$ ), and consumed rut life can be determined by defining a terminal rut depth of for example 20 mm.

#### 4 CONCLUSIONS AND RECOMMENDATIONS

In chapter 4 and 6 it was concluded that the current mechanistic design procedure in South Africa using distress determinants vertical subgrade strain ( $\epsilon_{vs}$ ) and horizontal asphalt strain ( $\epsilon_{ha}$ ) is a sound one. Proper fatigue relationships have been established for these parameters. This makes the use of the linear summation of cycle ratios applicable to both distress criteria: fatigue cracking and deformation rutting. The generalized relationship, ( $N = (\frac{1}{\epsilon})^b$ ), described by Snaith et al. (1980) can thus be used to

TABLE C.1. Values for  $b_o$  and  $b_1$  to be used in the calculation of the permanent deformation (Molenaar, 1983)

Materials	$U_p = U_e * b_o * n^{b_1}$	Modulus (MPa)
Bituminous layers	$U_e * 4,49n^{0,25}$	5 000 (summer)
Stone base	$U_e * 2n^{0,3}$ if $n < 0,12$ m	500
	$U_e * 2n^{0,2}$ if $n < 0,12$ m	
Lean concrete base	-	1 500
Granular subbase	$U_e * 2n^{0,3}$	200
Subgrade	$U_e * (1 + 0,7 \log n)$	5, 10, 20, 40

determine remaining life for both distress criteria. The more critical value can then be used in the selection of an overlay, as described in Appendix D. Although Freeme et al. (1982a) give a fundamental basis to rehabilitation design in their description of the mechanistic design procedure, it is felt that, particularly in the case of establishing criteria to determine consumed life due to rutting, some advances can be made. This would again be possible with the information available from HVS tests and observed field data. In this regard the approach by Treybig et al. (1978), where the deformation contributions of each layer is better represented by the computed stresses and strains of each layer, should be pursued with the available data.

It is clear too that the approach to relate the remaining life of the pavement to other structural indicators such as the equivalent layer approach shows much promise. The structural performance model suggested by Molenaar (1983) was developed specifically for a three-layered pavement structure and therefore it is obvious that it would not be possible to use this approach in all cases. Instead it is suggested that, with the previously mentioned information available on pavement performance in South Africa, the performance model be established with values determined from regression analyses. This approach would then take into consideration factors



such as the deflection basin measuring device, deflection basin parameter selected and pavement structure classification described previously.

The model relating permanent deformation and elastic deformation to the number of load applications seems a sound approach. It would also be possible to establish these relationships with the regression analysis of the information available for the South African condition.



## **APPENDIX D**

### **CRITERIA FOR OVERLAY**



## 1 INTRODUCTION

This section is a logical continuation of the discussion in Appendix C. In general, the decision to overlay a pavement under analysis will be based on criteria related to the remaining life or consumed life. The distress criteria, fatigue cracking and permanent deformation rutting, are considered separately to determine the remaining life of the pavement. The decision to overlay the pavement is based on the more conservative of the two criteria, but both criteria are checked again to ensure that the prolonged life (remaining life after the overlay) would indeed be achieved. As in any situation where various possible alternatives are generated, sound engineering judgement is influenced by economic considerations. The latter type of decision strongly indicates the typical considerations of a maintenance or pavement management programme and should be viewed against that broader background although the focus here is on a project level based on deflection basin related criteria.

## 2 RUTTING CRITERIA

Snaith et al. (1980) describe how on the basis of the theory of cumulative damage, the remaining life can be determined. In general this remaining life, as described in Appendix C, would be expressed as:  $R_1 = N_1 - n_1$  or  $R_1 = 1 - n_1/N_1$ . Snaith et al. (1980) do not mention any specific criteria related to this remaining life for decisions to overlay or not. Anderson (1977) bases the decision to overlay or not on the length of the remaining life. If the anticipated or estimated future traffic is more than the remaining life, an overlay is needed. If the remaining life is more than the anticipated traffic over the functional life of the pavement, no overlay is needed. An overlay may be required for other functional reasons such as improving the skid resistance of the riding surface. It is in this regard that Anderson (1977) states that even a nominal thickness of asphalt concrete placed on an existing pavement gives the pavement a new "life" by removing the surface deformation. "There is no theoretical or practical

evidence which suggests that the permanent deformation which existed before rehabilitation will affect the future performance of the pavement."

In general Anderson (1977) does support the analysis procedure described by Snaith et al. (1980). For the generalized fatigue relationship ( $N = (\frac{1}{\epsilon})^b$ ) the aim of an overlay would be to reduce the strain level ( $\epsilon_{vs}$ ) to the level where the anticipated traffic would meet the prolonged life or remaining life after overlay. This process is shown in Figure D.1 and in a more general form in Figure D.2. The formulation of the fatigue relationship considered by Treybig et al. (1978) (as discussed in chapter 6 and Appendix C) is obviously more complicated. Although no specific mention is made of any criteria for overlays related to remaining life the reasoning above was evidently followed.

Molenaar (1983) does not use his permanent deformation model (see Appendix C) in his proposed overlay design. It is obvious though that this model, if properly calibrated to field performances, would also be able to provide the same criteria based on remaining life as described in Appendix C. If an overlay is needed, the aim would be to reduce the elastic deformation ( $U_e$ ) and resulting permanent deformation ( $U_p$ ) of each layer in order to meet the required prolonged life.

### 3 FATIGUE CRACKING CRITERIA

Remaining life ( $N_1 - n_1$ ) compared with the anticipated or future traffic is the general criterion for overlays, based on analysis using the cumulative damage (linear summation ratio) theory. This has already been briefly described on the basis of the discussion by Snaith et al. (1980) (see Appendix C and sections 2).

In considering the previously defined remaining life, Anderson (1977) also considers the cracked state of the existing asphalt concrete layer and whether the pavement has an asphalt concrete layer when establishing criteria for considering an overlay. The remaining life is automatically zero if the pavement is cracked

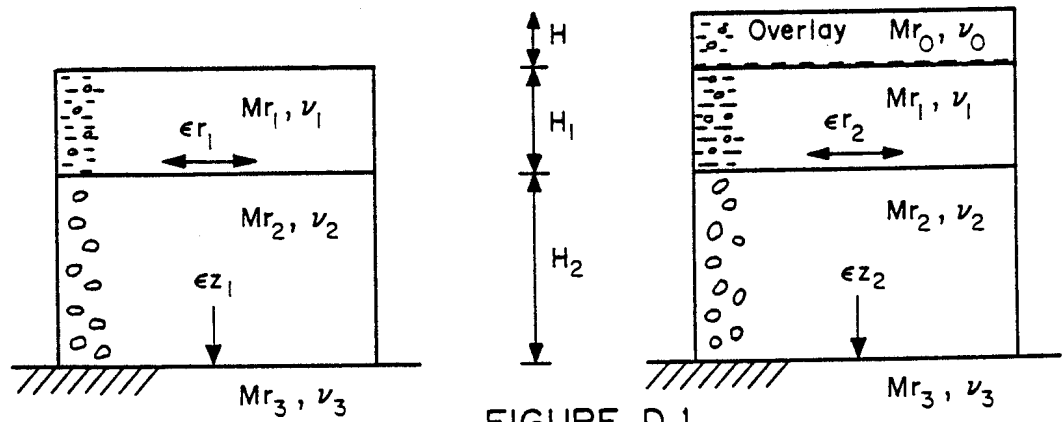
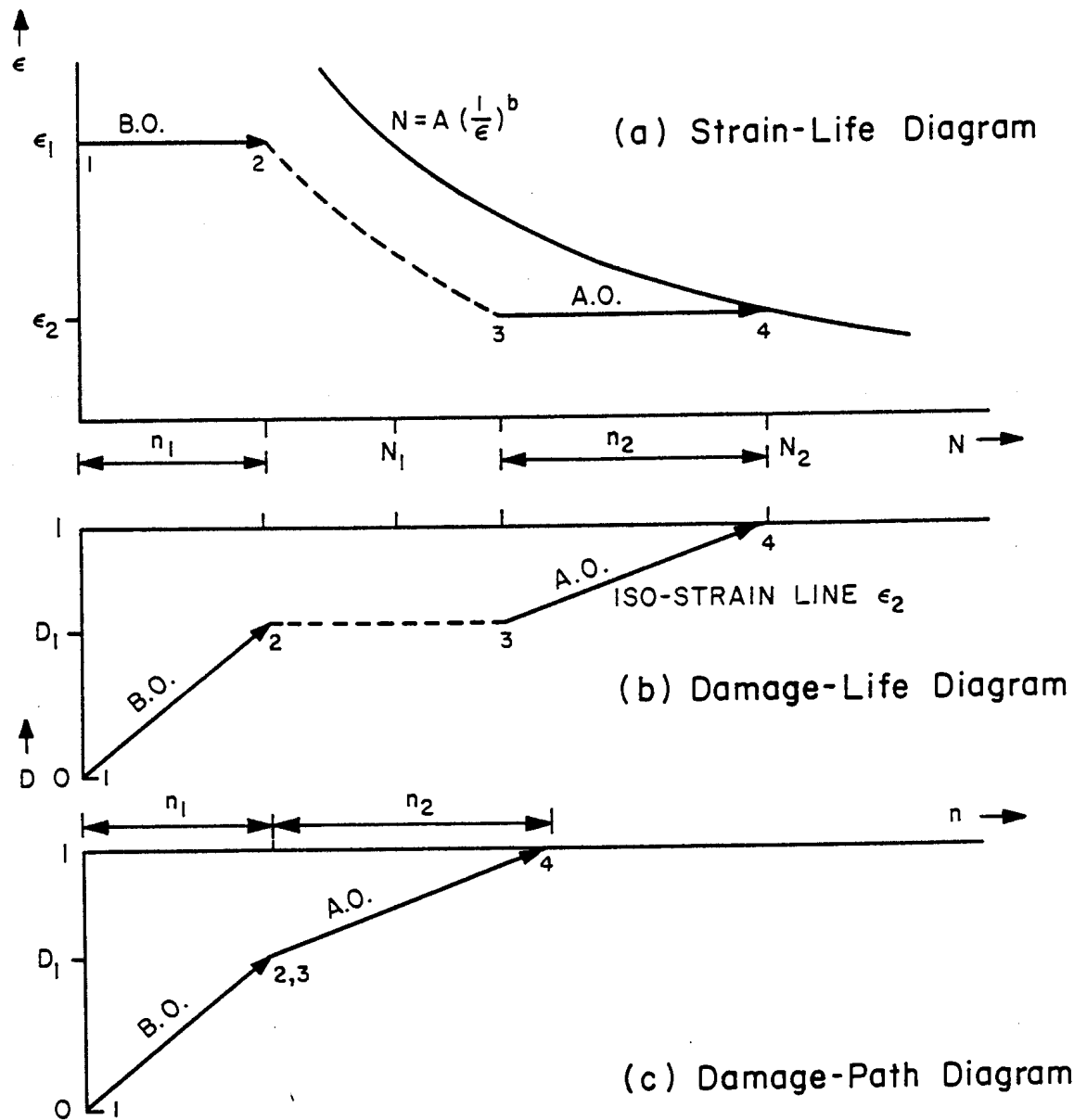


FIGURE D.1  
CHANGES IN STRAIN LEVELS DUE TO OVERLAY.



NOTE : B.O. - BEFORE OVERLAY    A.O. - AFTER OVERLAY

FIGURE D.2  
DAMAGE PROCESS IN A PAVEMENT  
STRUCTURE WITH A SINGLE OVERLAY.

( Snaith, et al., 1980 )

and warrants consideration for an overlay, or if there is no asphalt concrete layer yet. If the remaining life is less than the anticipated traffic an overlay may be considered. If the remaining life is more than the anticipated traffic no overlay is needed. When an overlay is considered as was discussed in section 2 (referring to Figures D.1 and D.2), the aim would again be to reduce the strain level ( $\epsilon_{HA}$ ) to accommodate a prolonged life or remaining life after the overlay, which would meet the required anticipated traffic life. Analysing various pavements in this way, Anderson (1977) arrived at characteristic curves as shown in Figure D.3. In this figure remaining life is expressed as a percentage of the overlay thickness. The latter value of overlay thickness corresponds to the reduction in strain level ( $\epsilon_{HA}$ ). Comparing these results with those of a fully cracked asphalt concrete layer with no remaining life, Anderson (1977) concludes that it will always be more economical to neglect any existing asphalt when the remaining life is below 75 per cent. In this overlay design procedure, a "critical" remaining life of 50 per cent was adopted, this being the point at which the existing life is disregarded in designing an overlay. This approach, based on the fatigue relationships described in chapter 6, was also followed by Monismith and Markevich (1983).

The approach by Molenaar (1983), using the structural performance model, obviously differs from the one described above. Molenaar (1983) is quoted as follows:

"Although Miner's law is applicable to the development of one crack, further extension of cracks is dependent on the redistribution of the stresses, and in this case Miner's law may not be fully applicable. Furthermore Miner's law defines a clear failure condition which occurs at e.g. the fracture of a test specimen. Such a failure point does not exist in the case of pavements. A 100 per cent cracked pavement surface can still be used as a reasonable driving surface unless large deformations and/or pot-holes occur. Therefore a straightforward use of Miner's law in the estimation of overlay thicknesses is not considered to be a proper approach, since this will result in an unrealistic overlay design especially in those cases where Miner's ratio comes close to

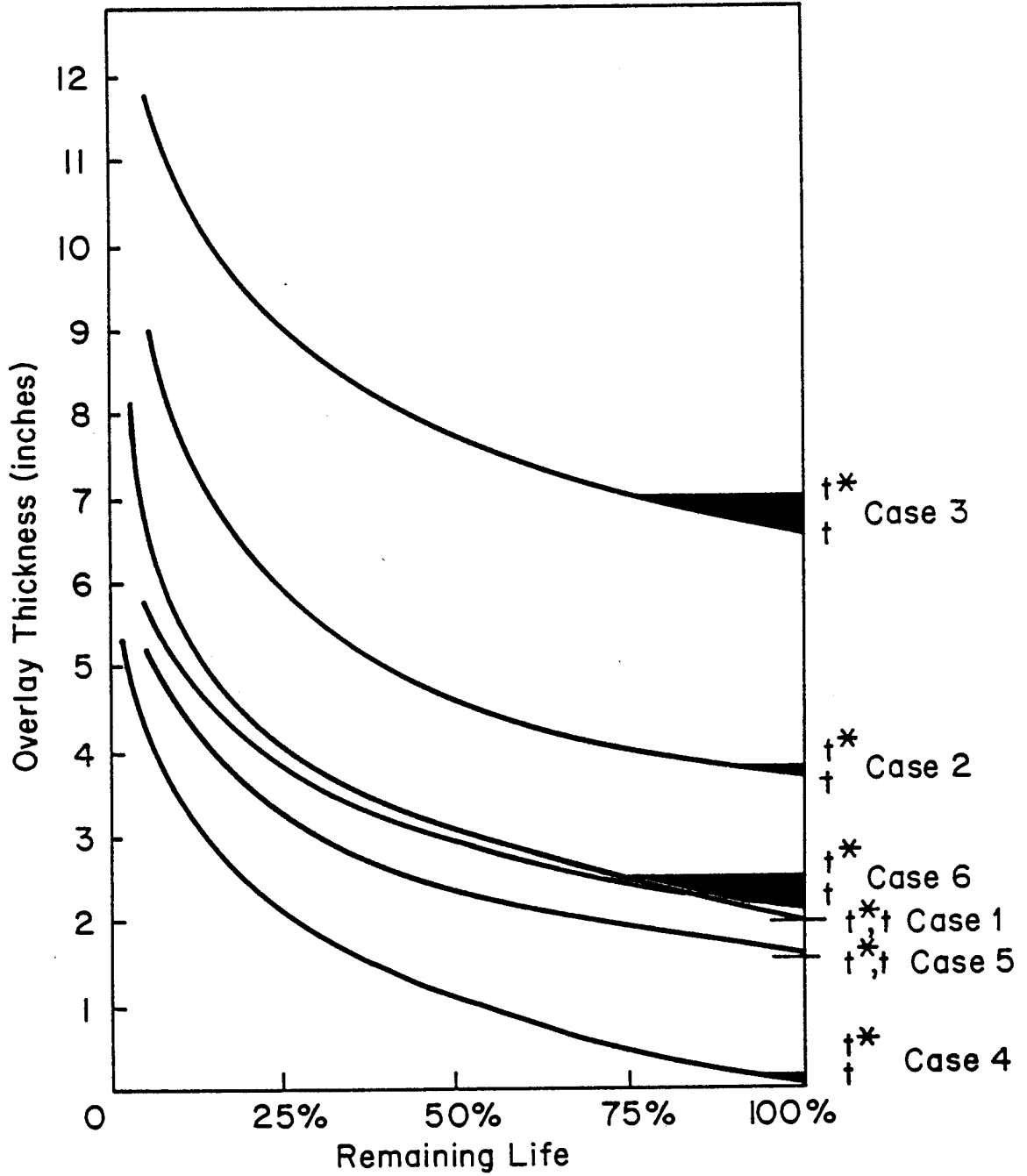


FIGURE D.3  
EFFECT OF REMAINING LIFE ON OVERLAY  
THICKNESS (Anderson, 1977)

one."

This supports the reasoning of Anderson (1977), but also points to the possibility of the structural performance model being used to give a more realistic estimate of the structural life of a bitumen pavement. Molenaar (1983) does not give any specific indication of criteria for decisions on overlays. It is evident from the reasoning, however, that the remaining life determined in this way, would also be used, but with different preconditions.

#### 4 DETERMINATION OF OVERLAY THICKNESS

The two distress criteria, fatigue cracking and permanent deformation rutting have deliberately been considered separately. The reasoning behind this is explained by Koole (1979):

"In determining the thickness required for an overlay, the subgrade-strain and asphalt-strain criteria should be considered, separately; it is quite possible that the design criterion that did not govern the original pavement design will become limiting for the overlay thickness."

In this section an overlay thickness is thus decided upon by means of the limiting life of the two defined criteria described in section 2 and 3. The resulting lower distress criteria parameters ( $\epsilon_{HA}$  and  $\epsilon_{VS}$ ) are usually calculated for the possible thicknesses considered. Anderson (1977) calculates these relationships for the various thicknesses of overlays by means of the techniques described in chapter 4. This is shown in Figures D.4 and D.5 for reduction in subgrade strain ( $\epsilon_{VS}$ ) and asphalt tensile strain ( $\epsilon_{HA}$ ). In Figure D.3 only pavements with more than 50 mm of asphalt concrete prior to overlaying are considered. The reason was discussed in chapter 6 and in Figure 6.2 what the effect of relatively thin asphalt concrete layers (50 to 75 mm) on tensile strain in asphalt concrete was shown. From the quotation by Koole (1979) above it is obvious that an overlay of for example 25 mm on the existing 25 to 40 mm of asphalt for rut requirements, could in fact shorten the remaining life of the fatigue cracking requirements. The desired

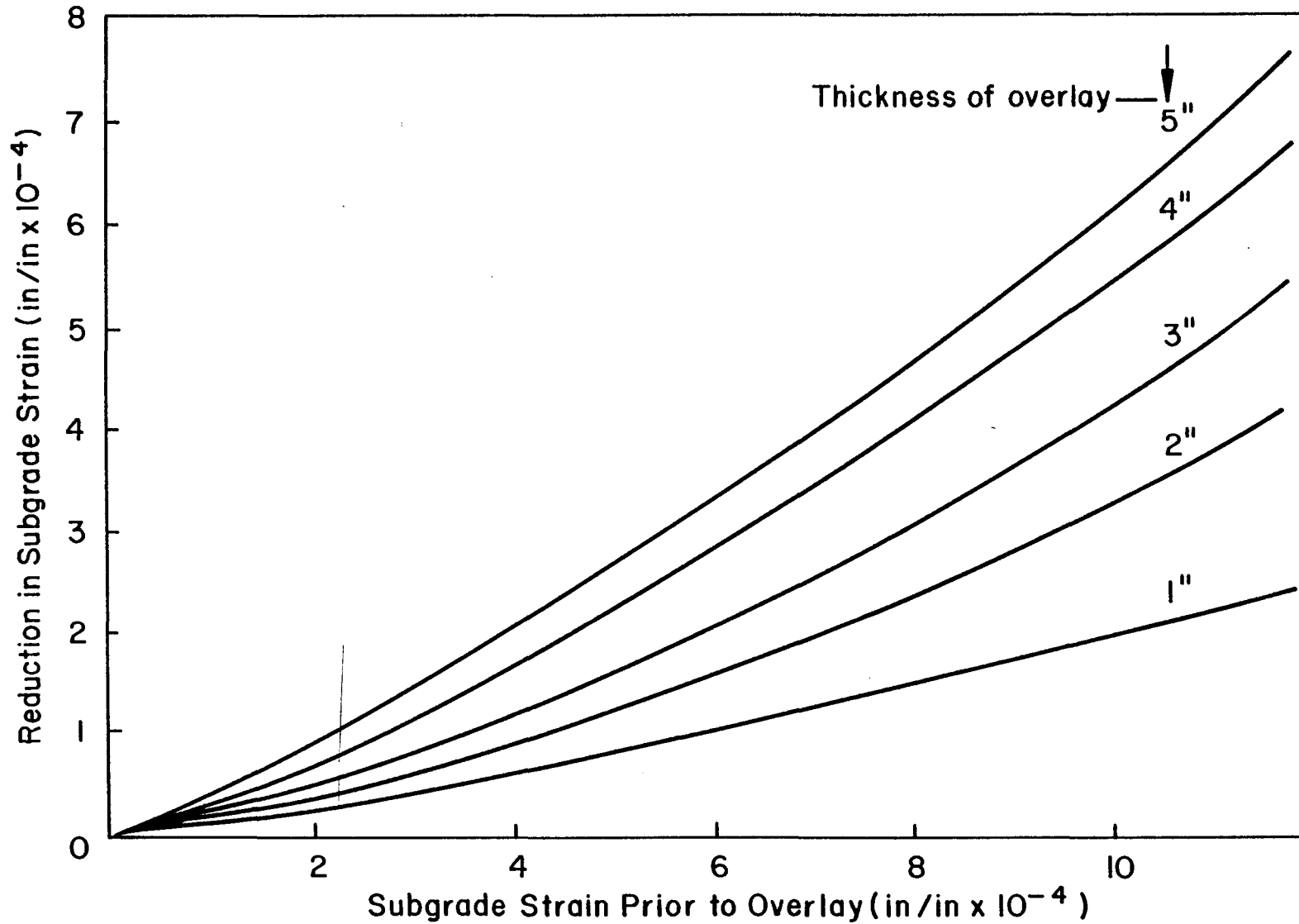
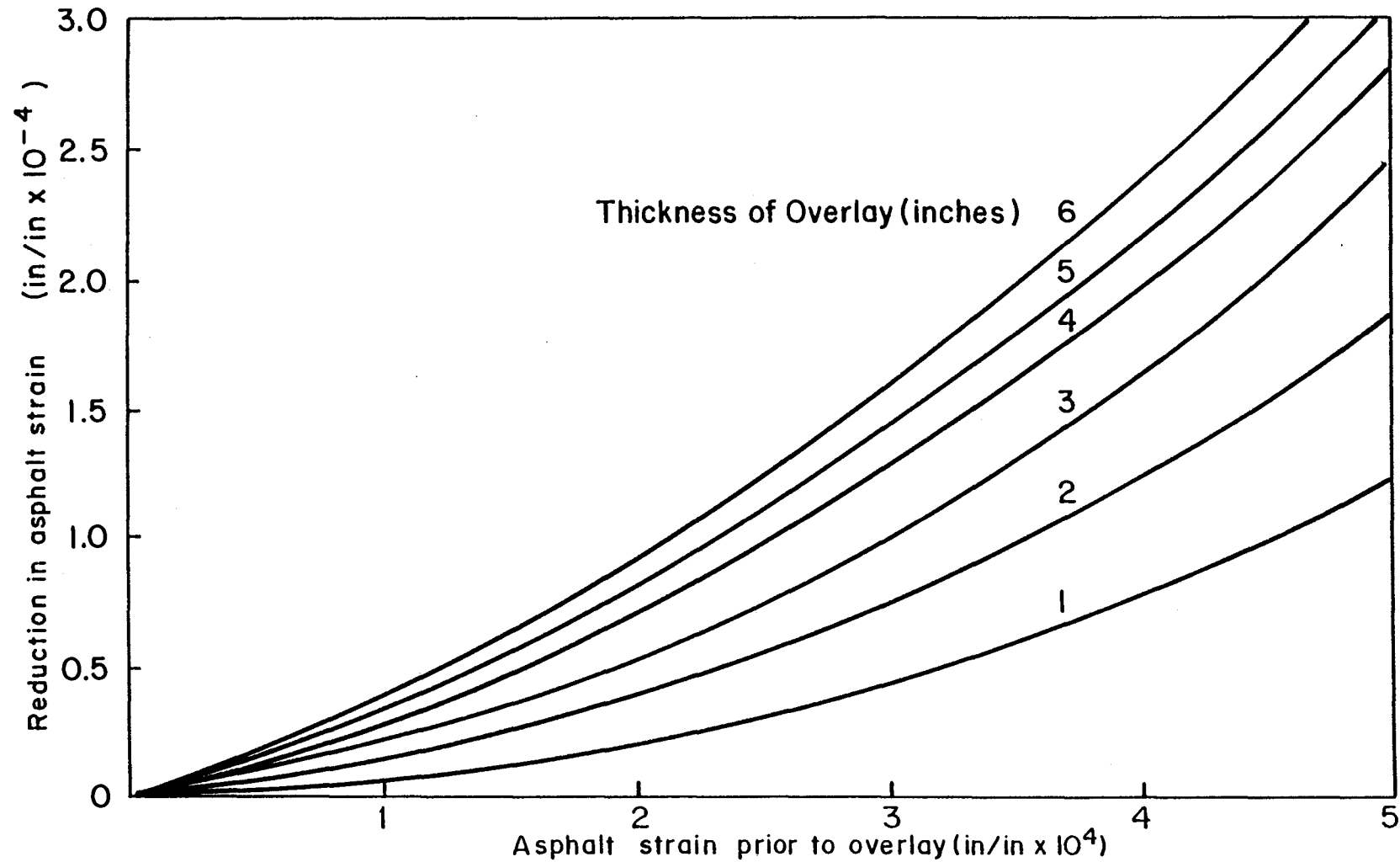


FIGURE D.4

REDUCTION IN SUBGRADE STRAIN DUE TO OVERLAY (Anderson, 1977)



**FIGURE D.5**  
**REDUCTION IN ASPHALT TENSILE STRAIN DUE TO OVERLAY**  
**(Pavements with more than 2" of asphalt concrete prior to overlaying)**  
**(Anderson, 1977)**



reduction in strain level can also be expressed in terms of the selected deflection basin parameters, as shown in Figure D.6, according to Anderson (1977). Similarly the desired lower deflection basin parameter such as surface curvature index (SCI) can be related to a higher equivalent layer thickness ( $H_e$ ) (see Figure 4.10) according to the analyses of Molenaar (1983).

Treybig et al. (1978) established the most comprehensive procedure for considering the effect of fatigue cracking and rutting simultaneously. This is shown in Figure D.7 where the existing asphalt concrete layer is regarded as uncracked. The overlay thickness required, is determined by selecting the thicker of the two thicknesses related to the various criteria for the desired load repetitions.

Koole (1979) also describes how three separate overlay thicknesses are determined. This includes the previously discussed criteria for fatigue cracking and rutting, and also a method of determining thickness based on the assumption that the existing pavement has deteriorated to such an extent that the asphalt concrete layer is treated as a granular layer and the overlay as a "new" asphalt concrete layer.

The latter approach is also suggested by Thompson and Hoffman (1983) when the asphalt concrete layer displays interconnected Class 2 cracking.

## 5 CONCLUSIONS AND RECOMMENDATIONS

Remaining life in relation to the distress criteria, rutting and fatigue cracking, is the main criterion in the consideration of overlays. The remaining life determined by methods described in chapter 6 was determined for each of the distress criteria separately. For the rutting criterion the views on remaining life vary considerably. The view that remaining life is completely restored by an overlay removing the deformations is widely accepted in overlay design. Using the various models discussed in Appendix C it is possible to determine the prolonged life by lowering the

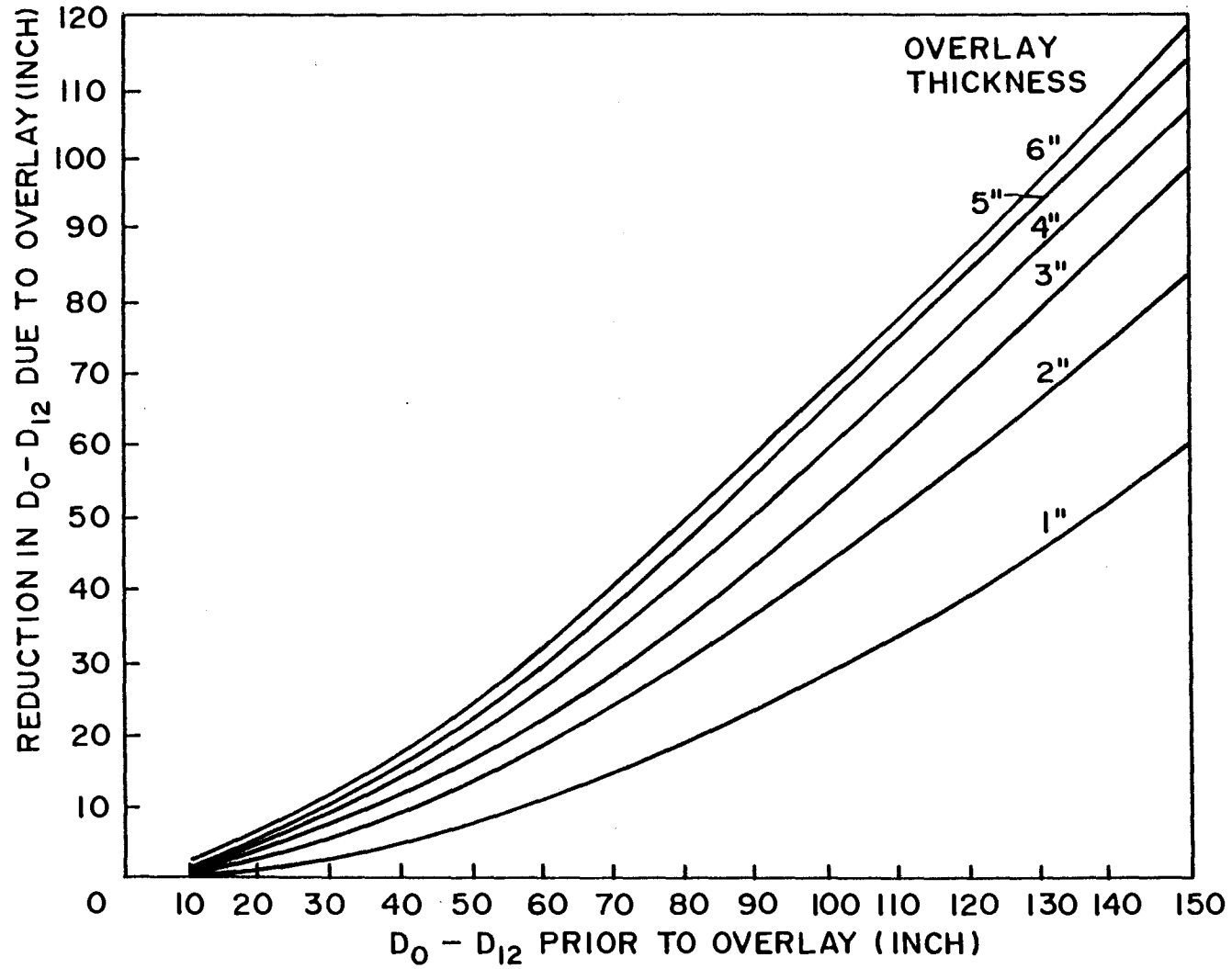


FIGURE D.6  
REDUCTION IN  $D_0 - D_{12}$  DUE TO OVERLAY  
(Anderson, 1977)

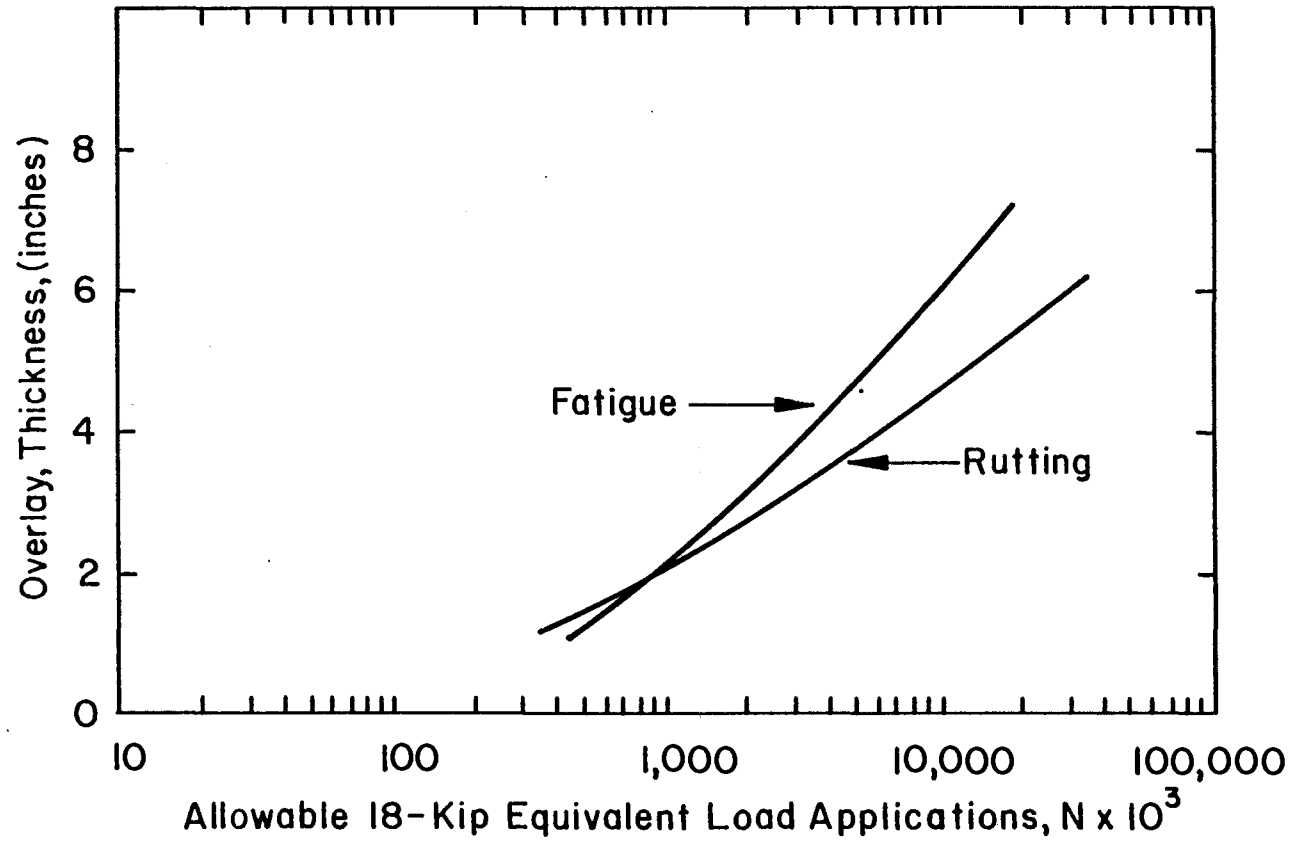


FIGURE D.7  
SAMPLE OVERLAY THICKNESS DESIGN CURVES

vertical subgrade strain ( $\epsilon_{vs}$ ) for example. The more comprehensive model proposed by Treybig et al. (1978) warrants a closer look if it were to be related to the South African situation as were the other proposals and recommendations mentioned before. This may all be incorporated in a proposed catalogue of overlay designs, which would be similar to the existing TRH4 (NITRR, 1985a).

In consideration of remaining life as a criterion for fatigue cracking, the consideration of cracking only leads to some uneconomical overlay proposals. Anderson (1977) indicates that a 50 per cent remaining life for fatigue cracking should be a critical value. The structural performance model by Molenaar (1983) attempts to be more economical by considering the structural value of the cracked asphalt layer. It also offers better consideration of the use of other new materials like bitumen-rubber.

In the final selection of the thickness of the proposed overlay for the critical strain parameter, the emphasis is on checking the other parameter again in order to ensure that the overlay does not shorten remaining life after overlay for the previously non-critical parameter value. From Anderson's (1977) work it is obvious that this would be of particular importance with thin overlays on thin asphalt concrete layers. The approach by Treybig et al. (1978) to plot overlay thickness for both criteria simultaneously in relation to remaining life gives a good graphical indication of such trends.

It has been stated that the selection of an overlay must be seen against the background of maintenance or rehabilitation management systems. The models discussed for analysis are not always applicable to the South African situation. It is therefore suggested that the recommendations in regard to pavement performance and structure were made in previous sections be extended to this area of overlay design in order to make the whole design procedure mechanistically sound. This could easily be incorporated in the suggested catalogue of overlay designs, mentioned above.



## **APPENDIX E**

### **CRACK MOVEMENT CALCULATIONS WITH DEFLECTION BASIN MEASUREMENTS ON N4/3**

## 1 INTRODUCTION

In Appendix B it was mentioned that there exists a good correlation between the measurements of the Crack-Activity-Meter (CAM) and deflection basin parameters as measured with the Road Surface Deflectometer (RSD). The normal procedure of initial assessment according to the draft TRH12 (1983) guidelines are carried out on a typical cemented base pavement. In the detailed assessment stage the question whether the cracks recorded on specific sections are active or not must then be addressed with confidence. The new service of the NITRR where the CAM and the RSD are combined can then give the required information to make a sound decision in regards to the rehabilitation option. Various cracks with related block sizes and degrees of severity are selected on such a section under investigation. At the same point (crack) the CAM and RSD are set up and measurements are taken with the Benkelmanbeam truck travelling over the crack following the WASHO procedure. The crack activity measurements are then correlated with various other parameters such as block size and deflection basin parameters (Rust, 1984). This appendix therefore describes how such an analysis on the N4/3 was used to verify the rehabilitation option selected in terms of its crack attenuation.

## 2 PROBLEM DESCRIPTION

The cemented base of N4/3 is cracked and urgently needs rehabilitation. Crack movement measurements were taken in October (Rust, 1986). It was found that there exists sections of road where the crack movements are very high. The block sizes were found to be relatively large. This means that the crack movements are likely to increase as the block sizes break down to a smaller size. The rehabilitation option that was selected is to overlay the existing pavement with a 100 mm G1 crushed stone base and 40 mm asphalt surfacing. The analysis described in this technical note is to determine what the effectiveness of the overlay is to reduce crack movement. In the analysis use was made of measured deflection basins and the correlation thereof with crack movement measurements. This was followed with a mechanistic analysis of the rehabilitation

option to calculate the deflection basin and predicted crack movements.

### 3 CRACK MOVEMENT AND DEFLECTION BASIN CORRELATION

On each of the measuring points of the CAM the deflection basin was also measured with the RSD. The measurement of the whole deflection basin with the RSD makes it possible to determine various deflection basin parameters. The most common deflection basin parameters (Rust, 1986) that can be calculated from RSD measurements are listed in Table 1.1 with their respective formula. The maximum horizontal crack movements (HMAX) and the maximum vertical crack movements (VETOT) in micro-meters were correlated with various deflection basin parameters. The results were as follows:

$$\begin{aligned} \text{HMAX} = & 904,271 * (\text{MAX. DEFL})^{2,6} - 9,483\text{E-}6 * (\text{SCI}_{915})^{2,5} + \\ & 3,086\text{E-}3 * (\text{SCI}_{610})^{1,5} - 2,538\text{E-}2 * (\text{DI}_1)^{1,3} + \\ & 9,81 * (\text{SCI}_{305})^{1,4} + 71,765 \end{aligned}$$

$$\text{R-squared} = 0,69$$

$$\begin{aligned} \text{VETOT} = & 4931,765 * (\text{MAX. DEFL})^{5,2} - 1,813\text{E-}12 * (\text{SCI}_{915})^{5,1} + \\ & 4,312\text{E-}8 * (\text{SCI}_{610})^{3,6} + 1,65\text{E-}3 * (\text{DI}_1)^{1,9} - \\ & 1,887\text{E-}3 * (\text{SCI}_{305})^{1,9} + 49,713 \end{aligned}$$

$$\text{R-squared} = 0,83$$

Where: SCI = Surface curvature index with the subscripts indicating the offset for deflection in mm.

$\text{DI}_1$  = Deflection Index which is the difference in deflection at 127 mm and 305 mm.

MAX. DEFL = Maximum deflection in mm.

VETOT = Total vertical movement in micrometer.

The regression analysis indicate that VETOT correlated better with the deflection basin parameters than HMAX. The reason for that can clearly be related to the relatively large block sizes (Rust, 1986).

#### 4 CALCULATED DEFLECTION BASIN PARAMETERS

The pavement structures as shown in Figure E.1 for the existing pavement and the rehabilitated pavement were analysed mechanistically with the computer program ELSYM5. The input values are as indicated in the figure. The stress directly on top of the cemented base was calculated before and after the G1 crushed stone base overlay. The calculated vertical stress was 374 kPa and after the overlay it was reduced to 111 kPa. This is a drastic reduction in the calculated stress values and clearly indicates that the overlay did indirectly reduce the possible crack movements.

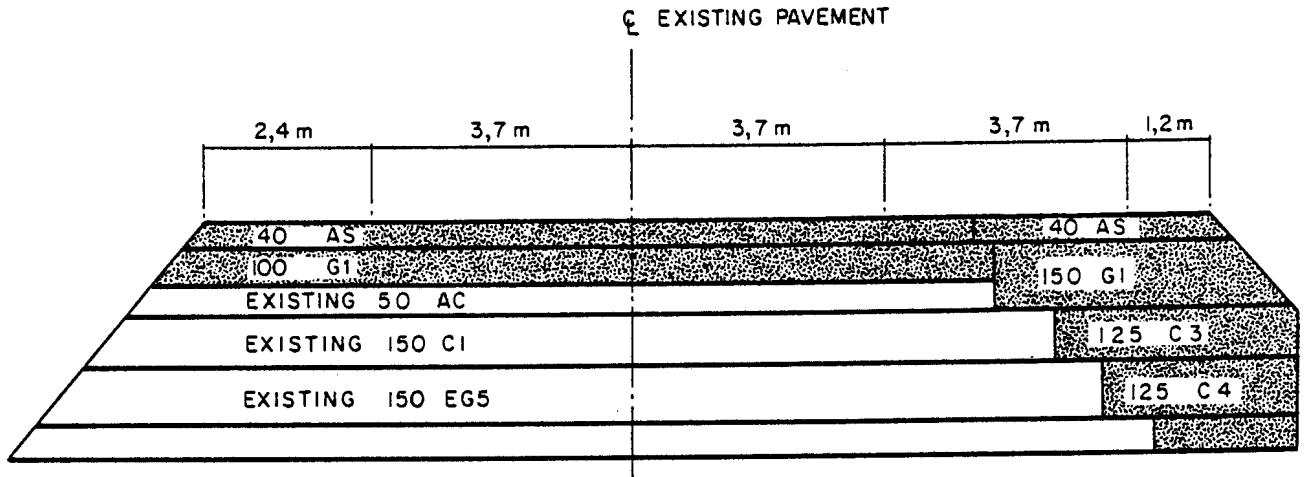
During the mechanistic analysis the deflection basin was calculated for the two pavement structures. In Table E.1 the relevant deflection basin parameters are indicated. The deflection basin parameters on top of the old cemented base (now sub-base) and on top of the overlaid pavement are shown.

TABLE E.1 Calculated deflection basins

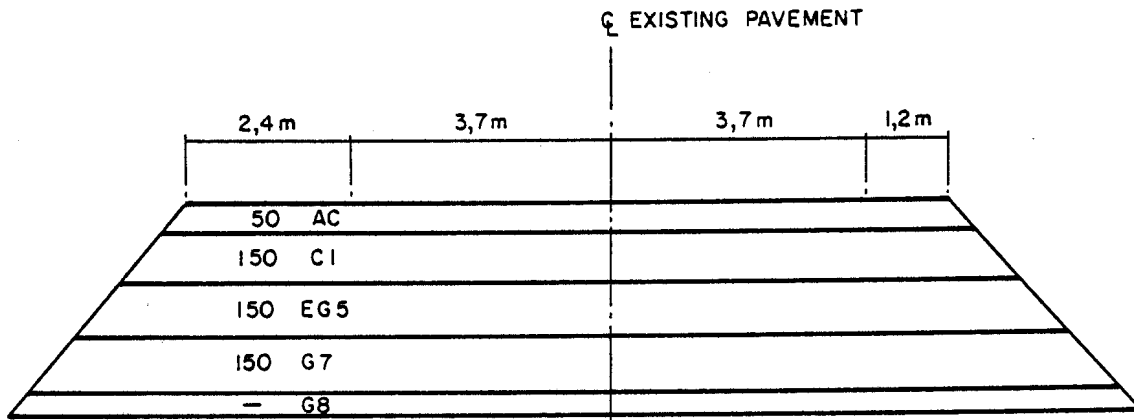
Pavement	Depth (mm)	Deflection basin parameters (mm)				
		MAX. DEFL	SCI <sub>915</sub>	SCI <sub>610</sub>	SCI <sub>305</sub>	DI <sub>1</sub>
Existing	0	0,434	0,300	0,245	0,144	0,098
Overlaid	0	0,373	0,253	0,209	0,135	0,084
	140	0,351	0,230	0,186	0,108	0,075

When comparing the deflection basin parameters calculated on the surface directly it is shown in Table E.1 that the overlay reduces the deflection basin parameters values drastically. This reduction in the respective deflection basin parameter values are even more when the values calculated on top of the cemented base are compared.





OPTION 1



EXISTING PAVEMENT

FIGURE E.1  
REHABILITATION OPTION ON N4/3

The regression analysis described earlier were also used to calculate the respective predicted crack movements. These results are shown in Table E.2.

TABLE E.2 Calculated crack movements (micro-meter)

Pavement	Depth (mm)	HMAX	VETOT
Existing	-	175	144
Overlaid	140	131	71

The results in Table E.2 show that there is a drastic reduction in the vertical and the horizontal crack movements. In the case of the vertical crack movements the reduction was more. This vertical movement was the more severe case for crack movement due to the relatively large block sizes.

## 5 CONCLUSIONS

- (a) The crack movements (HMAX and VETOT) were correlated with various deflection basin parameters as measured with the CAM and the RSD.
- (b) The vertical stress calculated on top of the cemented base show a drastic reduction in values when compared with the vertical stress values calculated on top of the cemented sub-base of the overlaid pavement. This reduction indicates that there should be a reduction in crack movements too.
- (c) The deflection basin parameters were calculated for the existing pavement and the overlaid pavement. These calculated deflection basin parameters were used in the correlation relationships to determine the calculated crack movements. There is a drastic reduction in the crack movements on top of the cemented base due to the overlay.



## **APPENDIX F**

### **APPLICATION OF EQUIVALENT LAYER THICKNESS CONCEPT**

## 1 INTRODUCTION

Odemark's (1949) equivalent layer thickness concept is used as a simple method of approximation. It enables the transformation of a multi-layered system into a single layer with equivalent thickness. The principle is that the equivalent layer has the same stiffness as the original layer, so as to give the same pressure distribution underneath the layer. This concept of classifying a pavement with one number that represents more or less the bearing capacity of that pavement is clearly illustrated by Molenaar and Van Gorp (1980) and Molenaar (1983). The typical South African pavement structures that were analysed in chapter 7 were also converted to the equivalent layer thickness. The equivalent layer thickness values calculated were then related to various distress determinants and fatigue life in order to evaluate this concept as a possible aid in the mechanistic rehabilitation design procedure.

The equivalent layer thickness is calculated as follows:

$$H_e = a \sum_{i=1}^{L-1} h_i \left| \frac{E_i (1-\nu_s^2)}{E_s (1-\nu_i^2)} \right|^{1/3}$$

where

$a = 0,9$  for flexible pavements

$h_i$  = thickness of layer  $i$  in m

$E_i$  = elastic modulus of layer  $i$  in  $N/m^2$

$E_s$  = elastic modulus of subgrade in  $N/m^2$

$\nu_i$  = Poisson ratio of layer  $i$

$\nu_s$  = Poisson ratio of subgrade

layer with value equal to 0,35

$L$  = Number of layers

## 2 EQUIVALENT LAYER THICKNESS RELATIONSHIPS

Molenaar (1983) and Molenaar and Van Gorp (1980) analysed a typical three-layered pavement structure. The typical flexible pavement

structures referred to in this Appendix differ from this three-layered system in the sense that the pavement structures are either four layered or five-layered systems with a different standard wheel load and tyre pressure. The bitumen base pavements analysed resemble these three-layered pavements most closely in terms of thickness of the bitumen bases. Most of the typical flexible pavement structures analysed, though, have thin asphalt surfacings ( $\leq 40$  mm).

In Figures F.1 and F.2 typical relationships of  $H_e$  versus deflection basin parameters, shape factor (F1) and slope of deflection (SD) are shown as calculated for bituminous base pavements. The purpose is to show that some deflection basin parameters like SD, R, SCI, BCI and BDI can discern between the various subgrade elastic moduli while others, such as F1, F2, S, A and Q cannot. In Figure F.3 surface curvature index (SCI) is shown for bituminous and granular bases versus  $H_e$ . In both cases SCI can discern between the various subgrade effective elastic moduli. The gradients for these functions of the bitumen base pavements correlate well with bitumen base pavements with three layers (SCI with  $r = 500$  mm) (Molenaar and Van Gorp, 1980). The gradients for the relationships of the granular base pavements though, are shallow and reflect a greater sensitivity to changes in  $H_e$ .

Flexible pavements in general were grouped together in Figure F.4 to show that  $H_e$  correlates well with vertical subgrade strain ( $\epsilon_{vs}$ ). The various values of effective elastic moduli of the subgrade lead to different relationships as shown in Figure F.4. In Figure F.5 the other distress determinant, horizontal asphalt tensile strain ( $\epsilon_{HA}$ ), at the bottom of the bituminous base, is shown versus  $H_e$ . Here again, there is a clear discernment between the elastic moduli of the subgrade. It is however not possible to develop the same relationship between  $\epsilon_{HA}$  and  $H_e$  for the thin surfacings of granular base pavements. One of the reasons for the latter situation seems to be that the thickness, Poisson ratio and elastic modulus ratio of the thin surfacing, compared to that of the base and even subgrade, differ markedly from that of a bituminous base pavement. This is

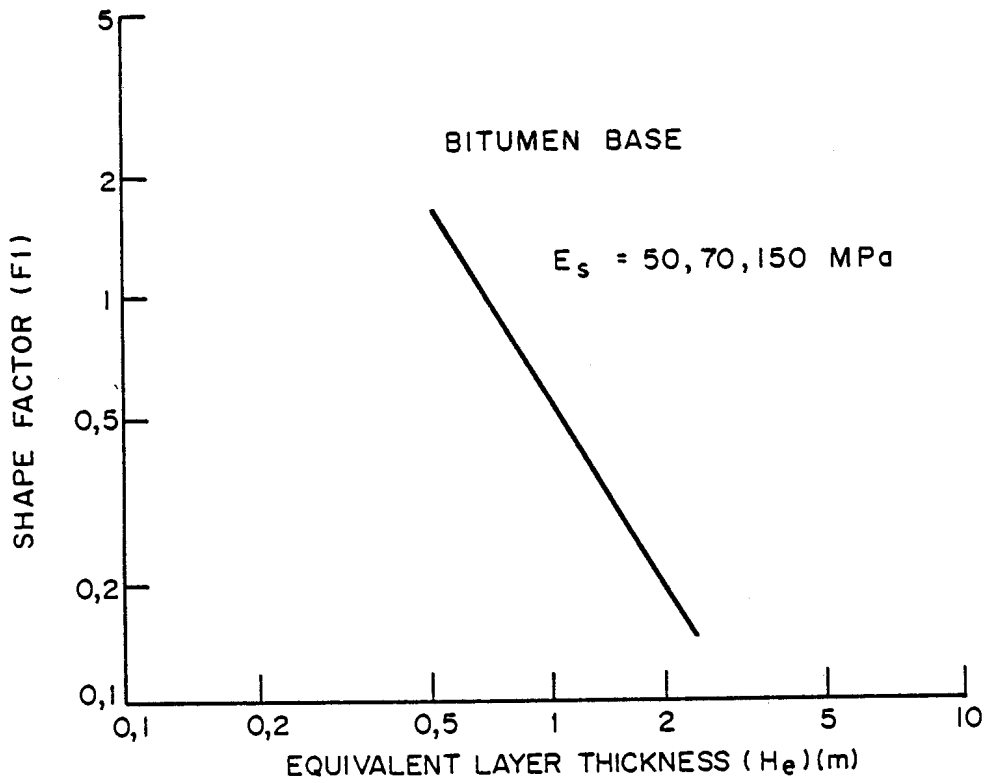


FIGURE F.1  
EQUIVALENT LAYER THICKNESS VERSUS SHAPE FACTOR F1

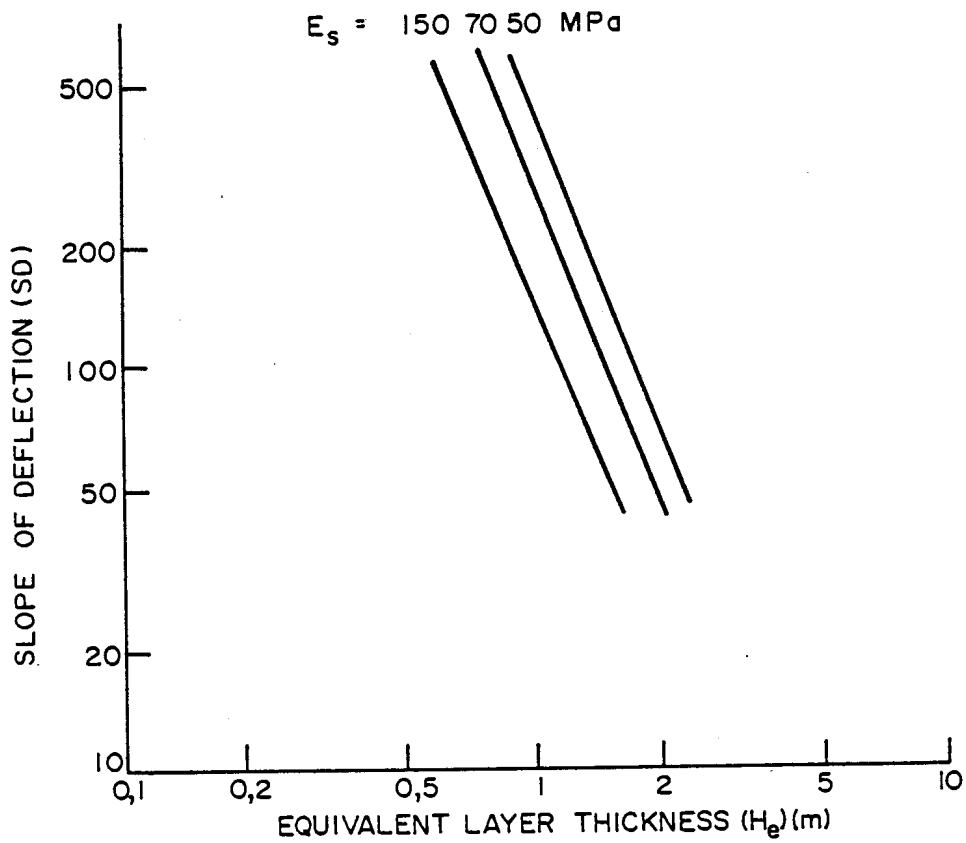


FIGURE F.2  
EQUIVALENT LAYER THICKNESS VERSUS SLOPE OF DEFLECTION

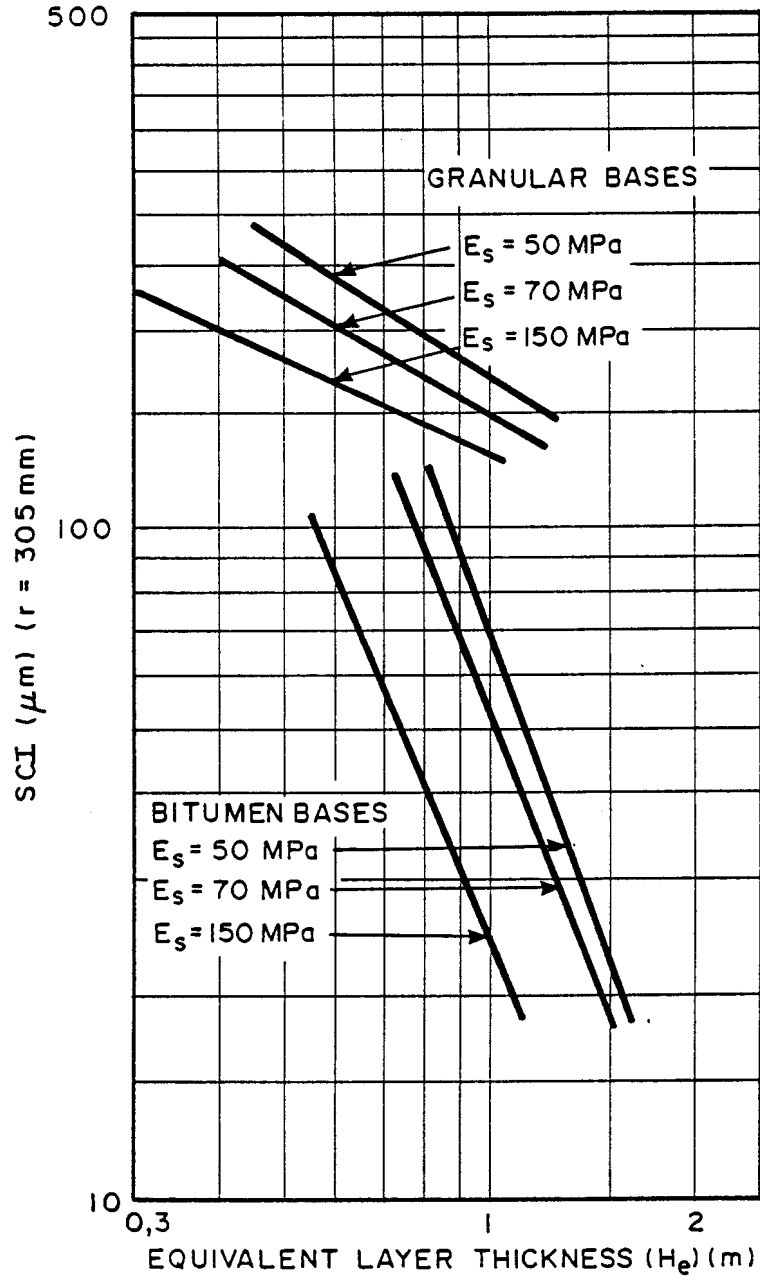


FIGURE F.3  
Equivalent layer thickness versus  
surface curvature index

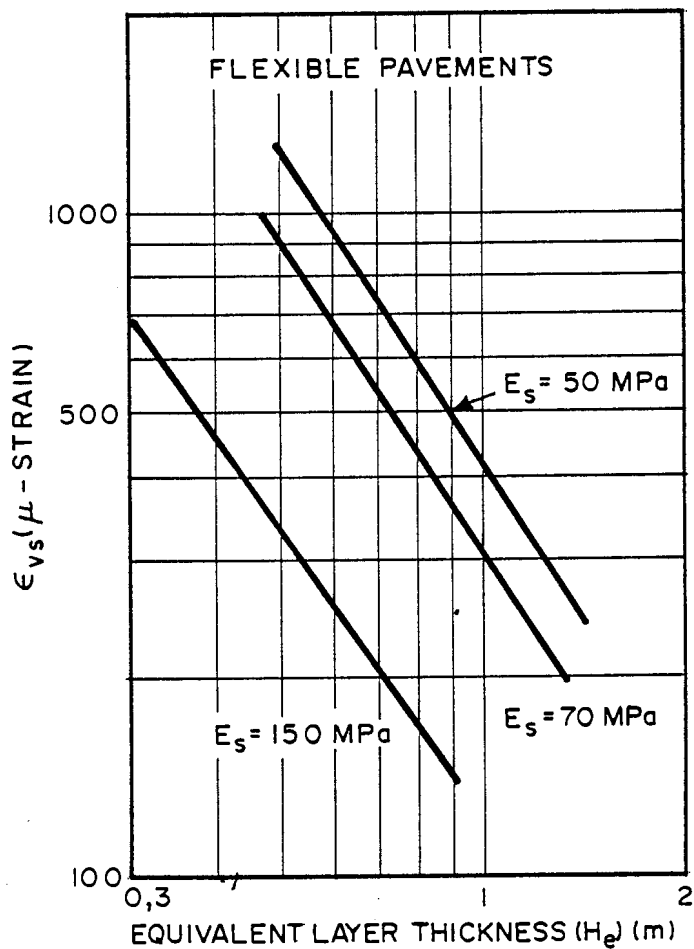


FIGURE F.4  
VERTICAL SUBGRADE STRAIN VERSUS  
EQUIVALENT LAYER THICKNESS FOR  
FLEXIBLE PAVEMENTS



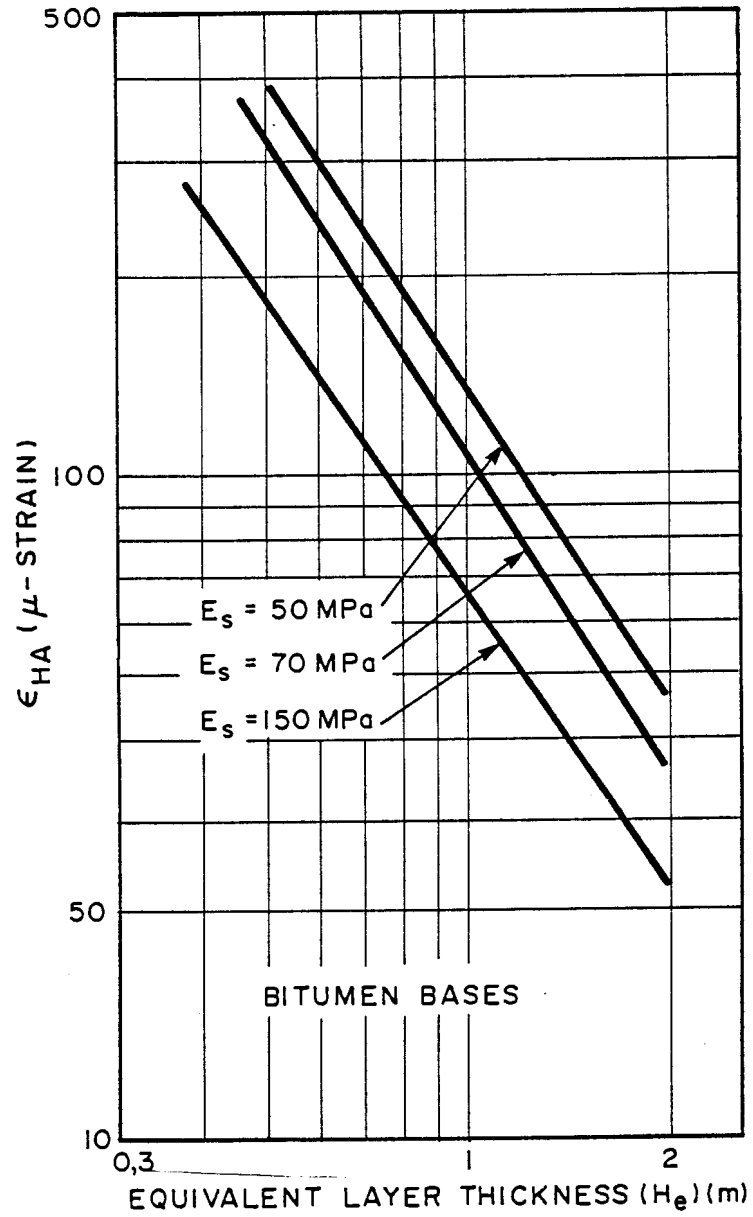


FIGURE F.5

EQUIVALENT LAYER THICKNESS VERSUS  
MAXIMUM ASPHALT STRAIN FOR  
BITUMEN BASE PAVEMENTS

clear when one looks at the formula for the calculation of  $H_e$ , given earlier.

Equivalent layer thickness ( $H_e$ ) can be used to indicate whether a pavement structure with cemented subbases or bases is in the flexible state, with the cemented layers in the cracked phase exhibiting equivalent granular behaviour according to the definition given by Freeme (1983). In Figure F.6,  $H_e$  for the pre-cracked life of pavements with cemented subbases and bases is shown in terms of standard 80 kN axle repetitions (E80s) determined as prescribed by Freeme et al. (1982a). A distinction can be made based on the variance of the elastic modulus of the subgrade. It can be seen, however, that an  $H_e$  value of at least 1,1 m is required for a subgrade modulus of 70 MPa to have any significant pre-cracked life of cemented layers. This is rather high and reaffirms that the major portion of the structural life of typical TRH4 (NITRR, 1985a) pavement structures with cemented layers is in the cracked phase or flexible behaviour state.

The recommended vertical subgrade strain ( $\epsilon_{vs}$ ) criteria for different road categories (Freeme et al., 1982a) were used to calculate the standard 80 kN axle repetitions for all the flexible pavement structures for their respective values of  $H_e$ . This relationship between  $H_e$  and E80s is shown in Figure F.7 for all flexible pavement structures. In this figure the fatigue life of bitumen base pavements was also calculated with respect to maximum asphalt strain ( $\epsilon_{HA}$ ) and correlated with the respective  $H_e$  value. The recommended fatigue life criteria for thick bitumen base pavements were used in the calculation (Freeme et al., 1982a). The recommended shift factors shown in Table F.1 were applied to the calculated fatigue lives.

TABLE F.1 - Shift factors for bituminous bases

Road category		
A	B	C
2	5	10

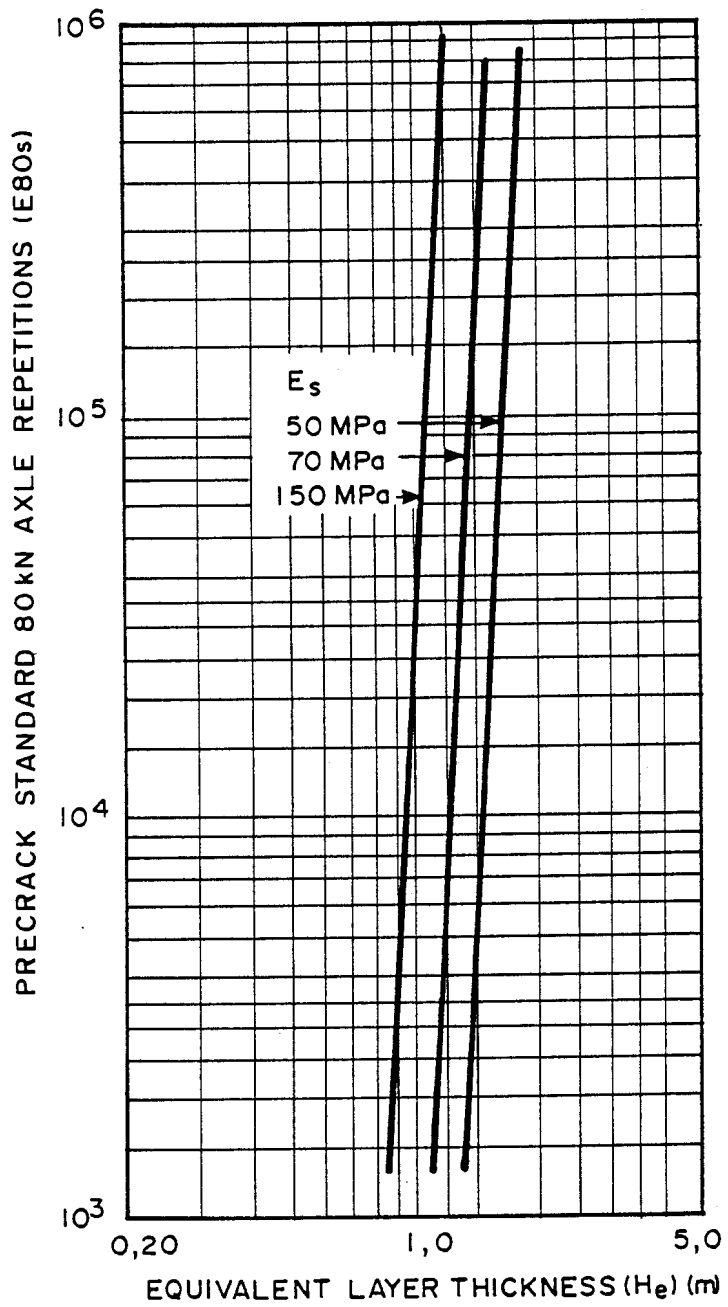


FIGURE F.6  
Initiation of cracking of cemented bases and subbases in terms of equivalent layer thickness

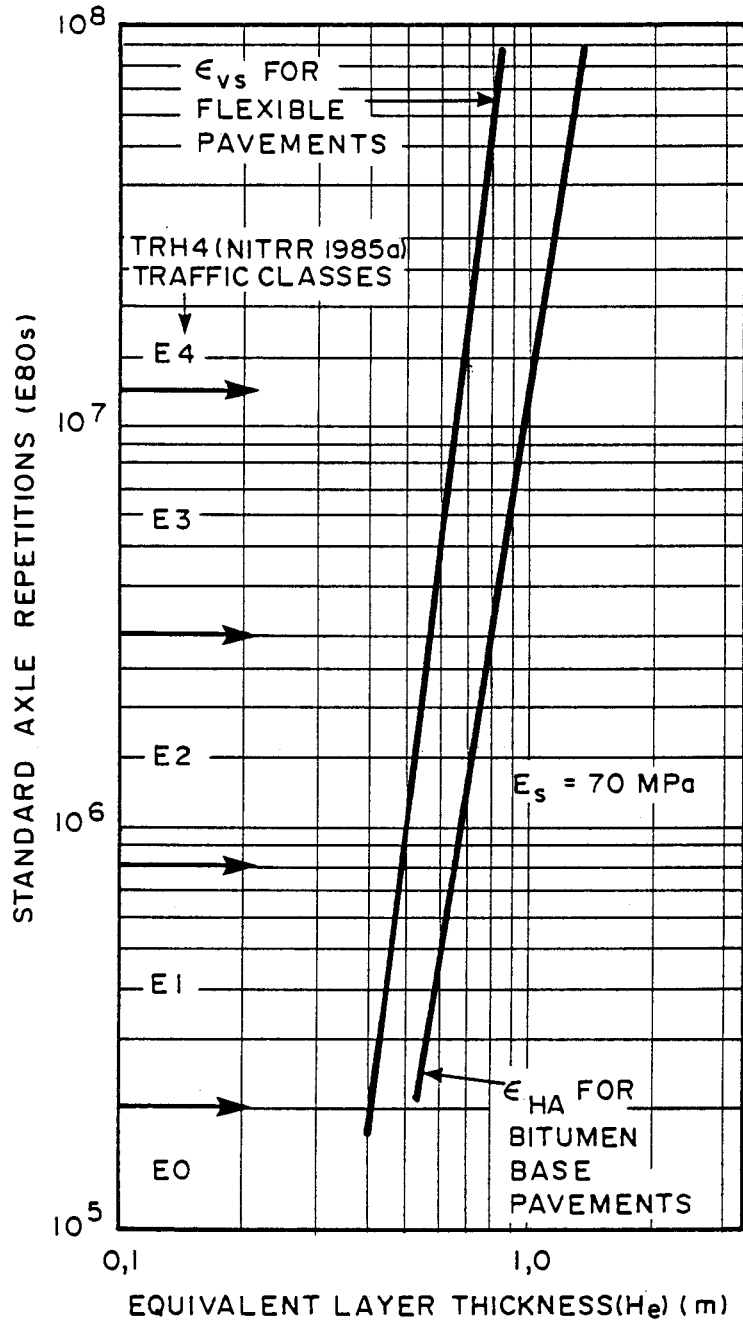


FIGURE F.7

Pavement life for maximum asphalt strain and vertical subgrade strain criteria in terms of equivalent layer thickness

### 3 CONCLUSIONS AND RECOMMENDATIONS

The equivalent layer thickness ( $H_e$ ) concept proved to be a concept that more or less represents the structural capacity of flexible pavements. Deflection basin parameters correlate well with a value such as  $H_e$  in general, as calculated for flexible pavements. It is however only such deflection basin parameters, that normally use points of deflection near each other in the calculation procedure (e.g. SCI, R, BCI, BDI and SD), that can discern the effect of variance in subgrade elastic moduli. Such relationships however do not have much value except as for an interim step towards establishing relationships between the distress determinants ( $\epsilon_{HA}$  and  $\epsilon_{VS}$ ) and  $H_e$ .

$H_e$  correlates well with subgrade vertical strain ( $\epsilon_{VS}$ ) for flexible pavement structures and discerns the effect of variance of subgrade elastic moduli. Granular bases on the other hand do not give any clear relationships between maximum asphalt strain ( $\epsilon_{HA}$ ) and  $H_e$  as is the case with bitumen base pavements. The reason seems to be the ratios of the thickness, elastic modulus and Poisson ratio of the surfacing and the base as well as that of the subgrade, in the calculation of  $H_e$ , which leads to this marked difference between granular and bitumen bases.

The value of  $H_e$  can be used in a mechanistic design or analysis procedure to establish the structural life of a flexible pavement with regard to the distress determinants ( $\epsilon_{VS}$  and  $\epsilon_{HA}$ ). The pre-cracked life of a cemented base and subbase layer can be determined. It must be remembered though, that in order to use  $H_e$  in such a way, the effective elastic moduli of all the layers as well as the thicknesses have to be known. This restricts  $H_e$  to an interim value in the determination of the distress determinants ( $\epsilon_{VS}$  and  $\epsilon_{HA}$ ) in the mechanistic analysis of a pavement.



## REFERENCES

## REFERENCES

- ABBOT, L M. (1977). Stresses and strains in layered systems, CHEV4. NITRR, Computer program guideline, P4. (CSIR, Pretoria)
- ANANI, B A (1979). An evaluation of in situ elastic moduli from surface deflection basins of multi-layer flexible pavements. Ph.D Thesis, Department of Civil Engineering, Pennsylvania State University, University Park, Pennsylvania.
- ANDERSON, D T. (1977). The design of asphalt concrete overlays for flexible highway pavements. Department of Civil Engineering, University of California, Berkeley.
- ANDERSON, D T. (1984) A new approach to asphalt overlay design. Proc.. 11TH ARRB Conf., 12(3), pp. 55-66.
- ASPHALT INSTITUTE, (1977). Asphalt overlays and pavement rehabilitation. MS-17 College Park, Maryland.
- BASSON, J E B. (1985). The measurement of the deflection and curvature of a road surface when loaded by a standard axle. NITRR Technical Note, TP/71/85 (CSIR, Pretoria).
- BASSON, J E B, WIJNBERBER, O J and SKULTETY, J. (1980). The multi depth deflectometer: A multistage sensor for the measurement of resilient deflections and permanent deformation at various depths in road pavements. NITRR Technical Note, TP/85/80. (CSIR, Pretoria).
- BEDFORD, F W and DIVIVEDI, T D. (1970). Vector calculus. McGraw-Hill Book Company.
- BERGER, L and GREENSTEIN, J. (1985). Use of pocket computers for rehabilitation or rural roads in Dominica. TRB, Transportation Research Record 997, Washington, DC.
- BROWN, S F. (1979). The characterization of cohesive soils for flexible pavement design. Proc. 7th Euro. Conf. Soil Mech. and Fnd. Engrg., Vol. 2. pp. 15-22.
- BURMISTER, D M. (1945). The theory of stresses and displacements in layered soil systems. Journal of Applied Physics, Vol. 16.
- BUSH, A J. (1980). Non-destructive testing for light aircraft pavements, Phase I, Evaluation of non-destructive testing devices. Final report prepared for U.S., DOT, Federal Highway Administration.
- CLEASSEN, A I M and DITMARSCH, R. (1977). Pavement evaluation and overlay design, The SHELL Method. Proc. of the 4th Int. Conf. on the Structural Design of Asphalt Pavements. Vol. I. Ann Arbor.
- COETZEE, C H. (1982). CHEVRON program for calculating stresses, strains and displacement in a layered pavement system having a maximum of fifteen layers. NITRR Technical Note TC/27/82. (CSIR, Pretoria).
- COETZEE, C H and HORAK, E. (1981). "Passing van elastisiteitsmoduli van plaveisellae met die CHEVRON program vir dubbelwiele en defleksie gemeet op



die laagvlakke-CHEVMF Program". NITRR, Technical Note TC/44/81. (CSIR, Pretoria).

COETZEE, N F and MONISMITH, C L. (1979). Analytical study of minimization of reflection cracking in asphalt concrete overlays by use of a rubber-asphalt interlayer. TRB, Transportation Research Record No. 700.

DE BEER, M. (19983). HVS site selection and material description at Malmesbury test sections - Report on Main Road 18. NITRR Technical Note TP/50/83. (CSIR, Pretoria).

DE BEER, M. (1986). Die ontwikkeling van 'n DKP-klassifikasiesisteem vir plaveiselstrukture met ligte gesementeerde lae. NITRR Technical Note TP/53/86. (CSIR, Pretoria).

DEHLEN, G L. (1961). The use of Benkelman beam for the measurement of deflections and curvatures of a road surface between dual wheels. CSIR Special report R.2 NITRR, RS/11/61. (CSIR, Pretoria).

DEHLEN, G L (1962a). A simple instrument for measuring the curvature included in a road surfacing by a wheel load. The Civil Engineer in South Africa. Vol. 4, No. 9.

DEHLEN, G L. (1962b). Flexure of road surfacings, its relation to fatigue cracking and factors determining its severity. HRB, Highway Research Board Bulletin No. 321.

DORMAN, G M and METCALF, C T. (1963). Design curves for flexible pavements based on layered system theory. Highway Research Record No. 71, Washington, D.C.

EPPS, J A and HICKS, R G. (1982). Moderator's summary papers in Session V, Rehabilitation of pavements. Proc. of the 5th Int. Conf. on the Structural Design of Asphalt Pavements. Vol. II.

FEDERAL AVIATION ADMINISTRATION (U.S.) (1979). Use of non-destructive testing devices in the evaluation of airport pavements. Advisory Circular No. 150/5370-11. Washington, D.C.

FEDERAL HIGHWAY ADMINISTRATION (FHWA). U.S. DEPARTMENT OF TRANSPORTATION. (1984). Synthesis study of non-destructive testing devices for use in overlay thickness design of flexible pavements. FWHA/RD-83/097. Washington, DC.

FORD, Jr. M C and BISSETT, J R. (1962). Flexible pavements performance studies in Arkansas. Highway Research Board Bulletin 321.

FREEME, C R. (1983). Evaluation of Pavement Behaviour for Major Rehabilitation of Roads. NITRR Technical Report RP/19/83 (CSIR, Pretoria).

FREEME, C R, MAREE, J H and VILJOEN, A W. (1982a). Mechanistic design of asphalt pavements and verification of designs using the Heavy Vehicle Simulator. Proc. 5th Int. Conf. on the Structural Design of Asphalt pavements. Vol. 1, pp 156-173 (CSIR Reprint RR362).

FREEME, C R, MAREE, J H and WALKER, R N. (1982b). User's experience with the South African Heavy Vehicle Simulators. Proc. of Bearing Capacity of



Roads and Airfields. Vol. II. The Norwegian Institute of Technology, Norway.

FREEME, C R, MEYER, R G and SHACKEL, B. (1981). A method for the adequacy of road pavement structures using a heavy vehicle simulator. Paper presented at the Int. Road Federation World Meeting in Stockholm.

FREEME, C R. SERVAS, V P and WALKER, R N. (1986). Pavement behaviour as determined from Heavy Vehicle Simulator Testing. Paper prepared for the 1986 Int. Conf. on Bearing Capacity of Roads and Airfields.

FRÝBA, L. (1967). Vibration of solids and structures under moving loads. Research Institute of Transport, Prague. Noordhof International Publishing, Groningen.

GRANT, M C and CURTAYNE, P C. (1982). Rehabilitation design incorporating past experience of pavement behaviour. Proc. of the 5th Int. Conf. on the Structural Design of Asphalt Pavements. Vol. II. Delft.

GRANT, M C, MARAIS, C P and UYS, D G. (1979). An investigation of an asphalt overlay on a lightly trafficked road showing premature cracking. Proc. of the 3rd Conf. of Asphalt Pavements for Southern Africa. Vol. I. University of Natal, Durban.

GRANT, M C and WALKER, R N. (1972) The development of overlay design procedures based on the application of elastic theory. Proc. 3rd Int. Conf. on the Structural Design of Asphalt Pavements. Vol. 1, pp 1155-1166. (CSIR Reprint RR145).

GREENSTEIN, J. (1982). Pavement evaluation and upgrading of low-cost roads. TRB, Transportation Research Record 875. Washington, D.C.

HETÉNYI, M. (1971). Beams on elastic foundation. Theory with applications in the fields of civil and mechanical engineering. Ann Arbor. The University of Michigan Press. Ninth edition.

HOFFMAN, M S and THOMPSON, M R. (1981). Mechanistic interpretation of non-destructive pavement testing deflections. Transportation Engineering Series No. 32. Illinois Co-operative Highway and Transportation Research Program Series No. 190. University of Urbana-Champaign.

HOGG, A H A. (1944). Equilibrium of a thin slab on an elastic foundation of infinite depth. Phil. Mag. Vol. 35 (234), pp 265-276.

HORAK, E. (1984). Deflection-based mechanistic overlay design for flexible pavements in South Africa: A literature survey. NITRR Technical Report RP/7/84. (CSIR, Pretoria)

HORAK, E. (1985). Curve fitting of deflection basin measurements. NITRR Technical Note TP/82/85. (CSIR, Pretoria).

HORAK, E. (1986a) Analysis of deflection basins measured during accelerated testing. NITRR Technical Note TP/34/86. (CSIR, Pretoria).

HORAK, E. (1986b) Investigation of relationships between deflection basin parameters, distress determinants and overlay thickness for flexible pavements. NITRR Technical Note TP/29/86. (CSIR, Pretoria).



- HORAK, E (1986c). Effective elastic moduli determined from Road surface Deflectometer measurements. NITRR Technical Note TP/40/86. (CSIR, Pretoria).
- HORAK, E and MAREE, J H. (1982). Behaviour of a slag base pavement structure in Heavy Vehicle Simulator testing in the Transvaal. NITRR Technical Report. RP/5/82. (CSIR, Pretoria).
- HORAK, E and OTTE, J R. (1985). Deflection basin data preparation for curve fitting and parameter calculation. NITRR, Technical Note TP/96/85. (CSIR, Pretoria).
- HOYINCK, W T, VAN DER BAN, R and GERRITSEN, W. (1982). Lacroix overlay design by three-layer analysis. Proc. 5th Int. Conf. on the Structural Design of Asphalt Pavements. Vol. I Delft.
- HUSIAN, S and GEORGE, K P. (1985). In situ pavement moduli from Dynaflect deflection. Paper prepared for presentation at the Transportation Research Board Meeting, Washington D.C.
- HVEEM, F N. (1955). Pavement deflection and fatigue failures. Highway Research Board Bulletin 114.
- IRWIN, L H. (1981). User's guide to MODCOMP. version 1.0. Cornell University.
- JORDAAN, G J. (1986). The classification of pavement rehabilitation design methods. NITRR Technical Note, TC/12/86. (CSIR, Pretoria).
- JORDAAN, G J and SERVAS, V P. (1983). Suggested condition classification for flexible pavements in pavement rehabilitation design. Technical report, RC/7/83. (CSIR, Pretoria).
- KENNEDY, C K and LISTER, N W. (1978). Deflection and pavement performance: The experimental evidence. TRRL Laboratory Report No. 833. Great Britain.
- KILARESKI, W P and ANANI, B A. (1982). Evaluation of in situ moduli and pavement life from deflection basins. Proc. 5th Int. Conf. on the Structural Design of Asphalt Pavements. Vol. 1.
- KLEYN, E G, FREEME, C R and TERBLANCHE, L J. (1985). The impact of the Heavy Vehicle Simulator testing in the Transvaal. Annual Transportation Convention. Session: Transport Infrastructure: Accelerated testing of pavements. Pretoria.
- KLEYN, E G and VAN HEERDEN, M J J. (1984). Swaarvoertuigspektrumsimulasie met behulp van enkelvoudige verkeerstellings. Paper presented at the Annual Transportation Conference, Pretoria.
- KLEYN, E G, VAN HEERDEN, M J J and ROSSOUW, A J. (1982). An investigation to determine the structural capacity and rehabilitation. Utilization of road pavement using the Pavement Dynamic Cone Penetrometer. Proc. Bearing Capacity of Roads and Airfields. Vol. II. The Norwegian Institute of Technology, Trondheim, Norway.



- KOOLE, R C. (1979). Overlay design based on Falling Weight Deflectometer measurements. TRB, Transportation Research Record No. 700. Washington D.C.
- KUNG, K Y. (1967). A new method in correlation study of pavement deflection and cracking. Proc. of the 2nd Int. Conf. on the Structural Design of Asphalt Pavements. Ann Arbor.
- LISTER, N E and KENNEDY, C K. (1977). A system for the prediction of pavement life and design of pavement strengthening. Proc. of the 4th Int. Conf. on the Structural Design of Asphalt Pavements. Vol. 1 Ann Arbor.
- MARCHIONNA, A, CESARINI, M FORNACI, M G and MALGARINI, M. 1985). Pavement elastic characteristics measured by means of tests conducted with the FWD. (Method for flexible and semi-rigid pavements considered as non-linear multi-layer structures). Paper prepared for TRB meeting, Washington D.C.
- MAREE, J H. (1978) Ontwerpparameters vir klipslag in plaveisels. M.Sc. (Eng.) Thesis (in Afrikaans). University of Pretoria, October 1972.
- MAREE, H J and FREEME, C R. (1981a). The mechanistic design method used to evaluate the pavement structures in the Catalogue of the Draft TRH4, 1981, NITRR, Technical Report RP/2/81. (CSIR, Pretoria).
- MAREE, J H, FREEME, C R, VAN ZYL, N J W and SAVAGE, P F. (1982). The permanent deformation of pavements with untreated crushed stone bases as measured in Heavy Vehicle Simulator tests. Proc. 22nd ARRB Conf. 2(2), pp 16-28 (CSIR Reprint RR355).
- MAREE, J H, VAN ZYL, N J W and FREEME, C R. (1981b). The effective moduli and the stress-dependence of pavement materials as measured in some Heavy Vehicle Simulator tests. Paper prepared for TRB meeting, Washington, D.C. Also as NITRR Technical Report RP/7/81. (CSIR, Pretoria).
- MOLENAAR, A A A. (1983). Structural performance and design of flexible road constructions and asphalt concrete overlays. Thesis for the Doctor in Technical Science. Technische Hogeschool, Delft, The Netherlands.
- MOLENAAR, A A A. (1984). Structural performance of flexible pavements. Proc. 11th AARB Conf. 12(3), pp 48-54.
- MOLENAAR, A A A and KOOLE, R C. (1982). Moderator's report. Papers in session III. Pavement evaluation. Proc. of the 5th Int. Conf. on the Structural Design of Asphalt Pavements. Vol. II Delft.
- MOLENAAR, A A A and VAN GURP, C A P M. (1980). Optimization of the thickness design of asphalt concrete. 10th ARRB Conf. 10(2) pp 31-44.
- MONISMITH, C L (1966) Design considerations for asphalt pavements to minimize fatigue distress under repeated loading. Berkeley, University of California.
- MONISMITH, C L. (1977). Pavement evaluation and overlay design: Summary of methods. Transport Research Record No. 700, Transport Research Board. Washington, D.C.



- MONISMITH, C L and DEACON, J A. (1969) Fatigue of asphalt paving mixtures. Transportation Engineering Journal of the ASCE, May 1969.
- MONISMITH, C L. and MARKEVICH, N (1983). Progress report on structural pavement evaluation and overlay design for low volume roads. Dept. of Civil Engineering, University of California, Berkeley.
- MONISMITH, C L and McLEAN, D B. (1982). Structural design considerations. Symposium on the technology of thick asphalt construction. Proc. of the Association of Asphalt Technologists.
- MONISMITH, C L, SECOR, K E and BLACKMER, E W. (1961). Asphaltic mix behaviour in repeated flexure. Proc. of the Association of Asphalt Technologists. Vol. 30. Minneapolis.
- MOORE, W M HANSON, D I and HALL, J W. (1978). An introduction to non-destructive structural evaluation of pavements. TRB, Transportation Research Circular No. 189.
- NATIONAL INSTITUTE FOR TRANSPORT AND ROAD RESEARCH. (1971). Bituminous surface treatments for newly constructed rural roads. TRH3. (CSIR, Pretoria).
- NATIONAL INSTITUTE FOR TRANSPORT AND ROAD RESEARCH. (1978). Selection and design of hot-mix asphalt surfacings for highways. TRH8. (CSIR, Pretoria).
- NATIONAL INSTITUTE FOR TRANSPORT AND ROAD RESEARCH. (1983). Structural design of pavement rehabilitation. Draft TRH12. (CSIR, Pretoria).
- NATIONAL INSTITUTE FOR TRANSPORT AND ROAD RESEARCH. (1985a). Structural design of inter-urban and rural road pavements. TRH4 (CSIR, Pretoria).
- NATIONAL INSTITUTE FOR TRANSPORT AND ROAD RESEARCH. (1985b). Standards for road construction materials. TRH14 (CSIR, Pretoria).
- NIE, N H, HULL, C H, JENKINS, J G, STEINBRANNER, K AND BRENT, D H. (1975). SPSS Statical package for the social sciences. Second Edition. McGraw-Hill Publishing Company.
- ODEMARK, N. (1949.) Investigations as to the elastic properties of soils and design of pavements according to the theory of elasticity. Statens Vaeginstitut, Stockholm, Sweden.
- OPPERMAN, R A. (1984). Die swaarvoertuignaboorsertoetse (SVN-toetse) op Pad 30, naby Hornsnek. NITRR Technical Report, RP/3/84 (CSIR, Pretoria).
- OPPERMAN, R A, HORAK, E and VILJOEN, A W. (1983). The Heavy Vehicle Simulator (HVS) tests on freeway N3/1 between Paradise Valley and Farnningham interchange. NITRR Technical Report, RP/7/83 (CSIR, Pretoria).
- PATTERSON, W D O. (1985). Prediction of road deterioration and maintenance effects: Theory and quantification. The highway design and maintenance standards study. Draft Vol. III. Transportation Department. The World Bank, Washington, D.C.

- PATTERSON, W D O and VAN VUUREN, D J (1974). Diagnosis of working strains in a pavement using deflection profiles. ARRB Proc., Vol. 7, Part 6.
- PERMANENT INTERNATIONAL ASSOCIATION OF ROAD CONGRESSES. (1983). Technical committee report on flexible roads. XVII World Road Congress, Sydney, Australia.
- PRONK, A C and BUITER, R. (1982). Aspects of the interpretation and evaluation of Falling Weight Deflectometer (FWD) measurements. Proc. of the 5th Int. Conf. on the Structural Design of Asphalt Pavements. Vol. 1 Delft.
- RHOLF, J G and ROGNESS, R O. (1985). Multivariate analysis of pavement Dynaflect deflection data. Paper prepared for the Transportation Research Board Meeting, Washington, D.C.
- ROBINSON, B. (1984). SPSS subprogram Non-linear regression. Vogelback Computer Centre, Illinois.
- RUST, F C. (1984). Load-associated crack movements in road pavements. Paper presented at the Annual Transportation Conference, Pretoria.
- RUST, F C. (1985). Summary of crack movement measurement results on the MR27- Stellenbosch to Somerset West. NITRR Technical Note TP/149/85. (CSIR, Pretoria).
- RUST, F C. (1986). Crack movement measurements on the N4/3. NITRR Technical Note, TP/86/86. (CSIR, Pretoria).
- SHACKEL, B. (1980). The Heavy Vehicle Simulator system in South Africa. NITRR Technical Report RP/3/80. (CSIR, Pretoria).
- SHELL INT. PETROLEUM CO. ((1978). Shell pavement design manual: Asphalt pavements and overlays.
- SLAVIK, M M and BOSMAN, J. 1984. Estimation of pavement loads from traffic observations.. Paper presented at the Annual Transportation Conference, Pretoria.
- SNAITH, M S, McMULLEN, D, FREER-HEWISH, R J and SHEIN, A. (1980). Flexible pavement analysis. Final Report. Dept. of Transportation and Environmental Planning, University of Birmingham.
- STUBSTAD, R N and CONNER, B. (1983). Use of the Falling Weight Deflectometer to predict damage potential on Alaskan Highways during spring thaw. TRB, Transportation Research Record 930.
- STUBSTAD, R N and HARRIS, T B. (1984). Personal communication. Dynatest Consulting, Ojia, California.
- SWIFT, G. (1972). A graphical technique for determining the elastic moduli of a two-layered structure for measured surface deflections. Research Report No. 136-3, Texas Transportation Institute.
- SZENDREI, M E. (1974). Evaluation of Benkelman beam field data supplied in the form of a deflection distance chart. NITRR Technical Note TI/8/74. (CSIR, Pretoria).



- SZENDREI, M E. (1975). Benk 5 - An improved version of Benk 1. NITRR Technical Note TI/4/75 (CSIR, Pretoria).
- SZENDREI, M E. (1975b). A computer program to evaluate road deflections at various depths. NITRR Technical Note TI/5/75. (CSIR, Pretoria).
- TAM, W S. (1985). Report on design of overlays for bituminous pavements. Report No. WST/1. Department of Civil Engineering, University of Nottingham.
- TAUTE, A, McCULLOUGH, B G and HUDSON, W R. (1981). Improvements to the materials characterization and fatigue life prediction methods of the Texas rigid pavement overlay design procedure. Research report 249-1. (University of Texas at Austin.) Centre for Transportation Research, Bureau of Engineering Research, Austin.
- THOMPSON, M R. (1982). Concepts for developing a non-destructive based asphalt concrete overlay thickness design procedure. Illinois Dept. of Transportation Bureau of Materials and Physical Research. FHWA/IL/UI-194.
- THOMPSON, M R and ELLIOTT, R P. (1986). ILLI-PAVE-Based algorithms for design of conventional flexible pavements. TRB, Transportation Research Record No. 1043.
- THOMPSON, M R and HOFFMAN, M S. (1983). Concepts of developing an NDT-based design procedure for determining asphalt concrete overlay thickness. TRB, Transportation Research Record No. 930.
- TREYBIG, H J, McCULLOUGH, B F, FINN, F N, McCOMB, R and HUDSON, W R. (1978). Design of asphalt concrete overlay thickness. Proc. of the 4th Int. Conf. on the Structural Design of Asphalt Pavements. Vol. I., Ann Arbor.
- ULLIDTZ, P (1982). Management system for pavement maintenance and rehabilitation based on analytic methods of pavement evaluation. TRB, Transportation Research Record 930.
- ULLIDTZ, P and PEATTIE, K R. (1980). Pavement analysis by programmable calculators. Transportation Engineering Journal of the American Society of Civil Engineers. Vol. 106, No. TE5.
- ULLIDTZ, P and PEATTIE, K R. (1982). Programmable calculators in the assessment of overlays and maintenance strategies. Proc. of the 5th Int. Conf. on the Structural Design of Asphalt Pavements. Vol. I., Delft.
- UNIVERSITY OF CALIFORNIA. (1972). ELSYM5. Unpublished report, Berkeley, California.
- UNIVERSITY OF DUNDEE, DEPARTMENT OF CIVIL ENGINEERING. (1980). Pavement evaluation based on surface deflection. Dundee.
- VAN DE LOO, P J. (1976). A practical approach to the prediction of rutting in asphalt pavements - the Shell method. Transportation Research Board, Washington, D.C.

- VAN ZYL, N J W and FREEME, C R. (1984). Determination of relative damage done to roads by heavy vehicles. Paper presented at the Annual Transportation Conference, Pretoria.
- VAN ZYL, N J W and TRIEBEL, R. (1984). Drie-maandelikse vorderingsverslag vir die tydperk Mei tot Julie 1982. NITRR Technical Note TP/82/82. (CSIR, Pretoria).
- VASWANI, N K. (1971). Method for separately evaluating structural performance of subgrades and overlaying flexible pavements. HRB, Highway Research Record No. 362.
- VERSTRAETEN, J, VEVERKA, V and FRANCKEN, L. (1982). Rational and practical designs of asphalt pavements to avoid cracking and rutting. Proc. of the 5th Int. Conf. on the Structural Design of Asphalt Pavements. Delft. Holland.
- VEVERKA, V. (1979). Evaluation of rut depth in flexible pavements. La Technique Routiere. Vol. 24. No. 3.
- VILJOEN, A W and MEADOWS, K. (1981). The creep test - A mix design tool to tank asphalt mixes in terms of their resistance to permanent deformation under heavy traffic. NITRR, Technical Note TP/36/81. Pretoria).
- VISSER, A T, MAREE, J H and MARAIS, G P. (1983). Implications of light bituminous surface treatments on gravel roads. NITRR RR 350. Reprinted from Transportation Research Record No. 898, TRB, Washington, D.C.
- WALKER, R N, PATERSON, W D O, FREEME, C R and MARAIS, C P. (1977). The South African mechanistic design procedure. Proc. 4th Int. Conf. on the Structural Design of Asphalt Pavements. Vol. 2, pp 363-415.
- WANG, M C, LARSON, T D, BHAHANDAS, A C and CUMBERLEDGE, G. (1978). Use of road rater deflections in pavement evaluation. TRB. Transportation Research Record 666.
- WHITCOMB, W G (1982). Surface deflections and pavement evaluation - Equipment and analysis techniques. Transportation Engineering Report 82-4. Dept. of Civil Engineering. Oregon State University, Cornwallis, Oregon.
- WISEMAN, G, UZAN, J, HOFFMAN, M S, ISHAI, I and LIVNEH, M. (1977). Simple elastic models for pavement evaluation. Proc. of the 4th Int. Conf. on the Structural Design of Asphalt Pavements. Ann Arbor, Vol. 2.
- YODER, E J and WITCZAK, M W. (1975). Principles of pavement design. Second Edition. John Willey and Sons. Inc.

TABLE I.1 : SUMMARY OF DEFLECTION BASIN PARAMETERS.

Parameter	Formula
1. Maximum deflection	$\delta_0$
2. Radius of curvature	$R = \frac{r^2}{2\delta_0(\delta_0/\delta_r - 1)} ; r = 127 \text{ mm}$
3. Spreadability	$S = \frac{[(\delta_0 + \delta_1 + \delta_2 + \delta_3)/5]100}{\delta_0} ; \delta_1 \dots \delta_3 \text{ spaced } 305 \text{ mm}$
4. Area	$A = 6[1 + 2(\delta_1/\delta_0) + 2(\delta_2/\delta_0 + \delta_3/\delta_0)]$
5. Shape factors	$F = (\delta_0 - \delta_2)/\delta_1 ; F_2 = (\delta_1 - \delta_3)/\delta_2$
6. Surface curvature index	$SCI = \delta_0 - \delta_r ; r = 305 \text{ or } 500 \text{ mm}$
7. Base curvature index	$BCI = \delta_{610} - \delta_{915}$
8. Base damage index	$BDI = \delta_{305} - \delta_{610}$
9. Deflection ratio	$Q_r = \delta_r/\delta_0 ; \text{ where } \delta_r \approx \delta_0/2$
10. Bending index	$BI = \delta_0/a ; \text{ where } a = \text{deflection basin length}$
11. Slope of deflection	$SD = \tan^{-1}(\delta_0 - \delta_r)/r ; \text{ where } r = 610 \text{ mm}$
12. Tangent slope	$ST = (\delta_0 - \delta_r)/r ; \text{ where } r = \text{distance to inflection point}$
13. Radius of influence	$RI = R'/\delta_0 ; \text{ where } R' \text{ is the distance from } \delta_0 \text{ to where basin is tangent to horizontal.}$

TYPICAL DEFLECTION BASIN

